Coordinated Operation of the Electric Power System with Water Distribution Systems:

Modeling, Control, Simulation, and Quantification of Resilience

by

Scott Zuloaga

A Dissertation Presented in Partial Fulfillment
of the Requirements for the Degree
Doctor of Philosophy

Approved April 2020 by the
Graduate Supervisory Committee:

Vijay Vittal, Chair
Junshan Zhang
Larry Mays
Meng Wu

ARIZONA STATE UNIVERSITY

May 2020

ABSTRACT

The electric power system (EPS) is an extremely complex system that has operational interdependencies with the water delivery and treatment system (WDTS). The term water-energy nexus is commonly used to describe the critical interdependencies that naturally exist between the EPS and water distribution systems (WDS). Presented in this work is a framework for simulating interactions between these two critical infrastructure systems in short-term and long-term time-scales. This includes appropriate mathematical models for system modeling and for optimizing control of power system operation with consideration of conditions in the WDS. Also presented is a complete methodology for quantifying the resilience of the two interdependent systems.

The key interdependencies between the two systems are the requirements of water for the cooling cycle of traditional thermal power plants as well as electricity for pumping and/or treatment in the WDS. While previous work has considered the dependency of thermoelectric generation on cooling water requirements at a high-level, this work considers the impact from limitations of cooling water into network simulations in both a short-term operational framework as well as in the long-term planning domain.

The work completed to set-up simulations in operational length time-scales was the development of a simulator that adequately models both systems. This simulation engine also facilitates the implementation of control schemes in both systems that take advantage of the knowledge of operating conditions in the other system. Initial steps for including the influence of anticipated water availability and water rights attainability within the combined generation and transmission expansion planning problem is also presented.

Lastly, the framework for determining the infrastructural-operational resilience (IOR) of the interdependent systems is formulated.

Adequately modeling and studying the two systems and their interactions is becoming critically important. This importance is illustrated by the possibility of unforeseen natural or man-made events or by the likelihood of load increase in the systems, either of which has the risk of putting extreme stress on the systems beyond that experienced in normal operating conditions. Therefore, this work addresses these concerns with novel modeling and control/policy strategies designed to mitigate the severity of extreme conditions in either system.

ACKNOWLEDGMENTS

I would like to give thanks to my advisor, Dr. Vijay Vittal, for giving me the opportunity to work under him on this extremely interesting project. I appreciate his guidance and for always being there with an open door to answer questions and provide direction. I also thank the other co-principal investigators on this project, Dr. Junshan Zhang, Dr. Larry Mays, and Dr. Virginia Kwan for their advice, suggestions and feedback throughout the completion of this project and during the revisions for our published papers. I would like to acknowledge my fourth committee member, Dr. Meng Wu, for thoughtful questions and also thank my colleagues Beibei Liu and especially Puneet Khatavkar for the work on his part of the software engine that we developed and for helping to develop our resilience quantification methodology.

I would like to acknowledge Dr. Vittal and ECEE for providing my initial research funding. I would also like to acknowledge the National Science Foundation's Graduate Research Fellowship Program for funding all expenses related to my research for the last three years. I sincerely thank my three GRFP reference letter writers: David Tovar, Director of System Planning at El Paso Electric; Dr. Kyle Rawlings, physics professor at Scottsdale Community College; and Dr. Vittal for their time and recommendations as I have no doubt that played a large role in me receiving this prestigious fellowship.

This journey has not been easy and I would like to explicitly thank my parents, Richard and Jill; my sisters, Stacie and Kim; and brothers-in-law, Bo and Ryan. I very much appreciate their support and encouragement along the way, for always being there for me, and for their encouragement to persevere and stick it out through the tough times, thank you all so much.

TABLE OF CONTENTS

CHAPTER Page

CHAPTER Page

CHAPTER Page

CHAPTER Page

CHAPTER Page

LIST OF TABLES

Table Page

Table Page

Table Page

LIST OF FIGURES

Figure Page

Figure Page

Figure Page

Figure Page

Figure Page

Figure Page

Figure Page

GLOSSARY

Terms:

AGC	automatic generation control
CEED	combined economic and environmental dispatch
EPS	electric power system
LP	linear program
MILP	mixed-integer linear program
OPF	optimal power flow
SCUC	security constrained unit commitment
SCED	security constrained economic dispatch
WDS	water distribution system
WDTS	water delivery and treatment system

Sets and Indices:

g	generator index
g_{th}	thermoelectric generator index
G	set of all generators
G_{th}	set of thermoelectric generators, $G_{th} \subset G$
G_{AGC}	set of generators with AGC capability, $G_{AGC} \subset G$
G_n	set of generators at node (bus) n, $G_n \subset G$

$\overline{G}$	set of candidate generators, $\overline{G} \subset G$
i	index for cost segment i of generator g
l	index for transmission line or transformer
L	set of transmission lines and transformers
$\overline{L}$	set of candidate lines, $\overline{L} \subset L$
n	node (bus) index
q	index for year $q \in Q$
Q	set of all years
r	reference node (bus)
s	index for scenario $s \in S$
S	set of all scenarios
t	index for time-period $t \in T$
T	set of all time-periods
T_{24}	set of time-periods, $t_i \in \{t, \ldots, t + 24\}$
T_{ld}	set of limited day time-periods $T_{ld} \subset T$

Parameters:

α_{dn}	required percentage of net load for downward regulation reserve
α_{up}	required percentage of net load for upward regulation reserve
b_l	primitive susceptance for line l

c_l^{Inv}	investment cost for candidate line $l \in \bar{L}$
c_g^{Inv}	investment cost for candidate generator $g \in \bar{G}$
$C_{water,g}$	water cost for generator g
$cROC_t$	cumulative rate of change of averaged onsite storage tank level
$C_{g,i}$	fuel cost of segment i for generator g
CNL_g	no-load cost for generator g
CSU_g	startup cost for generator g
$CREGUP_g$	upward regulation reserve cost for generator g
$CREGDN_g$	downward regulation reserve cost for generator g
$CNSPIN_g$	non-spinning reserve cost for generator g
$CSPIN_g$	spinning reserve cost for generator g
d	discount factor
DT_g	minimum down time for generator g
$\delta_{fuelCost}$	objective function weight for fuel cost
$\delta_{waterCost}$	objective function weight for water cost
EF	elasticity of supply for the price of water
$G_{TP,g}$	value assigned to generator g based on type

HCF_g	historical capacity factor of generator g
LMF_t	load multiplier factor for scaling active and reactive loads in the EPS simulation, time-period t
M_l	large positive number
$P_{load,nt}$	active power demand, bus n, period t
$P_{g,max}$	maximum active power output for generator g
$P_{gi,max}$	maximum active power output for segment i, generator g
$P_{g,min}$	minimum active power output for generator g
$\overline{P_{gt}}$	fixed active power output of generator g, time-period t
$P_{l,max}$	maximum active power flow through element l, steady-state
$P_{l,min}$	minimum active power flow through element l, steady-state
$P_{l,maxC}$	maximum active power flow through element l, Rate C limit
$P_{l,minC}$	minimum active power flow through element l, Rate C limit
$P_{pload,nt}$	active WDS pump power demand, bus n, time-period t
Φ_{gt}	fixed active power output for generator g, time-period t, input for contingency analysis

$Q_{t,g}$	cooling water supplied from wds to generator g, time-period t
$R_{g,hr}$	hourly ramp rate for generator g
ROC_t	onsite storage tank rate of change averaged over last 24 time-periods
$\mathrm{TC}_{\mathrm{tankRefill}}$	time constant for WDS node demand adjustment factor
TL_g	on-site water storage tank level, generator g
TPF	tank percentage factor, percentage water tank level can change over time duration
RSU_g	startup ramp rate for generator g
RSD_g	shutdown ramp rate for generator g
$RREG_g$	regulation ramp rate for generator g
$RSPIN_g$	spinning ramp rate for generator g
$RNSPIN_g$	non-spinning ramp rate for generator g
sl	transmission line index function calculation parameter
UT_g	minimum up time for generator g
$\overline{u_{gt}}$	fixed on/off status for generator g, time-period t

$W1$	objective function weight for the transmission investment terms
$W2$	objective function weight for the generation investment terms
$W3$	objective function weight for the SCUC terms
Υ_{gt}	fixed on/off status for generator *g*, time-period *t*, input to CEED
WA_{gqs}	water rights obtained for generator g $\in \overline{G}$ for all periods *t* in year *q* of scenario *s*.
WCRg	water consumption rate (gal/MWH) of generator g
W_{derate}	weight for derating LP

Variables:

$dAdj_{xf,n,t}$	load reduction amount, *xf* ∈{*sf, mf*}, bus *n*, time *t*, from consumer survey results
$LOL_{n,t}$	loss of load, bus *n*, time-period t
mf_n	fraction of multi-family (m*f*) homes in residential component of load, bus *n*
$P_{l,t}$	active power flow on line *l*, time-period *t*
$P_{g/g_{th},t}$	active power output for generator g/g_{th}, time-period *t*
$P_{g/g_{th}ti}$	active power output for segment i, generator g/g_{th}, time-period *t*

r_{gt}^{c}	active generation change for generator g, time-period t, generator contingency
$r_{gt,spin}$	spinning reserve for generator g, time-period t
$r_{gt,nonspin}$	non-spinning reserve for generator g, time-period t
$r_{gt,regup}$	five-minute upward regulation reserve, generator g, time-period t
$r_{gt,regdn}$	five-minute downward regulation reserve for generator g, time period t
sf_n	fraction of single-family (*sf*) homes in residential component of load at bus n
s_l	slack variable for transmission line l
$s_{t,g}$	slack variable for time-period t, generator g
Θ_{nt}	voltage angle of bus n, time-period t
TL_{gt}	water tank level for generator g, time-period t
u_{gt}	on/off status for generator g, time-period t
v_{gt}	startup status for generator g, time-period t
w_{gt}	shutdown status for generator g, time-period t
y_{gt}	investment decision variable for generator $g \in \overline{G}$, time-period t

z_{lt}	investment decision variable for line $l \in \bar{L}$, time-period t
WDS_{DA}	demand adjustment factor for cooling water requirement for altering node demands of generators within WDS simulation

Resilience Nomenclature

Index Functions:

R_{CW}^{g}	cooling water index function, generator g
R_{DS}^{n}	demand supplied (overall) index function, bus n
R_{PL}^{n}	demand supplied (WDS pumps) index function, bus n
R_{TL}^{l}	transmission line thermal limit index function, branch l
R_{V}^{n}	voltage index function, bus n

Operational Resilience Measures of Performance (RMP):

$Res_{R_{CW}^{g},t}$	RMP for cooling water supply, time-period t
$Res_{R_{DS}^{n},t}$	RMP for demand supplied (overall), time-period t
$Res_{R_{PL}^{n},t}$	RMP for demand supplied (WDS pumps), time-period t
$Res_{R_{TL}^{l},t}$	RMP for transmission lines, time-period t
$Res_{R_{V}^{n},t}$	RMP for voltage, time-period t
$R_{EPS,IND}$	EPS independent OR terms: voltage, transmission line, overall load supplied

$R_{EPS,INTR}$ EPS interdependent OR terms: thermoelectric cooling water supplied and WDS pump load supplied

$Res_{EPS,TOT}(t)$ overall EPS operational resilience at time t

Infrastructural Robustness Metrics (IRM):

$M_{ED,n}$ connectivity IRM for bus n

$M_{EB,l}$ betweenness IRM for transmission line element l

$M_{EFF,n}$ efficiency IRM for bus n

$M_{SCW,g}$ EPS generator cooling water significance IRM for generator g

Infrastructural-Operational Resilience (IOR) Functions:

$R_{R^n_{V},t}$ final resilience value for voltage, IOR based calculation, time t

$R_{R^l_{TL},t}$ final resilience value for transmission elements, IOR based calculation, time t

$R_{R^n_{DS},t}$ final resilience value for overall demand satisfied, IOR based calculation, time t

$R_{R^n_{PL},t}$ final resilience value for pump demand supplied, IOR based calculation, time t

$R_{R^g_{CW},t}$ final resilience value for thermoelectric generators, IOR based calculation, time *t*

Total IOR Values:

$R_{EPS,IND}$ EPS independent IOR terms: voltage, transmission line, overall load supplied

$R_{EPS,INTR}$ EPS interdependent IOR terms: thermoelectric cooling water supplied and WDS pump load supplied

$R_{EPS,TOT}(t)$ ESP total IOR value

$R_{WDS,IND}$ WDS independent IOR term: pressure

$R_{WDS,INTR}$ WDS interdependent IOR terms: pump power availability and demand satisfaction

$R_{WDS,TOT}(t)$ WDS total IOR value

$R_{TOT}(t)$ final combined WDS and EPS IOR value

IOR Quantification Metrics:

M_{ROB} metric quantifying system robustness to disturbance

$M_{RAPI,DP}$ metric quantifying system ability to limit rate of impact by disturbance

$M_{RAPI,RP}$ metric quantifying system ability to rapidly recover from disturbance

M_{RA} metric quantifying system ability to reach pre-disturbance resilience value

M_{TAPL} metric quantifying performance loss of system during disturbance

M_{TOT} metric quantifying overall system response to disturbance

Weights:

w_{ov}, w_{otl}, w_{ocw} weights associated with voltage, transmission element, cooling water, overall and WDS pump demand supplied terms for EPS OR

w_{ods}, w_{opl}

w_p, w_{pow}, w_{dem} weights associated with pressure, pump power and demand satisfaction terms, respectively, for WDS IOR

w_1, w_2 weights associated with the independent and interdependent terms, respectively, for total IOR

$w_v, w_{tl}, w_{cw}, w_{ds}, w_{pl}$ weights associated with voltage, transmission element, cooling water, overall demand supplied and WDS pump demand supplied terms, respectively, for EPS IOR

LIST OF PAPERS RESULTING FROM THIS WORK

Journal Papers:

S. Zuloaga, P. Khatavkar, V. Vittal, and L. W. Mays , "Interdependent electric and water infrastructure modeling, optimization and control," IET Energy Syst. Integr. J., vol. 2, no. 1, pp. 9–21, March, 2020.

S. Zuloaga, P. Khatavkar, L. W. Mays, and V. Vittal, "Resilience of Cyber-Enabled Electrical Energy and Water Distribution Systems Considering Infrastructural Robustness Under Conditions of Limited Water and/or Energy Availability," *IEEE Trans. Eng. Manag.*, in press/Early Access Available, pp. 1–17, Sep. 2019.

S. Zuloaga and V. Vittal, "Integrated Electric Power/Water Distribution System Modeling and Control under Extreme Mega Drought Scenarios," submitted to *IEEE Trans. Power Syst*, March, 2020.

S. Zuloaga and V. Vittal, "Quantifying Power System Operational and Infrastructural Resilience under Extreme Conditions within a Water-Energy Nexus Framework," submitted to *IEEE Trans. Smart Grid*, April, 2020.

Conference Publications:

S. Zuloaga and V. Vittal, "Metrics for Use in Quantifying Power System Resilience with Water-Energy Nexus Considerations: Mathematical Formulation and Case Study," in *Proc. 2019 IEEE Power and Energy Society General Meeting*, Atlanta, GA, Aug. 2019.

CHAPTER 1

INTRODUCTION

1.1 Background and Motivation

The electric power system (EPS) and the water delivery and treatment system (WDTS) have several interdependencies that have been recognized and informally defined as the water-energy nexus. These interdependencies arise because power generation via thermoelectric plants requires water for the plants' cooling cycle and because water taken from its source requires electricity for pumping and/or treatment needs before its final delivery to the end user. The energy requirements for the water distribution system (WDS) can be a large portion of the total energy requirements of a city or state, as evidenced in California in 2005 when the state required 19% of its total energy use for water system requirements [1]. More recently in 2012, it was estimated that 12.3% of the total energy consumption in the US was for water related uses [2]. Likewise, water usage in the power system can constitute a large percentage of the total water demands, being up to as much as 45% of the total daily water withdrawn from water sources in the U.S. [3]. It is also seen from the data in [3] that the usage of water by the power production sector in each state varies quite widely, with values totaling over 80% of daily water withdrawals in Alabama, Illinois, and S. Carolina down to much smaller values including approximately only 1.71% for thermoelectric power generation in Arizona. Although water for thermoelectric generation may represent a small amount of the overall demand in the WDS, the converse is not necessarily true. Figure 1.1 shows the percentage of thermoelectric generation (calculated from overall energy production) in Arizona from 1990 through 2018 and it is

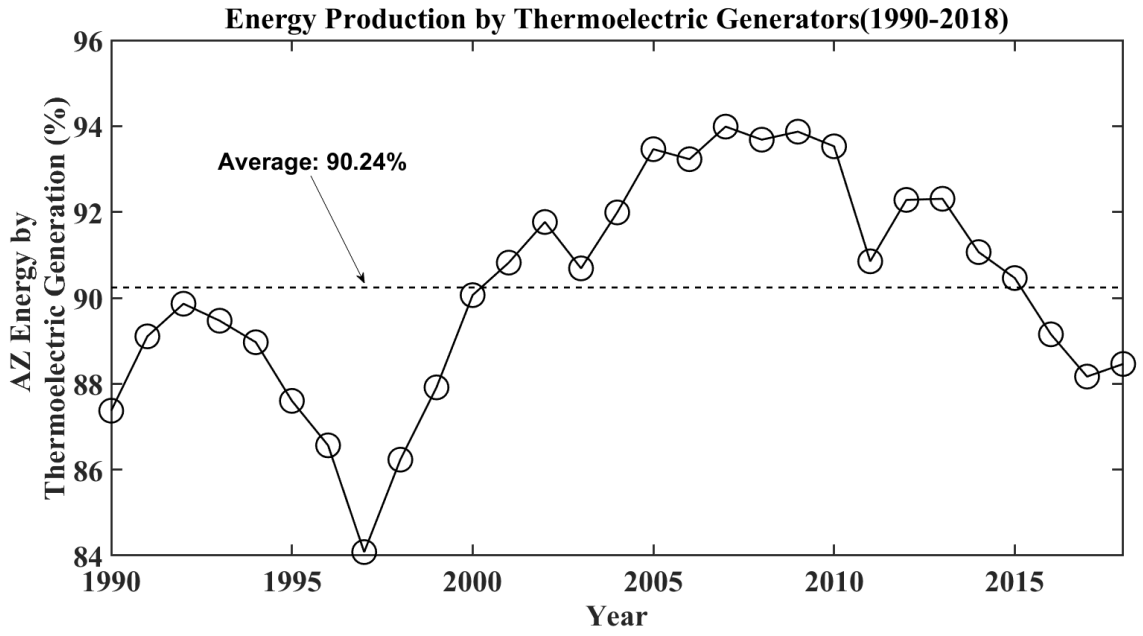

Figure 1.1 AZ Energy Production by Thermoelectric Generation 1990-2018 (data:[4])

seen that a little over 90 percent of all electric demand in this time-period is served by thermoelectric generation. Thus, this serves as an example of the importance of having adequate supplies of cooling water to maintain grid integrity.

Given that the two systems do in fact interact as described above, it is reasonable to assume that the need to study the interaction of the two systems and to develop models with which to perform these studies will be essential to maintaining satisfactory operation of both systems in the future. This is a consequence of the fact that increased demand or even unforeseen events will cause the two critical infrastructure systems to be more heavily burdened. Several examples have already arisen which exemplify the interdependence of the two systems. Recently, a long-term outage of a water treatment facility in Tampa, Florida [5] due to an electrical failure resulted in accompanying health concerns due to a

lack of pressure within the underground water system pipes which normally keeps pollutants from entering and contaminating the water supply.

Natural events can also disrupt normal operation of either system, such as when drought conditions in the southeast [6] resulted in the need to reduce certain nuclear generation by almost 50%. Massive flooding in Iowa resulted in substation outages which affected the ability of WDS pumping stations to prevent water from entering and contaminating a water treatment facility [7]. Other evidence of previous disruptions can be seen in places such as Howard County, MD, where electrical outages to two distribution feeders after Hurricane Sandy caused an overflow at the Little Patuxent sewage plant and the spillage of almost 20 million gallons of untreated effluent [8]. This prompted the building of onsite generation which can completely supply the treatment plant's electrical needs [9]. The South Monmouth Regional Sewerage Authority provides an example [10] of preemptive action taken to safeguard against a catastrophic failure like the one at Little Patuxent. Here, the sewerage authority built a mobile trailer to house the plant's primary controls and electric equipment and this allows the equipment to be moved to safety and temporarily replaced with a cheaper set of electronics during storms. Following Hurricanes Irene and Sandy, a savings of approximately $1.5 million in repair costs was achieved using this setup.

With events such as the ones just discussed as background, attention is turned towards the Southwest where thermoelectric generation is directly at risk because of the area's dry climate and the increased risk of extreme drought conditions [11]. These events and prediction of future risks confirm that modeling and studying the interactions between

these interdependent systems will be necessary to enable the operation of the two systems in a reliable way and to provide a means for them to be designed in a more resilient manner in the future.

1.2 Problem Statement

It is desired to study the interactions between the two systems in a way that is in contrast with the existing methods of studying the water-energy nexus. Most of these studies, which are detailed in Chapter 2, provide overall and aggregate trends or relationships between interdependent quantities because they look at the interactions between the systems with very high-level types of analysis. Some studies that have conducted lower level analysis have examined, for example, a particular type of generation's water consumption. This approach is still at too high of a level since the methodology is normally to use cumulative historical data or to examine vast spatial areas. Other low-level studies take no consideration of the WDS impact on thermal generation, long-term system operations, or contingencies. Some other studies only examine an aspect of the water-energy nexus, such as the pump loads within the EPS and many only have considerations towards normal system operating conditions. These approaches, therefore, do not help in determining how the two systems can be operated so that there is a smaller impact on overall system performance when contingencies arise in either system.

Consequently, a need exists for the formulation of appropriate mathematical models for the systems as well as models for the optimization of the systems' controls. The models presented in this work enable the relationships that exist between the two systems to be studied with a resolution of interaction at the individual component level. The use of

these models allows insight to be gained in how the two systems respond to stresses imposed by different contingencies of varying severity. The contingencies that are studied within both systems can be due to natural events which fall into the category of "high-impact, low frequency(probability) [12]", such as the flooding seen in the previous section, or due to "normal" failures such as pipes bursting (WDS) or a generator being tripped offline (EPS).

1.3 Research Objectives

The work that is presented in the following chapters implements models for control and system models for the optimal operation of the EPS with consideration of knowledge about operating conditions in the WDS. The work completed has aimed to accomplish the following goals:

1) To find the appropriate mathematical model for system analysis
2) To develop novel system control models and strategies
3) To develop the framework for the combined electric power and water network system simulations that encapsulates the implemented system models and control schemes
4) To simulate a variety of contingencies in both systems to observe system behavior
5) To propose new policies to help mitigate undesired system behavior under extreme operating conditions
6) To develop a comprehensive and rigorous methodology for quantifying EPS resilience

7) To incorporate data which characterizes changes in consumer usage of water and electricity under different circumstances into the resilience calculations

8) To develop a long-term planning model which allows considerations of the electric power systems' key dependence on the WDS, water for the cooling cycle, to be included so that water availability can be used as a constraint and the anticipated water usage and associated costs can be calculated and evaluated

1.4 Dissertation Organization

The chapters of this dissertation are organized in the following manner. Chapter 2 presents a literature review of the main topics covered in this dissertation and summarizes the existing, relevant research that has been completed in the area of interdependent infrastructure systems, the Water-Energy Nexus, and resilience. Chapter 3 gives background information on network modeling in the power system and network solution techniques. Background information is also given on the mathematical formulations for system optimization that are used. Chapter 4 presents the mathematical models for the optimization of power system operation in both the short and long-term time-scales that are examined in this work. Chapter 5 details the simulation methodology, presents the test systems, and examines the proposed policies for short-term use in power system operation under extreme conditions. Chapter 6 and Chapter 7 present case studies for the combined WDS-EPS short-term simulations and the long-term planning problem, respectively. Chapter 8 presents a novel approach to quantifying power system resilience through metrics that reflect the interdependent systems' operation and power system topology and

looks at several case studies using this methodology. Lastly, Chapter 9 presents a short conclusion and lists topics for future work.

CHAPTER 2

LITERATURE REVIEW

This chapter presents a survey of literature that is relevant to this work.

2.1 Interdependent Systems

Modern infrastructure systems have grown increasingly complex in order to meet the needs of our technologically advanced society. The authors from the President's Commission on Critical Infrastructure Protection [13] highlight critical infrastructure systems in the US and the important role that these systems play in almost every aspect of our daily lives. Some of the systems highlighted in the report that are depended on heavily include the electric power system, transportation infrastructure, the oil and gas systems, water systems, and various communication systems. Although each system has complexity on its own, dependence of some systems on others and even interdependence between the systems exists. Another list of critical infrastructures along with events which have impacted these systems is given in the context of "Managing the cascading impacts from a long-term power outage" in [14].

A high level overview of the field of critical interdependent infrastructure systems is given by the authors in [15], where definitions of key terms such as "infrastructure", "infrastructure dependency", and "infrastructure interdependency" are provided. The term interdependency in the context of infrastructure systems is defined as "a bidirectional relationship between two infrastructures through which the state of each infrastructure influences or is correlated to the state of the other." This work also discusses types of

interdependencies that can exist, behavior of systems at the points of coupling, operation states, and issues in modeling and simulation. The authors in [16] have provided definitions and different types of dependencies that can exist between interdependent infrastructure systems as well as a general procedure for data collection and analysis of such systems. The authors in [17] discuss abstracting the concept of interdependent networks/systems by representing the networks as a "network of networks" and study this network's properties.

A thorough review of the existing literature on interdependent infrastructure systems at the time is presented in [18] and gives a comparison of the various different simulation and modeling approaches that have been used. In [19], interdependent infrastructure systems are examined using a graph theoretical approach in order to study the systems' susceptibility to cascading failure as a result of seismic activity. Here, modeling of the interdependence between the test electric power and water systems is accomplished with a conditional probability that quantifies the probability of the failure of an element (pump) in the water system given the failure of an element (substation) in the power system. Another effort made in order to study system failure with a graph theoretical approach is seen in [20].

2.2 Water-Energy Nexus Overview

The operational interdependencies that exist between the electric power system and water distribution systems have been identified and studied in broad generalities for some time. The primary interdependency of the electric power system on the water delivery and treatment system is the thermoelectric generator's usage of cooling water. Gerdes and Nichols [6] detail water usage for different types of power generation, such as subcritical

and supercritical pulverized coal plants, integrated gasification combined cycle (IGCC), natural gas combined cycle (NGCC) and nuclear plants and provide water consumption factors for each of the specific plant types. A comparison of water consumption for hydroelectric and thermoelectric generation is done in [21], with the conclusion that the average total water consumption from both types is about equal at the national level. Thermoelectric power plants with wet cooling cycles can be divided into two groups, with one group having open cycle cooling and the other group having a closed-loop cycle.

Water usage for power plants is defined in terms of water withdrawal and water consumption with the consumption of water being the difference between the amount of water withdrawn from a water source and the amount that is returned. Plants with an open cooling cycle, also known as once-through cooling, are seen to have high withdrawal rates from their source of water but relatively low consumption rates. Conversely, the water withdrawn by a plant with a closed-loop cooling cycle is seen to be much less, but the comparative consumption is high. It is also noted that even though water is used as the working fluid for the steam generation cycle, the cycle process used for this working fluid has much less water consumption than the cooling cycle.

The water losses associated with a wet, closed-loop cooling cycle are from evaporation, drift and blowdown. Evaporation is the process of water changing phases from liquid to vapor, drift is the loss of water droplets out of the cooling tower due to the airflow, and blowdown is the necessary removal of water to meet certain quality requirements as the cooling water is recirculated from the condenser to the heat exchange mechanism and back. These three components, which represent the majority of the water use by

thermoelectric generation, is illustrated on the right-hand side of the Figure 2.1 below. The withdrawal and consumption rates of modern power plants are dependent on many factors such as whether the plant has an open or closed cooling cycle, the types of equipped emission control schemes and the power plant's location. Recent efforts to reduce water consumption at power plants in Arizona resulted in using hybrid, wet-dry closed-loop cooling cycles [22].

Torcellini, Long, and Judkoff [23] conducted one of the early studies with the motivation of comparing the efficiency of cooling cycle methods of thermoelectric generation with that of evaporative cooling systems for buildings. Their findings, consistent with later ones, shows that the evaporative use of water by thermoelectric power

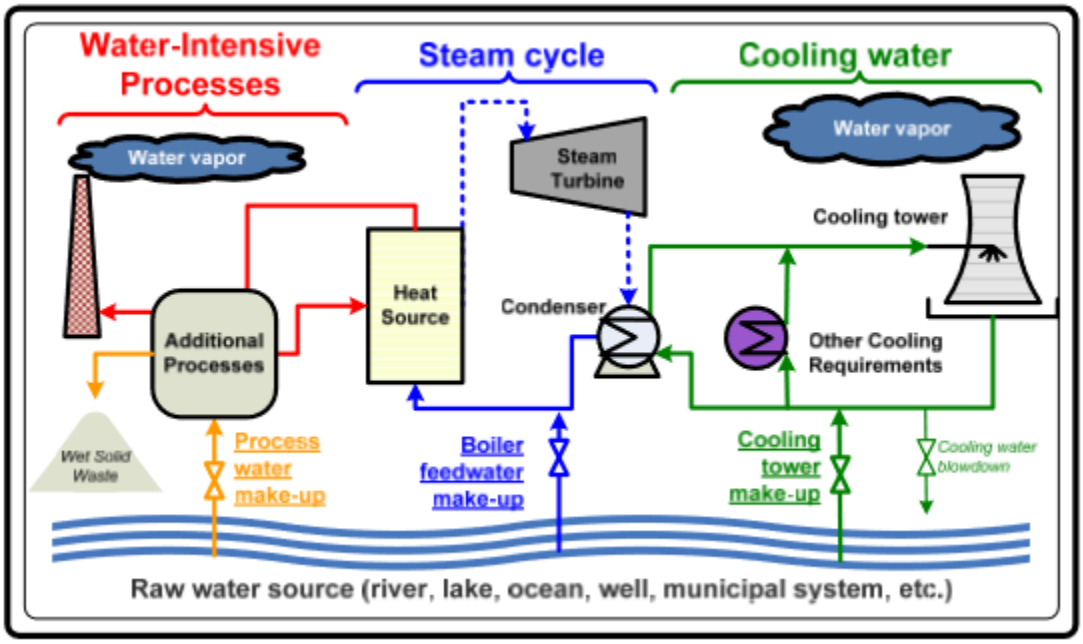

Figure 2.1 Water Usage in Thermoelectric Power Plants [6]

plants is a small fraction of the water withdrawn from all of the sources. Feeley, Green, Murphy, Hoffmann, and Carney [24] have another foundational report on the water-energy nexus which provides background information on thermoelectric generation's use of water and emerging cooling cycle technologies to help improve thermal cycle efficiency. In that work it is also noted that the main causes for the consumption of water can be attributed to evaporation, drift losses and required blowdown. The first two factors just listed are associated with the type and design of the cooling tower while the last factor is a design parameter dependent on water-quality. In [25] Feeley, Green, Murphy, Hoffmann, Duda, Kleinmann, and Ackman detail power generation's dependence on water and how low water availability is a limiting factor in supplying electric power. They also detail new water reuse and recovery methods and explore advanced cooling technology such as dry cooling, hybrid cooling using wet and dry cooling cycles, and advanced heat exchangers.

Maulbetsch and Barker [26] provide additional information on how more efficient or new technologies can be integrated into existing plants in order to more efficiently use the water that is needed. Roy and Chen [27] present a high level assessment of recent fresh water withdrawal trends at the county level across the country and through the use of a simple index, show that Southwest and High Plains states are at risk in the future due to using more water from groundwater sources than is replenished. Macknick, Newmark, Heath and Hallett [28] provide extensive data on water usage by power plants with great resolution based on the specific plant's fuel type and emission control schemes and gives factors for the withdrawal and consumption of water within those plants. Badr, Boardman and Bigger [29] provide a survey of water use in thermoelectric plants that includes a

breakdown on how water is used, some background and comparisons of cooling cycle technologies, a summary of previous studies done on the impact of drought conditions, and projections of the impact on future growth and demand.

The area of cooling tower performance [30]–[32] has also been explored in significant detail with structure shapes, flow rates, and types of heat exchangers all important in the final design characteristics and affecting everything from anticipated evaporation rates to the number of cycles of concentration that can be achieved. Wolfe [33] provides background on how new technology can be used to increase the efficiency of water use by power plants. Another broad overview of cooling systems, cooling technology and a summary of typical/generic design parameters for various cooling systems and technologies is given in [34].

The United States Geological Survey (USGS) and the United States Department of the Interior also track statistics on the uses of water by the power generation sector and the uses of water in the U.S more broadly. In [3], the withdrawals of water are broken down into many categories, such as by industry, and within each sector the state-by-state withdrawals of water are detailed. For thermoelectric power generation, the total water withdrawals are broken down by open (once-through) and closed (re-circulating) cycle cooling. Reference [35] details the water-energy nexus and discusses the interdependencies and details the need for continued earth science data collection and research in order to manage these resources. The USGS has also published a report [36] detailing methods for estimating the consumption of water by thermoelectric plants through the use of heat budgets and condenser duty, which is defined as the heat removed from the

steam in the working fluid cycle and transferred to water in the cooling cycle. A report by the International Energy Agency [37] details the use of water on a global scale, and presents the view that in the future, energy efficiency, increasing renewable penetration, and more advanced and efficient cooling cycle technologies will allow for the water requirements of the conventional thermoelectric power generation sector to be met.

Macknick, Sattler, Averyt, Clemmer and Rogers [38] provide an overall, system level view of the water use due to electric power generation through the consideration of four scenarios regarding anticipated policies on the emissions requirements of plants. Poch, Conzelmann, and Veselka [39] provide the results for case studies regarding capacity expansion planning with drought conditions where droughts are seen to significantly alter the future generation portfolio. Nearly all of the new generation added under the drought condition scenario is fueled by natural gas. The work in [40] includes approximations on how much total generation (hydro and thermoelectric) would be lost under various drought scenarios. The method used for calculating the amount of lost generation was a simple approximation base on the ratio of water flows during the drought to either average historical flows or the demand in a baseline drought year.

Several reports exist in the literature that look at the water-energy nexus in Texas. The authors in [41] detail the dependencies of each system on the other, describe the emerging technological trends which can improve power plant efficiencies and lower consumption, and, finally, estimate the demand of water due to future thermoelectric power production. A technical report [42] published just after the extreme drought conditions that Texas experienced in 2011 provides an in-depth look at plant cooling technologies, use of

water overall and within the power sector, and a case study highlighting the negative consequences of implementing a "one-type only" cooling technology mandate. The report also provides an interesting comparison on the amount of water used to generate a household's electricity versus the much larger amount of average household water consumption. The authors in [43] study the impact of the 2011 drought and the benefits to system resilience during droughts brought about by the increase in combustion turbine and combined cycle plants due to their lower water consumption rates.

Many papers and reports in the area of the water-energy nexus are focused on policy level analysis and feature proposals for resource management and regulation. The authors in [44] give a high-level overview of the water-energy nexus which provides an understanding of how the importance of this infrastructure interdependency has grown and give background on the water-energy nexus. The various dimensions related to the interdependencies as well as a review of the scope, focus and method of various studies in this area is presented in that work as well. The authors in [45] highlight the so-called "energy-water-food (EFW) nexus" and presents the interactions between the systems and highlights the needs of models, analytical methods and larger data sets on these interdependent systems moving forward. Another review highlighting the different types of studies that have been conducted between various combinations of infrastructures in the water, energy, and food nexus is presented in [46].

The water-energy nexus outside the US has also been examined, with [47] and [48] offering analysis on the water usage for the power production sector in Europe and in China, respectively. Finally, a discussion of the water-energy nexus in China is presented

in [49] and also contains a discussion on the price elasticity of water, which is the change in demand due to a change in price.

2.3 System Modeling, CEED, UC, Expansion Planning

The unit commitment (UC) problem is a non-convex, non-linear problem in its basic form due to the highly non-linear equations governing the power network and non-convexity arising from the binary commitment variables that denote the on/off status of a generating unit. Methods for solving the unit commitment problem have varied historically from the Lagrange relaxation formulation presented by Li, Svoboda, Tseng, and Johnson [50] to the dynamic programming approach by Snyder, Powell, and Rayburn [51]. The formulation of the unit commitment problem through a mixed integer linear program (MILP) [52] is now widely used with Pandzic, Qiu, and Kirschen [53] presenting some of the state of the art formulations. The formulations differ in the number of unit commitment variables used (1, 2 or 3), which in turn are dependent on the type of system modeling being implemented.

Stott, Jardim and Alsac [54] show how an optimal power flow (OPF) can be used for determining the dispatch of generation. Also detailed in that work are the linear approximations to the network equations normally used within the UC and OPF problems that, along with careful formulation of any constraints, avoids any non-linearities. OPF solution techniques, developments and a survey of the OPF literature can be found in [55]–[57]. Stott and Marinho [58] explain the preference for a linear program formulation in that the existence of robust and fast solution algorithms makes this problem formulation appropriate for large scale, power system applications.

Talaq, El-Hawary and El-Hawary [59] summarize modified versions of the OPF which consider environmental aspects such as emissions and which is sometimes called the combined economic and environmental dispatch (CEED). Yokoyama, Bae, Morita and Sasaki [60] also include environmental concerns in their examination of multi-objective generation dispatch formulations. While the previous work includes environmental concerns in the form of emissions, it has not been until recently that constraints relating to generator's use of water have begun to garner interest. The authors in [61] examine the effects on thermoelectric generation dispatch for units that have once-through cooling and that are physically located on the same waterway. This is accomplished with the inclusion of water constraints that limit the water temperature difference between inlet and outlet, maximum inlet water flow rate, and equations for calculating the inlet temperatures of units downstream. Tidwell, Bailey, Zimlick and Moreland [62] integrate water supply constraints into the transmission expansion planning problem by including the amount of available water in the watershed of the physical locations of generation units and these restrictions related to water are now being considered within planning studies by using the Western Electricity Coordinating Council's (WECC) Long-Term Planning Tool (LTPT).

Following power system deregulation, the problems of transmission expansion planning (TEP) and generation expansion planning (GEP) now fall to different entities and thus are handled separately. The solution of the TEP problem is the determination of the necessary additional transmission lines that are needed to continue sufficient power delivery to loads while still meeting operating/security criteria. The solution of the GEP problem determines the proper mix of additional generation units to satisfy policy

requirements, load growth, and unit retirement. Because these are large-scale, difficult problems to solve, GEP [63]and TEP [64] are often examined separately in the literature. Ryan and Jin [65] present a formulation for the combined problem in the context of centralized planning for TEP and decentralized GEP. Another formulation of the problem by Kamalinia, Shahidehpour, and Khodaei [66] gives a security constrained GEP by which the build status of fast-start units with the presence of large scale wind integration can be determined.

2.4 Resilience

Increasing attention has been given to resilience calculations for various systems. The US National Infrastructure Advisory Council defines resilience [67] broadly with four distinct characteristics in the context of critical infrastructure systems. The first is robustness, which encompasses the ability of a system to remain operable after contingencies occur. The next two characteristics are resourcefulness and rapid recovery, which are the ability to manage disasters and limit the impact and the capacity within the system to get back to pre-disaster operating conditions, respectively. The last characteristic of a resilient infrastructure system is adaptability within the system and its operating procedures and policies in order to improve the robustness, resourcefulness, and recovery characteristics for future events. The Cabinet Office in the United Kingdom issued a report [68] detailing the importance of increasing resilience in critical infrastructure systems, with specific focus on natural hazards which were identified as one of the top risks in Britain's National Security Strategy. Hosseini, Barker, and Ramirez-Marquez [69] provide a recent review of the existing literatures use of the concept of resilience and methods of

quantification in many domains such as economics, social communities, and engineering. The President's Council of Economic Advisers along with the US Department of Energy's Office of Electricity Delivery and Energy Reliability and the White House Office of Science and Technology highlight the potential benefits resulting from the enhancement of system performance in the face of extreme events [70].

A conceptual framework for power system resilience is presented in [71] and the authors extend the idea of that framework and offer metrics for resilience quantification in [72] for the power systems area. The authors also show how the presented measures of resilience can be quantified using the results for case studies involving weather events that entailed transmission line operation in the face of high winds. Other works on the resilience of the power system while experiencing extreme weather conditions can also be found, with transmission line tower fragility modeling, resilience assessment and system resilience enhancement discussed in [73]. Metrics for quantifying the resilience of the power system with generation facing high temperatures while using once-through cooling is presented in [74]. Nan and Sansavini [75] have provided similar metrics and a general framework by which the overall system resilience of interdependent infrastructures can be calculated from specified measures of performance. These measures of performance are, in general, not system specific and allow for the convenient use of general metrics by which to quantify the main aspects that determine how resilient a given system is.

The aspects that have been proposed for quantifying resilience in [72], [75] are found by examining the behavior of certain measures of performance as functions of time before, during and after system disturbances. The process of quantifying a disturbance

includes measuring how low the measure of performance drops, how fast it both drops and recovers, and to what value the measure settles. These metrics are seen to correspond directly with the concepts of robustness, response, recovery, and adaptability [67], which are the terms for defining system resilience as outlined above.

2.5 Recent EPS Work on the Water-Energy Nexus

An optimal control methodology for the coordinated operation of the WDS and EPS is presented in [76]. This control methodology minimized operational costs for both systems but in contrast to the models presented in this work, it did not consider or include WDS real-time operation or emergency conditions. The optimization model in that work linearizes the WDS equations and the pump-scheduling problem is not considered. A unit commitment model is introduced, meaning a system representation at the transmission level, but there is no modelling of the effect on the EPS (other than varying pump loads) as a result of changing conditions in the WDS.

Co-optimization schemes for the two systems are presented in [77]–[79], where the emphasis on interdependency is again primarily one-way through the WDS pump loads in the EPS. In [77], the power system is represented via a distribution system only and the only coupling between the two systems is through the power consumed by the pumps. There are also other significant differences in the modeling and solution procedures, such as the lack of inter-temporal constraints in the power system and an algorithm that seeks to have both systems come to a consensus on the amount of power consumed by pumps. The other two algorithms presented in this paper are for the co-optimization of the operation of the two systems. The issue of pump scheduling is also not addressed, and the simulations

considered are short-term. Given the availability of storage at thermoelectric power plants and in the water towers in the WDS, it is essential to consider long-term simulations in order to examine the impact of disruptions. The authors in [78] and [79] represent the power system only at the distribution level and again the interdependency of the two systems is solely due to power consumed by WDS pumps. These papers also aim to co-optimize the operation of the two networks. Much of the effort in [76]–[79] is spent in eliminating the issues that arise from the non-convexity and non-linearity of the network equations for use in their optimization procedure(s). Again, pump scheduling is not considered in any of these short-term simulations.

In summary, [77]–[79] model the EPS at the distribution system level only and those references along with [76] have no consideration towards the consequences of WDS operations on thermoelectric generation. In addition, these works do not consider anything other than normal system conditions in the simulations conducted, which is in contrast to one of the main motivations behind this work, which aims to consider the impact of large disruptions in both the WDS and EPS.

2.6 Summary

This chapter has detailed the relevant literature associated with the subject matter that is being studied.

CHAPTER 3

BACKGROUND INFORMATION FOR SYSTEM MODELING AND OPTIMIZATION

Mathematical models that are used for the EPS simulation are presented in this chapter as well as background information on the optimization models that will be detailed in Chapter 4. A brief look at the modeling of the water distribution system that was used in the completion of the case studies in Chapter 6 is also presented. The power system is, in general, described mathematically by a system of non-linear differential-algebraic equations (DAE) of the form [80]–[82]:

$$\dot{x} = f(x,y,u) \tag{3.1}$$

$$g(x,y) = 0 \tag{3.2}$$

where x is a vector of state variables (flux linkages or currents), y is a vector of algebraic network variables, and u is a matrix of control variables. Because of the time-scales involved for certain quantities of interest in the water-energy nexus, a specific version of (3.2) is of interest.

3.1 Modeling of the Power System for Network Solution [83], [84], [85]

The steady-state analysis of the power system involves finding a solution to the power flow problem. The analysis techniques for finding a solution to this problem differs from other types of linear analysis, such as phasor analysis, which are conducted in AC networks. The reason for this is that sources in linear analysis methods are treated as

voltage or current sources while the sources (loads) within the power system are treated, in the simplest case, as sources (sinks) of active and reactive power.

The solution of a power system network is achieved when four quantities at every bus (node) within the system can be specified. These quantities include the net active and reactive power injections into the network from the bus, where the calculation of the net injections at a bus is the algebraic sum of all generation and load at that bus (where generation is by convention positive). The two other quantities are the magnitude of the bus voltage and the phase angle of the bus voltage relative to some reference angle. From these quantities, other values of interest such as flows through transmission lines or transformers and power losses in transmission lines can be calculated if knowledge of the system topology and component parameters is known.

3.1.1.Power flow data setup

The first step in solving the power flow is gathering all the needed data regarding the system in order to proceed towards a solution. The data that is needed includes bus data detailing any generation and load information, transmission line data giving the series resistance, reactance, and shunt susceptance, and data pertaining to transformers in the system.

At the transmission system level, the common assumption of balanced system operating conditions is used. This means that generators generate perfect sinusoidal voltages of equal magnitude with 120 degrees of phase shift between each of the three phases. With this assumption, all loads (or equivalent impedances) can be converted to the

"wye" equivalent and it is seen that balanced impedances draw balanced currents from balanced voltage sources and the resulting neutral current is zero. A single-phase equivalent representation of the three-phase system is thus sufficient and all desired quantities (other phases or three-phase totals) can be calculated after solving for the solution of the chosen phase within the network.

For systems with unbalanced conditions, a convenient analytical technique for network analysis has been developed through the use of symmetrical components [86]. Symmetrical components allow for a transformation by which a system of *n* unbalanced phasors can be transformed into *n* sets of balanced phasors. In the case of fault analysis, the complicated solution of unbalanced phases in the network is conveniently simplified into a network solution where the three sequence networks are coupled at the point of imbalance (the fault). For use in this work, knowledge of how to get from the phase representation of series impedances to the sequence representation is sufficient. The relationship between the phase voltages (*a*,*b*,*c*) and the zero, positive, and negative sequence voltages (0,1,2) is:

$$\underline{V_{ph}} = \mathrm{A}\underline{V_s} \tag{3.3}$$

where $\underline{V_{ph}}$ and V_s are 3x1 vectors of the phase voltages and sequence voltages, respectively, and

$$\mathrm{A} = \begin{bmatrix} 1 & 1 & 1 \\ 1 & a^2 & a \\ 1 & a & a^2 \end{bmatrix} \tag{3.4}$$

where a is the operator $1\angle 120°$. A similar relationship between phase currents exists. The relationship between the phase voltages and the currents is found through

$$\begin{bmatrix} V_a \\ V_b \\ V_c \end{bmatrix} = \begin{bmatrix} Z_{aa} & Z_{ab} & Z_{ac} \\ Z_{ba} & Z_{bb} & Z_{bc} \\ Z_{ca} & Z_{cb} & Z_{cc} \end{bmatrix} \begin{bmatrix} I_a \\ I_b \\ I_c \end{bmatrix} \tag{3.5}$$

which can be written more compactly as

$$\underline{V_{ph}} = \underline{Z_{ph} I_{ph}} \tag{3.6}$$

Substitution of the right-hand side of (3.3) and the analogous current relationship into (3.6) gives:

$$\mathrm{A}\underline{V_s} = \underline{Z_{ph}}\mathrm{A}\underline{I_s} \tag{3.7}$$

which after solving for $\underline{V_s}$ and simplifying yields:

$$\underline{V_s} = \underline{Z_s I_s} \tag{3.8}$$

From (3.8), it is clearly seen that

$$\underline{Z_s} = \mathrm{A}^{-1}\underline{Z_{ph}}\mathrm{A} \tag{3.9}$$

This relationship therefore provides a method for converting phase impedances (balanced or not) into an equivalent sequence representation which can be used with other positive sequence data for a power flow solution.

3.1.2.Power Flow Bus Types

The equations necessary for the power flow solution depend on what elements are present at a given bus. If a bus has a generator connected to it, the bus type is "PV" since active power output (P) and the regulated terminal voltage magnitude (V) are specified in the input data and the voltage angle and reactive power outputs need to be determined. If a bus does not have any generation then it denoted as a "PQ" bus since active (P) and reactive power (Q) are specified (having values of zero if no load is present) and the voltage angle and magnitude need to be determined. The last type of bus is the reference, or swing bus. As a result of the equations that arise in the power flow solution, only the angle differences between the buses need to be considered and therefore one bus, the swing bus, can have both its voltage magnitude (V) and voltage angle (δ) specified. The active power at this reference bus is then equal to the sum of what is required to balance any remaining difference between generation and load plus any losses within the system. A summary of these bus types, the known quantities, and the quantities found by the solution process is in Table 3.1.

Table 3.1 Bus Type Summary

Bus Type	Known	Found
Swing	V, δ	P, Q
PV	P, V	δ, Q
PQ	P, Q	V, δ

3.1.3.Power Flow Equations

With the assumption of a balanced, three-phase system, net bus injections can be specified with the familiar relationship between voltage, current injection and complex power:

$$S_k = V_k I_k^* \tag{3.10}$$

where * denotes the complex conjugate operator. Additionally, the current injections can be specified in terms of the bus voltages and the network bus-admittance matrix, Y_{bus}:

$$I = Y_{bus} V \tag{3.11}$$

Extracting the *k*-th element from the vector I and substituting into (3.10) yields

$$S_k = V_k (\sum_n Y_{kn} V_n)^* \tag{3.12}$$

Writing the voltages V_k and V_n in complex polar form and writing Y_{kn} in complex, rectangular form using its conductance and susceptance components yields:

$$S_k = |V_k| \angle \theta_k (\sum_n (G_{kn} + jB_{kn})(|V_n| \angle \theta_n))^*$$

$$= \sum_n (G_{kn} - jB_{kn})(|V_k||V_n| \angle (\theta_k - \theta_n)) \tag{3.13}$$

Converting the expression for complex power from polar to rectangular form gives:

$$S_k = \sum_n (G_{kn} - jB_{kn})(|V_k||V_n| (cos(\theta_k - \theta_n) - jsin(\theta_k - \theta_n)) \tag{3.14}$$

which can be simplified and separated into real and imaginary parts:

$$S_k = P_k + jQ_k = \sum_n (|V_k||V_n|)(G_{kn}cos(\theta_k-\theta_n) + B_{kn}sin(\theta_k-\theta_n))$$

$$+j\sum_n (|V_k||V_n|)(G_{kn}sin(\theta_k-\theta_n) - B_{kn}cos(\theta_k-\theta_n)) \quad (3.15)$$

$$P_k = \sum_n (|V_k||V_n|)(G_{kn}cos(\theta_k-\theta_n) + B_{kn}sin(\theta_k-\theta_n)) \quad (3.16)$$

$$Q_k = \sum_n (|V_k||V_n|)(G_{kn}sin(\theta_k-\theta_n) - B_{kn}cos(\theta_k-\theta_n)) \quad (3.17)$$

Letting N denote the total number of buses and the number of generators be denoted as G, a quick examination of the number of knowns and unknowns in these equations reveals the following. First, after neglecting k=1 in (3.16) for the slack bus, P_k is known at N-1 buses since P is specified at all PV and PQ buses. Q_k is specified at all PQ buses and thus N-G variables in (3.17) are known. There is no knowledge of any bus voltage angle values at any of the buses besides the swing bus, giving N-1 unknowns. Further, the voltage magnitude is not known at any of the N-G PQ buses. The difference between known values and unknown variables is found as:

$$\text{Total Unknowns} = (N\text{-}1+N\text{-}G)-(N\text{-}1+N\text{-}G) = 0 \quad (3.18)$$

Given that the number of known values on the left hand sides of all equations represented by (3.16) and (3.17) is equal to the number of unknown voltage angles and magnitudes in the equations, a solution to the power flow problem can be found.

3.1.4.Newton-Raphson Solution

The Newton-Raphson solution technique is an iterative algorithm that uses a Taylor series expansion in order to find the zeros for, in this case, a multi-variable function. With the ability to calculate the real and reactive components of net bus complex power injections, the set of non-linear equations for the *N*-1 buses can be written in terms of a vector of state variables, defined here as:

$$x = \begin{bmatrix} \theta_2 \\ \vdots \\ \theta_N \\ |V_2| \\ \vdots \\ |V_N| \end{bmatrix} \tag{3.19}$$

Since (3.16) and (3.17) are defined in terms of *x* and it is desired to have the specified input values of P_k and Q_k be equal to the calculated values of real and reactive power, $P_k(x)$ and $Q_k(x)$, a state vector function can be formulated as:

$$f(x) = \begin{bmatrix} P_2\text{-}P_2(x) \\ \vdots \\ P_N\text{-}P_N(x) \\ Q_2\text{-}Q_2(x) \\ \vdots \\ Q_N\text{-}Q_N(x) \end{bmatrix} \tag{3.20}$$

The previous statement leads to the conclusion that (3.20) should be equal to zero:

$$f(x) = \begin{bmatrix} P_2\text{-}P_2(x) \\ \vdots \\ P_N\text{-}P_N(x) \\ Q_2\text{-}Q_2(x) \\ \vdots \\ Q_N\text{-}Q_N(x) \end{bmatrix} = \begin{bmatrix} \Delta P_2 \\ \vdots \\ \Delta P_N \\ \Delta Q_2 \\ \vdots \\ \Delta Q_N \end{bmatrix} = \underline{0} \tag{3.21}$$

For a single variable equation $h(x) = 0$, the Taylor series expansion is

$$h(x+\Delta x) = h(x) + h'(x)\,\Delta x + H.O.T = 0 \tag{3.22}$$

where H.O.T are the higher order terms. Neglecting the H.O.T and solving for Δx gives

$$\Delta x = -\,h'(x)^{-1}\,h(x) \tag{3.23}$$

Assuming the present value of x does not satisfy the equation $h(x) = 0$, a new value of h can be calculated after updating x by

$$x^{new} = x + \Delta x = x - h'(x)^{-1}\,h(x) \tag{3.24}$$

The procedure for calculating a new x value via (3.24) can be repeated until the equation for h is equal to zero, assuming convergence to a valid solution is reached.

Expanding on this procedure and realizing that the multi-variable equivalent for $h'(x)^{-1}$ is the Jacobian matrix, the algorithm for the Newton-Raphson method is:

1. Calculate P_k and Q_k using equations (3.16) and (3.17)

2. Calculate $f(x)$ from (3.20)

3. Calculate the Jacobian matrix, J

4. Solve the matrix equation $J\Delta x = f(x)$ for Δx

5. Calculate $x^{new} = x + \Delta x$

The calculation of the Jacobian matrix is computationally expensive. The matrix can be divided into four sections of partial derivatives, with terms below:

$$\frac{\partial P}{\partial |V|}, \frac{\partial P}{\partial \theta}, \frac{\partial Q}{\partial |V|}, \frac{\partial Q}{\partial \theta} \tag{3.25}$$

The expressions for these equations are well-known and can be found in, for example, [83], [84]. The stopping criteria for the algorithm is based on the mismatch vector $f(x)$. The power flow solution algorithm can be made more complex with the inclusion of generator reactive power limits as bus-type switching must implemented in order to turn generators which are on their reactive power limits from PV to PQ buses. More complicated models and system requirements add complexities in the power flow algorithm as well as voltage controls through switched devices, more complicated load models, and AGC representation are included [87].

3.2 Modeling of the Power System for Control Optimization

This section covers the basic formulations of the power system controls that are implemented in this work. The optimal power flow aims to dispatch generation to achieve the lowest total system operating cost subject to certain network constraints. The determination of which generators should be committed (turned on), and when, in order to

meet the forecasted demand at the lowest system cost is found through the solution of the unit commitment problem. Both models use a simplified network model based on the assumptions detailed in the next sub-section.

3.2.1.DC Power Flow Model

The DC power flow model is a linear approximation that is based on the observation of several characteristics in the physical power systems as well as on engineering insights into power flow solutions. First, the following assumptions are made:

1. Neglect the dependence of active power on voltage magnitude, which means that the corresponding Jacobian entry can be expressed as:

$$\frac{\partial P}{\partial |V|} = 0 \tag{3.26}$$

2. Neglect the dependence of reactive power on voltage phase angle, which means that the corresponding Jacobian entry can be expressed as:

$$\frac{\partial Q}{\partial \theta} = 0 \tag{3.27}$$

3. Assume that θ_k-θ_n is small, which allows for the use of the small angle approximations:

$$cos(\theta_k - \theta_n) \cong 1 \tag{3.28}$$

$$sin(\theta_k - \theta_n) \cong 0 \tag{3.29}$$

4. Assume that the series primitive resistance, *r*, is much smaller that the series reactance, *x*.

With these assumptions, the power flow equations can be written as:

$$\begin{bmatrix} \frac{P_2-P_2(x)}{|V_2|} \\ \vdots \\ \frac{P_N-P_N(x)}{|V_N|} \end{bmatrix} = B' \begin{bmatrix} \Delta\theta_2 \\ \vdots \\ \Delta\theta_N \end{bmatrix} \tag{3.30}$$

$$\begin{bmatrix} \frac{Q_2-Q_2(x)}{|V_2|} \\ \vdots \\ \frac{Q_N-Q_N(x)}{|V_N|} \end{bmatrix} = B'' \begin{bmatrix} \Delta|V|_2 \\ \vdots \\ \Delta|V|_N \end{bmatrix} \tag{3.31}$$

The previous assumptions lead to the so-called decoupled power flow of (3.30) and (3.31). Because the stopping criteria is the same as the full Newton-Raphson solution, namely driving the mismatch vector in (3.20) to zero, the decoupled power flow in theory will arrive at the same solution. The DC power flow is formulated by neglecting reactive power completely in (3.31) and by assuming constant bus voltage magnitudes (normally 1.0 pu):

$$\begin{bmatrix} P_2-P_2(x) \\ \vdots \\ P_N-P_N(x) \end{bmatrix} = B' \begin{bmatrix} \Delta\theta_2 \\ \vdots \\ \Delta\theta_N \end{bmatrix} \tag{3.32}$$

where the elements of *B'* are calculated from the primitive series reactance values:

$$B_{ii} = \sum \frac{1}{x_{ik}} \tag{3.33}$$

$$B_{ik} = -\frac{1}{x_{ik}} \tag{3.34}$$

3.2.2.Optimal Power Flow

The optimal power flow (OPF) is an extension of the basic economic dispatch calculation (EDC). This calculation minimizes system operating costs (generator fuel costs) while ensuring the total generation meets demand. The most basic formulation of the EDC problem involves no consideration of the transmission network and thus its solution represents a lower bound on the OPF solution. The OPF extends the EDC by taking generation and transmission constraints into account. The general formulation of such an optimization problem that minimizes costs while considering generation and transmission constraints for a single time-period is:

$$\text{Minimize} \qquad \sum_g F(P_g) \tag{3.35}$$

where $F(P_g)$ is the function relating generation output to cost and can be, in general, quadratic or piece-wise linear. The basic EDC constraint is still used:

$$\sum P_{load} + \sum P_{loss} = \sum_g P_g \tag{3.36}$$

The constraints on maximum and minimum outputs of generators are:

$$P_{g,min} \leq P_g \leq P_{g,max} \tag{3.37}$$

And finally, the limit on flows through transmission elements is:

$$P_{l,min} \leq P_{lt} \leq P_{l,max} \tag{3.38}$$

3.2.3.Unit Commitment

The unit commitment problem is normally a multi-time-period method of determining which units should be on, for what time-periods, and at what output levels. The problem solution in its basic form therefore involves determining the values of the two decision variable that are unit on/off status, $u_{g,t}$ and real power outputs $P_{g,t}$. A simple, mixed-integer linear program can then be stated as:

$$\text{Minimize} \qquad \sum_t \sum_g \left(F\left(P_{g,t}\right) + CSU_g\right) u_{g,t} \tag{3.39}$$

subject to unit minimum and maximum values

$$u_{g,t} P_{g,min} \leq P_{g,t} \leq P_{g,max} u_{g,t} \tag{3.40}$$

and load-generation balance constraint at each time-period

$$\sum P_{load} + \sum P_{loss} = \sum_g P_{g,t} u_{g,t} \tag{3.41}$$

The difference between (3.40) and (3.37) and between (3.41) and (3.36) is the addition of the on/off variable $u_{g,t}$. Additional constraints can be added to make the model more realistic and complex.

3.3 Modeling of Water Distribution System [88]

The water system network solution is obtained by solving a set of non-linear equations for nodes and loops within the WDS. Equation (3.42) represents the conservation of mass at each node in the WDS and ensures continuity:

$$\sum_j Q_{ij} - D_i = 0 \tag{3.42}$$

The second equation is a conservation of energy around loops in the system and is specified by the flow-head loss relationship:

$$H_{i,t} - H_{j,t} = f(Q_{i,j})_t \tag{3.43}$$

The gradient descent method in the solution procedure used in [88] updates nodal heads using the Jacobian matrix A by solving the matrix equation:

$$AH = F \tag{3.44}$$

where the elements of the flow vector F are updated with:

$$F_i = \sum_j Q_{ij} - D_i + \sum_j y_{ij} + \sum_f p_{if} H_f \tag{3.45}$$

and y_{ij} and p_{ij} are correction factors. Equations (3.42)- (3.45) are made more complex when the actual expressions for nodal head, H, and flows, Q, as well as the elements for A are used.

3.4 Summary

This chapter covered some background information on the solution techniques for the system models as well as basic formulations to be built upon in the development of the EPS optimization models.

CHAPTER 4

OPTIMIZATION AND CONTROL OF POWER AND WATER SYSTEMS – MATHEMATICAL FORMULATIONS FOR SHORT AND LONG-TERM SIMULATIONS

This chapter presents the optimization models and the control/operational strategies used in this work. The model used for the short-term, operational length simulations includes unit commitment and unit dispatch formulations. The long-term, planning simulations consist of a more complicated unit commitment model and a security constrained economic dispatch. Several policies related to the short-term operation of the power system under severe conditions such as those exemplified in Chapter 1 are also discussed.

4.1 Short-Term Optimization Models for Operational Length Simulations

4.1.1. CEED Formulation

In this section, the optimization model for the dispatch of generation using information from the water distribution system is presented. This optimization model determines the real power set-points for the units which have been committed from the solution of the short-term unit commitment problem. The formulation of the dispatch model is based upon modifications of the combined economic and environmental dispatch formulation (CEED). Historically, CEED has been formulated as either an economic dispatch or an optimal power flow. The formulation of the CEED problem is presented below:

Minimize $$\sum_t \left(\delta_{fuelCost} \sum_g \sum_i \left(C_{gi} P_{gti} \right) + \delta_{waterCost} \sum_{gth} \left(WCR_g C_{water,g} \sum_i P_{gthi} \right) \right) \quad (4.1)$$

subject to $$P_{gt1} = P_{g,min} \Upsilon_{gt} \quad (4.2)$$

$$0 \le P_{gti} \le P_{gi,max} \Upsilon_{gt} \quad (4.3)$$

$$P_{gt} = \sum_i \left(P_{gti} \right) \quad (4.4)$$

$$P_{lt} - b_l \left(\theta_{n(to),t} - \theta_{n(from),t} \right) = 0 \quad (4.5)$$

$$P_{l,min} \le P_{lt} \le P_{l,max} \quad (4.6)$$

$$\theta_{rt} = 0 \quad (4.7)$$

$$\sum_{g \in G_n} P_{gt} + \sum_{\forall l(to)} P_{lt} - \sum_{\forall l(from)} P_{lt} - \left(P_{load,nt} + P_{pload,nt} \right) = 0 \quad (4.8)$$

$$P_{g,min} \Upsilon_{gt} \le P_{gt} \le P_{g,max} \Upsilon_{gt} \quad (4.9)$$

Here, the modified CEED objective function is the weighted sum of two cost functions. The first function is the cost related to fuel consumption which is the unit's incremental cost of fuel, in \$/MW·Hr, multiplied by the current active power output of the unit. The fuel cost curves are assumed here to be, in general, piece-wise linear functions of the unit's output with values of the *i*-th piece-wise segment's cost equal to C_{gi}.The second term in the objective function gives an operational cost to the amount of cooling water that is consumed. The incremental cost of water (C_{water}), in \$/gal, is itself a variable and the

setting and adjustment of this value is discussed in the simulation methodology chapter of this report. The term $WCR_{water,g}$ is the consumption rate of water, in gal/MW·Hr. This can be calculated from historical data or given a variable value based on known conditions such as ambient temperature and air conditions at the generation site if this level of accuracy is desired and such information is known. Since the fuel cost of a given unit is usually inversely related to its water consumption rate, the two cost terms are in direct competition with each other and therefore neither can be minimized, except for the extreme case of large weights, $\delta_{fuelCost}$ or $\delta_{waterCost}$. The summation for both terms is over all time-periods (e.g. 24-hours) and over all generators for the fuel cost term and over the subset of all thermal units for the term constituting operational water costs. The first segment of the piece-wise real power output curve is ensured to be zero in (4.2) if the unit commitment on/off variable is zero for all generators and for all time-periods. In (4.4), the active power output of the unit is set equal to the sum of the individual segments of the piece-wise linear curve. The linear approximation for the power flow across a transmission element is given in (4.5), where the active power flow magnitude is equal to magnitude of the difference between the to bus voltage angle and the from bus angle multiplied by the element's primitive susceptance. Constraint (4.6) limits the line flows to be between a line's minimum and maximum values. In (4.7), the voltage angle of the reference node, *r*, is stated to be zero. The node supply-demand balance equation is given in (4.8). The equation, going over terms in words from left to right, states that the sum of all generation at a bus plus the sum of all real power leaving through transmission elements at that bus is equal to the real power coming into the bus through terminating transmission elements plus the real power demand at the bus. Note that the demand is specified explicitly in terms of the electric system load

at the bus plus any WDS pump load ($P_{pload,nt}$) present at the bus, thus capturing the key dependency of the WDS on the EPS in this part of the formulation. Lastly, constraint (4.9) ensures that a unit's output is between its minimum and maximum output values when the unit is on and zero when the unit is off, dictated by the on/off variable input from the unit commitment solution, Υ_{gt}.

4.1.2.Short Term Unit Commitment Model

The unit commitment model seeks to minimize the total operating cost, subject to operating constraints that will be described. The total operating cost is the sum of all the unit start-up costs, no-load costs, and fuel costs. The decision variables are the piece-wise power outputs, the unit commitment variables (on/off, start-up, shutdown), and the spinning and non-spinning reserve requirements.

Minimize $$\sum_t \sum_g \left(\sum_{\forall i} \left(C_{gi} P_{gti} \right) + CNL_g u_{gt} + CSU_g v_{gt} \right) \quad (4.10)$$

$$0 \le P_{gti} \le P_{g,max} u_{gt} \quad (4.11)$$

$$P_{gt1} = P_{g,min} u_{gt} \quad (4.12)$$

$$P_{gt} = \sum_{\forall i} \left(P_{gti} \right) \quad (4.13)$$

$$P_{gt} + r_{gt,spin} \le P_{g,max} u_{gt} \quad (4.14)$$

$$P_{g,min} u_{gt} \le P_{gt} \quad (4.15)$$

$$r_{gt,nonspin} \leq R_{g,tm}(1\text{-}u_{gt}) \tag{4.16}$$

$$0 \leq r_{gt,spin} \tag{4.17}$$

$$0 \leq r_{gt,nonspin} \tag{4.18}$$

$$\sum_{\forall g}\left(r_{gt,spin}\right) \geq \frac{1}{2}\left(\max_g\left(P_{g,max}\right)\right) \tag{4.19}$$

$$\sum_{\forall g}\left(r_{gt,spin}+r_{gt,nonspin}\right) \geq \left(\max_g\left(P_{g,max}\right)\right) \tag{4.20}$$

$$P_{lt}\text{-}b_l\left(\theta_{n(to),t}\text{-}\theta_{m(from),t}\right) = 0 \tag{4.21}$$

$$P_{l,min} \leq P_{lt} \leq P_{l,max} \tag{4.22}$$

$$\theta_{rt} = 0 \tag{4.23}$$

$$\sum_{g \in G_n} P_{gt} + \sum_{\forall l(to)} P_{lt} - \sum_{\forall l(from)} P_{lt} - P_{load,nt} = 0 \tag{4.24}$$

$$u_{gt} \in \{0, 1\} \tag{4.25}$$

$$0 \leq v_{gt} \leq 1 \tag{4.26}$$

$$0 \leq w_{gt} \leq 1 \tag{4.27}$$

$$v_{gt}\text{-}\ w_{gt}\text{=}u_{gt}\text{-}u_{g,t\text{-}1} \tag{4.28}$$

$$\sum_{s=t-UT_g+1}^{t} v_{g,s} \leq u_{gt} \qquad \forall g,\ t \in \{UT_g, \ldots, T_{24}\} \quad (4.29)$$

$$\sum_{s=t-DT_g+1}^{t} w_{g,s} \leq 1-u_{g,t} \qquad \forall g,\ t \in \{DT_g, \ldots, T_{24}\} \quad (4.30)$$

$$P_{gt}-P_{g,t-1} \leq R_{g,hr}u_{g,t-1} + RSU_g v_{g,t} \quad (4.31)$$

$$P_{g,t-1} - P_{g,t} \leq R_{g,hr}u_{g,t} + RSD_g w_{gt} \quad (4.32)$$

The SCUC objective minimizes the operating costs related to power generation for the period under study with a piece-wise linear incremental cost curve and costs related to no-load operation and unit startup. The piece-wise linear cost function is modeled in (4.11) through (4.13). In (4.14) and (4.15), the power output and assigned reserve are ensured to be within a units' maximum and minimum output values. Likewise, (4.16) - (4.18) ensure positive reserve values and limit the non-spinning reserve to be for units that are off. System wide minimum values for the spinning and non-spinning reserve values are provided in (4.19) and (4.20). The DC approximation for line flow is given in (4.21) and states that the active power flow across a line is equal to the angle difference between the from and to bus of the line multiplied by the line's primitive susceptance. Constraint (4.22) constrains the line flow magnitude to its maximum steady-state, or Rate *A*, value. In (4.23), the reference bus angle is set to zero. Given in (4.24) is a nodal power-balance equation stating the sum of all line flows into and generation at a bus is equal to the demand at that bus and any line flows from the bus. The constraints and relationships between the unit commitment variables u_{gt}, v_{gt} and w_{gt} are seen in (4.25) - (4.30). The minimum up and down time constraints are facets and defined by (4.29) and (4.30). In (4.31) and (4.32), the

generation levels between time-periods are constrained to the hourly ramp rate, if a unit is on, and the start-up ramp rate, if the unit is off, in the upward direction and by the hourly ramp rate and the shutdown rate in the downward direction.

The following equations and constraints relate to ensuring an *N*-1 secure dispatch.

SCUC Transmission Contingencies:

$$P_{lt} - b_l(\theta_{n(to),t} - \theta_{m(from),t}) = 0 \tag{4.33}$$

$$P_{l,minC} \leq P_{lt} \leq P_{l,maxC} \tag{4.34}$$

$$P_{kt} = 0 \tag{4.35}$$

$$\sum_{g \in G_n} \Phi_{gt} + \sum_{\forall l(to)} P_{lt} - \sum_{\forall l(from)} P_{lt} - P_{load,nt} = 0 \tag{4.36}$$

For each transmission line outage that is outaged, its flow is set to zero in (4.35). New line flows are calculated based upon (4.36). These new line flows must satisfy the DC power flow (4.33) while being within the line's Rate C, or short-term emergency limit (4.34).

SCUC Generator Contingencies:

$$P_{lt} - b_l(\theta_{n(to),t} - \theta_{m(from),t}) = 0 \tag{4.37}$$

$$P_{l,minC} \leq P_{lt} \leq P_{l,maxC} \tag{4.38}$$

$$\sum_{g \in G_n} (\Phi_{gt} + r^c_{gt}) + \sum_{\forall l(to)} P_{lt} - \sum_{\forall l(from)} P_{lt} - P_{load,nt} = 0 \tag{4.39}$$

$$\sum_{\forall g} r^{c}_{gt} = \Phi_{g=c,t} \tag{4.40}$$

$$\Phi_{g=c,t} = 0 \tag{4.41}$$

$$r^{c}_{g=c,t} = 0 \tag{4.42}$$

$$r^{c}_{gt} \leq r_{gt,spin} \tag{4.43}$$

$$P_{g,min} Y_{gt} \leq \Phi_{gt} + r^{c}_{gt} \tag{4.44}$$

Similar to the transmission line outage constraints, the generator contingency outage must satisfy the line flow and limit constraints (4.37), (4.38) and the nodal generation-demand balance (4.39). The generation is re-dispatched so that the reserve meets the amount of lost generation (4.40). In (4.41) and (4.42), the contribution to the reserve and the nominal power output are forced to be zero for the outaged unit. Lastly, constraint (4.44) ensures the re-dispatched units all stay above their minimum power outputs.

4.2 Long-Term Optimization Models for Planning Length Simulations

The planning model is an optimal investment/SCUC problem. As can be seen, this formulation gives a mixed-integer, linear model with a multi-term objective function.

4.2.1. Optimal Investment/SCUC

Minimize $W_1 \cdot T_1 + W_2 \cdot T_2 + W_3 \cdot T_3$ (4.45)

$$T_1 = \sum_{\forall t \in T_{ld}} \left(\sum_{\forall l \in \bar{L}} \left(c_l^{Inv} \left(\frac{z_{lt} - z_{l,t-1}}{(1+d)^{t-1}} \right) \right) \right) \tag{4.46}$$

$$T_2 = \sum_{\forall t \in T_{ld}} \left(\sum_{\forall g \in \bar{G}} \left(c_g^{Inv} \left(\frac{y_{gt} - y_{g,t-1}}{(1+d)^{t-1}} \right) \right) \right) \tag{4.47}$$

$$T_3 = \sum_{\forall g,t \in T_{ld}} \begin{pmatrix} \sum_{\forall i} \left(C_{g,i} P_{gti} \right) + CREGUP_g r_{gt,regup} + CREGDN_g r_{gt,regdn} + \\ CSPIN_g r_{gt,spin} + CNSPIN_g r_{gt,nonspin} + CNL_g u_{gt} + CSU_g v_{gt} \end{pmatrix} \tag{4.48}$$

Term *T1* in the SCUC objective relates to the investment costs of candidate lines $\bar{L}$. The term c_l^{Inv} is the cost of line *l* and depends on the line location, length, rating, configuration and required right-of-way. The binary variables z_{lt} are decision variables equal to 1 if a line is built and 0 if it is not. Term *T2* is similar to *T1* but captures the investment costs for generators with the decision variables y_{gt}. Term *T3* captures the operating costs related to power generation for the period under study with a piece-wise linear incremental cost curve and costs related to regulation up and down, both spinning and non-spinning reserve and a units' startup and no-load costs. Given that this optimal investment/operational problem has multiple terms in its objective function, the weights *W1*, *W2*, and *W3* can be assigned values as the planner sees fit. The constraints accompanying the objective function in (4.45) are:

subject to *Power output, regulation and reserve constraints*

$$0 \le P_{gti} \le P_{gi,max} u_{gt} \tag{4.49}$$

$$P_{gt1} = P_{g,min} u_{gt} \tag{4.50}$$

$$P_{gt} = \sum_{\forall i} \left(P_{gti} \right) \tag{4.51}$$

$$P_{gt} + r_{gt,regup} + r_{gt,spin} \leq P_{g,max} u_{gt} \tag{4.52}$$

$$P_{g,min} u_{gt} \leq P_{gt} - r_{gt,regdn} \tag{4.53}$$

$$0 \leq r_{gt,regup} \leq RREG_g u_{gt} \tag{4.54}$$

$$0 \leq r_{gt,regdn} \leq RREG_g u_{gt} \tag{4.55}$$

$$r_{gt,regup} = 0 \tag{4.56}$$

$$r_{gt,regdn} = 0 \tag{4.57}$$

$$r_{gt,regup} + r_{gt,spin} \leq RSPIN_g u_{gt} \tag{4.58}$$

$$r_{gt,nonspin} \leq RSPIN_g (1 - u_{gt}) \tag{4.59}$$

$$0 \leq r_{gt,spin} \tag{4.60}$$

$$0 \leq r_{gt,nonspin} \tag{4.61}$$

$$\sum_{\forall g} \left(r_{gt,regup} \right) \geq \alpha_{up} \sum_{\forall n} \left(P_{pload,nt} \right) \tag{4.62}$$

$$\sum_{\forall g}\left(r_{gt,regdn}\right) \geq \alpha_{dn} \sum_{\forall n}\left(P_{pload,nt}\right) \tag{4.63}$$

$$\sum_{\forall g}\left(r_{gt,spin}\right) \geq \frac{1}{2}\left(\max_g\left(P_{g,max}\right)\right) \tag{4.64}$$

$$\sum_{\forall g}\left(r_{gt,spin}+r_{gt,nonspin}\right) \geq \left(\max_g\left(P_{g,max}\right)\right) \tag{4.65}$$

Power flow constraints:

$$-(1-z_{lt})M_l \leq P_{lt}-b_l(\theta_{nt}-\theta_{mt}) \leq (1-z_{lt})M_l \tag{4.66}$$

$$z_{lt}P_{l,min} \leq P_{lt} \leq z_{lt}P_{l,max} \tag{4.67}$$

$$\theta_{rt}=0 \tag{4.68}$$

$$\sum_{g\in G_n} P_{gt} + \sum_{\forall l(to)} P_{lt} - \sum_{\forall l(from)} P_{lt} - P_{load,nt} = 0 \tag{4.69}$$

Constraint (4.49) and (4.50)-(4.51) model the piece-wise linear cost function. The purpose of (4.52) and (4.53) is to ensure the power output and assigned regulation are within a units' maximum and minimum output values. Constraints (4.54)-(4.55) and (4.56) - (4.57) constrain the regulation up and down to be zero for those units not available for AGC and within a five-minute ramp rate for generators available for AGC. Constraints (4.58) - (4.61) ensure positive reserve values and limit the spinning and non-spinning reserve for units that are on and off, respectively. Constraints (4.62) - (4.65) provide system wide minimum values for the regulation and reserve values. Constraint (4.66) is a disjunctive constraint which keeps the model linear and the selection of a large enough

value of *M* ensures that the constraint is non-binding if the line is not built. Similarly, (4.67) forces the line flow to be zero if a candidate line is not built. The reference bus angle is state to be zero in (4.68) and (4.69) is a nodal power-balance equation stating the sum of all line flows into and generation at a bus is equal to the demand at that bus and any line flows from the bus.

TEP binary constraints:

$$z_{lt} \in \{0,1\} \tag{4.70}$$

$$z_{lt} \geq z_{l,t\text{-}1} \tag{4.71}$$

$$z_{lt} = 1 \qquad \forall l \in L,\ l \notin \bar{L} \tag{4.72}$$

$$z_{lt} = 0 \qquad \forall l \in \bar{L},\ t=1 \tag{4.73}$$

GEP binary constraints:

$$y_{gt} \in \{0,1\} \tag{4.74}$$

$$y_{gt} \geq y_{g,t\text{-}1} \tag{4.75}$$

$$y_{gt} = 0 \qquad \forall g \in \bar{G},\ t = 1 \tag{4.76}$$

$$z_{lt} = y_{g \in G_n = L(n),t} \qquad \forall g \in \bar{G},\ l \in \bar{L} \tag{4.77}$$

The decision variables for transmission expansion are given in constraint (4.71) and equations (4.72) - (4.73) and (4.70). They express that z_{lt} is a binary, that once a line is built it must stay built and that z_{lt} is one for all pre-existing lines. The corresponding constraints and equations for the generation expansion decision variables are shown in (4.74)-(4.76). In (4.77), it is ensured that if a candidate generator is built, the corresponding transmission line connecting it to the existing system will be built.

UC binary constraints:

$$u_{gt} \in \{0,1\} \tag{4.78}$$

$$u_{gt} \leq y_{gt} \tag{4.79}$$

$$0 \leq v_{gt} \leq 1 \tag{4.80}$$

$$v_{gt} \geq u_{gt} - u_{g,t-1} \tag{4.81}$$

$$\sum_{s=t-UT_g+1}^{t} v_{g,s} \leq u_{gt} \tag{4.82}$$

$$\sum_{s=t-DT_g+1}^{t} v_{g,s} \leq 1 - u_{g,t-DT_g} \tag{4.83}$$

$$P_{gt} - P_{g,t-1} \leq R_{g,hr} u_{g,t-1} + RSU_g v_{g,t} \tag{4.84}$$

$$P_{g,t-1} - P_{g,t} \leq R_{g,hr} u_{g,t} + RSD_g \left(v_{gt} - u_{gt} + u_{g,t-1} \right) \tag{4.85}$$

The constraints and relationships between the unit commitment variables u_{gt} and v_{gt} are seen in (4.78) - (4.83). In (4.79), it ensures that no candidate generator is on if it has not been built. The minimum up and down time constraints are facets and defined by (4.82) and (4.83). Lastly, (4.84) and (4.85) constrain the generation levels between time-periods to the hourly ramp rate if a unit is on and the start-up ramp rate if not in the upward direction and by the hourly ramp rate and the shutdown rate in the downward direction.

4.2.2.Security Constrained Economic Dispatch (SCED)

The two main differences between OPF formulations and SCED implementations are the addition of voltage angle constraints and contingency constraints for the SCED [89]. Additionally, a more complex objective function is used to capture the total operating cost.

$$\text{Minimize} \qquad \sum_{\forall g}\begin{pmatrix}\sum_{\forall i}\left(C_{g,i}P_{gti}\right)+CREGUP_g r_{gt,regup}\\ +CREGDN_g r_{gt,regdn}+CSPIN_g r_{gt,spin}\end{pmatrix} \tag{4.86}$$

subject to

$$0 \le P_{gti} \le P_{g,max}\overline{u_{gt}} \tag{4.87}$$

$$P_{gt1} = P_{g,min}\overline{u_{gt}} \tag{4.88}$$

$$P_{gt} = \sum_{\forall i}\left(P_{gti}\right) \tag{4.89}$$

$$P_{gt} + r_{gt,regup} + r_{gt,spin} \le P_{g,max}\overline{u_{gt}} \tag{4.90}$$

$$P_{g,min}\overline{u_{gt}} \le P_{gt} - r_{gt,regdn} \tag{4.91}$$

$$0 \leq r_{gt,regup} \leq RREG_g \overline{u_{gt}} \tag{4.92}$$

$$0 \leq r_{gt,regdn} \leq RREG_g \overline{u_{gt}} \tag{4.93}$$

$$r_{gt,regup} = 0 \tag{4.94}$$

$$r_{gt,regdn} = 0 \tag{4.95}$$

$$r_{gt,regup} + r_{gt,spin} \leq RSPIN_g \overline{u_{gt}} \tag{4.96}$$

$$0 \leq r_{gt,spin} \tag{4.97}$$

$$\sum_{\forall g} \left(r_{gt,regup} \right) \geq \alpha_{up} \sum_{\forall n} \left(P_{load,nt} \right) \tag{4.98}$$

$$\sum_{\forall g} \left(r_{gt,regdn} \right) \geq \alpha_{dn} \sum_{\forall n} \left(P_{load,nt} \right) \tag{4.99}$$

$$\sum_{\forall g} \left(r_{gt,spin} \right) \geq \frac{1}{2} \left(\max_g \left(P_{g,max} \right) \right) \tag{4.100}$$

$$P_{lt} - b_l (\theta_{nt} - \theta_{mt}) = 0 \tag{4.101}$$

$$-P_{l,min} \leq P_{lt} \leq P_{l,max} \tag{4.102}$$

$$\theta_{rt} = 0 \tag{4.103}$$

$$\sum_{g \in G_n} P_{gt} + \sum_{\forall l(to)} P_{lt} - \sum_{\forall l(from)} P_{lt} - P_{load,nt} = 0 \tag{4.104}$$

The constraints and equations in (4.87) - (4.104) describe the security constrained economic dispatch problem modeled in this project. The equations are similar to their corresponding SCUC definitions with the exception of fixed decision variables u_{gt} (and by extension y_{gt}), v_{gt}, and z_{gt}. The process by which the SCED was performed will be detailed in Chapter 5. Also, it can be noted that the inter-temporal constraints (4.84) and (4.85) are not used for the SCED.

4.2.3.*N*-1 Contingency Analysis:

Transmission contingencies

$$P_{lt}\text{-}b_k(\theta_{nt}\text{-}\theta_{mt})=0 \tag{4.105}$$

$$P_{l,minC} \leq P_{lt} \leq P_{l,maxC} \tag{4.106}$$

$$P_{lt}=0 \tag{4.107}$$

$$\sum_{g \in G_n} \overline{P_{gt}} + \sum_{\forall l(to)} P_{lt} \sum_{\forall l(from)} P_{lt} \; - \; P_{load,nt} = 0 \tag{4.108}$$

Generator contingencies

$$P_{lt}\text{-}b_k(\theta_{nt}\text{-}\theta_{mt})=0 \tag{4.109}$$

$$P_{l,minC} \leq P_{lt} \leq P_{l,maxC} \tag{4.110}$$

$$\sum_{g \in G_n} (\overline{P_{gt}} + r^c_{gt}) + \sum_{\forall l(to)} P_{lt} - \sum_{\forall l(from)} P_{lt} \; - \; P_{load,nt} = 0 \tag{4.111}$$

$$\sum_{\forall g} r_{gt}^{c} = \overline{P_{g=c,t}} \tag{4.112}$$

$$P_{g=c,t} = 0 \tag{4.113}$$

$$r_{g=c,t}^{c} = 0 \tag{4.114}$$

$$r_{gt}^{c} \leq r_{gt,spin} \tag{4.115}$$

$$P_{g,min}\overline{u_{gt}} \leq \overline{P_{gt}} + r_{gt}^{c} \tag{4.116}$$

The constraints related to ensuring an *N*-1 secure dispatch are given in (4.105) - (4.116). The constraints and equations in (4.105) - (4.108) are related to ensuring line flows are less than their Rate C rating for transmission line outages while (4.109) - (4.116) do the same for generator outages.

4.2.4.Environmental Analysis

$$\sum_{t \in q} P_{gt} \cdot WCR_g \cdot \sum_T 1 \leq WA_{gqs} \qquad \forall s,q,g \in \overline{G} \tag{4.117}$$

Lastly, constraint (4.117) can be used to constrain the water usage of a candidate generator. This has the effect of limiting the water consumption (by limiting the power output) of a candidate generator to a value less than the anticipated water rights acquisition at the proposed plant site. This might be desirable due to the forecasted water available during a drought, for example, or other weather scenarios. The indexing is given as it will be used in a future implementation of this planning model where the water availability, *WA*, is for all scenarios in all years for all of the expansion candidate generators.

4.3 Modeling of Time-Period End Points

The different models used in the simulations that will be shown were run for a finite number of time-periods at different points within each simulation. The data within the simulation and the values that used as output need to make sense within this environment and thus the issue of how to handle end-points becomes important, especially for constraints involving multiple time-periods, such as the minimum up and down times for a unit.

The first approach that was used in the context of the short-term optimization model is shown in Figure 4.1. Here, more time-periods are used as input into the unit commitment and OPF models than are needed, the simulation is run for this longer duration, and the desired outputs at a given time-period (CEED), e.g. t = t1, or for a set of desired time-periods (UC), e.g. t ∈ {t1,…,t2}, are used.

Figure 4.1 Optimization Model End-Point Modeling Method 1

The second method shown in Figure 4.2 was used in the long-term planning model.

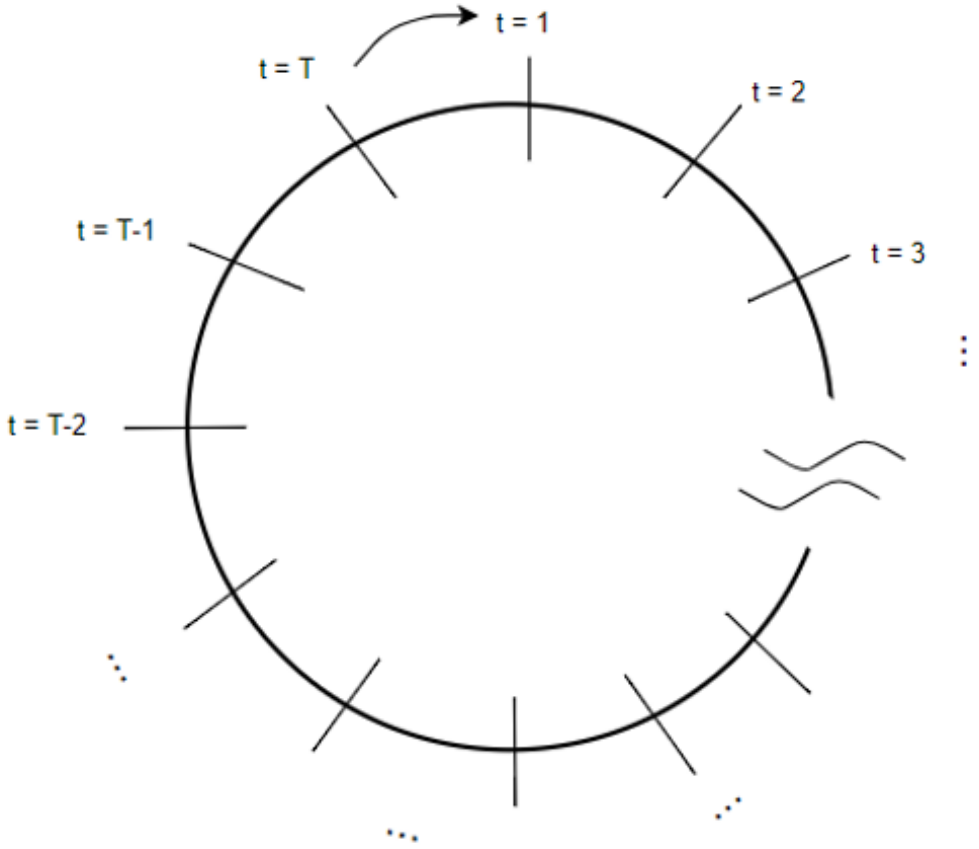

Figure 4.2 Optimization Model End-Point Modeling Method 1

Here, the end time-period, denoted by “T”, is linked to the first time-period, t = 1. This is more important in this model where the consideration of constraints involving end-point time-periods can become critical due to the implementation of a limited day SCUC. The implementation involves the modification of the equations involving the unit commitment binary variables, where at least one additional constraint for each of the original equations is added to ensure this linking of beginning and ending time-periods.

4.4 Proposed Policies with Consideration of External System Data

The availability of information to the EPS from the WDS allows for new decisions to be made with regards to the operation of the power system. The following three policies are for use in the operational length simulations. The first adjusts the maximum output of generators experiencing extreme conditions to ensure that unit's availability for a longer period of time. The second is a more immediate measure and is an adjustment of the operational cost of water based on the recent supply of cooling water demands. The third affects the nodal demand of cooling water requirements which are seen within the WDS.

4.4.1.Policy I: Unit Derating, LP Model

This section presents a method for curtailing a unit's output under extreme conditions. The number of high impact, weather related electric power grid disturbance has been growing [90], and that report also describes how just under 50% of large blackouts in the US have been caused by severe weather. Given that the majority of non-regulatory stay actions for thermoelectric generation experiencing cooling water issues have been the curtailment of generation [91], a method for determining the maximum output of such units is desired. There is some additional post-processing that is done which will be detailed while addressing the simulation methodology in Chapter 5. The mathematical formulation of the model follows.

$$\text{Minimize} \qquad -\sum_{t,g} P_{t,g} + \sum_{t,g} 1\text{x}10^{10} s_{t,g} \tag{4.118}$$

subject to

$$P_{t,g} \leq P_{g,max} \Upsilon_{gt} \tag{4.119}$$

$$(P_{t,g} - P_{t\text{-}1,g}) \cdot (1 - \text{abs}(\Upsilon_{g,t\text{-}1} - \Upsilon_{gt})) \leq R_{g,hr} \tag{4.120}$$

$$(P_{t\text{-}1,g} - P_{t,g}) \cdot (1 - \text{abs}(\Upsilon_{g,t-1} - \Upsilon_{gt})) \leq R_{g,hr} \tag{4.121}$$

$$(P_{t,g} - P_{t\text{-}1,g}) \cdot (1 - \Upsilon_{g,t-1}) \leq RSU_g \tag{4.122}$$

$$(P_{t\text{-}1,g} - P_{t,g}) \cdot (1 - \Upsilon_{gt}) \leq RSD_g \tag{4.123}$$

$$\sum_t P_{t,g} \cdot WCR_g \cdot T - s_{t,g} \leq \sum_t Q_{t,g} \cdot T + TPF \cdot TL_g \tag{4.124}$$

$$s_{t,g} \geq 0 \tag{4.125}$$

The objective function shown in (4.118) seeks to maximize the $P_{t,g}$ value over the time-periods of concern (last 24 hours). The variable $P_{t,g}$ is used to avoid confusion with a unit's nominal maximum output power, $P_{g,max}$. Similar to the CEED formulation, the unit commitment variables are used in (4.119) to determine $P_{g,max}$ for the units which are committed in each time-period. Constraints (4.120) and (4.121) seek to keep the fluctuation of $P_{g,max}$ within the running ramp rates of the units. Similarly, constraints (4.122) and (4.123) handle the ramp rates if the unit is committed or turned off during one of the time-periods of this model's implementation. Constraint (4.124) utilizes input data from the WDS simulation. In words, the left hand side is the algebraic sum of two terms with the first being the product of the decision variable, which again is a proxy for a new

$P_{g,max}$, and the unit's water consumption rate and the second being the slack variable. The right-hand side is the sum of all the water flows into generator storage tank nodes from all connections to the WDS plus a slack factor that is discussed below. So, this constraint seeks to keep the water consumed less than the water supplied, plus an additional quantity determined by the current onsite water storage tank level. Lastly, (4.125) keeps the slack variables positive so that they are minimized as shown in the objective function. The right-most term in constraint (4.124) is the product of the tank percentage factor and the tank level at the current iteration of the simulation. This factor is defined mathematically as:

$$TPF = W_{derate} \cdot \left(1 - \frac{TL_g}{TL_{g,initial}}\right) \tag{4.126}$$

where $TL_{g,initial}$ is the initial onsite storage tank level, TL_g is the tank level in the current iteration and W_{derate} is a weight determined from sensitivity analysis.

4.4.2.Policy I: Unit Derating, Empirical Model

The following exponential model is presented as an alternative to the implementation of a unit derating scheme such as the above LP model. Here, an exponential function is used along with a bias term and an appropriate multiplier for the exponential in order to maintain the curtailed $P_{g,max}$value between the unit's nominal $P_{g,max}$ and $P_{g,min}$ values. A choice for the exponent was determined through trial and error and presented as:

$$T1 = \frac{TL_{g,,initial} - ave_{t\text{-}24:t}(TL_g)}{TL_g \cdot WCR_g} \tag{4.127}$$

where the $ave_{t\text{-}24:t}$ operator indicates a running average over the previous 24 simulation time-periods. With the quantity *T1* calculated, the unit's P_{max} value can be determined using the unit's nominal maximum ($P_{g,max0}$) and minimum ($P_{g,min0}$) outputs from :

$$P_{g,max} = P_{g,min0} + (P_{g,max0} - P_{g,min0}) \cdot e^{-T1} \tag{4.128}$$

4.4.3.Policy II: Operational Water Cost Adjustment

In extreme drought scenarios, it might also be desirable to further influence the dispatch of generation in the affected spatial area in order to keep units operational for as long as possible through the frugal use of water stored onsite. The approach presented here accomplishes this through the adjustment of the operational water cost in (4.1) and seeks to discourage the dispatch of affected generation based on how the onsite cooling water demands are being met. Defining a tank level rate of change term as:

$$ROC_t = ave_{t\text{-}24:t}(s(t)) \tag{4.129}$$

where the $ave_{t\text{-}24:t}$ operator is as defined in the previous section and the quantity *s* is defined as being proportional to the difference between the cooling water which was supplied by the water system and that which was actually requested (consumed) by the unit.

$$s(t) = \frac{Q_{t,g,supplied} - Q_{t,g,requested}}{P_{g,max0} \cdot WCR_g} \tag{4.130}$$

A cumulative rate of change is then defined as

$$cROC_t = cROC_{t\text{-}1} - ROC_t \tag{4.131}$$

Finally, the operational cost of water which is analogous to the incremental fuel cost, is calculated in equation (4.132) using an assumed elasticity of supply factor, EF.

$$C_{water,i} = C_{water,initial} \cdot (1 + cROC_t \cdot EF) \tag{4.132}$$

4.4.4.Policy III: Modification of Cooling Water Make-up Requirements

Since the WDS optimization is adjusting the demands which are supplied based on the time of day and other constraints, the cooling water make-up requirements that are used as node demands within the WDS simulation are adjusted in order to help refill onsite storage tank levels after they have dropped. The node demands which are used as input for the WDS simulation therefore consist of both the actual cooling water requirements for the given simulation time-period as well as a demand adjustment component. This demand adjustment factor has two elements. The first part of this factor considers whether the make-up requirements were satisfied in the previous simulation time-period. The second component is composed of a term which aims to bring the tank level back to its original value. The components of the demand adjustment factor, $WDS_{DA,1}$ and $WDS_{DA,2}$, are then calculated from:

$$WDS_{DA,1} = \frac{Q_{t,g,requested} - Q_{t,g,supplied}}{TC_{tankRefill}} \tag{4.133}$$

$$WDS_{DA,2} = \left(1 - \frac{mod(TL_g, TL_{g,initial})}{TL_{g,initial}}\right) \frac{TL_{g,initial}}{TC_{tankRefill}} \tag{4.134}$$

where mod is the modulus or remainder operator. The demand adjustment factor value is then calculated as the algebraic sum of (4.133) and (4.134):

$$WDS_{DA,Tot} = WDS_{DA,1} + WDS_{DA,2} \quad (4.135)$$

4.5 Summary of Short Term WDS Mathematical Model [92], [93]

The demands at each node throughout the WDS are used as inputs to the hydraulic simulation model within EPANET [88] which then ensures that all zonal demands throughout the system at each time-period are satisfied. Under situations where the demands may not be fully satisfied due to low water availability or a lack of electrical power, an amount of demand that is lower in value than what was actually requested may still be satisfied. This reduced value of demand that can still be satisfied under contingency scenarios is denoted for zone z during time-period t as $D_{sat,\,z,\,t}$. The objective function for the WDS optimization is therefore to minimize the difference between demands required and demands supplied. The optimization model given was extended to include the water quality constraints for a WDS as follows.

$$\text{Minimize} \qquad \text{obj} = \sum_{t}^{t=T} \sum_{z}^{z=Z} \left[\left(D_{req,\,z,t} - D_{sat,z,t} \right) Qb_z \right]^b \theta_{z,t} \quad (4.136)$$

The constraints are summarized below:

1. The EPANET hydraulic analysis equations
2. The EPANET water quality analysis equations
3. The lower and upper bounds on pump operation time
4. Limits on the number of times a pump switches on or off
5. The power requirement of the pumps
6. The bounds on nodal pressure head, including tank levels
7. The lower and upper bound on demand satisfaction

8. Upper and lower bounds on contaminants/nutrients for water quality

The solution to this optimization was obtained by using a Genetic Algorithm after the extensive problem listed above was reformulated by a relaxation that brings the constraints into the objective function. The control variables for this model are the satisfied demand pattern multipliers ($D_{sat,z,t}$) and the on/off status for all pumps.

4.6 Summary

This chapter has presented the operational time-scale unit commitment model used for an *N*-1 secure commitment of generation units as well as the model used for dispatching the committed generation while taking environmental aspects such as water cost and consumption into consideration. Also presented in this chapter were the mathematical formulations for three implemented control policies. The first policy presents a logical way to curtail the output of generation based upon how cooling water make-up requirements are being met as well as the availability of the generator's onsite water storage. The second policy aims to dispatch generation in a way that encourages less use of cooling water for those units that are experiencing water shortages. The third policy alters the perceived cooling water requirements that are seen within the WDS simulation. The model used for the long-term problem of the combined generation expansion and transmission expansion planning was presented. The model includes the optimal investment/SCUC model for use in a limited-day application as well as the SCED model that is used for determining operating costs and levels of water consumption for generation. Lastly, the optimization model used for the WDS simulation was summarized. The next chapter covers the methodology for simulations in both time-scales.

CHAPTER 5

SIMULATION METHODOLOGY

The framework for the simulations that were conducted will now be presented. The sections that follow present the methodology of simulations in both time-scales considered in this work, a description of the test systems used, and details on the implementation of the control policies introduced in Chapter 4. The framework and methodology for the operational length simulations and optimization of operations of the EPS and WDS under extreme conditions was presented in [94].

5.1 Operation Length Simulations

Because the rate of change of quantities of interest within the power system is relatively slow, the simulation of the power system network for the operational time-frame simulations was accomplished using time-series power flows. The power system control optimization was implemented by a combination of unit commitment for determining the on/off status of all the generators and a modified DC optimal power flow (DCOPF) for determining generator output set-points. The water system simulation was accomplished by solving quasi-dynamic system equations using controls determined from the optimization model summarized in the previous chapter.

The coupling between the water system and the power system was achieved through alternatively exchanging data between the power system and water network simulations via a program control overlay developed in Python. Figure 5.1 shows this concept at a high level. The relevant simulation data exchanged between the power system

and water network simulations included electric power system network configurations, pump power consumption for inclusion in power system loads, and thermal generation cooling water requirements that were used as node demands within the water system. The temporal dependence of one system on the other is accomplished through the modification of loads within the power system and the modification of demands within the water system. The spatial relationship between the two systems is accounted for by placing those loads or demands at the appropriate location within the EPS and WDS.

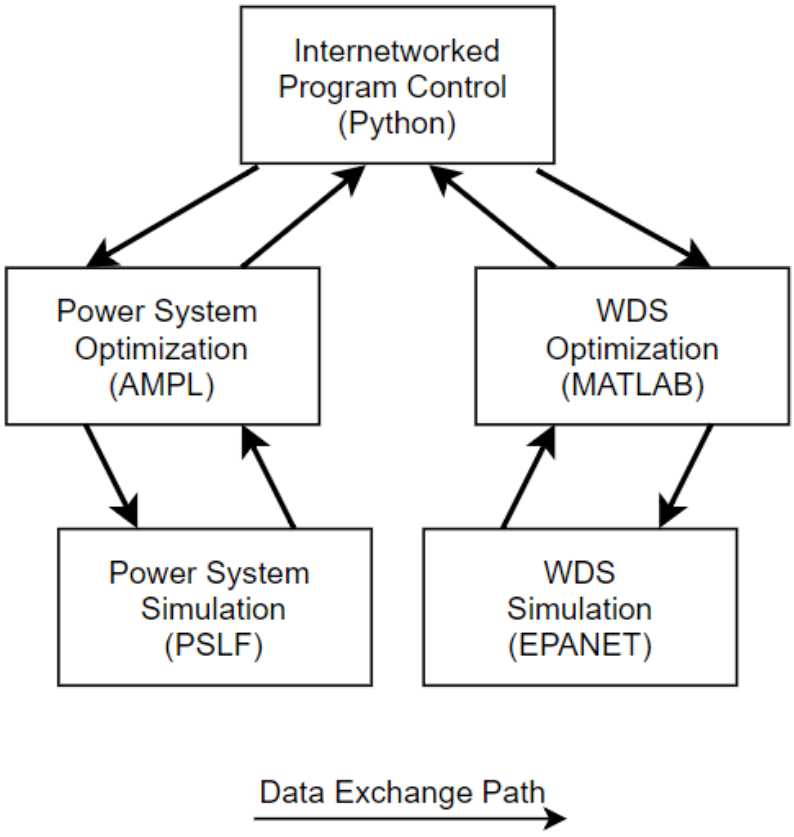

Figure 5.1 Internetworked Simulation Overview

All of the models for the optimization and control of the power system were solved via implementation within the AMPL programming language [95] along with an appropriate solver, in this case Gurobi [96]. The complete electric power system network solution which obtained the net active and reactive power injections as well as the voltage magnitudes and angles at each bus was obtained using GE's PSLF software [97]. The EPANET software was used for the extended period simulation of the water distribution system being analyzed, while a MATLAB toolkit [98] was used to implement the optimization procedure and to interface the WDS simulation with the optimization procedure.

The overall real-time operation of the WDS is described as follows:

1. Update topology (pump status) from electrical energy input from EPS and update WDS data (tank levels, status of valves, and flows)
2. Run WDS optimization model to determine the pump operations and demand pattern given the scenario defined water availability and the available electrical energy input from the EPS.
3. Make the outputs of pump load data and cooling water flows to generators for the correct hour available to the EPS

The overall real-time operation of the EPS is described as follows:

1. Update topology (bus and branch status) from scenario contingency definition
2. Update WDS related quantities (pump loads and generator node water flows)

3. Run EPS optimization model to determine the unit commitment and unit dispatch using the results from 1 and 2.
4. Calculate updated cooling water requirements and make policy adjustments
5. Make network topology and new generator node demands available for the WDS

A high-level flow chart that shows the simulation procedure and all of the software used in the implementation of the extended time-period simulation engine is shown in Figure 5.2 and Figure 5.3.

The simulation initialization includes the specification of the scenario being simulated. This consists of defining the amount of water available to the water system for each hour in the simulation. The power system scenario is defined by listing the outages which occur and at which hours these outages take place. From initial simulations that were conducted, the power test system was seen to be quite robust to the scenarios with branch outages, so worst-case bus outages are considered in this work.

Electric utilities keep records on the amount of cooling water used by their different generating stations. Based on this information, the utilities have tabulated accurate annual characterizations of cooling water requirements for different thermal prime mover fuel types. This characterization, along with a plant's total annual energy output, can be utilized to determine an averaged cooling water requirement rate in gallons per megawatt-hour. Utility data has been acquired [22], and a summary of average water consumption rate, in gal/MW-Hr, is shown for different fuel types in Table 5.1 below.

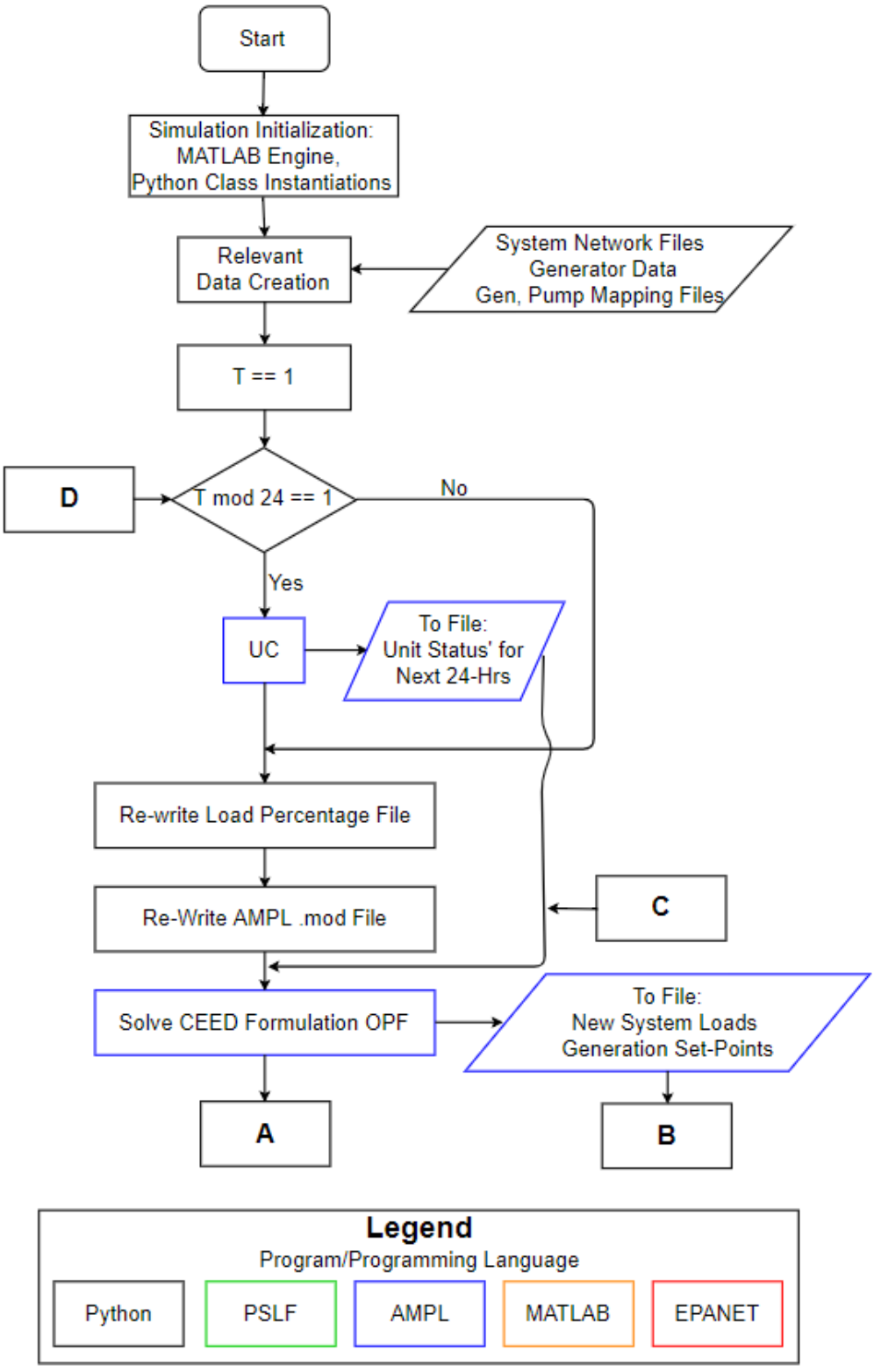

Figure 5.2 High Level Simulation Flow Chart 1/2

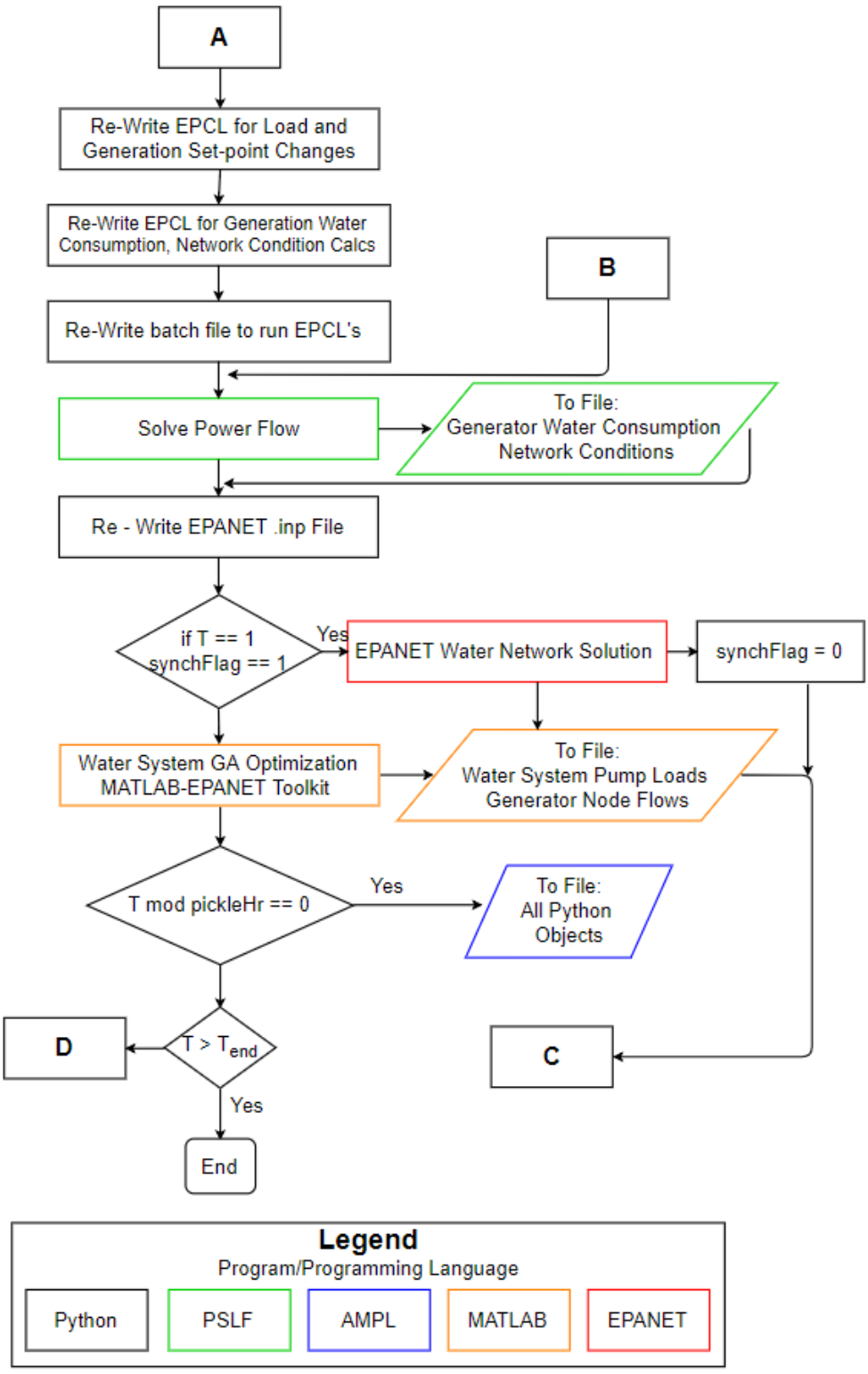

Figure 5.3 High Level Simulation Flow Chart 2/2

Table 5.1 Generator Water Consumption Rates by Fuel Type, WCRg

Generator Type	WCR_G (gal./MWH)
Npp	764
IGCC	600
CCGT	312
CT	231

The task of running extended period time-domain simulations inherently involves some amount of uncertainty as various items related to the simulation process must be forecasted. These items include the residential water demands, initial water storage at water distribution tanks and at the power plants, available generation mix, transmission assets in service, and accuracy of the short to medium-term forecasted load. In order to create time varying system loads, historical load data [99] was normalized and used as load multiplier factors (*LMF*) within the EPS simulation. Constant power factor of the load was assumed so the loads at each time-period *t* were calculated as shown:

$$P_{load,t} = P_{load,nominal} \cdot LMF_t \tag{5.1}$$

$$Q_{load,t} = Q_{load,nominal} \cdot LMF_t \tag{5.2}$$

The short-term security constrained unit commitment was run every 24 hours during the simulation using the next 24 *LMF*s which had their indices offset according to the current time-period in the simulation. Figure 5.4 shows the *LMF* pattern that was used for the power system.

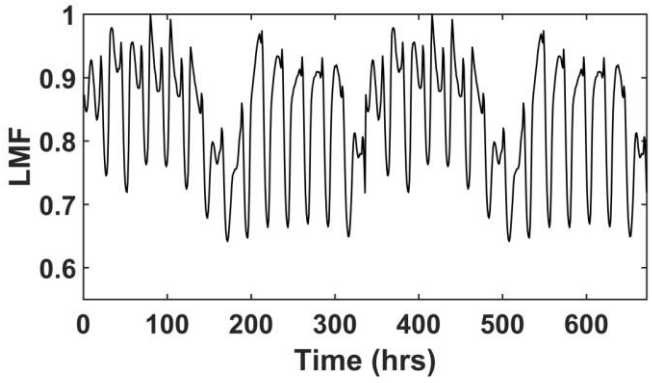

Figure 5.4 LMF for 28-day (672 Hr) Simulation

5.2 Planning Length Simulation

The task of power system planning also involves uncertainty with regards to the various items related to the planning process that must be forecasted. In contrast to the operational time-frame, these items include load growth, regulatory and policy decisions, and the anticipated mix of new network equipment and unit retirements. One way to handle this uncertainty is to create a representative sample of scenarios that could reasonably represent the future, each being arrived at by assuming different driving factors from the initial starting point in the present. For example, the Western Electric Coordinating Council (WECC) defines four such scenarios for use in their Study Case Development Tool (SCDT), Network Expansion Tool (NXT), and long-term planning tools (LTPT) [100]. The scenarios arise as a response to their focus question, repeated here as "How will demand for electric power services in the WECC regions change in the future (10/20 years) and how will electric power supply services (and related transmission networks) change to accommodate that demand?" The scenarios are presented with their driving factors and the relevant data used in this project in Table 5.2. The adjusted load growth is determined from

the anticipated future load minus anticipated policy driven load reduction plus anticipated policy driven electrification.

Table 5.2 Planning Scenarios Considered

Scenario	Summary	Adjusted Load Growth (%/yr.)
Reference	-	1.4
1	Wide-spread economic growth in WECC region Increasing standards of living Evolutionary changes in supply and distribution technology	1.6
2	Scenario 1, but: Paradigm changes in supply and distribution technology	0.1
3	Narrow, slow economic growth in the WECC region Stagnating standards of living Evolutionary changes in supply and distribution technology	0.8
4	Scenario 3, but: Paradigm changes in supply and distribution technology	1.0

The analysis was performed as follows. First, a four-day SCUC was run to determine the investment and commitment decisions for each year considering *T*-1 security requirements. Then, the decision variables were fixed and the extended period SCED was performed. The system was seen to have over generation during certain time-periods, so these violations were recorded and the objective function for that time-period was adjusted to include only the operating costs. Finally, the environmental analysis was performed as shown by the left-hand side of (4.117). The values used to relate the power output of a given unit to the make-up requirements needed for the cooling cycle were averaged from historical data and are shown in Table 5.1. Figure 5.6 shows the flow chart for the simulation that was done for each scenario.

Load data for the limited day SCUC and yearly SCED models was generated from the test system's 24-hour and 336-hour load profiles [101]. These profiles were modified to achieve some type of seasonal variance using values inferred from [102] and which

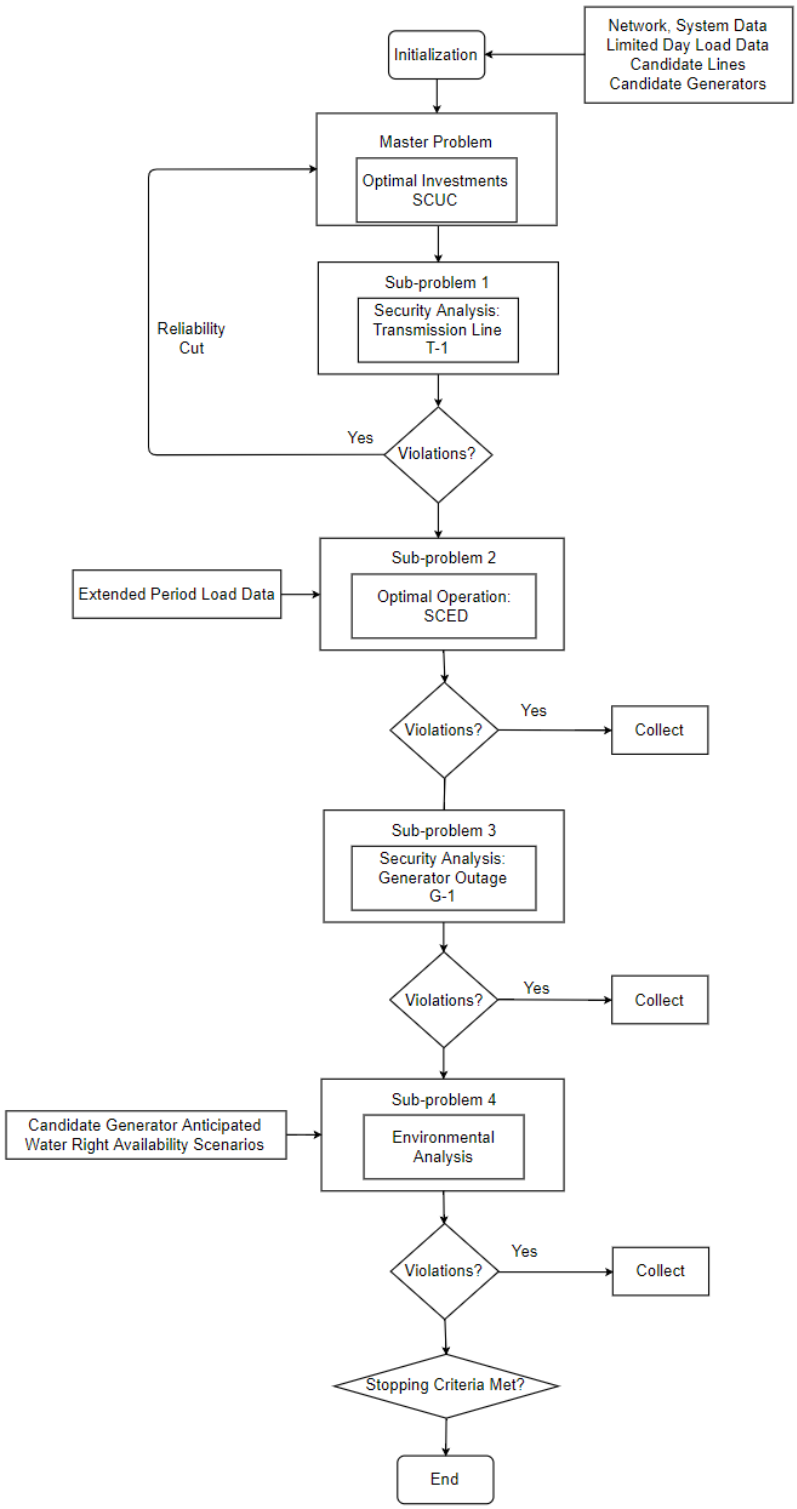

Figure 5.5 GTEP Simulation Flow Chart

represent the year 2032 WECC reference case relative system conditions for heavy summer (*HS*), light fall (*LF*), heavy winter (*HW*), and light spring (*LSP*). Using the *HS* case as the reference, the *LMF* values for each of the seasons was determined as:

$$LMF_{HS} = \frac{198\ GW}{198\ GW} = 1.00 \tag{5.3}$$

$$LMF_{LF} = \frac{105\ GW}{198\ GW} = 0.53 \tag{5.4}$$

$$LMF_{HW} = \frac{170\ GW}{198\ GW} = 0.86 \tag{5.5}$$

$$LMF_{LSP} = \frac{135\ GW}{198\ GW} = 0.68 \tag{5.6}$$

The *LMF* values for each year can then be adjusted for each scenario, considering the amount of load growth that has occurred (or not). The peak load for each scenario, relative to the reference scenario in year one, is shown below for years one and ten. These values are simply multipliers to the nominal, reference profile, for a given year, and are summarized in Table 5.3.

Table 5.3 Peak Load Relative to the Reference Year 1

	Peak Load, Relative to Reference, yr. 1	Peak Load, Relative to Reference, yr. 10
Reference	1.000	1.127
Scenario 1	1.041	1.220
Scenario 2	0.901	0.910
Scenario 3	0.960	1.040
Scenario 4	0.885	0.885

The curves for the limited-day SCUC/Expansion planning problem are shown below for each of the five scenarios (scenarios 1-4 and the reference case).

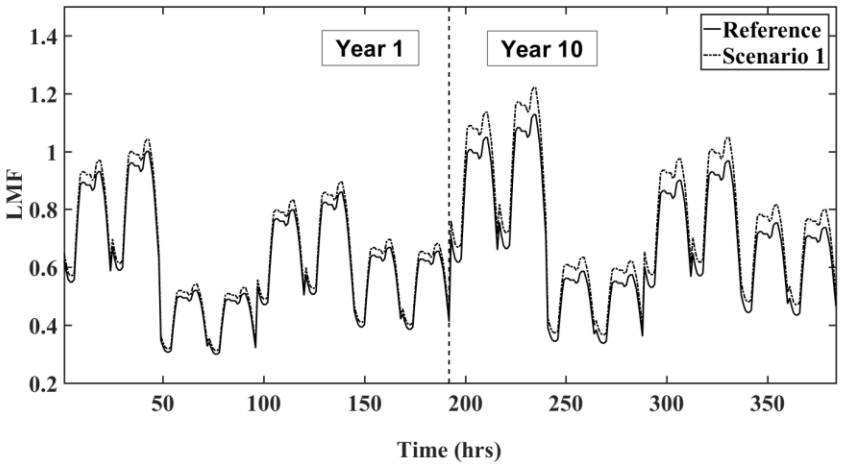

Figure 5.6 Limited Day SCUC Load Profile, Reference-Scenario 1 Comparison

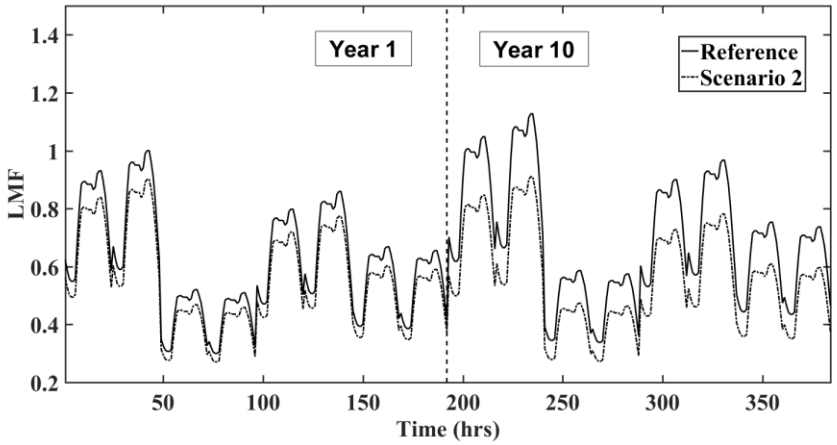

Figure 5.7 Limited Day SCUC Load Profile, Reference-Scenario 2 Comparison

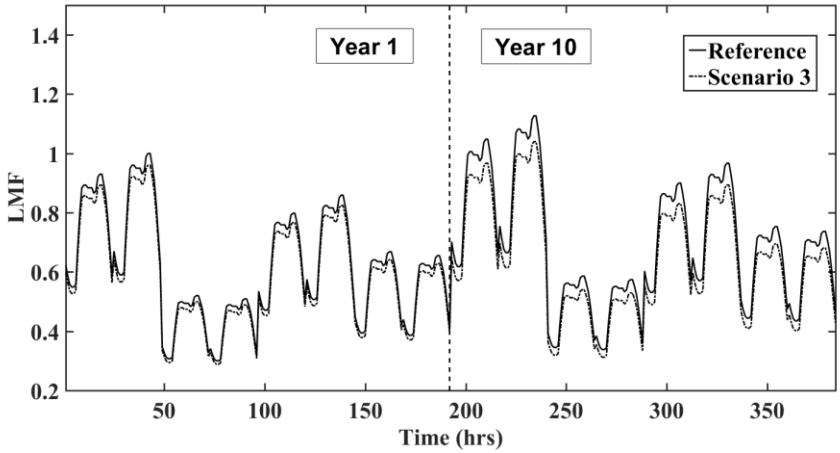

Figure 5.8 Limited Day SCUC Load Profile, Reference-Scenario 3 Comparison

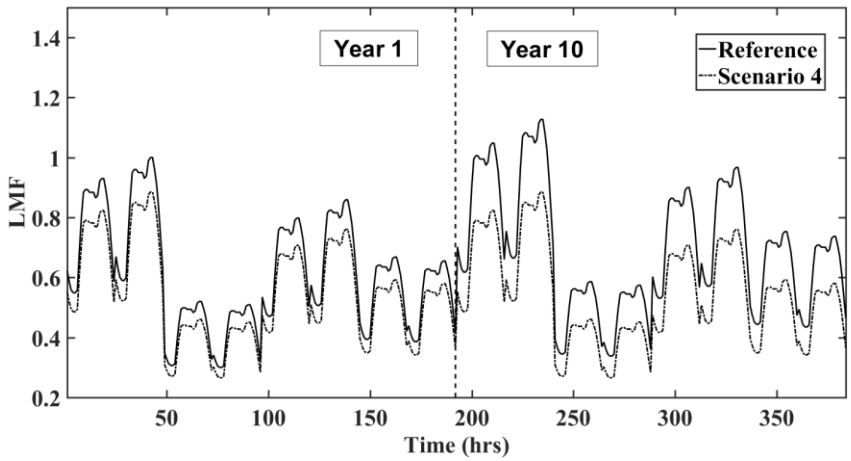

Figure 5.9 Limited Day SCUC Load Profile, Reference-Scenario 4 Comparison

The input to the SCED simulation was the hourly load profile for one year. In addition, the results from the optimal investment/SCUC problem were used so that the commitment variables for the different days within the limited day investment problem were extrapolated for an entire season in the SCED. A longer, 336-hr or two-week nominal load variation curve was used, and the seasons were again represented according to the *LMF* of the given season. Figure 5.10 below shows an example of this.

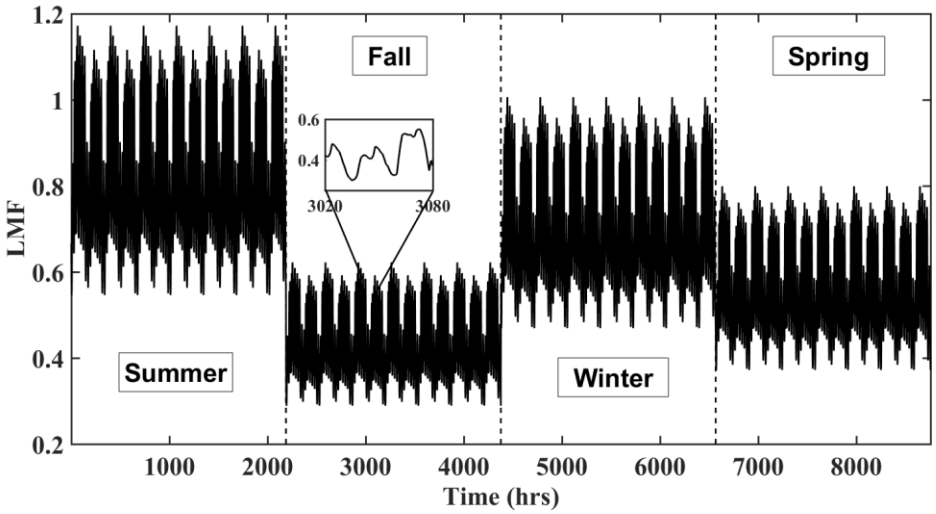

Figure 5.10 SCED Load Profile for Year 10, Reference Case

Investment cost data for both generation and transmission assets was then obtained from [102] and [103]. These values included generic capital cost per kW for various power generation types and an assortment of data related to various transmission line configurations. The generator types available to be installed were chosen to be: Nuclear(Npp), a coal fueled Integrated Gaseous Combined Cycle (IGCC), Aero-derivative Combustion Turbine (CT), and Combined Cycle Gas Turbine (CCGT). The transmission line costs are based on the assumption that a single circuit would be built, with the 115 kV cost estimated. The generator and transmission line data are summarized in Table 5.4 and Table 5.5.

Table 5.4 Generator Investment Costs

Generator Type	Cost($/MW)
Coal IGCC w/ CCS (IGCC)	8,000,000.00
Combustion Turbine – Aero (CT)	1,125,000.00
Combined Cycle Gas Turbine (CCGT)	1,200,000.00
Nuclear (Npp)	8,000,000.00

Table 5.5 Transmission Line Investment Costs

Transmission Line Voltage (kV)	Cost ($/mi.)
115	750,000.00
230	956,900.00
345	1,339,867.00
500	1,913,801.00

With the load-growth scenarios and a realistic data set for network expansion costs defined, other parameters related to the candidate generators and candidate line types were determined. Existing test system data for the system under study was used for the generation and transmission candidates. The candidate generators were assigned maximum

and minimum outputs and these values along with the total investment cost for each unit is shown in Table 5.6.

Table 5.6 Candidate Generator Descriptions

Generator Type	$P_{G,MAX}$ (MW)	$P_{G,MIN}$ (MW)	Total Cost ($)
IGCC	350	140	2.800×10^9
CT	100	25	112.5×10^6
CCGT	197	68.95	236.4×10^6
Npp	400	100	3.200×10^9

Table 5.7 shows the transmission line ratings selected for each voltage level, with the maximum output of the selected generators kept in mind during the selection and assumptions of line length of 50 mi., 100 mi, and 150 mi. for the voltage levels of 115 kV, 230 kV, and 345/500 kV, respectively.

Table 5.7 Candidate Transmission Line Descriptions

Transmission Line Voltage (kV)	Rate A (MW)	Rate C (MW)	Total Cost ($)
115	157	198	37.5×10^6
230	315	393	95.69×10^6
345	360	540	50.98×10^6
500	450	562.5	137.07×10^6

5.3 Test System Descriptions

5.3.1.Short-Term Simulation Test Systems

The example power system under consideration was a modified version of the IEEE 14-bus system [104], which is shown in . The modifications included the addition of representative distribution systems [105] to which the water system pumping station loads were mapped because WDS pumping stations are connected to the electric

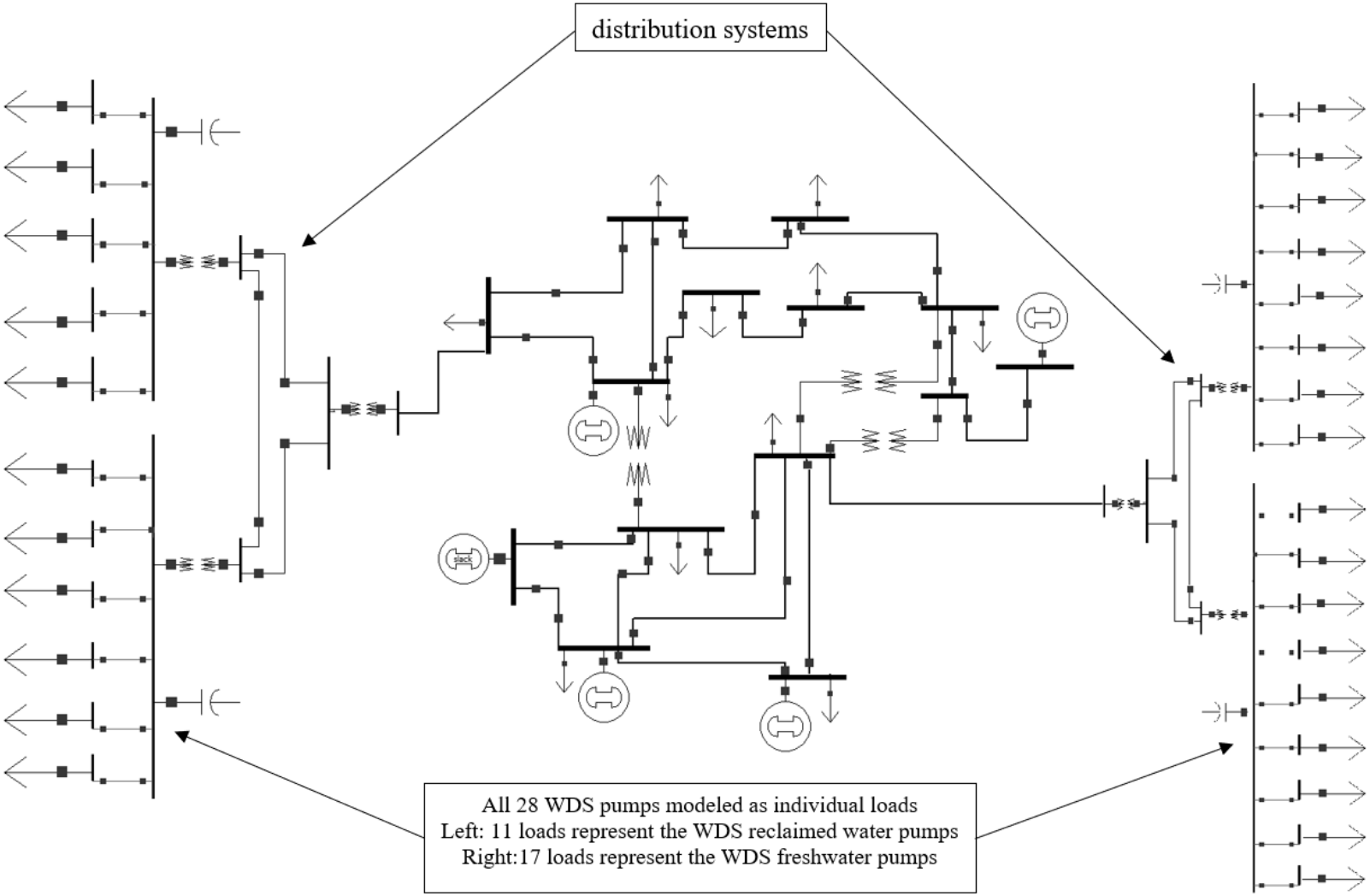

Figure 5.11 Short Term Simulation EPS Test System

power distribution system. In order to account for that and take into consideration thermoelectric generation that is in the bulk power system, the model presented in this section includes both levels of the system (transmission and distribution) in the network model. Data for the distribution systems was generated from the IEEE 34-bus test distribution system [106] by first converting the phase data to the sequence domain and then using the positive sequence results within both the AC and DC network models. This approach is equivalent to modeling the sub-transmission system voltages and above for all of the system except where the critical interdependencies of the power system with the water system lie. From [106], feeder configuration 300 was used for the line segments from nodes 802 to 806 and 812 to 814, which were chosen to represent segments between the high voltage bus and the distribution system transformers. The *Z* and *B* matrices are shown below.

$$Z = \begin{bmatrix} 1.3368+j1.3343 & 0.2101+ j0.5779 & 0.2130+ j0.5015 \\ 0.2101+ j0.5779 & 1.3238+ j1.3569 & 0.2066+j0.4591 \\ 0.2130+ j0.5015 & 0.2066+j0.4591 & 1.3294+ j1.3471 \end{bmatrix} \Omega/\text{mile} \qquad (5.7)$$

$$B = \begin{bmatrix} 1.9300+ j1.4115 & 0.2327+ j0.6442 & 0.2359+ j0.5691 \\ 0.2327+ j0.6442 & 1.9157+ j1.4281 & 0.2288+ j0.5238 \\ 0.2359+ j0.5691 & 0.2288+ j0.5238 & 1.9219+j1.4209 \end{bmatrix} \text{Siemens/mile} \qquad (5.8)$$

The transformation given in (3.9) was applied to both matrices and the (2,2) entry from each of the transformed matrices was selected and repeated here:

$$Z_{2,2} = 1.1201 + j0.8333\ \Omega/\text{mile} \qquad (5.9)$$

$$B_{2,2} = 0 + j\,6.1559 \text{ Siemens/mile} \tag{5.10}$$

A voltage of 69 kV was selected as a base value and along with the 100 MVA system complex power base and the distances given for these line segments, pu values for each segment quantity were found as

$$Z_{2,2,pu} = \frac{Z_{2,2}}{Z_{base}} \cdot length = 0.1325 + j0.0985 \text{ pu} \tag{5.11}$$

$$B_{2,2,pu} = B_{2,2,pu} \cdot Z_{base} \cdot length = j\,0.0017 \text{ pu} \tag{5.12}$$

between nodes 802 and 806 and values below between nodes 812 and 814.

$$Z_{2,2,pu} = \frac{Z_{2,2}}{Z_{base}} \cdot length = 0.0077 + j0.0057 \text{ pu} \tag{5.13}$$

$$B_{2,2,pu} = B_{2,2,pu} \cdot Z_{base} \cdot length = j0.0001 \text{ pu} \tag{5.14}$$

The distribution system data consisting of network topology and the series resistance and reactance along with the shunt susceptance values are shown in Table 5.8. This approach satisfies the need for transmission system level modeling to include thermoelectric generation along with the need to include the distributions system for capturing the WDS dependency on the EPS.

Other modifications included assigning generators in this test system the fuel types as shown in Table 5.9. The generator types available were chosen to be: Nuclear (Npp), coal fired (IGCC), Aero-derivative Combustion Turbine (CT), and Combined Cycle Gas

Table 5.8 Distribution System Data

	Line From Bus	Line To Bus	x	r	b
1	13	15	0.0800	0.0100	-
2	15	16	0.1325	0.0985	0.0017
3	15	17	0.1325	0.0985	0.0017
4	16	17	0.0770	0.0057	0.0001
5	16	18	0.0480	0.0190	-
6	17	19	0.0480	0.0190	-
7	14	31	0.0800	0.0100	-
8	31	32	0.1325	0.0985	0.0017
9	31	33	0.1325	0.0985	0.0017
10	32	33	0.0770	0.0057	0.0001
11	32	34	0.0480	0.0190	-
12	33	35	0.0480	0.0190	-

Turbine (CCGT). The minimum and maximum values were based on the nominal load in the IEEE 14-bus test system and given ratios equal to a recent estimate of the current portfolio of generation [107], excluding renewables. For use in other modeling aspects of the simulator, it was assumed, and stated here, that the Npp and IGCC plants are base load units while the units with gas turbines are the peaking units.

Table 5.9 Generator Data for Short Term Simulation

	Generator	Generator Bus	$P_{g,min}$ (MW)	$P_{g,max}$ (MW)
1	IGCC	1	55	89
2	Npp	2	40	66
3	CT	3	17	27
4	CT	6	17	27
5	CCGT	8	34	55

The test system for the WDS is shown in Figure 5.12. The interdependencies of the electric power system within the water system are expressed spatially in the simulation by the addition of power plant nodes in the water system to which the make-up water requirements at each iteration of the simulation can be expressed as node demands. The cooling water for the power plants is supplied from both a freshwater source and a

reclaimed wastewater source, denoted by the wastewater treatment plant (WWTP) in Figure 5.12. There is a total of 17 freshwater pumps and 11 reclaimed water pumps in the WDS, with 22 of them servicing the five power plants in the EPS. Each power plant in the system is equipped with water storage equivalent to 2-weeks-worth of average water consumption.

Figure 5.13 explicitly shows two views on how the generators in the EPS test system were mapped to the WDS and how the pumping stations within the WDS test system were mapped spatially to the EPS. The dashed lines show the connections between generators in the EPS (Gen x) and their nodes in the WDS (PWx).

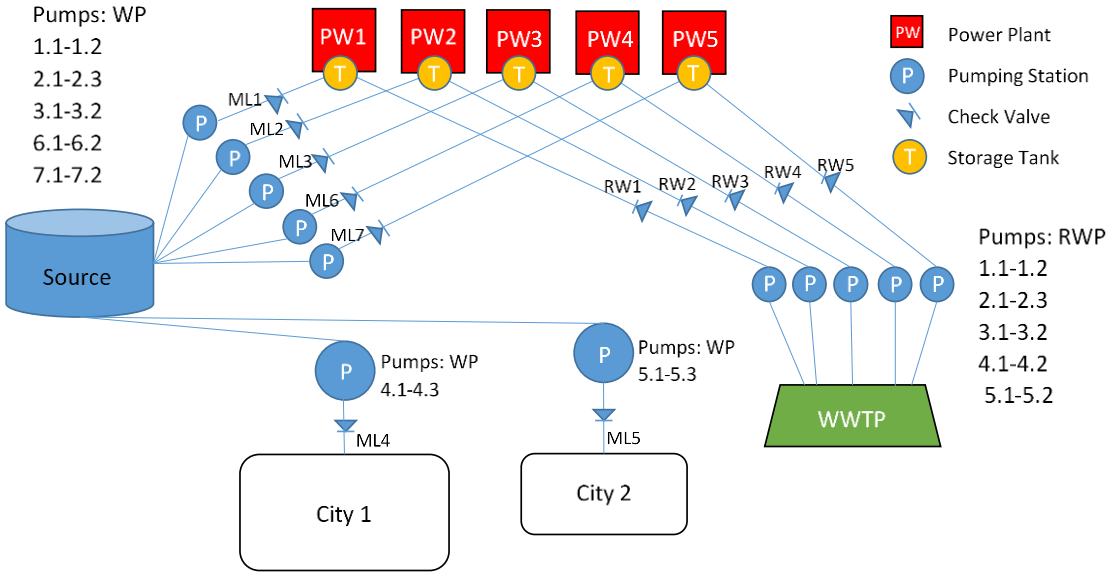

Figure 5.12 Short Term Simulation WDS Test System

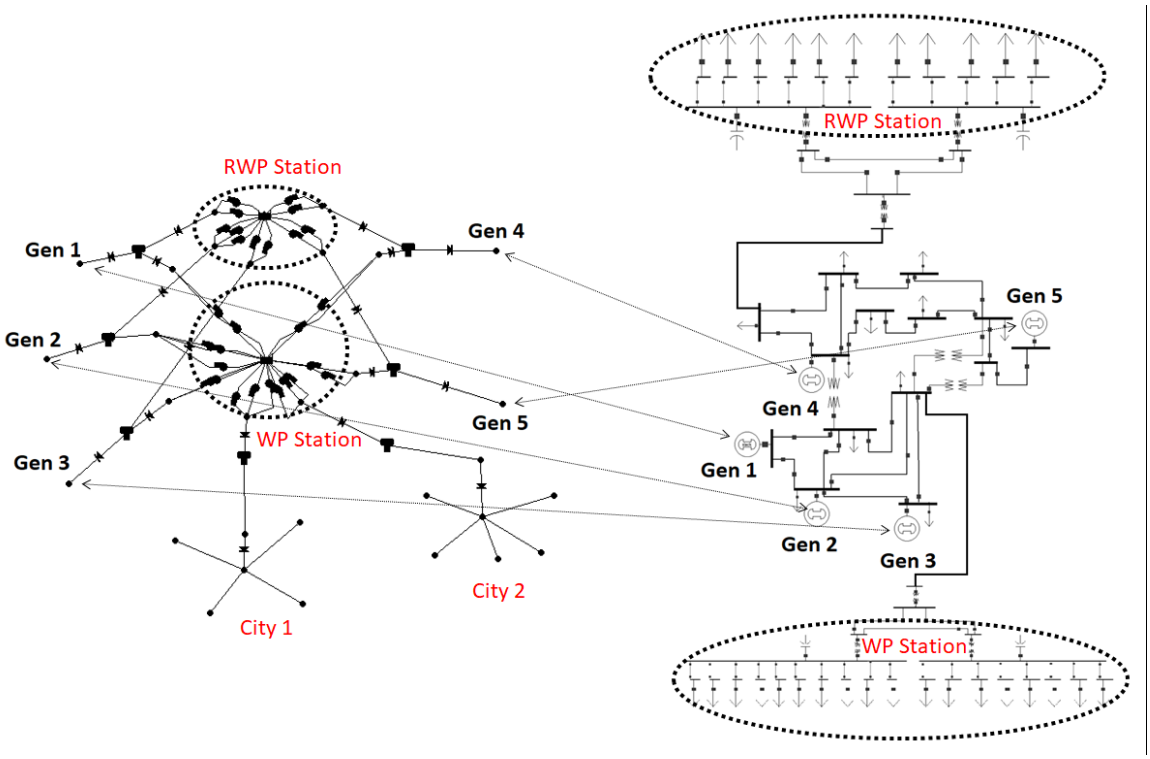

Figure 5.13 EPS and WDS Test System Spatial Relationship

5.3.2.Long-Term Simulation Test System

The test system used for the implementation of the planning model was a modified version of the three-area, 73-bus RTS96 test system [101]. This test system was designed for testing new algorithms and analysis methods and is not modeled after a real system. The nominal data has been modified and these modifications will be summarized. The continuous and short-term emergency MVA ratings of the transmission lines have been reduced by 10 percent and are shown below.

The generators were assigned one of nine types and the data for each type is summarized in the table below. Regulation up and regulation down were given costs equal to 5% and 4% of the largest marginal fuel cost value, respectively.

Table 5.10 Modified Branch Data

Line Type	Branch Number	Rate A (MVA)	Rate C (MVA)
1	1,10,41,50,78,87	157.5	180
2	2,3,4,5,6,8,9,11,12,13,14 42,43,44,45,46,48,49,51,52,53 79,80,81,82,83,85,86,88,89,90	157.5	198
3	24,62,99	315	393.75
4	7,15,16,17,18,47,54,55,56,57,84 91,92,93,94	360	540
5	19,20,21,22,23,25,26,27,28,29, 30,31,32,33,34,35,36,37,38,39, 40,58,59,60,61,63,64,65,66,67, 68,69,70,71,72,73,74,75,76,77, 95,96,97,98,100,101,102,103,104 105,106,107,108,109,110	450	562.5
6	111,112,113,114,115,116,117	649.8	803.7

Spinning reserve was given a cost of 2.5% of the largest marginal cost value while non-spinning reserve was assumed to be 1.5% of the marginal cost value.

Table 5.11 Modified Generator Data 1/2

	Fossil 1	Fossil 2	Fossil 3	Fossil 4	Fossil 5
$P_{g,max}$	12	100	155	197	350
$P_{g,min}$	2.4	25	54.25	68.95	140
RREG	5	35	0	15	0
RSPIN	10	70	30	30	40
RNSPIN	0	0	0	0	0
Fast Start	0	0	0	0	0
AGC	1	1	0	1	0
R_{hr}	12	100	155	180	240
RSU	12	100	155	197	350
RSD	12	100	155	197	350
CSU	571.2	4754.40	1696.34	6510.00	7953.04
CNL	72.68	839.45	252.67	1159.93	358.23
CREGUP	5.55	4.15	0	4.04	0
CREGDN	4.44	3.32	0	3.23	0
CSPIN	2.78	2.07	0.42	2.02	0.43
*CNSPIN*t	0	0	0	0	0

Table 5.12 Modified Generator Data 2/2

	Combustion Turbine	Combined Cycle	Hydro	Nuclear
$P_{g.max}$	20	76	50	400
$P_{g.min}$	15.8	15.2	0	100
RREG	15	0	50	0
RSPIN	20	20	50	200
RNSPIN	20	0	50	0
Fast Start	1	0	1	0
AGC	1	0	1	0
R_{hr}	20	76	50	400
RSU	20	76	50	400
RSD	20	76	50	400
CSU	75.85	1068.88	0	2400
CNL	1138.68	130.63	0	215.08
CREGUP	10.94	0	0	0
CREGDN	8.75	0	0	0
CSPIN	5.47	0.59	0	0.14
*CNSPIN*t	3.28	0	0	0

The cost information for each of the generator types is summarized in the table below.

Table 5.13 Piece-wise Linear Cost Curve Information

	P_{gt1}	$C_{g,1}$	P_{gt2}	$C_{g,2}$	P_{gt3}	$C_{g,3}$	P_{gt4}	$C_{g,4}$
Fossil 1	2.40	85.50	3.60	86.77	3.60	98.01	2.40	111.04
Fossil 2	25.00	67.95	25.00	73.15	30.00	79.13	20.00	82.97
Fossil 3	54.25	14.71	38.75	15.20	31.00	15.84	31.00	16.70
Fossil 4	68.95	70.12	49.25	74.20	39.40	77.49	39.40	80.81
Fossil 5	140.00	14.96	87.50	15.83	52.50	16.45	70.00	17.39
Combustion Turbine	15.80	149.56	0.20	153.81	3.80	216.51	0.20	218.86
Hydro	0.00	0.00	50.00	0.00	0.00	0.00	0.00	0.00
Combined Cycle	15.20	17.00	22.80	17.74	22.80	20.61	15.20	23.69
Nuclear	100.00	5.31	100.00	5.38	120.00	5.53	80.00	5.66

The system one-line diagram is shown in Figure 5.14 below.

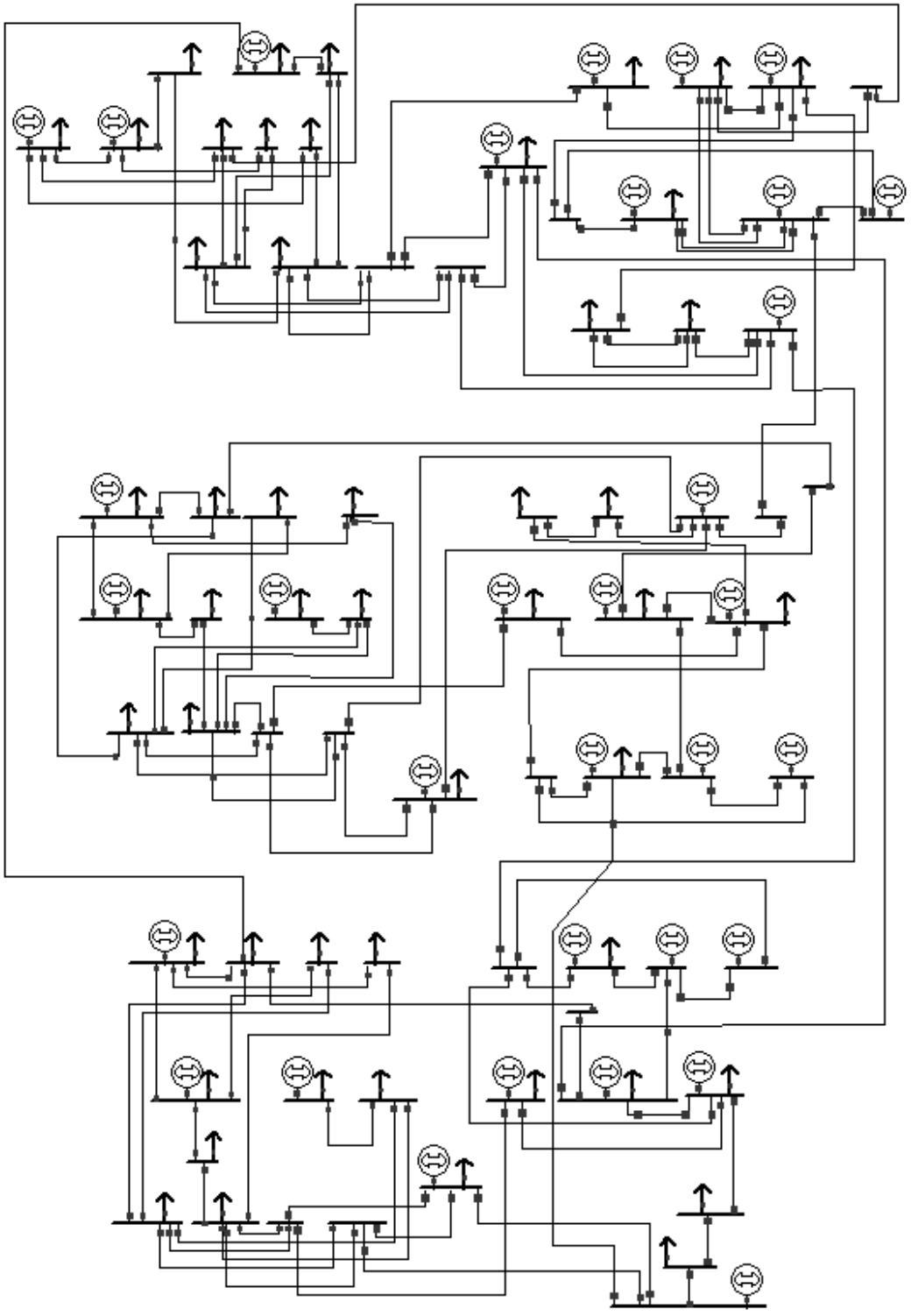

Figure 5.14 Test System for System Planning Model

5.4 Short-Term Thermoelectric Generation Control Policies

5.4.1. Unit Derating

The implementation of the empirical derating scheme detailed in Section 4.4.2 is straight forward in its application as the formula in (4.128) can be used directly. The output of the LP model described in Section 4.4.1, on the other hand, requires post-processing which is done through the averaging of two sets of data, as follows. First, the results for the 24 time-periods within the LP are averaged followed by the averaging of the previous 24 simulation time-period $P_{g,max}$ values, for each unit. Mathematically, this is accomplished by:

$$P_{max,i,g}^{*} = ave_{non\text{-}zero}\,(P_{1:24,g}) \tag{5.15}$$

$$P_{max,i,g} = ave(P_{max,\text{i-24:i-1},g} + P_{max,i,g}^{*}) \tag{5.16}$$

Additionally, the weight in (4.126), W_{derate}, was determined through sensitivity analysis and set to a value of 0.02 in all of the following simulations and results. The figure below shows plots of normalized tank level, which the unit is de-rated based upon, along with the normalized $P_{g,max}$ values for a comparison of the two models.

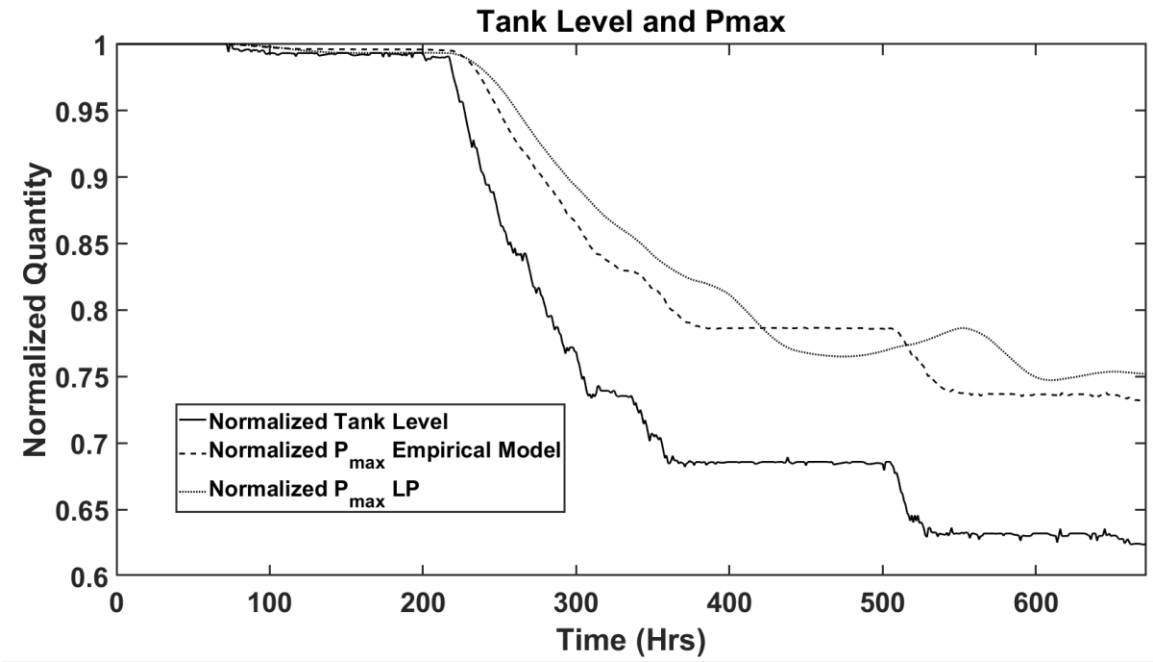

Figure 5.15 Comparison of Derating Schemes

As can be seen, both the empirical model as well as the more formal LP based derating scheme exhibit the desired behavior. This behavior includes tracking the tank level as it changes. As can be seen, due to the averaging that is done in post processing the data from the LP model, there is some lag between the storage tank level dropping and when the $P_{g,max}$ value starts to decrease. The LP model is what was included in the final implementation for combined simulations.

5.4.2. Operational Water Cost Adjustment

The setting of the operational water cost depends on the value that is used for the elasticity of water supply and this value was chosen as 0.08. The figure below shows the behavior of the incremental water cost to the ROC_t, $cROC_t$ and $C_{water,g}$ for a scenario during which the water storage tank level underwent the changes shown in Figure 5.17.

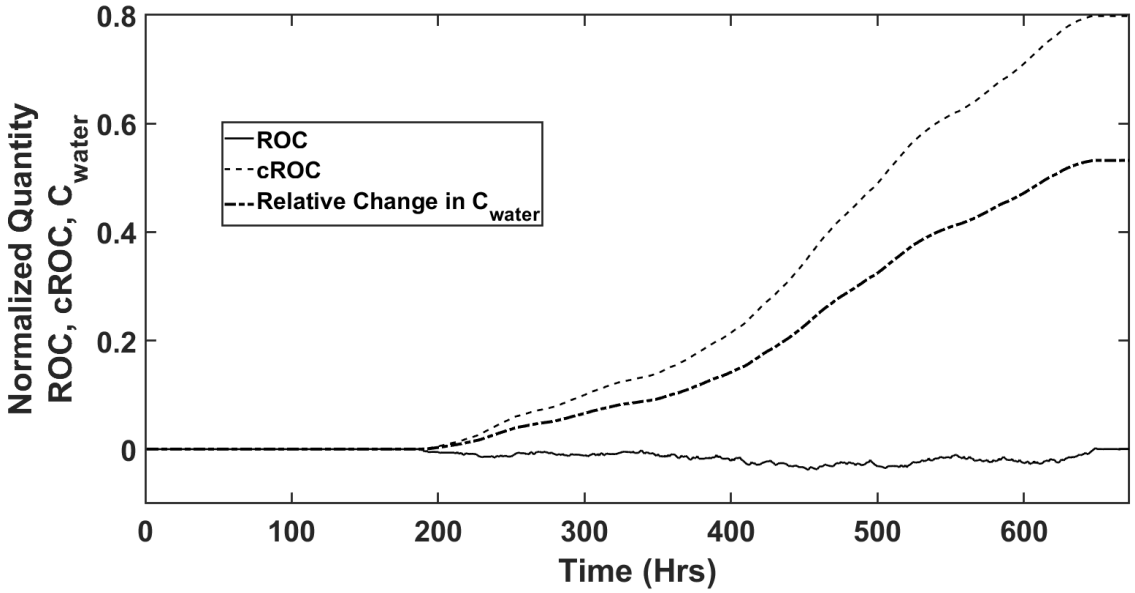

Figure 5.16 Implementation of Operational Water Cost Adjustment

The next figure shows the plots of fractional change in $C_{water,g}$ and the normalized tank level.

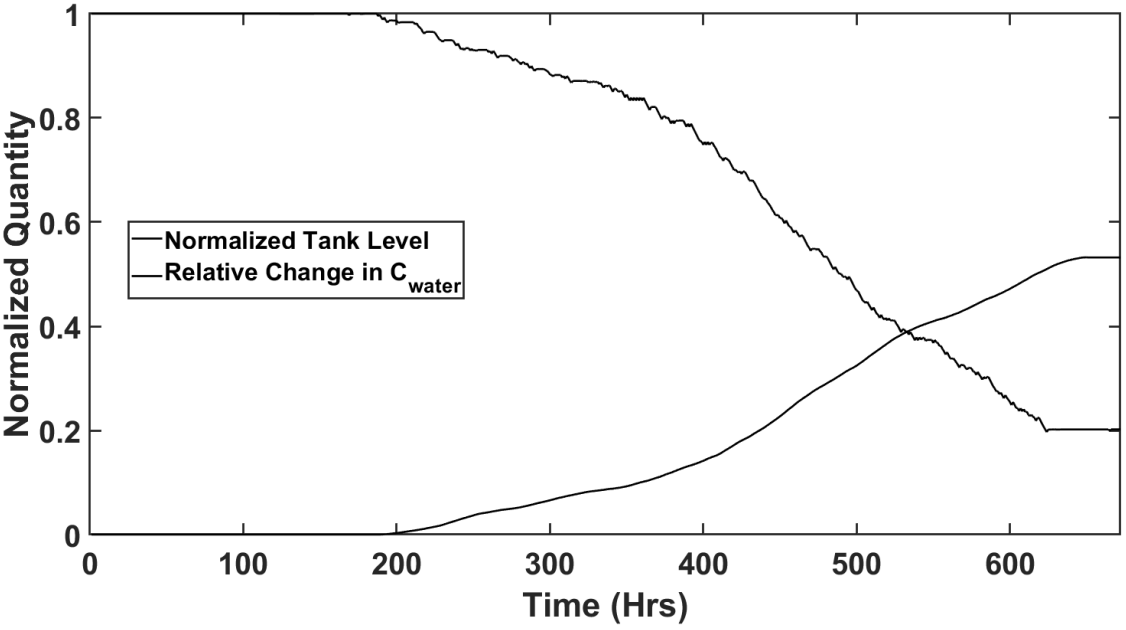

Figure 5.17 Comparison of Operational Water Cost and Onsite Tank Level

5.4.3.WDS Demand Adjustment

The purpose of the second WDS demand adjustment factor is to help drive the onsite storage tank level back to zero. Figure 5.18 shows how, in theory, a storage tank would refill if its only node demand in the WDS was that represented by $WDS_{DA,2}$. The effect of the refill time constant, $TC_{tankRefill}$, is also demonstrated in this figure.

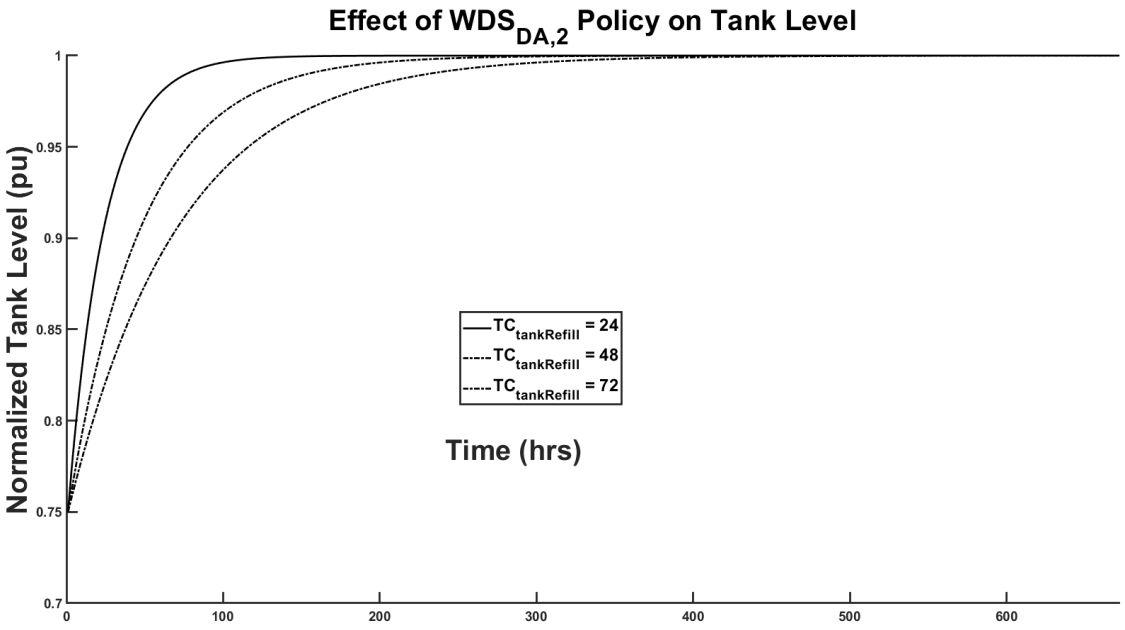

Figure 5.18 Tank Level Refill as a Function of $WDS_{DA,2}$ and $TC_{tankRefill}$ Parameter

The figure below shows the plots of the normalized tank level as well as the demand adjustment factor, on different ordinate scales. The main takeaway from the lower figure that plots WDS_{DA} is that there are two clearly visible components. The first is a gradual, slow increase in the demand adjustment factor. This corresponds to the corrective action because of (4.134) and as demonstrated above. The high frequency component in the figure

is the result of (4.133), which captures the time-period to time-period variations resulting from the thermoelectric cooling water make-up requirements being met or not.

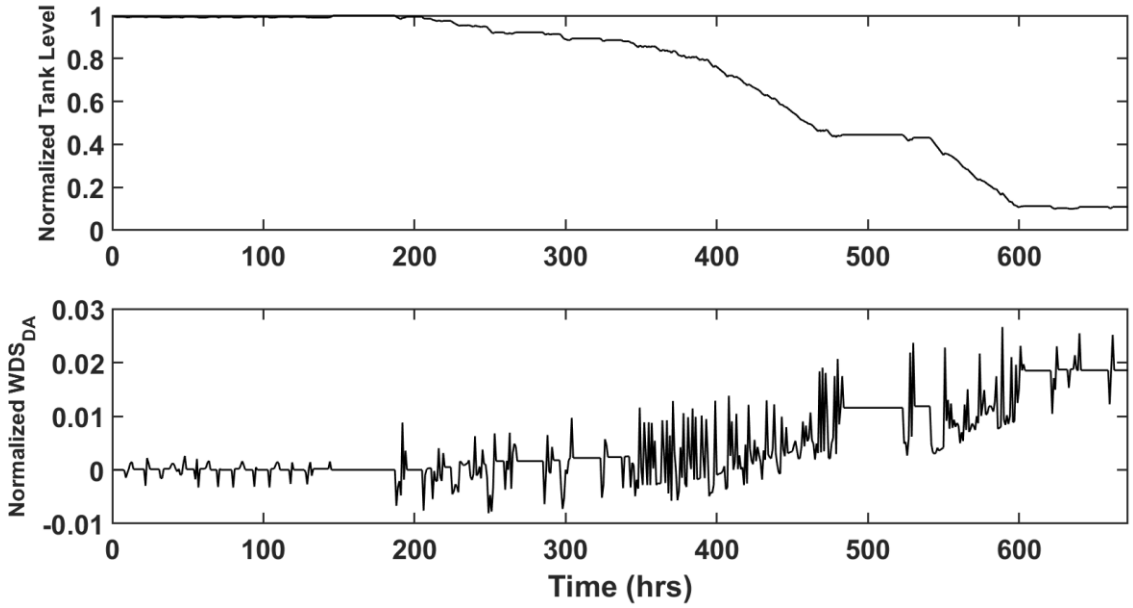

Figure 5.19 Onsite Storage Tank Level and WDS Demand Adjustment Factor (Bottom)

5.5 Summary

This chapter has detailed the simulation methodologies and given justification and examples for the proposed control policies. The test power system used for the planning simulation was described and details pertaining to the test EPS and WDS systems for use in the operation time-scale simulation were also given. The next two chapters present case studies to examine the performance of the presented models and policies for the operation and future expansion of the test systems.

CHAPTER 6

CASE STUDY AND RESULTS DISCUSSION – SHORT-TERM MODEL

This chapter presents case study results for the combined simulation of the water distribution system and electric power system. The case study is performed using the WDS and EPS test systems fully described in chapter 5. The scenario results provide a look at how the different policies can positively affect the operation of the two systems under extreme conditions. Comparisons showing the effects of the CEED implementation and operational water cost are presented and the application of the simulation methodology to a larger test system is shown. A sensitivity analysis is also shown which demonstrates that altering generation dispatch can result in lower overall system operating costs for the assumed system set-up.

6.1 Summary of Scenarios

This chapter presents three case studies as well as a demonstration of sensitivity analysis performed on the most extreme case. The test systems are the modified IEEE 14-bus system for the electric power system and the fictional WDS system presented in the previous chapter. Many simulations were run, and the results were examined in order to find extreme conditions that affected the operation of the two systems. The simple test systems were seen to be robust in their operation and ability to withstand these extreme conditions. The following cases build upon each other and were selected to demonstrate how the presented control models and policies affect the operation of the system. The general overview of the cases is as follows:

Case I: Shortage of total water availability in the WDS

Policy: WDS demand pattern adjustment, Operational water cost adjustment

Case II: Extreme shortage of total water availability in the WDS combined with extended periods of outages for a selection of WDS pumps

Policy: WDS demand pattern adjustment

Case III: Extreme shortage of total water availability in the WDS combined with extended periods of outages for a selection of WDS pumps

Policy: WDS demand pattern adjustment, Operational water cost adjustment, Unit curtailment, Load shed, Time dependent weights for WDS demand pattern satisfaction

Case IV: Sensitivity analysis of CEED weight on Case III scenario

Policy: WDS demand pattern adjustment, Time dependent weights for WDS demand pattern satisfaction

Case V: Sensitivity analysis of generator active power output and onsite water storage tank levels to different policy implementations

Case VI: Application of methodology to a larger test system

6.2 Case I: Shortage of Total System Water Availability

This scenario is representative of extreme drought conditions that could result in the severe limitation of water within the WDS for extended periods of time. Because WDSs are not interconnected, this contingency within the WDS represents a system wide event. Figure 6.1 shows the plot of water availability within the WDS versus time for the two-week, 672-hour simulation. This amount represents an upper bound on the total water that can be supplied to all the demands at the different nodes within the WDS, including residential and power plant nodes. With a total water demand mean of around 150,000 gpm, the simulation is clearly divided into periods which represent more water than needed (beginning and end), shortage of water (end of week 1, week 3, start of week 4) and a period during which demands should be able to be satisfied (week 2).

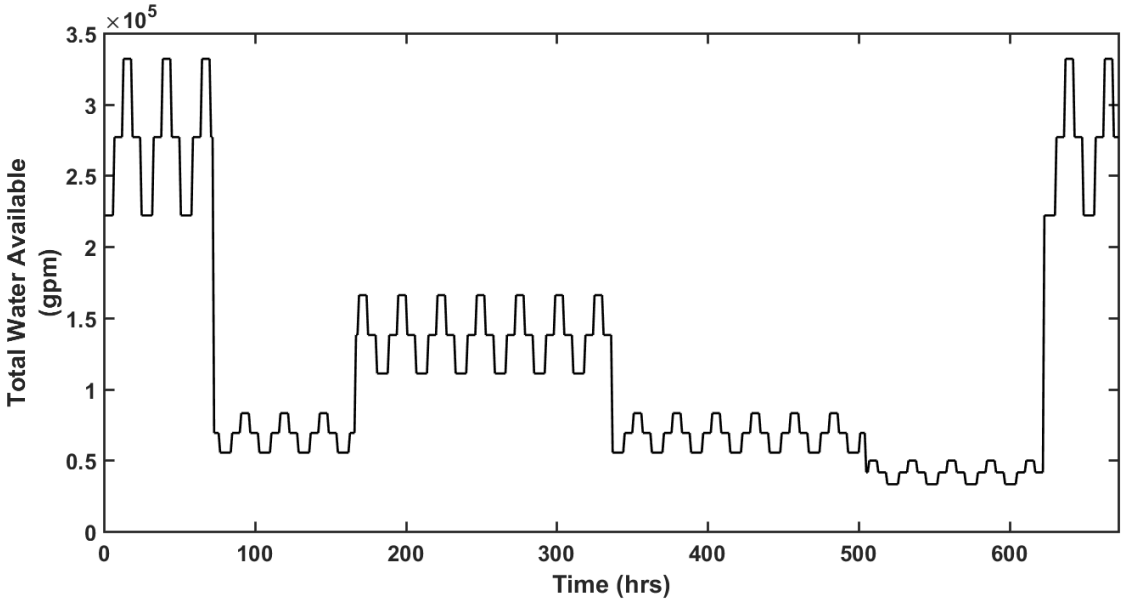

Figure 6.1 Case I-III Total WDS Water Availability

The simulation was run with a CEED $\delta_{fuelCost}$ weight of 0.7. The power outputs of the 5 units are shown below in Figure 6.2 and Figure 6.3. One of the policies that was

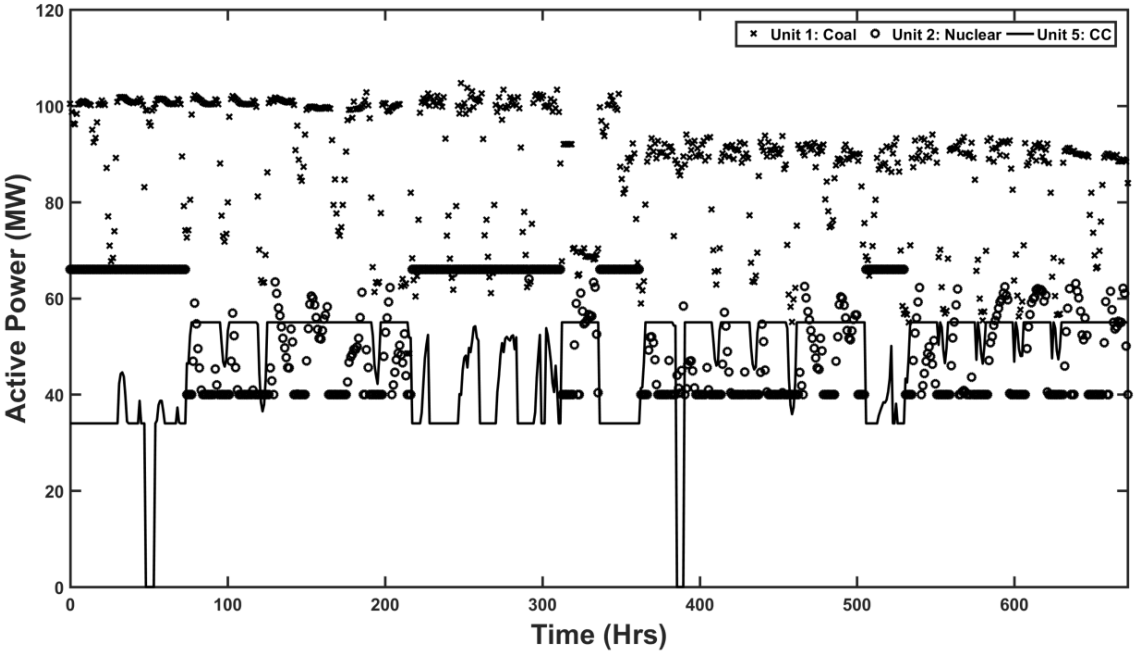

Figure 6.2 Case I Active Power Outputs, Generators 1, 2, and 5

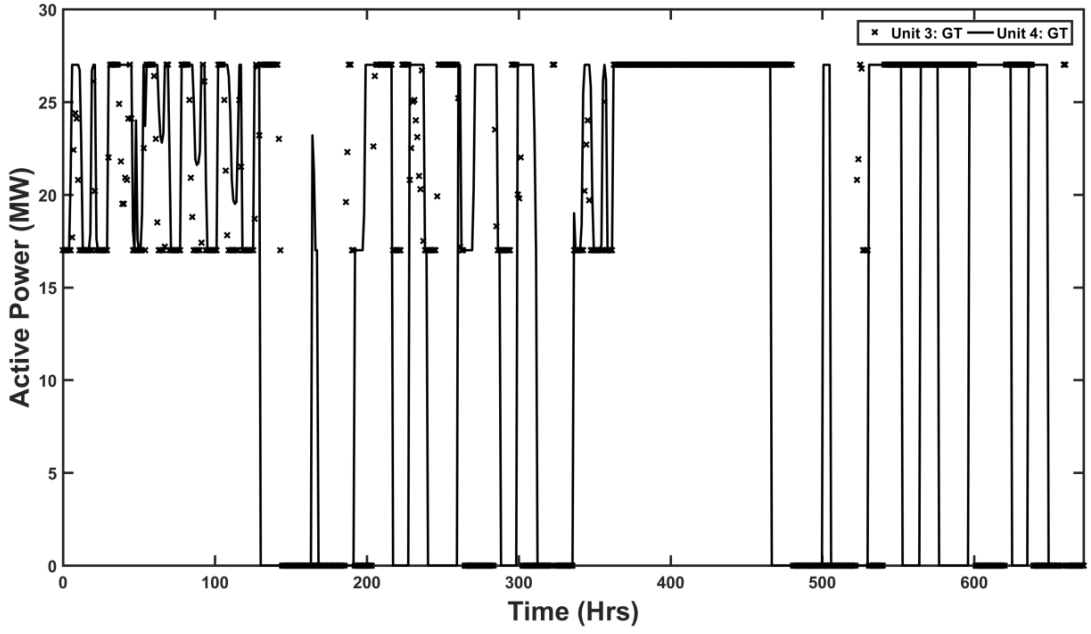

Figure 6.3 Case I Active Power Outputs, Generators 3, 4

implemented was the adjustment of the incremental cost of water. This can be seen to influence the dispatch of generation towards the end of the simulation as both Unit 1 and Unit 2 (coal and nuclear) are seen to have lower dispatches while the more expensive units (3, 4, 5) have higher dispatches because their operational water cost is comparatively less.

For completeness regarding quantities in the power system and for use in Chapter 8, the next two figures show the trends of all bus voltages and active power flows in the transmission elements in the system. The addition of the distribution system for the WDS pumps accounts for the number of curves in each plot.

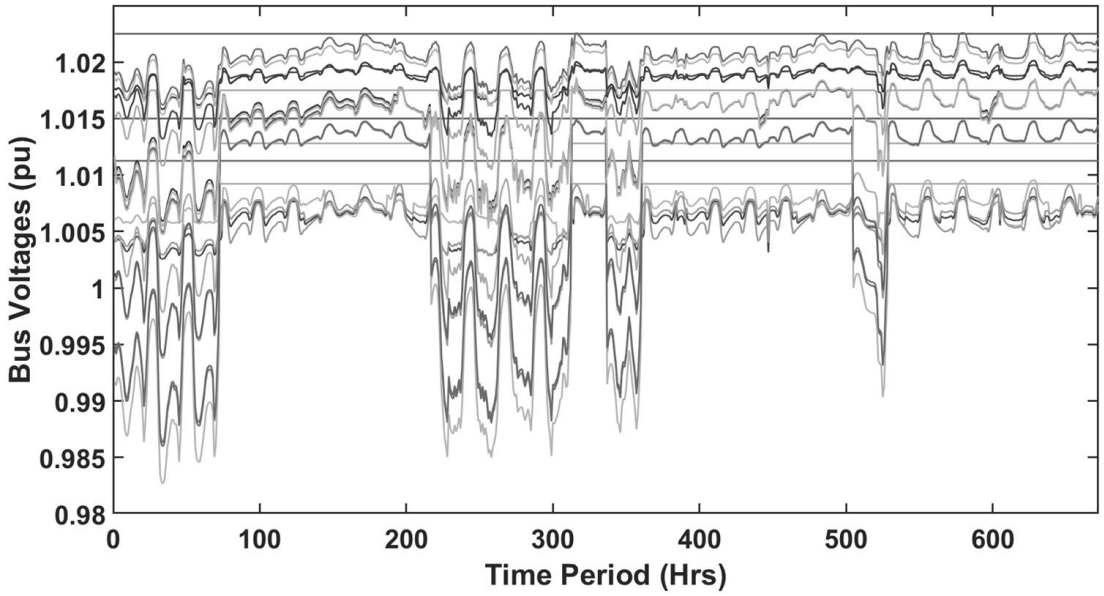

Figure 6.4 Power System Bus Voltage Profile

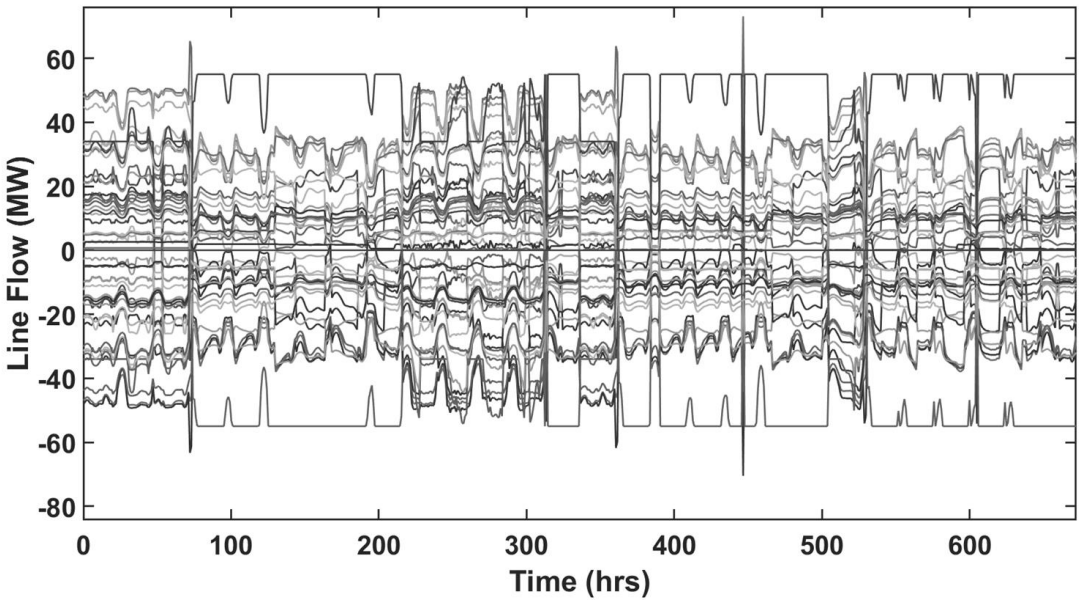

Figure 6.5 Power System Active Power Transmission Line Flows

The next figures show the cooling water make-up requirements of each unit as well as the supply of water from the WDS. Because only $WDS_{FD,1}$ (4.133) was implemented, the WDS is seen to oversupply the make-up requirements at times, but as will be seen shortly, these occasional oversupplies of demand do not significantly stop the onsite water storage tank levels from decreasing.

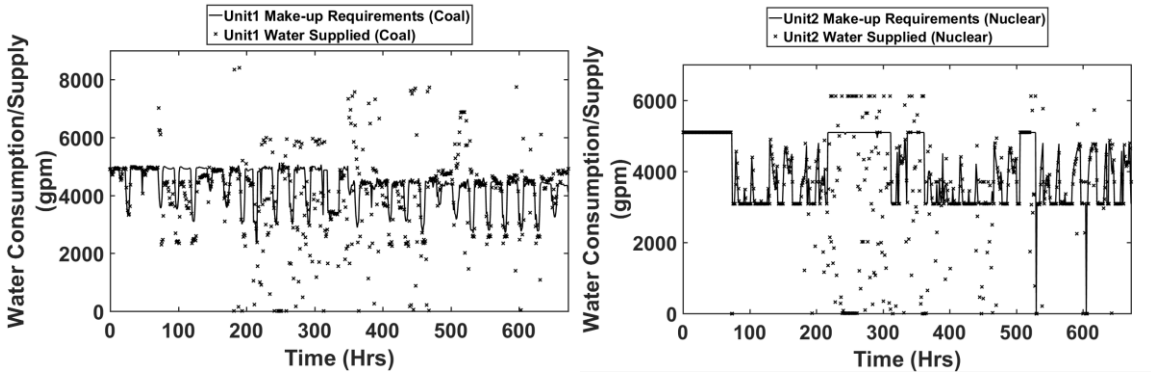

Figure 6.6 Unit 1(L) and 2(R) Cooling Water Requirements, Cooling Water Supplied

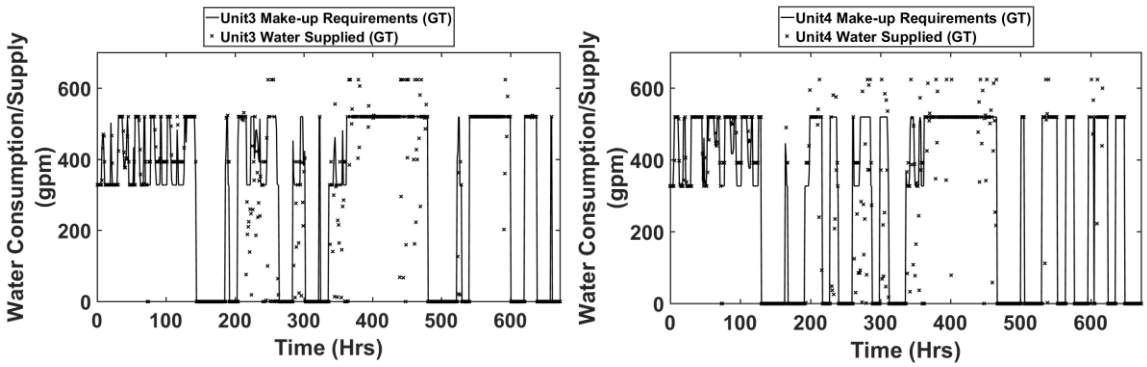

Figure 6.7 Unit 3(L) and 4(R) Cooling Water Requirements, Cooling Water Supplied

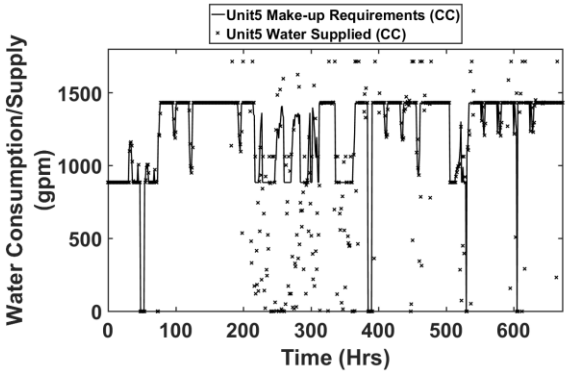

Figure 6.8 Unit 5 Cooling Water Requirements and Cooling Water Supplied

Unit 5 is supplied by the WDS with its cooling water requirements until about hour 210. This is during a period of high water availability within the WDS and therefore likely represents a time when the GA chose to satisfy other requirements within the WDS (due to pressure restrictions) rather than supply the required demand. The relationship between the quantities in the above plots is reflected by changes in the onsite water storage tank levels. The plots of tanks levels versus time are shown below. Unit 5 is seen to end the simulation with the lowest tank level, with its volume at 82.51% of its initial value.

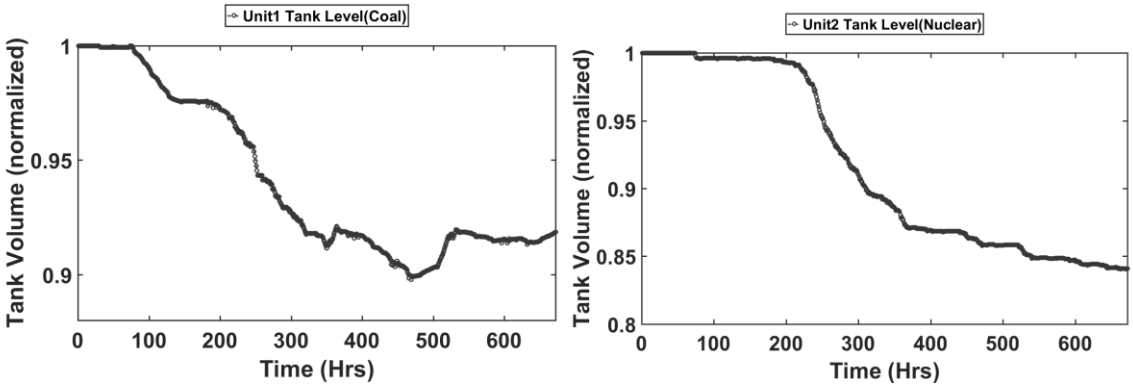

Figure 6.9 Unit 1(L) and 2(R) Onsite Water Tank Storage Levels

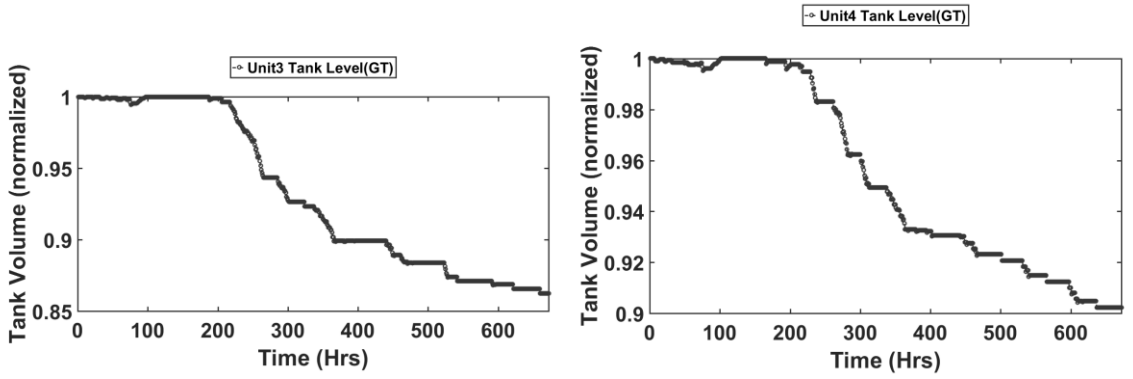

Figure 6.10 Unit 3(L) and 4(R) Onsite Water Tank Storage Levels

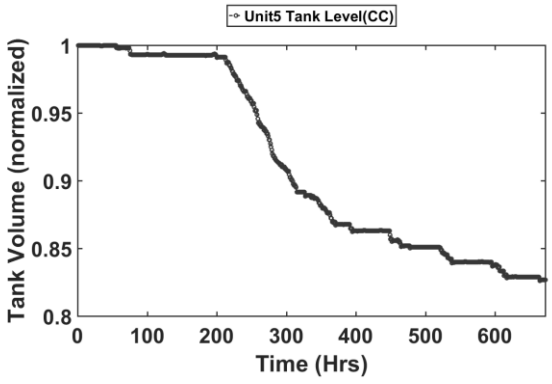

Figure 6.11 Unit 5 Onsite Water Tank Storage Levels

So, the tank levels for all the units are seen to decrease in value throughout the simulation while leveling off during the last two days of the simulation as the WDS system water availability increases and poses no limitation to the demand needing to be supplied.

In summary, the results of this case demonstrate that the generation dispatch can be influenced through the use of the operational water cost and that cooling water demands not being met by the WDS get reflected into future node demand values. This causes the WDS to oversupply water in some time-periods, but this is not enough to help the storage tanks to refill or even stop the tank levels from dropping. This issue will be addressed in the next two cases.

6.3 Case II: Shortage of Total System Water Availability and Long-Term WDS Pump Station Outages

This scenario is an extension of the extreme drought conditions that were examined in the previous case. Here, the addition of long-term power outages affecting the WDS pumping stations represent the more extreme system conditions. As discussed in the introduction, cases involving contingencies of both the water system and the power system have been observed historically. The hours during which the outages occurred in the simulation are shown below.

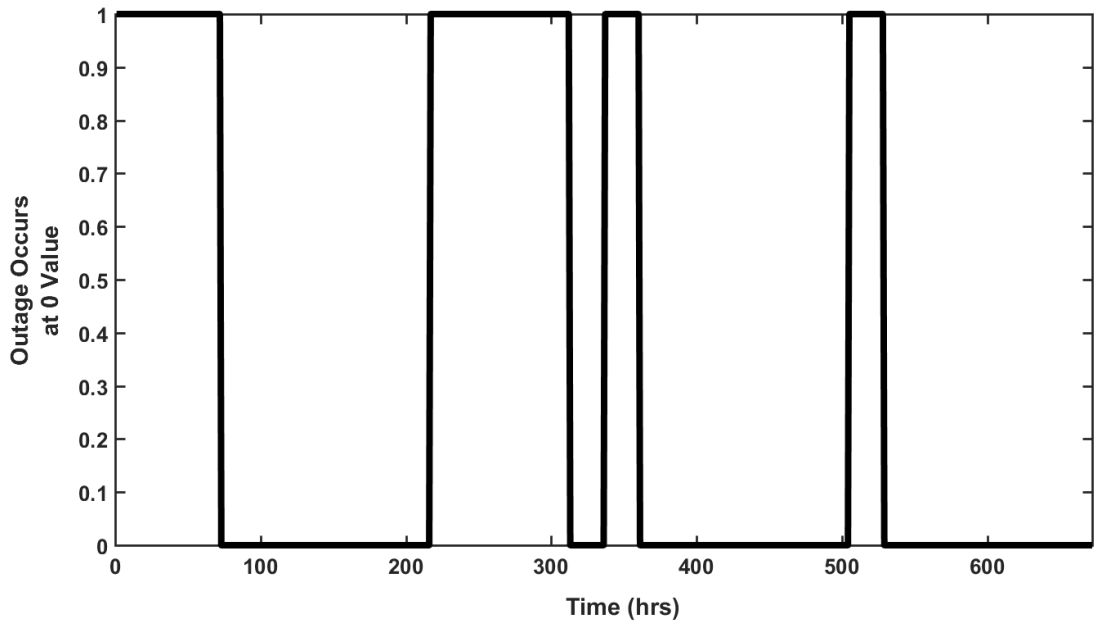

Figure 6.12 WDS Pump Outage Hours

This extreme contingency within the power system consists of several periods of long-term power outages where the two pumping stations experienced an outage which affected the freshwater pumping station supplying power plant 1 and the reclaimed water pumping station supplying power plant 2. The water availability is the same as was shown in Figure 6.1 and the figure and table below show the WDS pumps which were outaged and the physical location within the WDS.

Table 6.1 List of WDS Pumps to be Outaged

	Pump Name	WDS Node	EPS Bus
1	RWP2.1	1	22
2	RWP2.2	2	23
3	RWP2.3	3	24
4	WP1.1	6	36
5	WP1.2	8	37

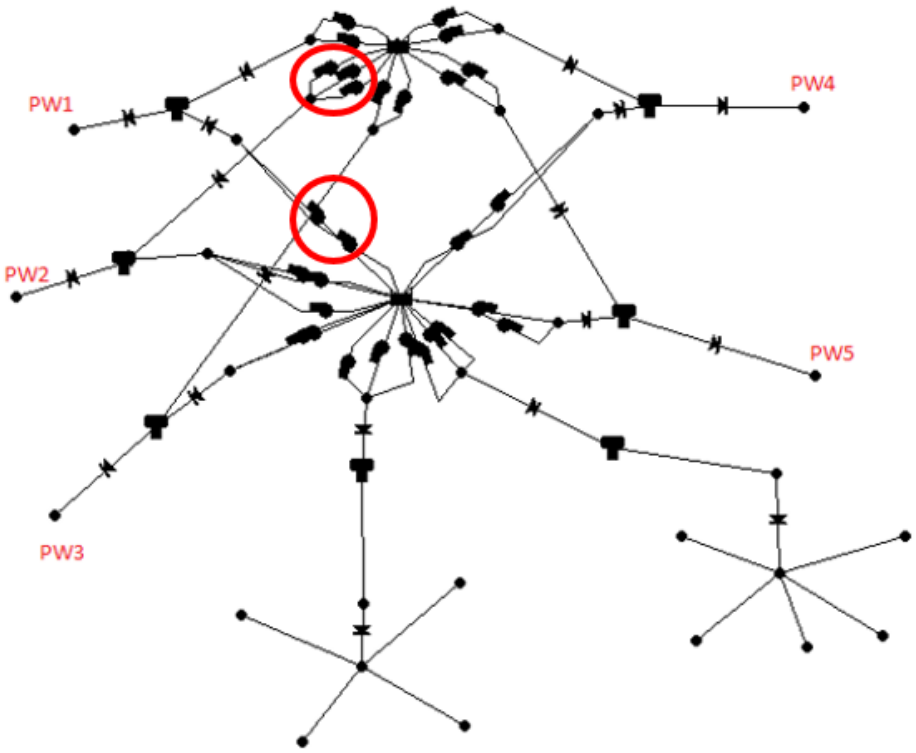

Figure 6.13 Location of Pumps to be Outaged

The plots of generator power outputs versus time are shown below. The simulation was run with a CEED $\delta_{fuelCost}$ weight of 0.9. The unit curtailment and operational water cost adjustments were not used. The WDS demands for the power plant nodes were altered using (4.133).

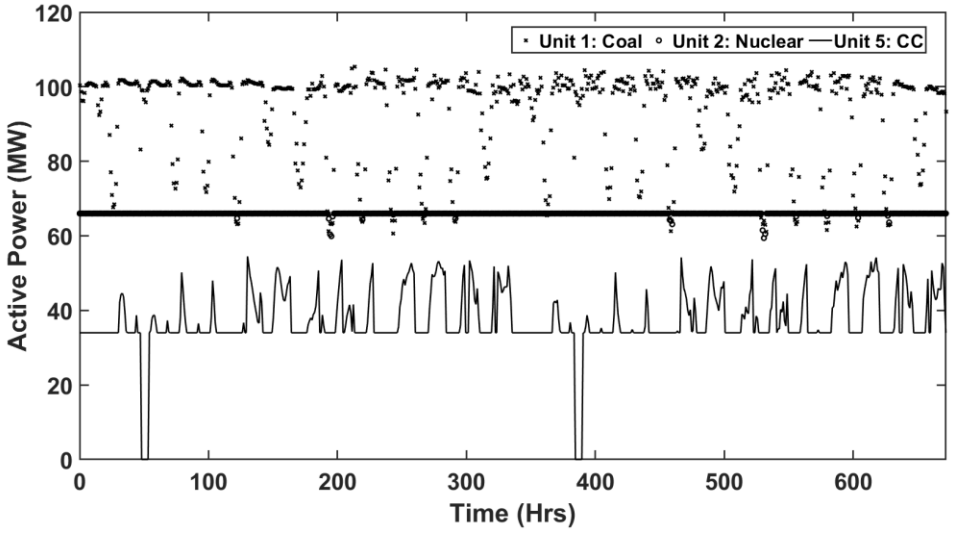

Figure 6.14 Case II Real Power Outputs, Generators 1, 2, and 5

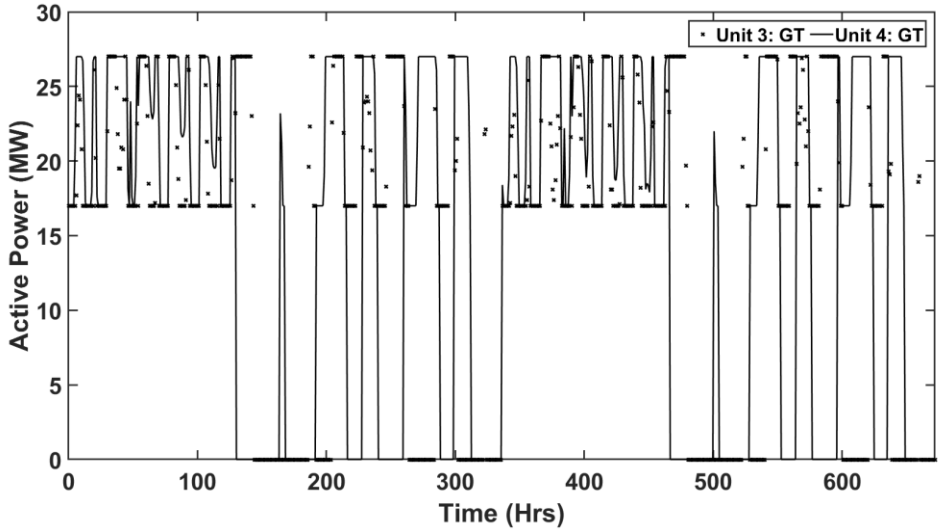

Figure 6.15 Case II Real Power Outputs, Generators 3, 4

As can be seen from Figure 6.14, the two units that have high water consumption values (coal and nuclear) are not seen to be dispatched at lower values as the simulation progresses. This is because there is no adjustment to the operational water cost and

therefore the cheapest units with respect to operational fuel costs will get dispatched. Figure 6.16 through Figure 6.21 shows plots of cooling water make-up requirements for all generators followed by each unit's onsite storage tank level versus time.

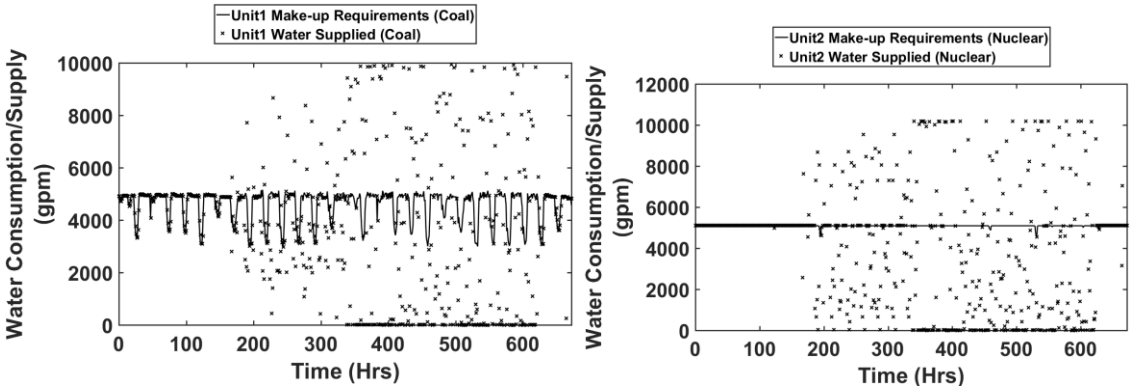

Figure 6.16 Unit 1(L) and 2(R) Cooling Water Requirements, Cooling Water Supplied

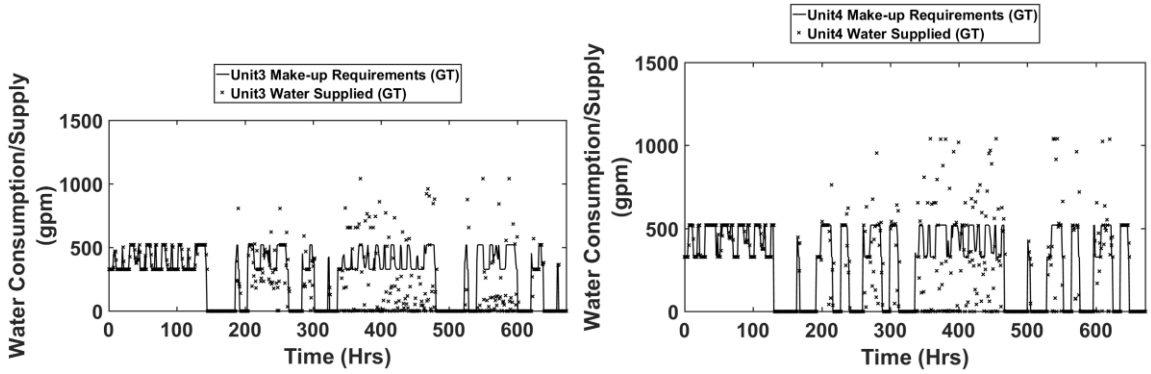

Figure 6.17 Unit 3(L) and 4(R) Cooling Water Requirements, Cooling Water Supplied

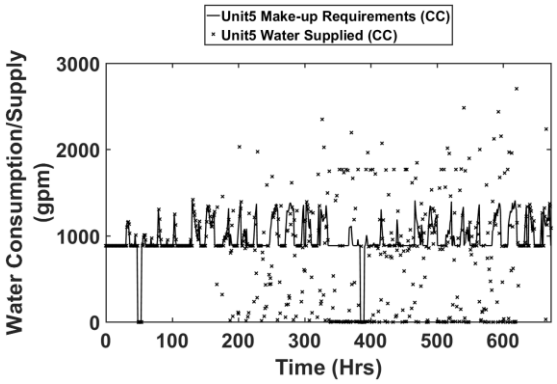

Figure 6.18 Unit 5 Cooling Water Requirements, Cooling Water Supplied

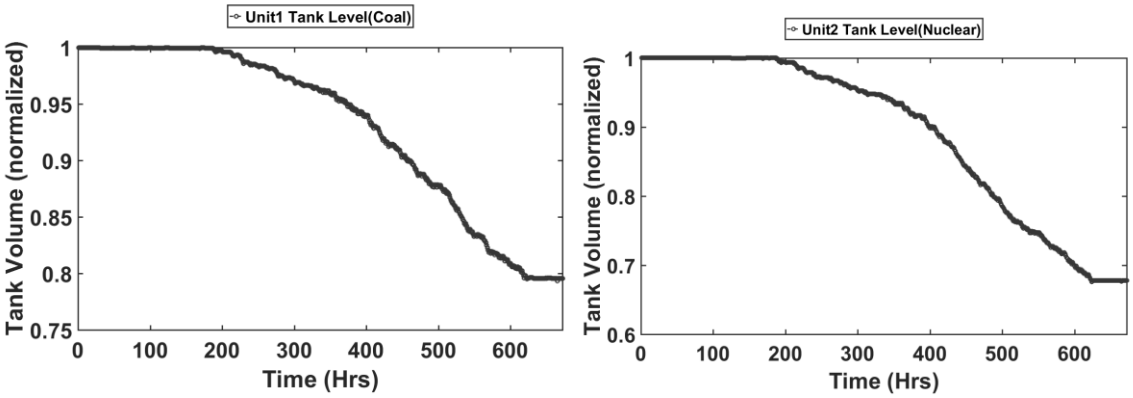

Figure 6.19 Unit 1(L) and 2(R) Onsite Water Tank Storage Levels

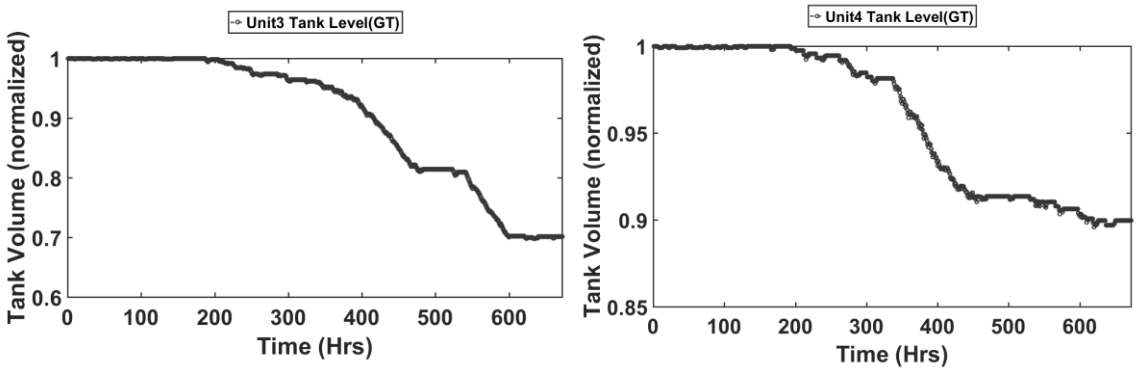

Figure 6.20 Unit 1(L) and 2(R) Onsite Water Tank Storage Levels

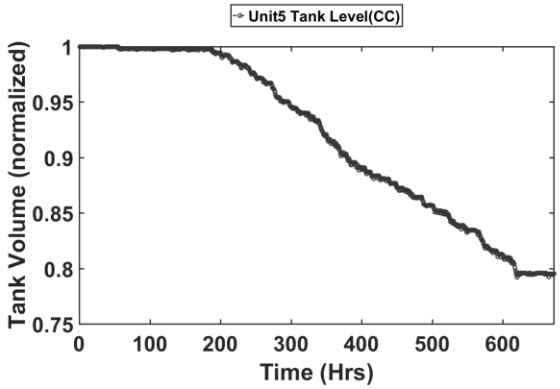

Figure 6.21 Unit 5 Onsite Water Tank Storage Levels

As can be seen, the severity of the contingency is reflected in the dramatic reduction in tank level value as compared with Case I. This is the result of the water system not being able to supply the make-up requirements from about hour 200 until the simulation hour 624, when the water restrictions are lifted. The figure below gives a glimpse of how the other demands in the water system were supplied during the simulation. Here, the supply to these demands is seen to not be met most obviously during the 200-350-hour range.

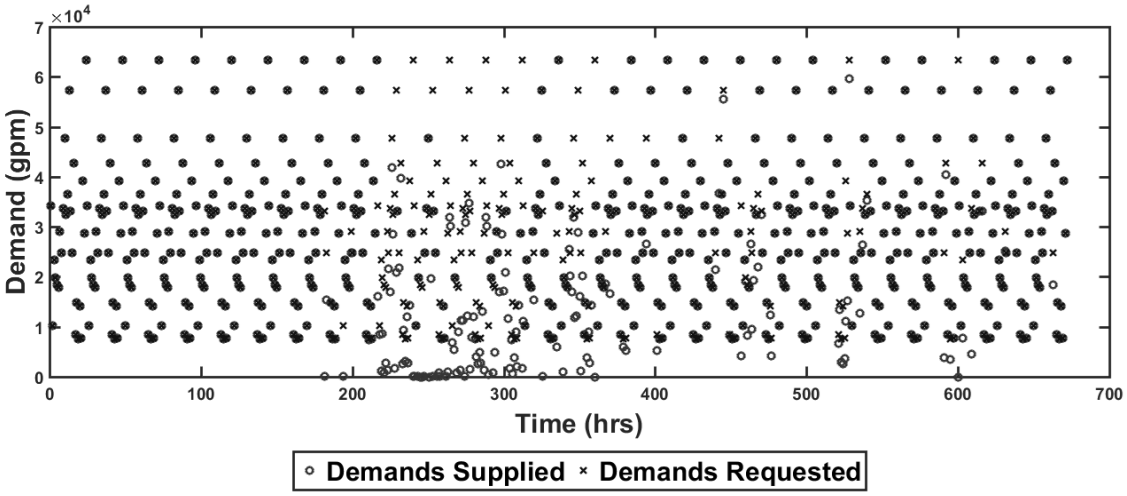

Figure 6.22 Residential Water Demands Supplied and Water Demands Requested

Lastly, as a comparison of how the WDS supply to the power plants suffered as a result of the pump outages experienced in the water system, the following figures demonstrate the demand deficits experienced by units 1 and 3. The demand deficit is the make-up requirement less the supplied value. The much larger deficits for Case II contribute directly to the Case I to Case II reductions in final tank levels of units 1 and 3 of 0.1274 pu and 0.1591 pu, respectfully. The reasons for this are two-fold. First, the pump outages directly affect water that is delivered by the WDS to Unit 1. This is further exacerbated by the fact the dispatch is not altered by the operational water cost adjustment, as in Case I, which is sensitive to the cooling water demands not being met and would reduce the dispatch in a situation like Case II.

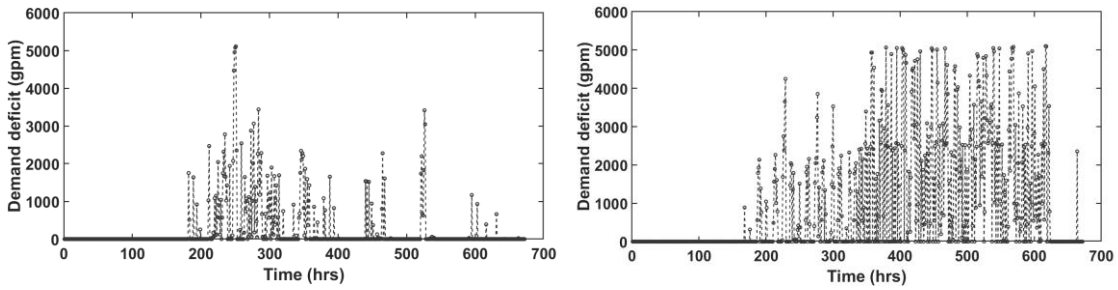

Figure 6.23 Unit 1 Cooling Water Demand Deficits, Case I (L) and Case II (R)

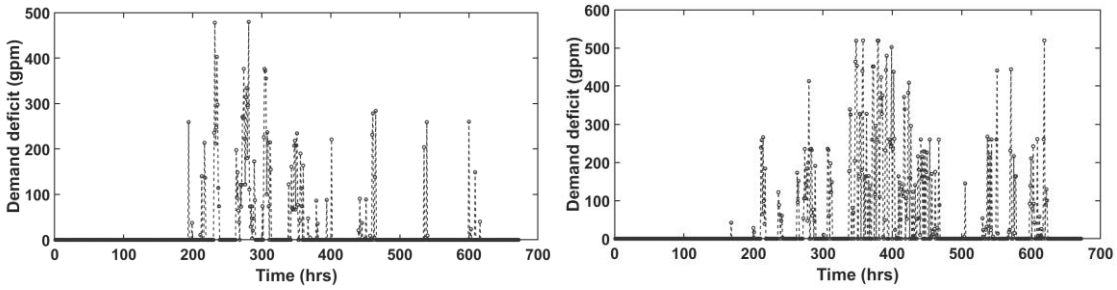

Figure 6.24 Unit 3 Cooling Water Demand Deficits, Case I (L) and Case II (R)

6.4 Case III: Shortage of Total System Water Availability and Long-Term WDS Pump Station Outages, All Policy Implementations

This study case is meant to exemplify the system performance under extreme conditions with all the controls and presented policies in place. The scenario set-up for contingencies is the same as in Case II, with water availability as defined in Figure 6.1 and power outages affecting WDS pumps as in Figure 6.12. The plot of unit real power output for all five units are shown in Figure 6.25 and Figure 6.26.

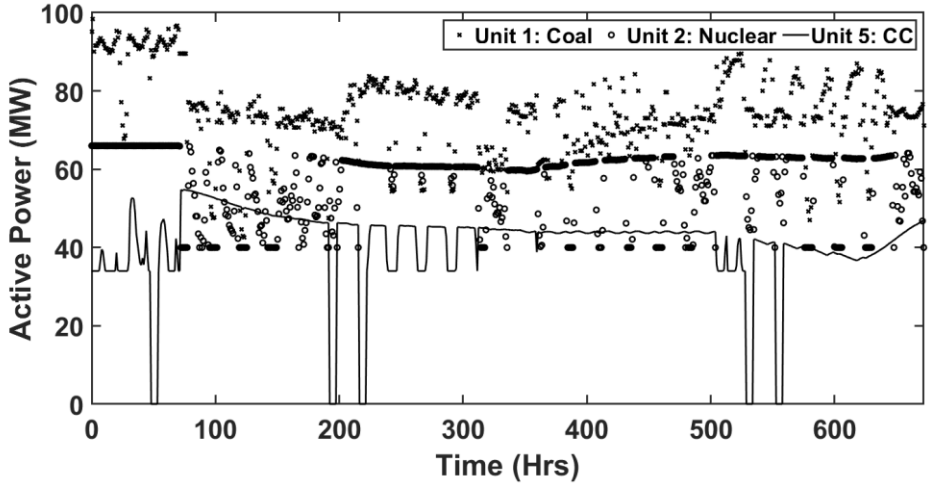

Figure 6.25 Case III Real Power Outputs, Generators 1, 2, and 5

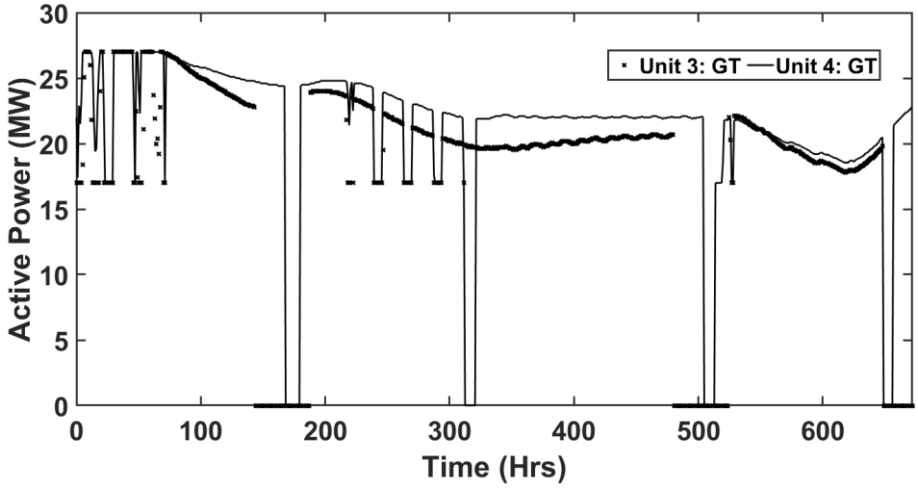

Figure 6.26 Case III Real Power Outputs, Generators 3, 4

Here, Unit 1 can be seen to be dispatched at much lower levels throughout the simulation as compared with the previous two cases. This is the result of the dispatch being influenced by the operational water cost. Unit 5 is seen to be cycled off 5 times, as compared with 2 times in the previous cases, and the two gas turbines (Units 3 and 4) are seen to be kept on much more in this particular case. In addition, it is observed quite clearly that there are some fluctuations that are not due to the varying loads over the course of the simulation. These slower fluctuations in the power outputs of each unit are due to the maximum output value being changed because of cooling demands not being met and/or onsite tank levels dropping, as dictated by (4.135).

The next figures show the cooling water demand make-up requirements from the power system, the demands which were requested by the power system to the WDS and the actual water that was supplied by the WDS. The observations from these plots include the overall trend of increasing demand requested because of tank levels dropping during the contingency. Superimposed on this overall increase, due to (4.134) trying to refill the tanks, are fluctuations due to (4.133) which is the result of recent cooling water consumed by a unit not being re-supplied by the WDS. The effect of trying to refill the onsite storage tanks is also evident by the units which cycle off, where the demands requested are seen to still have a finite value as dictated by (4.133). It can also be observed clearly in Figure 6.28 and Figure 6.29 that the requested demand rapidly decreases as the tank levels begin to refill post-water availability contingency. This operation can be contrasted with independent system control implementations where the demand on the water system from the power system would be purely due to current cooling water requirements and with no

consideration of the onsite tank levels or how power consumption (and therefore water consumption) was altered due to these tank levels.

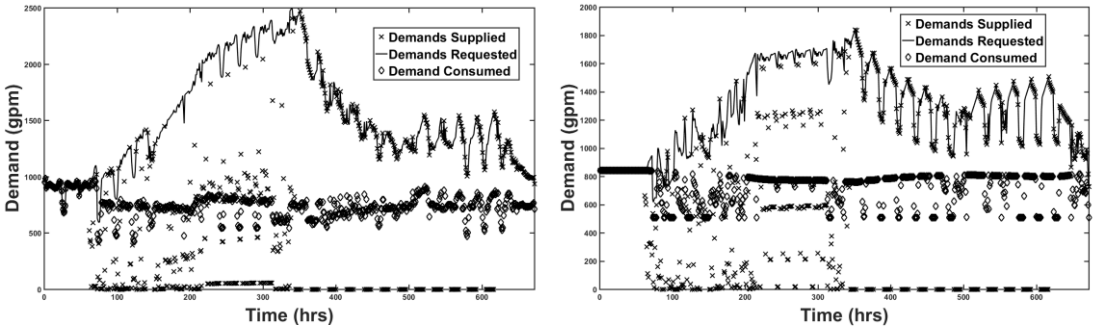

Figure 6.27 Unit 1(L) and 2(R) Cooling Water Requirements, WDS Water Requested, WDS Water Supplied

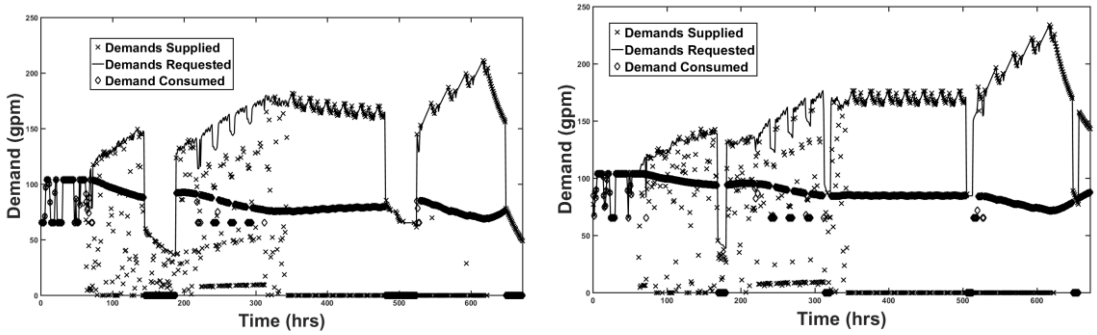

Figure 6.28 Unit 3(L) and 4(R) Cooling Water Requirements, WDS Water Requested, WDS Water Supplied

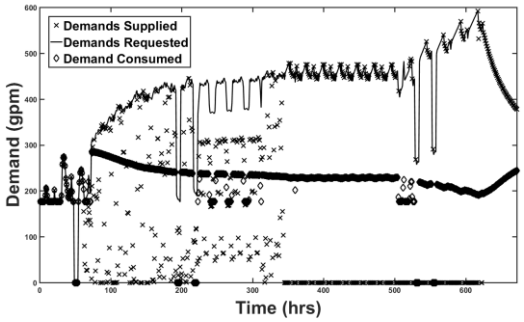

Figure 6.29 Unit 5 Cooling Water Requirements, WDS Water Requested, WDS Water Supplied

Figure 6.30 through Figure 6.32 show the storage tank volumes available onsite at each power plant. The tanks levels for the two base load plants are seen to drop less than the other units in terms of the percentage of water volume lost due to the water shortage, with the volume loss considerably less in the case of unit 2. This is due to a higher priority being placed on the base units' cooling water demands compared to the other peaking units by the WDS optimization model as it attempts to satisfy the residential demands with a higher priority during peak residential demand hours and the demands from power plants with a higher priority during the off-peak (night) hours. Contrasted with a policy of strictly residential demand satisfaction priority, this results in non-monotonically decreasing tank levels for the base load units and therefore has the additional benefit of extending the amount of time the onsite storage at the power plants will last. The effect of this time dependent weight on the demand satisfaction for different demands in the WDS can be seen in the tank level behavior shown in the inset of Figure 6.30. During the last week of the simulation, the amount of water available increases and even though there are power

outages the water system can meet the demands requested by the power plants and correspondingly the tank level for all five units increases.

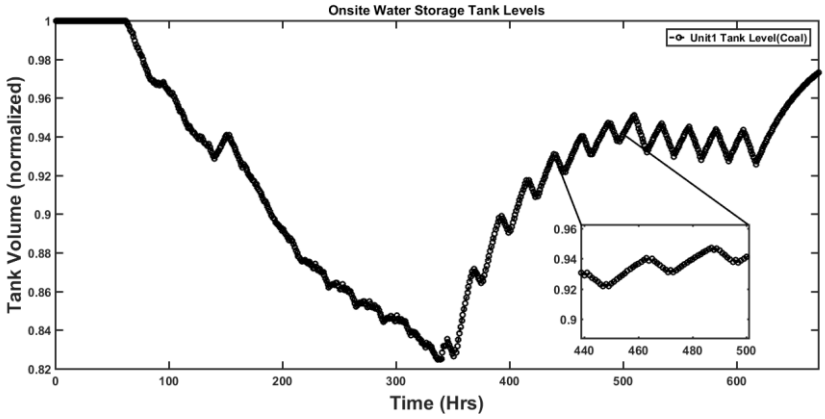

Figure 6.30 Unit 1 Onsite Water Tank Storage Levels

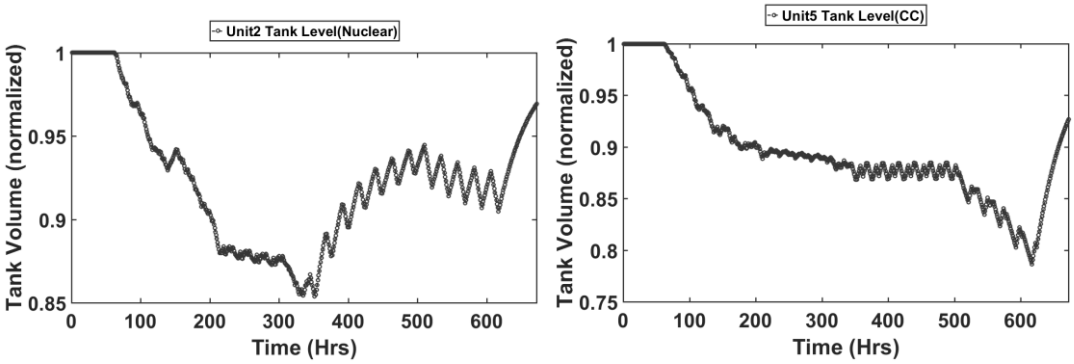

Figure 6.31 Unit 2(L) and 5(R) Onsite Water Tank Storage Levels

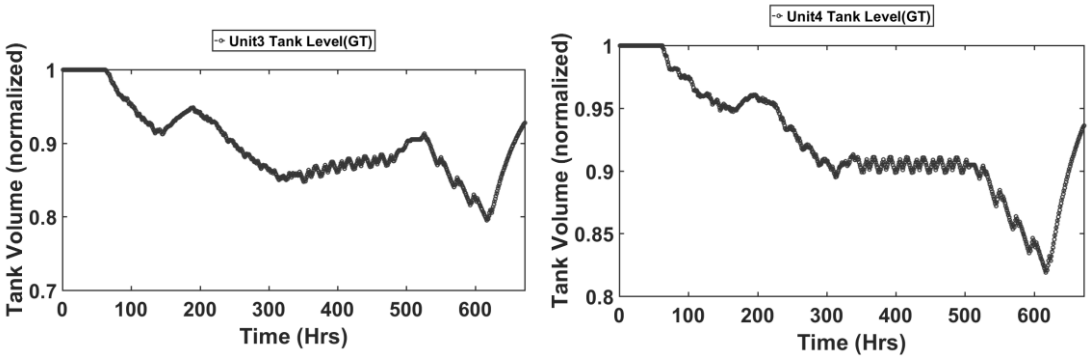

Figure 6.32 Unit 1(L) and 2(R) Onsite Water Tank Storage Levels

The next two figures show quantities within the water system, where it is noted that the reclaimed water flow to power plant 2 in Figure 6.33 is zero during the hours which the pumping station experiences outages. Figure 6.34 shows the residential demands for examination of the time-dependent demand satisfaction weights within the WDS system control optimization solution.

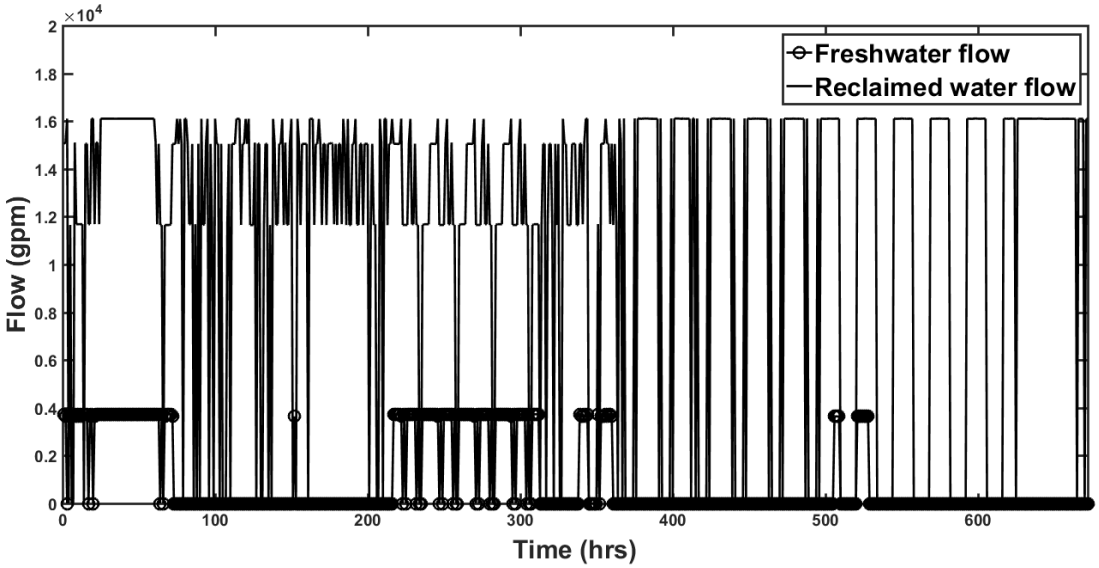

Figure 6.33 WDS Pump Flows to Unit 2 (Nuclear)

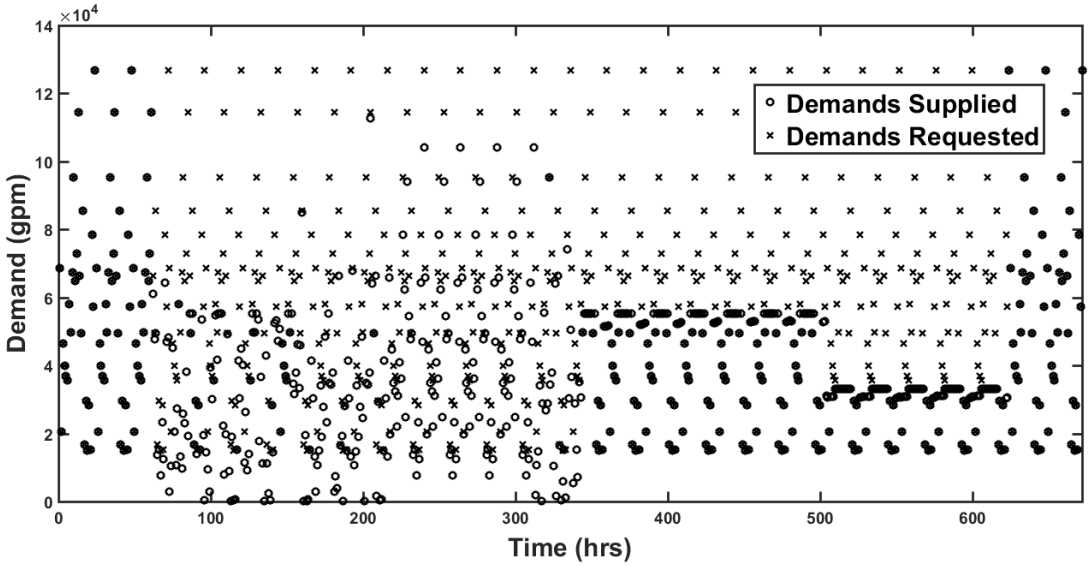

Figure 6.34 Residential Water Demands Supplied and Water Demands Requested

The next figures illustrate the effect of the unit curtailment policy on the maximum allowable power production at the five power plants in the power system. The trends of maximum allowable power production closely follow the water storage levels at the power plants with a slight delay due to the post procession of the output from the LP used to determine the appropriate curtailment based on recent WDS conditions.

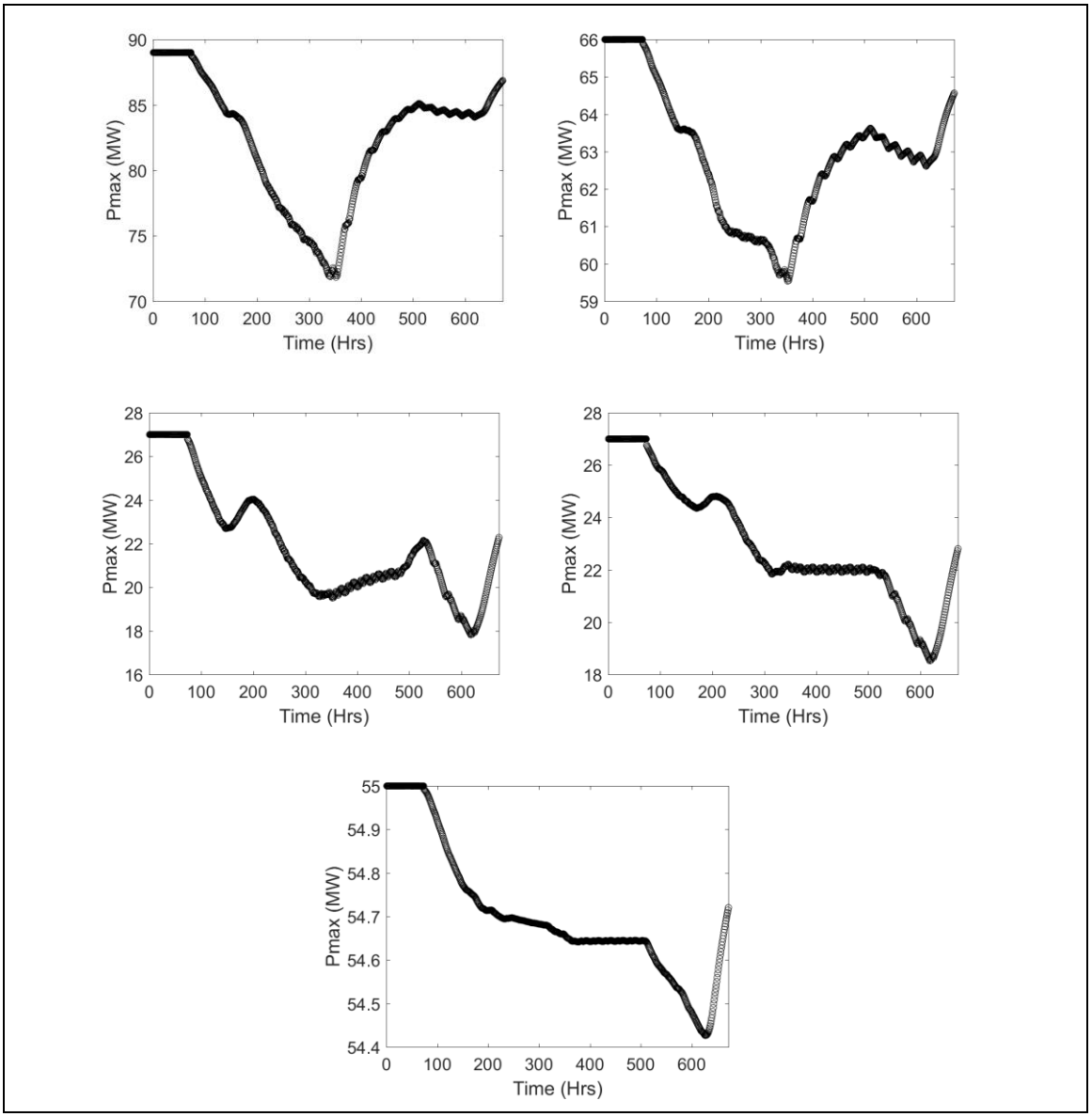

Figure 6.35 Units 1-5 P_{max} Values, From: Left to Right, Top to Bottom

The final power system quantities that will be examined for this case are the amounts of load that need to be shed during the simulation as a result of the unit curtailment demonstrated in the previous figure. Figure 6.36 and Figure 6.37 show the amount of load that is shed in pu on each load's nominal MW base. Because this is a small test system and the fact that it was designed to not have much margin between the maximum load conditions and the total capacity of the generation units, there are times when load is required to be shed. This could alternatively be viewed as the amount of power that would need to be imported if this were a more realistic simulation featuring a larger, interconnected system.

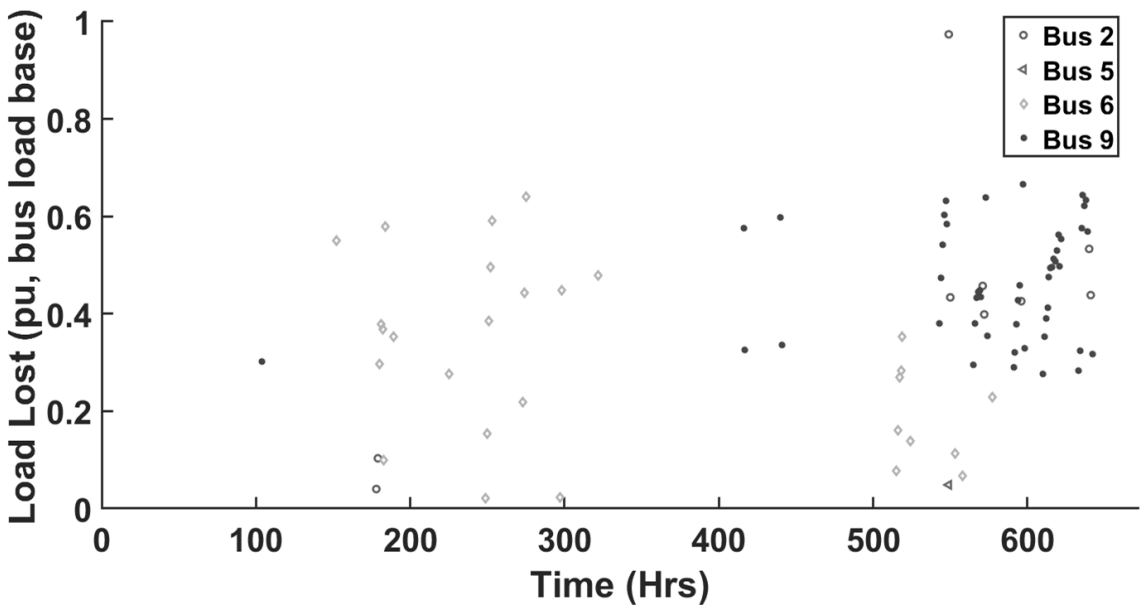

Figure 6.36 Load Curtailments, Bus 2, 5, 6 and 9

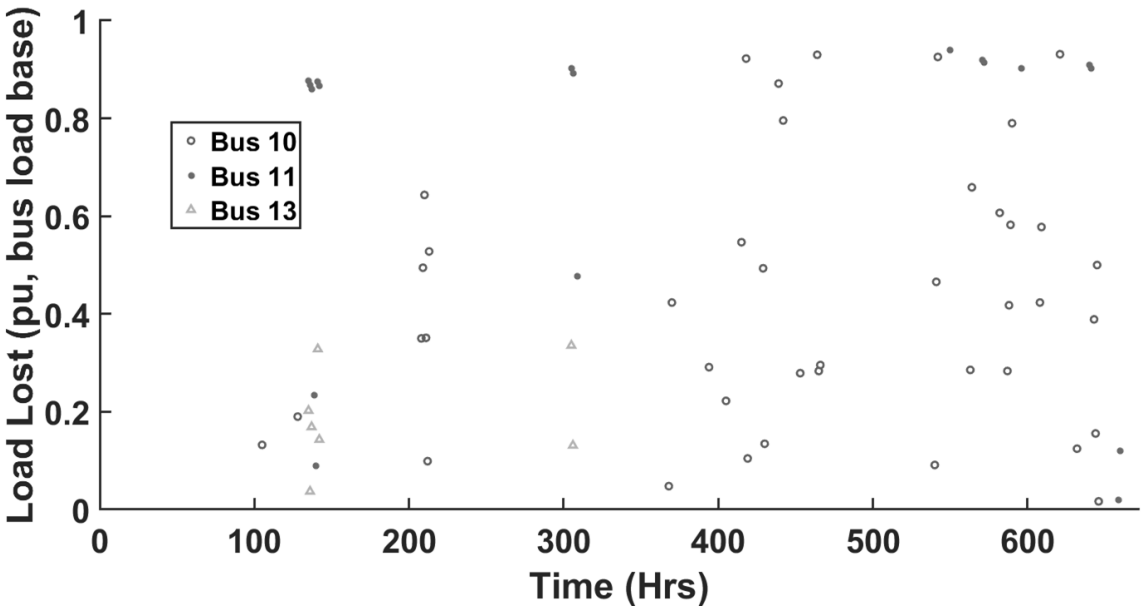

Figure 6.37 Load Curtailments, Bus 10, 11, and 13

Finally, as a comparison, the final onsite water storage tank levels (pu) and their minimum values (pu) are shown in Table 6.2.

Table 6.2 Onsite Storage Tank Level Comparison, Cases I – III, in pu

	Case I		Case II		Case III	
	Lowest	Final	Lowest	Final	Lowest	Final
Unit 1	0.9021	0.9229	0.7952	0.7955	0.8252	0.9731
Unit 2	0.8376	0.8376	0.6756	0.6777	0.8538	0.9693
Unit 3	0.8603	0.8603	0.6978	0.7012	0.7948	0.9276
Unit 4	0.9023	0.9023	0.8958	0.8995	0.8187	0.9361
Unit 5	0.8251	0.8251	0.7918	0.7951	0.7862	0.9266

6.5 Case IV: Sensitivity Analysis of CEED Objective Function Weight ($\delta_{fuelCost}$)

The next study done in this chapter is a sensitivity analysis for the combination water-system-power-system contingency looked at in Cases II and III. The values of unit

maximum output and the value of the operational water cost were kept at their nominal values throughout each simulation. While simulations were run for $\delta_{fuelCost} \in \{0.00, 0.25, 0.50, 0.75, 1.00\}$, the two figures below show the unit real power outputs for a normal OPF dispatch, corresponding to a CEED $\delta_{fuelCost}$ weight of 1, and for a dispatch only considering operational water costs, which is for a CEED $\delta_{fuelCost}$ weight of 0.

The main difference between the plots on the top and the plots on the bottom of Figure 6.38 and Figure 6.39 is the fact the the cheap (fuel) generation is dispatched when $\delta_{fuelCost}$ is equal to one while the cheap (water) generation is dispatched when $\delta_{fuelCost}$ is equal to zero, as expected. It is also interesting to note the similarities between the $\delta_{fuelCost}$ = 0 case and the results of Case III, where the effects of unit curtailment and operational water cost adjustment clearly move the resulting power outputs away from the traditional OPF dispatch and towards the environmental dispatch solution.

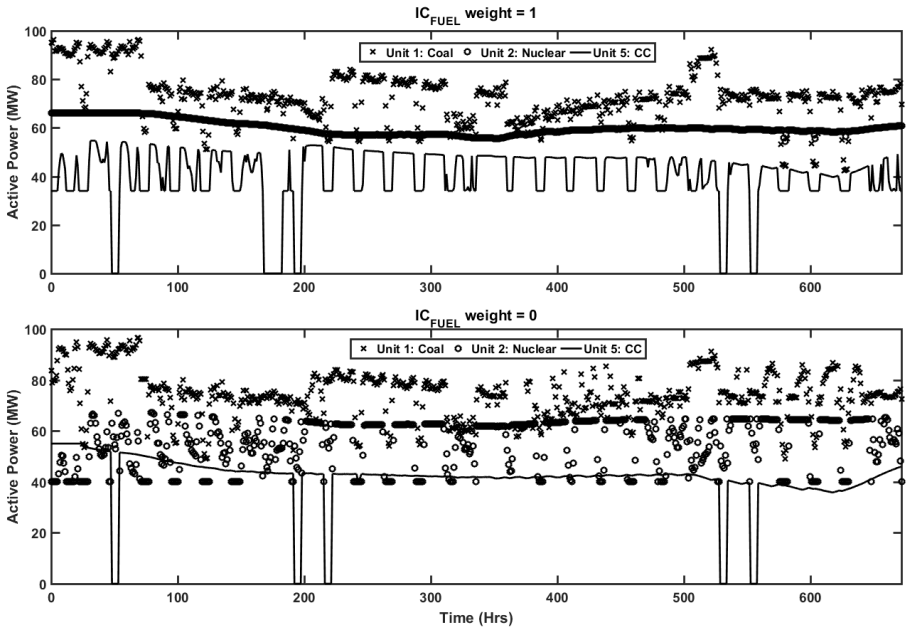

Figure 6.38 Real Power Outputs, Generators 1, 2, and 5, $\delta_{fuelCost}$ = 1 (Top) and $\delta_{fuelCost}$ = 0 (Bottom)

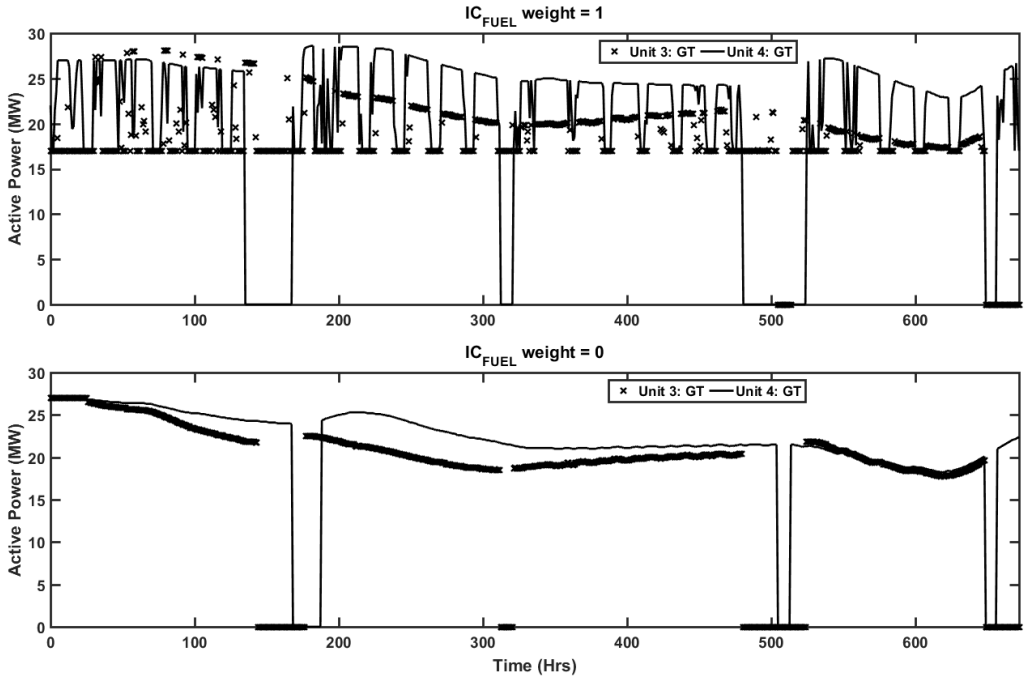

Figure 6.39 Real Power Outputs, Generators 1, 2, and 5, $\delta_{fuelCost}$= 1 (Top) and $\delta_{fuelCost}$ = 0 (Bottom)

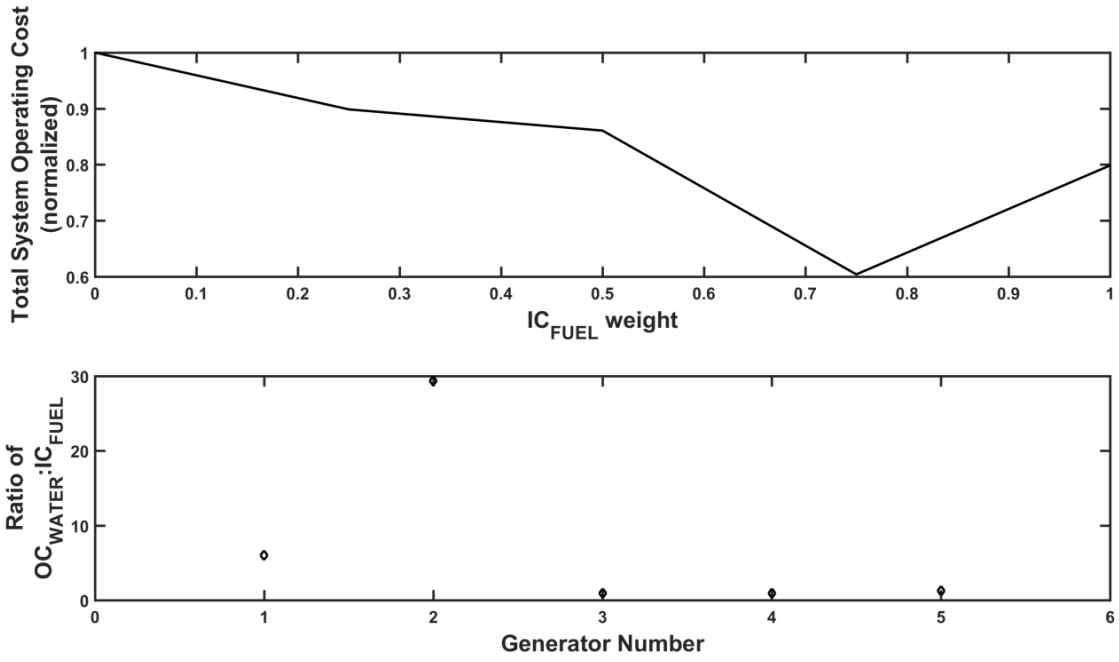

Figure 6.40 System Operating Cost Comparison (Top) and Operating Cost Component Ratios (Operational Water Cost to Incremental Fuel Cost)

The total system operating costs are seen to be lowest for a CEED weight of 0.75, as shown in the top plot of Figure 6.40 above. This fact is explained by consideration of the operational water cost to incremental fuel costs of the units. With $\delta_{fuelCost}$ = 0.75, the right combination of the more expensive (fuel) units get dispatched while their operating cost is offset by the units with much cheaper water costs. The plots below show the integral of the difference between the nominal onsite storage tank level and its value during simulation. If it is desired to keep the storage tanks full for as long as possible in order to keep the units operational, a lower value is desired.

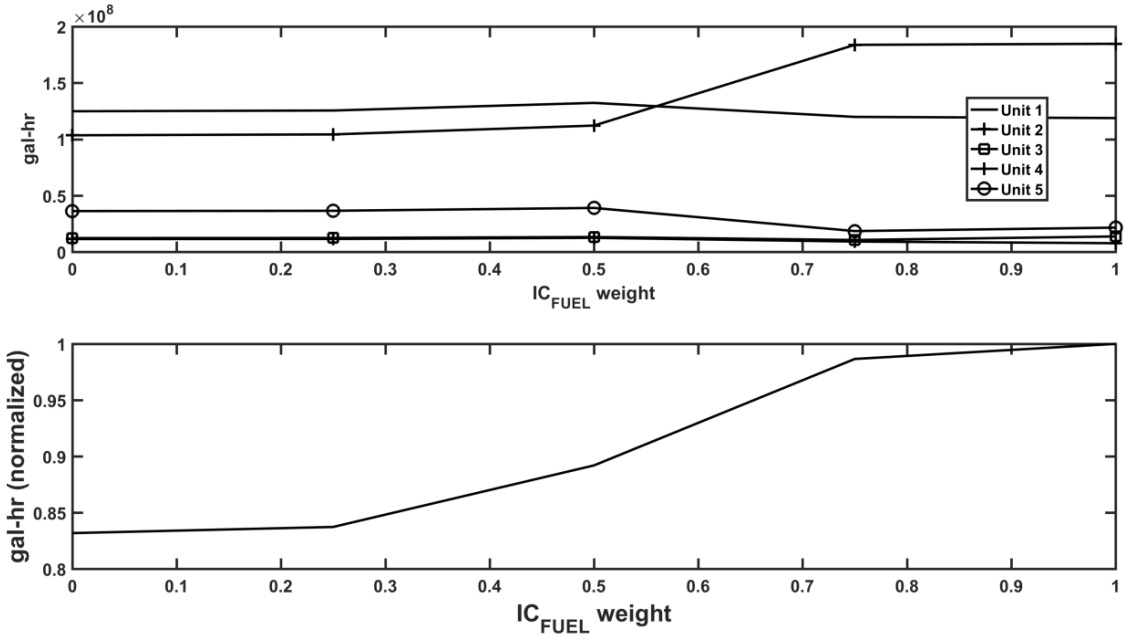

Figure 6.41 Integral of Tank Level Difference from Nominal over Full Simulation, Unit 1-5 (Top) and Total System (Bottom)

A quick note on solution times is given here. For this test system, the solution time for the SCUC is approximately 4 seconds using a relative MIP gap of 0.01% while the CEED takes about 250 milliseconds.

6.6 Case V: Sensitivity Analysis of Active Power Output and Tank Levels for Different Policy Implementations

This sensitivity analysis will examine the direct effect that different policy implementations have on system performance. The scenarios setup includes the long-term WDS pump power outages included in the previous cases and the total system water availability as show in Figure 6.42 below.

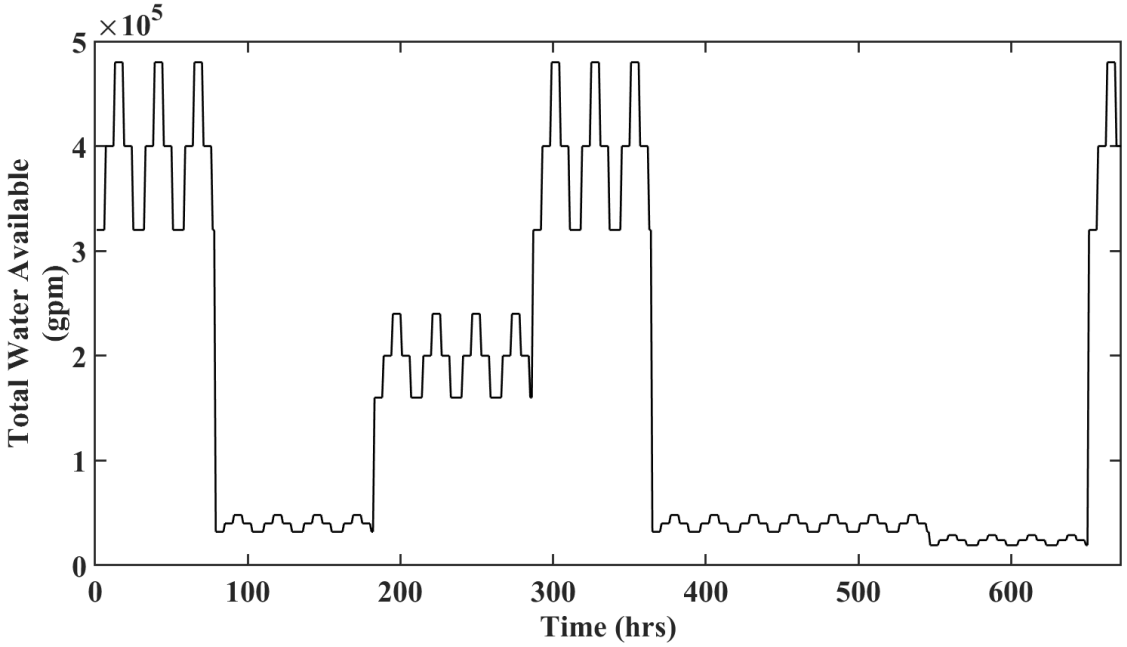

Figure 6.42 Sensitivity Analysis Total WDS Water Availability

Control Policy III (WDS demand pattern adjustment) and time dependent weights for WDS demand pattern satisfaction were used in the following cases. The weight chosen for $\delta_{fuelCost}$ was 0.5. The cases examined were:

Case 1 (C1): CEED only

Case 2 (C2): CEED with Policy II: Operational Water Cost Adjustment

Case 3 (C3): CEED with Policy I: Unit Derating, LP Model

Case 4 (C4): CEED with Policy I and Policy II

For these cases, like the previous ones, the curtailed maximum active power outputs of the units were not used within the unit commitment solution in order keep the MILP feasible. So, the adjusted maximum output values were used for determining a CEED solution only. The figures below show the outputs for the five units with a subplot in each figure corresponding to one of the cases (C1 through C4) above. It is readily apparent that the inclusion of the incremental cost adjustment causes much more variation in the dispatch of the coal and nuclear units (Units 1 and 2, respectively) since the cost to dispatch them becomes relatively more expensive as compared with the other three units that have lower water consumption rates. The effect of unit curtailment is also evident for all units in the bottom two subplots in each figure.

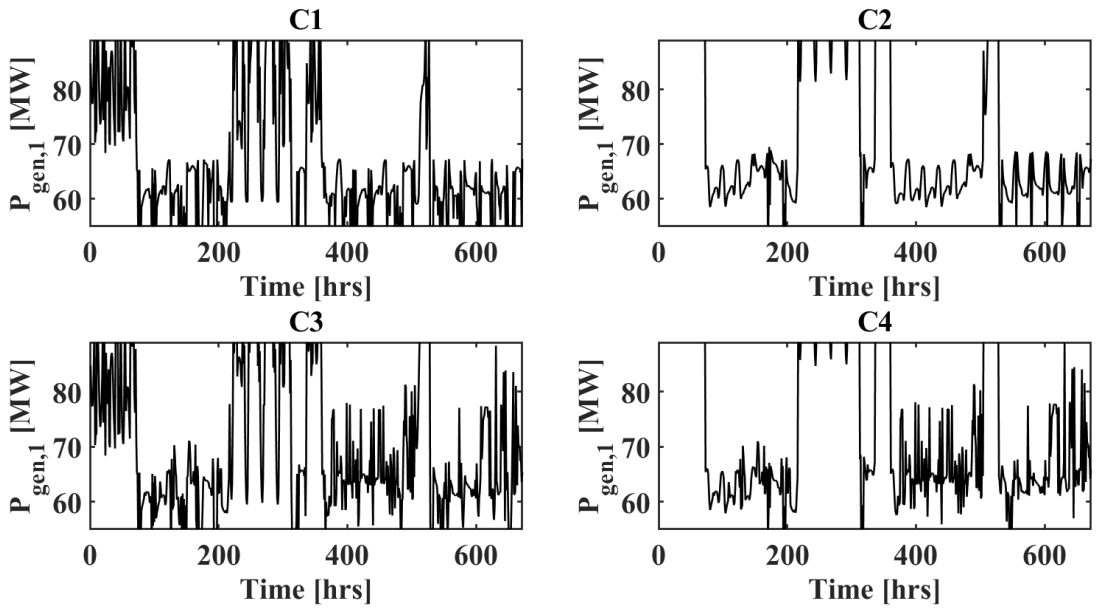

Figure 6.43 Unit 1 (Coal) Active Power, C1-C4

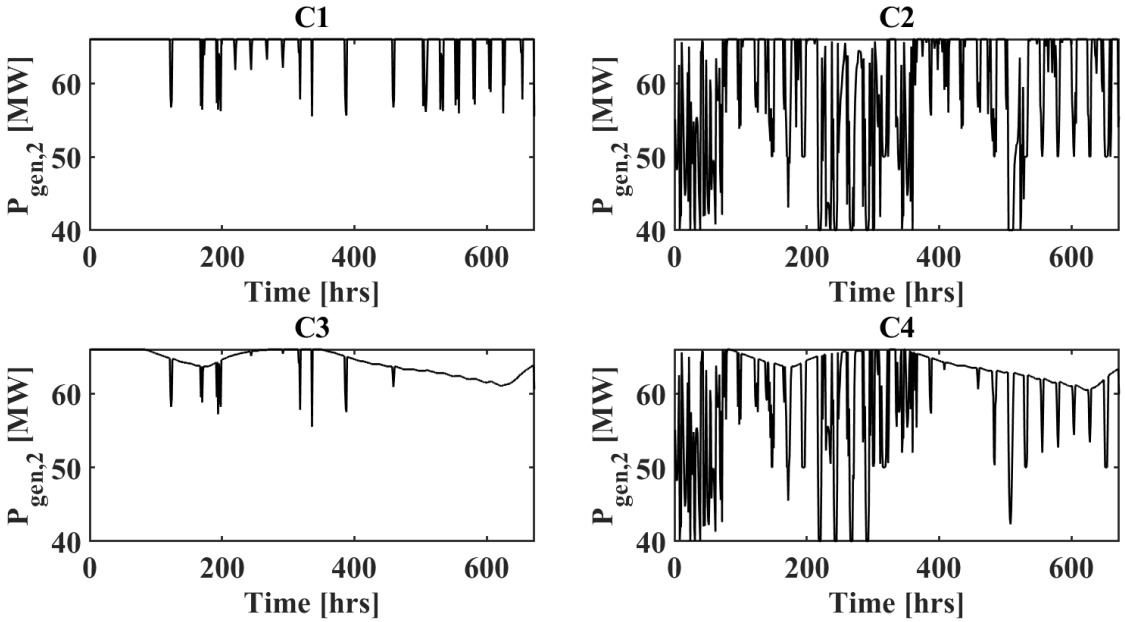

Figure 6.44 Unit 2 (Npp) Active Power, C1-C4

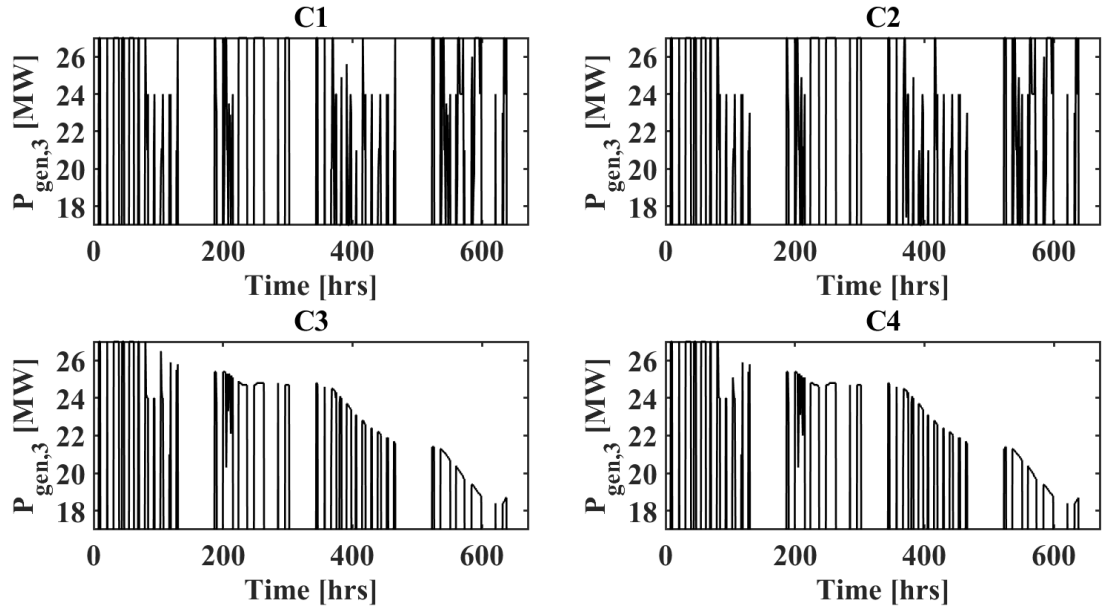

Figure 6.45 Unit 3 (CT) Active Power, C1-C4

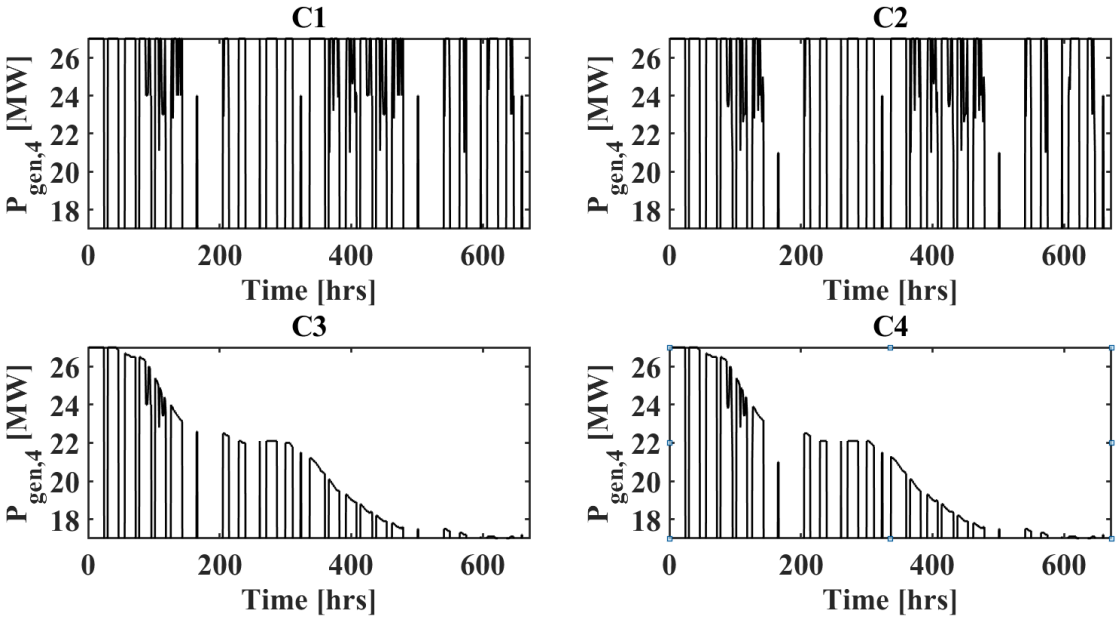

Figure 6.46 Unit 4 (CT) Active Power, C1-C4

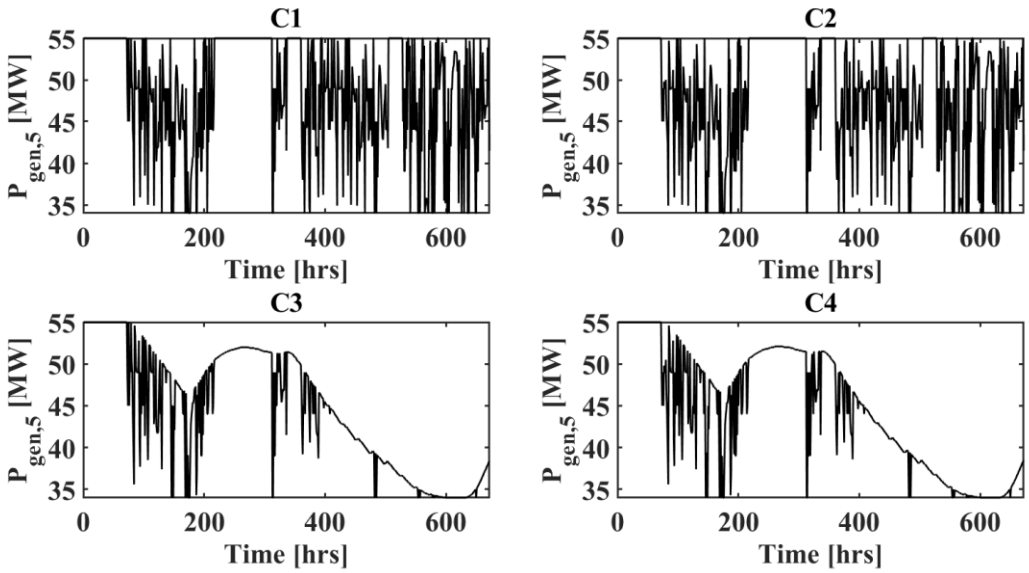

Figure 6.47 Unit 5 (CCGT) Active Power, C1-C4

The next figures show the levels of the onsite water storage for each case. The policy implementations are seen to result in improvements by increasing the minimum value in the storage tank levels as well as increasing the amount of water onsite at the end of the simulation, and this is particularly evident for Units 3-5.

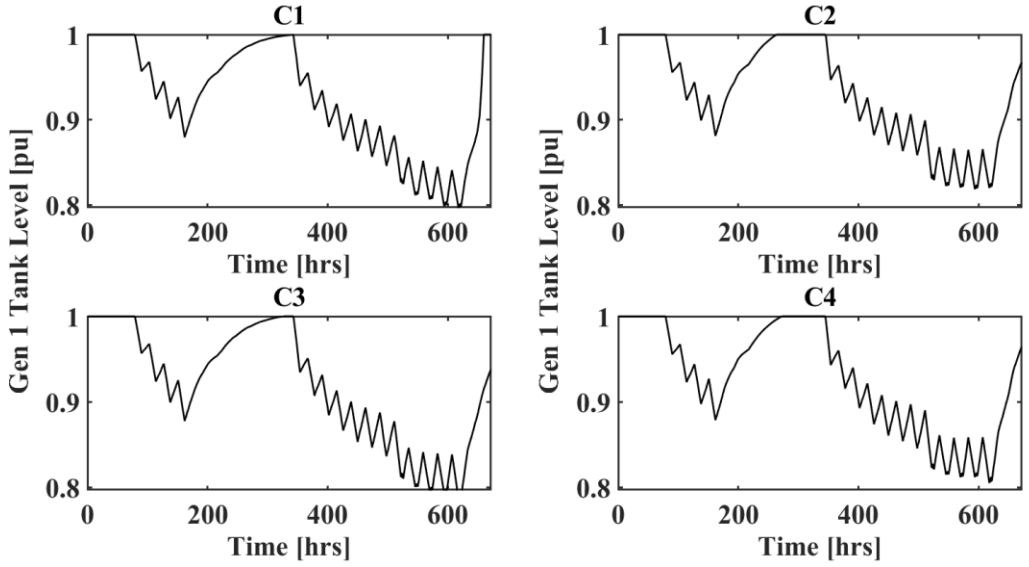

Figure 6.48 Unit 1 (Coal) Tank Level, C1-C4

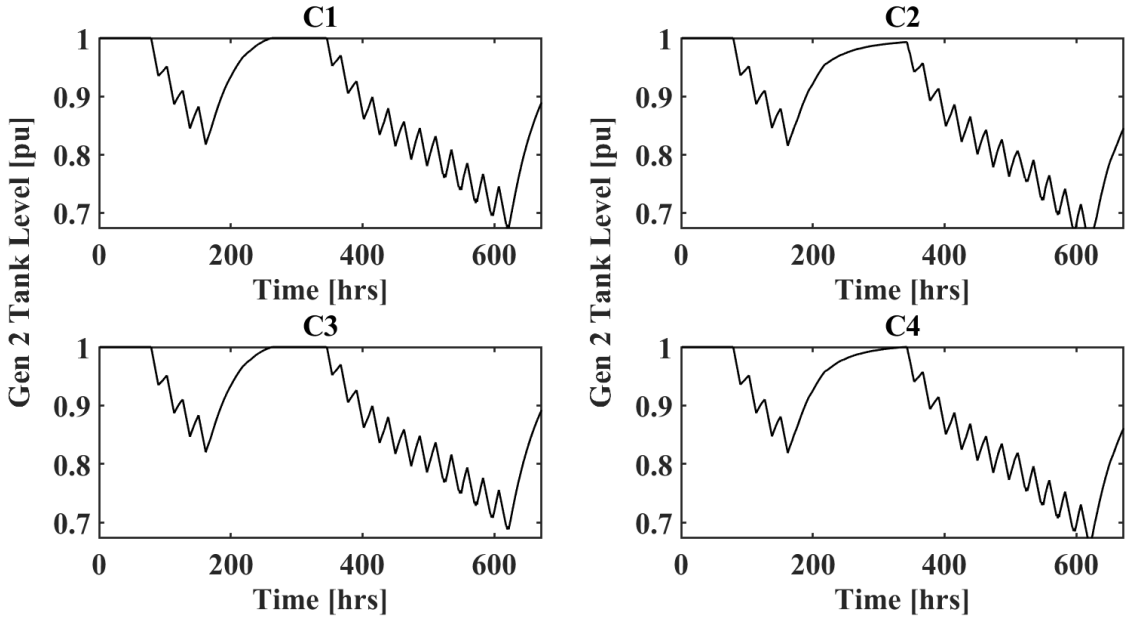

Figure 6.49 Unit 2 (Npp) Tank Level, C1-C4

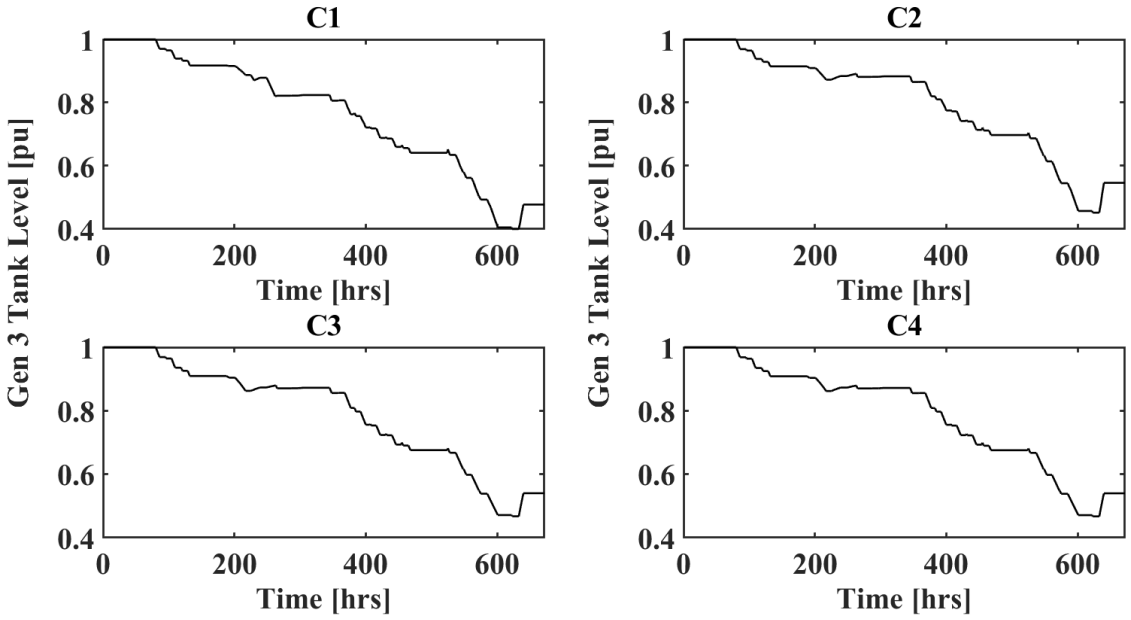

Figure 6.50 Unit 3 (CT) Tank Level, C1-C4

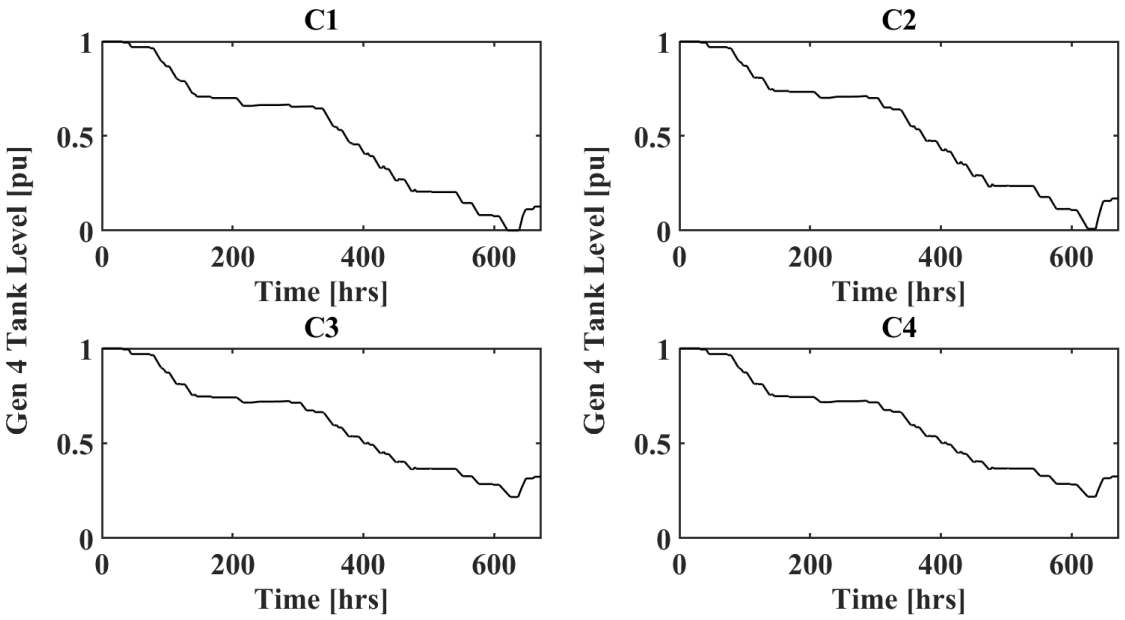

Figure 6.51 Unit 4 (CT) Tank Level, C1-C4

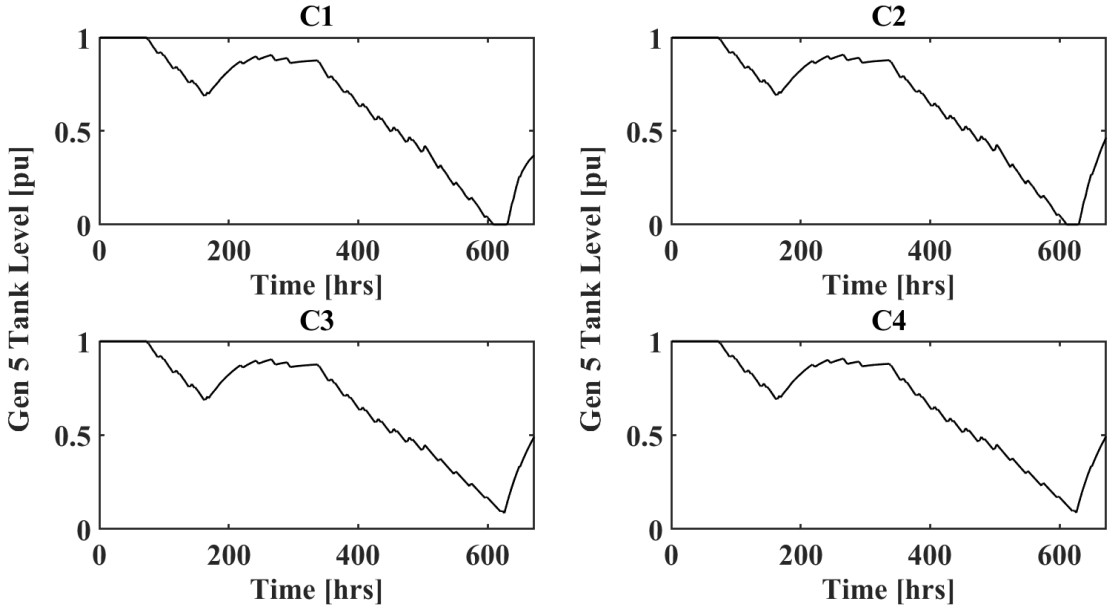

Figure 6.52 Unit 5 (CCGT) Tank Level, C1-C4

The effect of the WDS demand pattern weights is also evident in the tank levels as the lower priority peaking units have much larger decreases in their storage tank levels.

The tables below summarize data from these simulations. The average active power was calculated as the mean of the non-zero generation from each unit. The improvement in system performance for the cases in comparison to the CEED case (C1) by means of increased minimum tank levels and higher storage levels at the end of the simulation for all units is also noted.

Table 6.3 Generator Average Active Power Comparison, C1-C4

	Generator	C1 (MW)	C2 (MW)	C3 (MW)	C4 (MW)
1	IGCC	66.2	73.2	69.9	74.5
2	Npp	65.5	58.9	64.2	59.8
3	CT	24.0	23.9	23.2	23.2
4	CT	26.3	26.1	21.5	21.5
5	CCGT	48.8	48.6	44.5	44.4

Table 6.4 Generator Minimum Tank Level Comparison, C1-C4

	Generator	C1 (pu)	C2 (pu)	C3 (pu)	C4 (pu)
1	IGCC	0.7961	0.8183	0.7850	0.8049
2	Npp	0.6734	0.6439	0.6880	0.6637
3	CT	0.3989	0.4509	0.4663	0.4660
4	CT	0.0000	0.0089	0.2174	0.2187
5	CCGT	0.0000	0.0000	0.0849	0.0875

Table 6.5 Generator End of Simulation Tank Level Comparison, C1-C4

	Generator	C1 (pu)	C2 (pu)	C3 (pu)	C4 (pu)
1	IGCC	1.000	0.968	0.938	0.964
2	Npp	0.890	0.846	0.892	0.861
3	CT	0.477	0.545	0.539	0.539
4	CT	0.127	0.170	0.324	0.325
5	CCGT	0.372	0.466	0.491	0.494

Lastly, it is noted that the weight applied to the terms associated with water costs ($\delta_{waterCost}$) as well as the actual values of the operational cost of water ($C_{water,g}$) can have a substantial impact on the resulting dispatch of generation. Figure 6.53 and Figure 6.54 below illustrate this point by showing the active power for Units 2 and 5 for the C2 scenario and varying $\delta_{waterCost}$ values. The average values of active power are shown in Table 6.6, and it is again noted that the CEED moves from generation that is cheap (fuel) to generation that is cheap (water) and thus the output of Unit 2 decreases approximately 10.2% while Unit 5 increases approximately 6.8% as the objective function weight decreases.

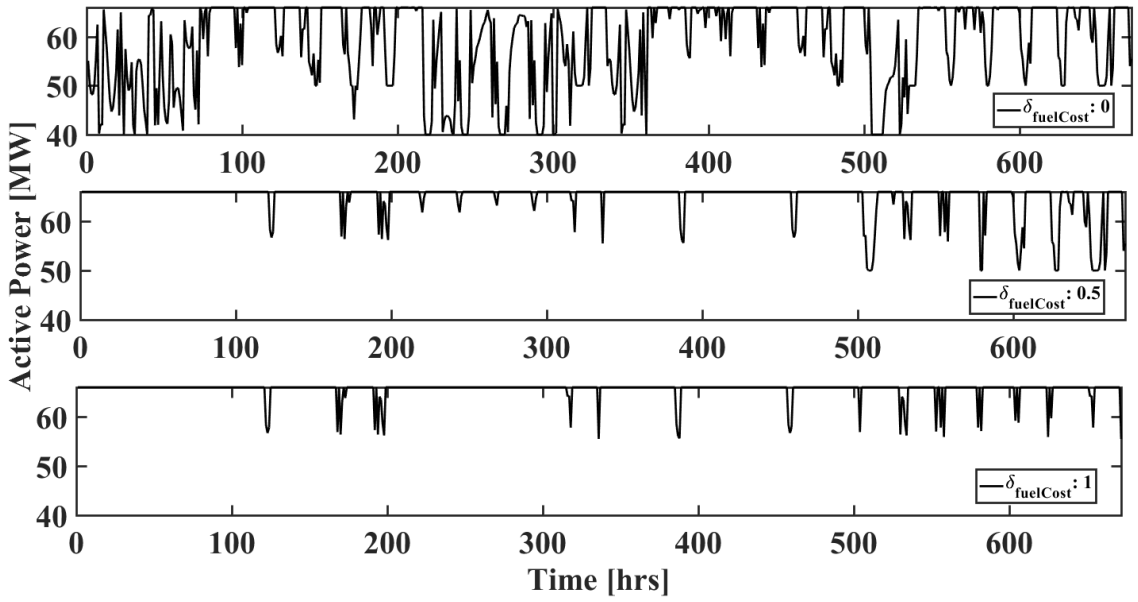

Figure 6.53 Unit 2 (NPP) Active Power, C3

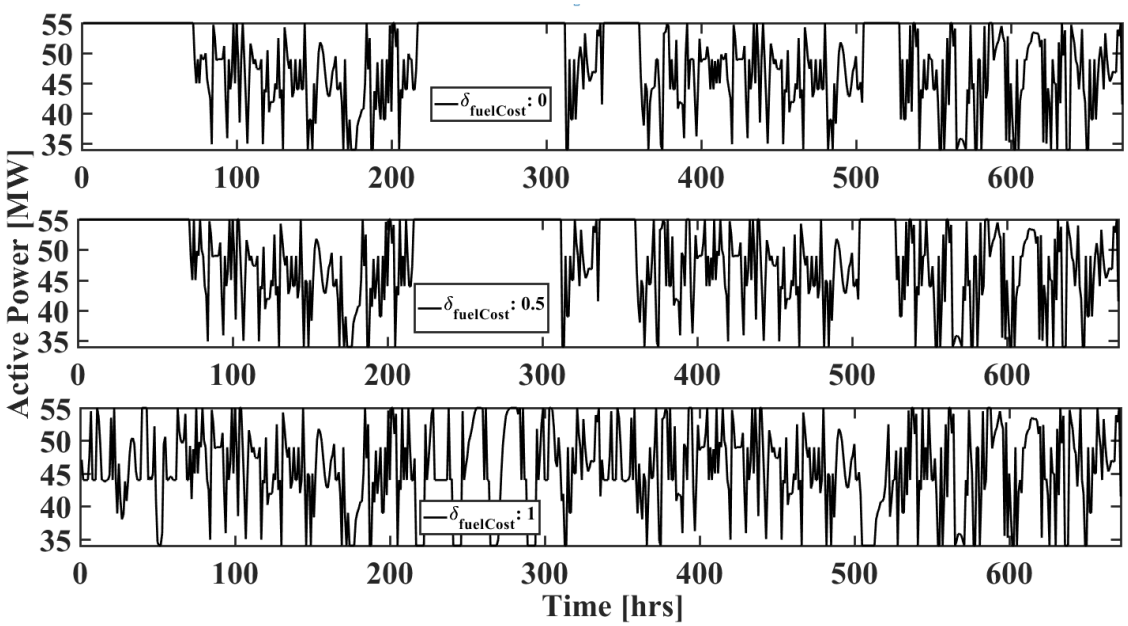

Figure 6.54 Unit 5 (CCGT) Active Power, C3

Table 6.6 Generator Average Active Power Comparison, C3

	Generator	$\delta_{fue;Cost}$ = 0.0	$\delta_{fue;Cost}$ = 0.5	$\delta_{fue;Cost}$ = 1.0
1	Npp	58.9	64.9	65.6
2	CCGT	48.7	48.8	45.6

6.7 Case VI: Application of CEED and Control Policies to a Larger Test System

The application of the simulations methodology to a larger test system is the last application that was examined. The long-term simulation test system was used along with the assumptions that follow. The effect of the control policies was under examination so the WDS was modeled implicitly. This means that the WDS network was not modeled but instead results from previous simulations were leveraged. The way that this was accomplished was by dividing the cooling water supplied by the WDS in each time-period by the amount of water consumed in that time-period. In effect, this gives a per-unit value of demand satisfied which can be used in other (these) simulations. These pu values were then used as the amount supplied to the respective thermoelectric fuel type within the larger

system. Because the WDS network solution and optimization was not modeled, the pump loads within the system are neglected as well.

The simulated scenario was the emulation of drought conditions in part of the system. The test system was divided into three areas as shown in Figure 6.55 below.

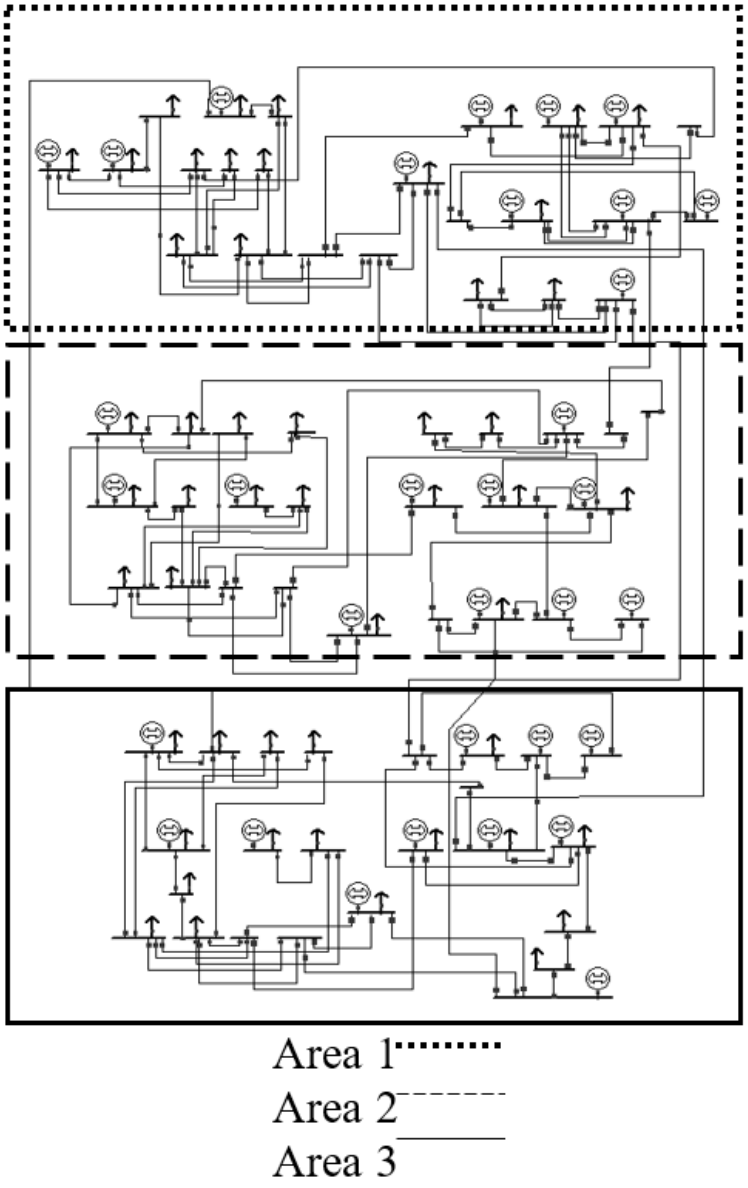

Figure 6.55 Areas of the Long-Term Simulation Test System

For each generator within Area 3 (the drought area), the cooling water supplied was set to equal to that of the corresponding type from the smaller test system. The cooling water supplied to units not in the drought area as well as to all hydro units was assumed to equal to whatever was requested for the purpose of this simulation scenario.

Simulation results are shown below for the cases of $\delta_{fuelCost}$ equal to 0.0, 0.5, and 1.0. The active power for NPP generators 24 and 90 as well as CCGT generators 7 and 74 are used to exemplify the results. Units 7 and 24 resided in the non-drought areas while Units 74 and 90 experienced the drought conditions. From, Figure 6.56 and Figure 6.57 it is seen that this base load unit is operated as such under the normal OPF dispatch ($\delta_{fuelCost}$= 1.0) and the dispatch point is moved around quite a bit otherwise. For decreasing values of $\delta_{fuelCost}$, it is seen in general and especially in the insets that the active power is consistently lower for smaller values of $\delta_{fuelCost}$= 1.0. Lastly, the effect of the curtailed $P_{g,max}$ values, denoted by the dotted lines in the figures, is clearly evident in Figure 6.56.

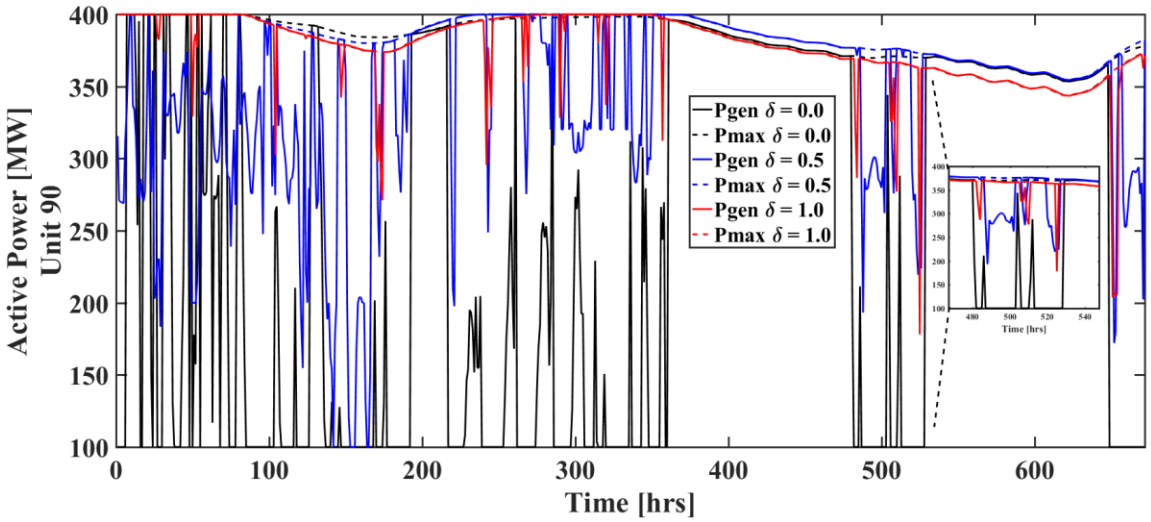

Figure 6.56 Unit 90 (NPP) Active Power Output, Unit in Drought Area

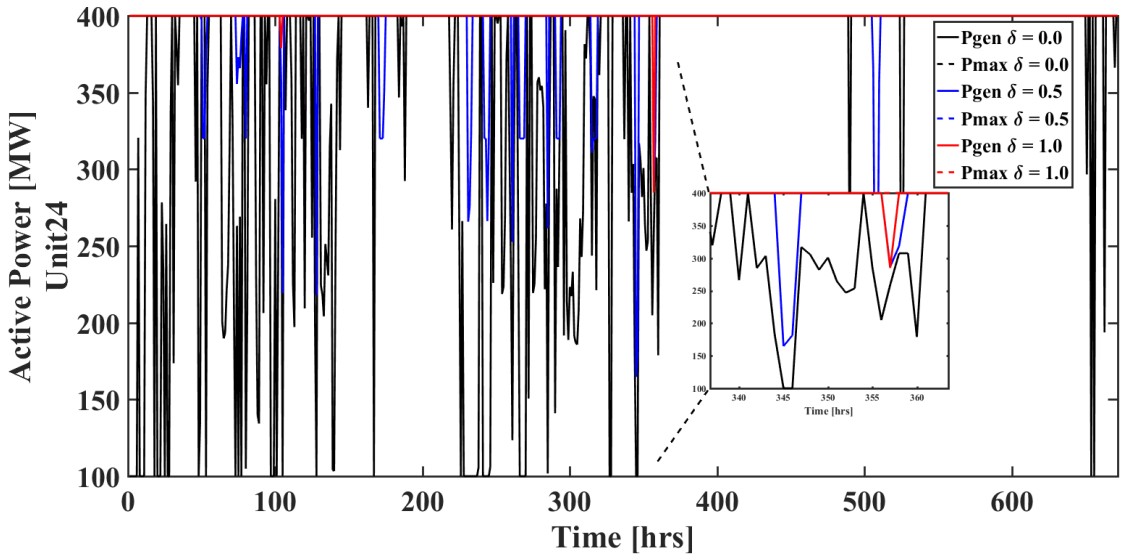

Figure 6.57 Unit 24 (NPP) Active Power Output, Unit not in Drought Area

The effect of $P_{g,max}$ reduction for Unit 74 is also quite evident from Figure 6.58 and while Unit 7 has time-periods where the output is reduced from its maximum, this is not the case for the curtailed unit.

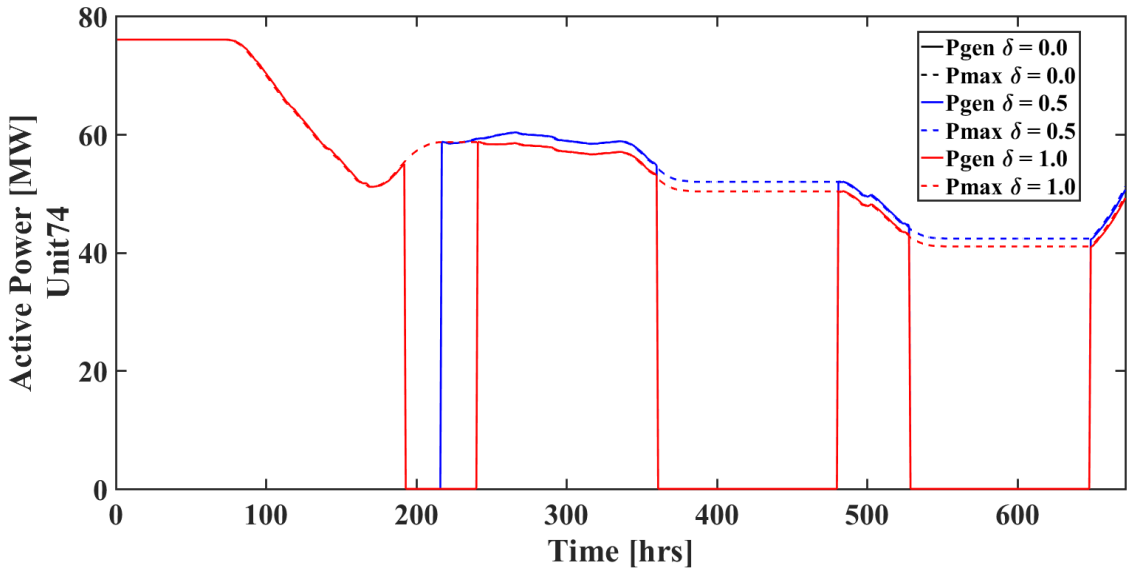

Figure 6.58 Unit 74 (CCGT) Active Power Output, Unit in Drought Area

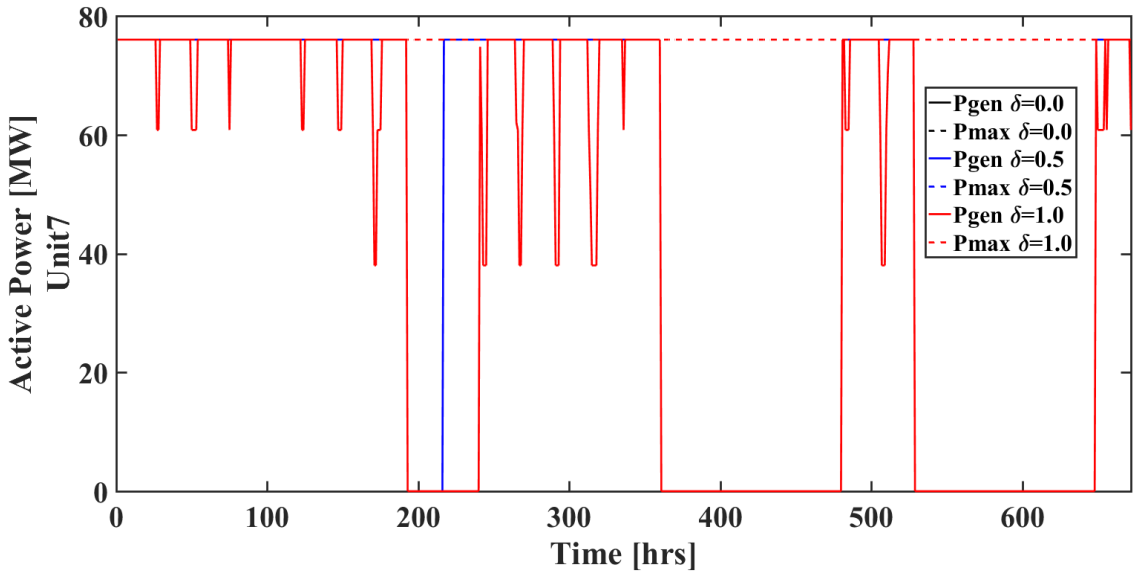

Figure 6.59 Unit 7 (CCGT) Active Power Output, Unit not in Drought Area

The other notable difference is that through the implementation of these policies, the unit dispatch is indirectly altered as Unit 74 is committed in hour 216 versus in hour 240 for the normal OPF dispatch.

Figure 6.60 and Figure 6.61show the normalized levels of onsite water storage for Unit 90 and Unit 74 (experiencing drought). Notice that the smaller difference in tank level between cases is smaller for Unit 74 due to smaller difference in dispatch between the cases.

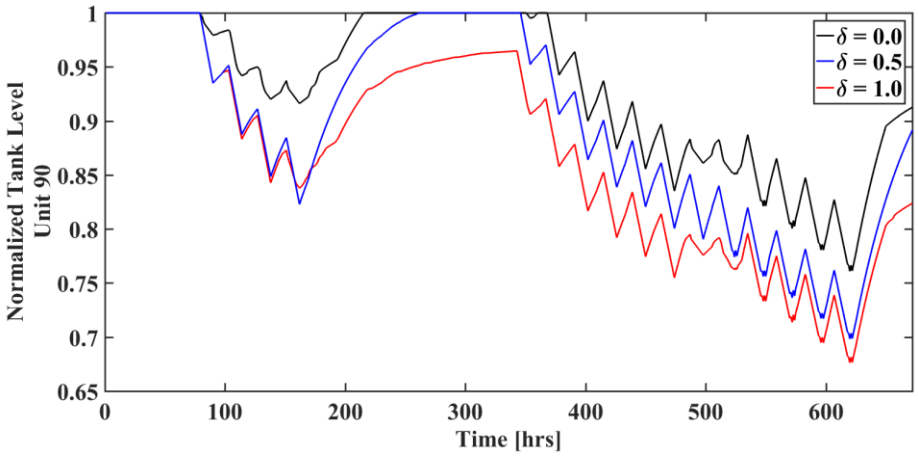

Figure 6.60 Onsite Water Storage Tank Level, Unit 90

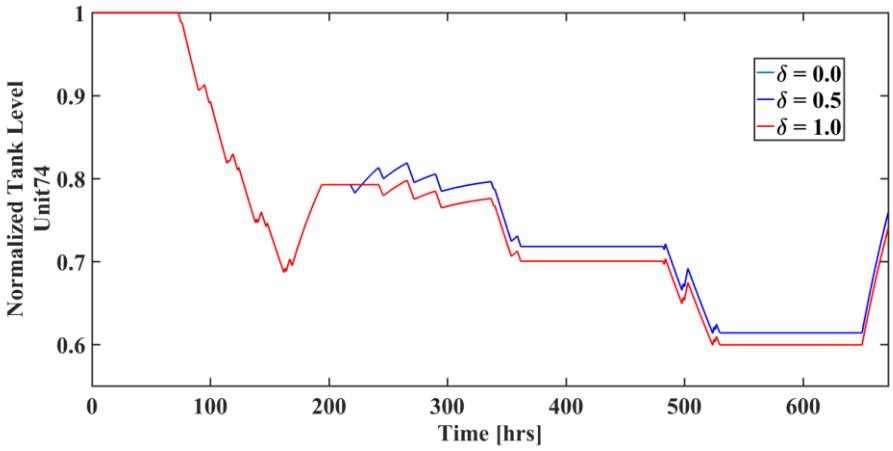

Figure 6.61 Onsite Water Storage Tank Level, Unit 74

Table 6.7 summarizes the system level data for water consumption and system operating cost for the different cases, normalized by the results from a simulation with a regular OPF and without the implementation of Policy I or II. Note that the total system cost is very sensitive to the ratio of fuel cost to operational water cost as well as to what value the operational water cost is given. A substantial reduction of water usage is seen by the whole system (29.7% decrease) and within the drought area (20.34% reduction) due to the implemented policies. Because a large portion of the reduction in water usage is already seen for $\delta_{fuelCost}$ = 1.0, it is therefore noted that the reduction of generation through the

curtailment policy is quite effective at lowering the system water consumption by reducing the active power output of affected units.

Table 6.7 Total Cost and Water Consumption Summary

	Case	Cost	Water Consumption (All)	Water Consumption (Drought Area)
1	OPF	1	1	1
2	$\delta_{fuelCost} = 0.0$	1.71202	0.70307	0.79663
3	$\delta_{fuelCost} = 0.5$	1.26186	0.71425	0.80481
4	$\delta_{fuelCost} = 1.0$	1.16834	0.707	0.82052

6.8 Summary

This chapter presented simulation results for several case studies that examined the performance of the two systems for different contingency scenarios and for different implementations of the policies presented in Chapter 4. The ability of the proposed policies to cause the desired behavior of units that are experiencing periods of extreme drought to be implemented was observed.

CHAPTER 7

CASE STUDY AND RESULTS DISCUSSION – LONG-TERM MODEL

With the test system information as described in Chapter 5, an actual set of candidate generators was chosen based on initial calculations of the total expected load in the growth scenarios as well as existing generation capacity. The transmission lines were selected by an initial simulation with a relaxed optimization model. Lastly, the objective function weightings were assigned to be 1, 0.01, and 1 for the transmission, generation, and operational terms, respectively. These weights were selected to yield total investment costs for transmission and generation as well as operational costs that were of the same magnitude. These weights can be selected by a decision maker or through sensitivity analysis.

7.1 Generation Expansion Candidates

Candidate generator buses were selected by identifying buses near large load pockets in the system and that had multiple existing outgoing transmission lines. The unit siting location and the bus to which the generator would be connected to or to which new transmission would need to be built from the plant site can be seen in Table 7.1

Table 7.1 Candidate Generator Interconnection Information

Generator Type	Bus	Connects to Bus
Npp	74	53
IGCC	75	9
IGCC	76	29
CCGT	77	58
CCGT	78	19
CT	79	34
CT	80	19

7.2 Transmission Expansion Candidates

A set of candidate transmission lines was determined by solving the biggest load-growth scenario with all Rate A line ratings twice as large as the nominal value. By examining the flows which would be violated, the candidate lines were selected and are listed in Table 7.2.

Table 7.2 Transmission Line Interconnection Information

Branch	Voltage (kV)	From Bus	To Bus
118	500	74	53
119	345	75	9
120	345	76	29
121	230	77	58
122	230	78	19
123	230	79	34
124	230	80	19
125	230	14	16
126	500	37	47
127	230	38	40
128	500	61	71
129	230	62	64
130	115	29	34
131	115	32	34
132	115	49	53
133	115	53	58
134	115	8	9
134	115	32	33

Figure 7.1 shows the test system configuration with the locations of the sites for the candidate generation shown by the large generator symbol (and fuel type) and with the candidate transmission lines shown in bold.

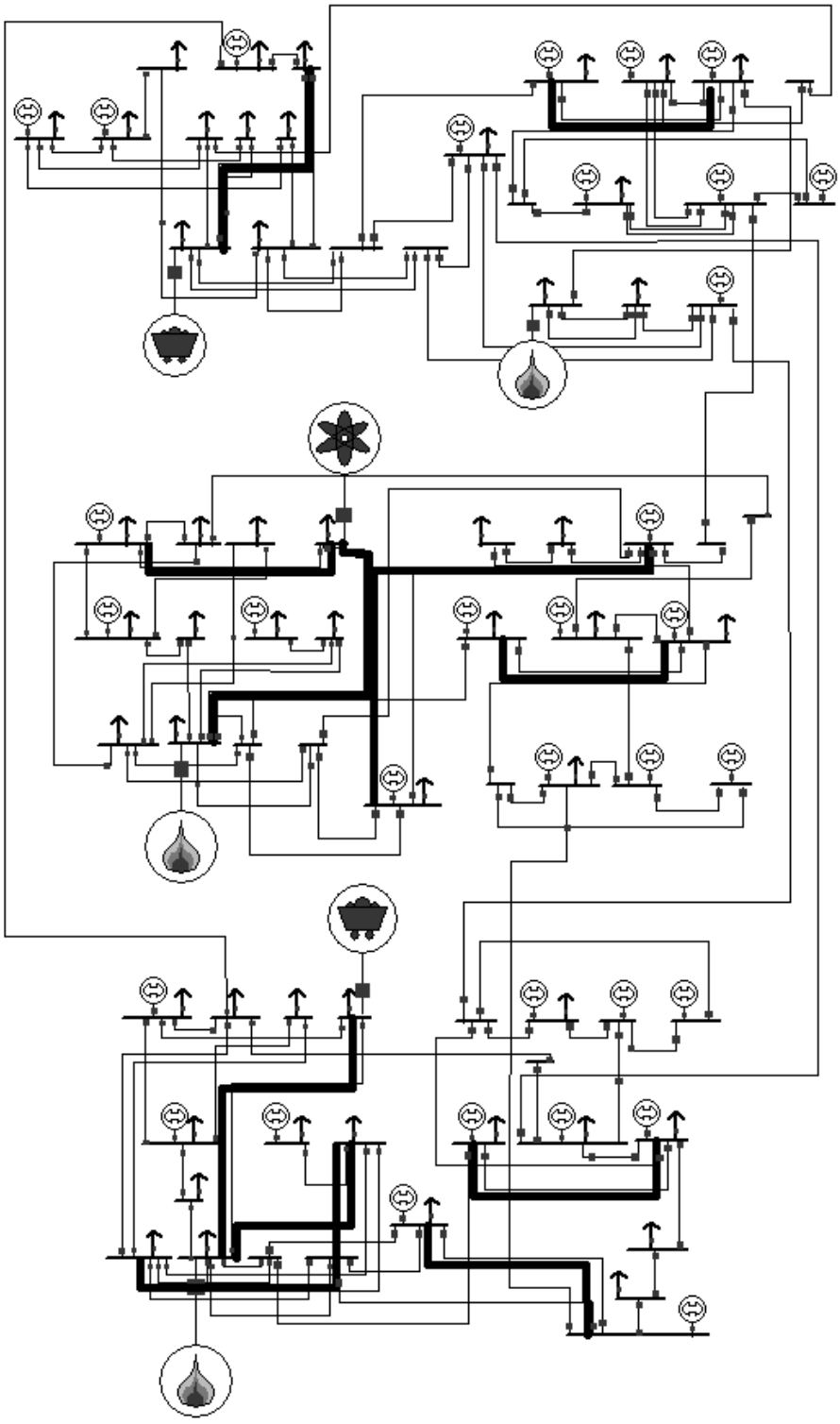

Figure 7.1 Test Expansion System with Generation Candidate Types/Locations and Transmission Line Locations

7.3 Scenario Results

The simulation results for the reference case are summarized in Table 7.3 through Table 7.6. Table 7.3 shows the generator investment decisions which were made, all in year 10, for this case with 1.4% load growth per year. It is seen that in addition to the five generators and their corresponding transmission lines an additional four transmission line circuits are required to be added to the system, including two which are added in the first year of the limited-day optimal investment/SCUC.

Table 7.3 Reference Case GEP Results

	Generator Added	Bus	Hour
1	Npp	53	102
2	CCGT	58	162
3	CCGT	19	160
4	CT	34	196
5	CT	19	160
	Total Investment Cost:	**$2,393,911,079.65**	

Table 7.4 Reference Case TEP Results

Line Added	118	121	122	123	124	125	127	129	133
Hour	102	161	160	196	160	68	18	160	102
	Total Investment Cost:		**$5,747,517.88**						

Table 7.5 shows the total operational costs for the system which were computed using the commitment variables from the optimal investment problem and updating the network to reflect the corresponding additions in the correct time-periods.

Table 7.5 Reference Case Operational Results

	Operational Years	8760 Hr x 2 SCED Cost ($)
1	1 & 10	1,431,850,000.00

The total water consumption for the units added in the reference case scenario is seen to be 1.215 billion gallons. As expected, the clear majority of this consumption comes from the nuclear unit, which is cheap to dispatch when considering only fuel costs. This issue was addressed in the operational length simulations in Chapter 6 and will be addressed in this context in future work, Chapter 9.

Table 7.6 Reference Case Environmental Results

Generator Added	On time (Hrs)	Energy (MWH)	Water Consumption (AF)
Npp	3737	1.436×10^6	3366.2
CCGT	1183	146.8×10^3	140.55
CCGT	1365	160.3×10^3	153.52
CT	728	31.95×10^3	22.647
CT	1456	68.59×10^3	48.624
	Total 3682.9 AF = 1.2150×10^9 gal		

Table 7.7 - Table 7.10 show the results for Scenario I, which has a slightly higher growth percentage as compared with the reference case. This is confirmed by the same units being chosen for generation expansion as the reference case along with the addition of one more coal unit. Even though the relatively cheaper generation was available due to the extra coal unit in this scenario, the operational costs were seen to be higher which suggests that the increase in system load outweighed the introduction of the cheaper generation.

Table 7.7 Scenario I TEP Results

Line Added	118	120	121	122	123	124	125	126	130	133
Hour	56	55	81	81	63	88	56	8	56	56
	Total Investment Cost:		**$7,030,515.55**							

Table 7.8 Scenario I GEP Results

	Generator Added	Bus	Hour
1	Npp	53	56
2	IGCC	29	55
3	CCGT	58	81
4	CCGT	19	81
5	CT	34	63
6	CT	19	88
	Total Investment Cost:	**$4,111,868,189.57**	

Table 7.9 Scenario I Operational Results

	Operational Years	8760 Hr x 2 SCED Cost ($)
1	1 & 10	1,493,956,000.00

The combined cycle and gas turbine units are seen to consume almost 977,000 more gallons of water than the previous scenario and the jump in overall water consumption can be attributed largely to the addition of the coal unit.

Table 7.10 Scenario I Environmental Results

Generator Added	On time (Hrs)	Energy (MWH)	Water Consumption (AF)
Npp	3737	1.493×10^6	3500.2
IGCC	3828	1.158×10^6	2132.3
CCGT	1183	143.7×10^3	137.55
CCGT	1365	150.9×10^3	144.51
CT	728	88.72×10^3	62.89
CT	1456	32.87×10^3	23.31
	Total 6000.76 AF = 1.955×10^9 gal		

Scenarios II and IV were both stated to have small net load growth per year and thus no new generation or transmission was required in the network. The year 1 and year 10 total operating costs for both Scenarios II and IV can be seen in Table 7.11. The total operational costs reflect lower the total load growth in year 10 as the values are seen to be much less than the reference scenario.

Table 7.11 Scenario II & IV Operational Results

Scenario	Operational Years	8760 Hr x 2 SCED Cost ($)
II	1 & 10	1,322,956,000.00
IV	1 & 10	1,264,202,000.00

Scenario III had a relatively larger load growth rate compared to Scenarios II and IV and, as a result, four additional generators were required. These were the smaller, less expensive units among the candidates for generator expansion and thus the total investment costs are observed to be much less than those seen for Scenario I and the reference case. Additionally, although the load growth was not as large for this case compared to the reference case, the operation costs were seen to be higher for Scenario III which can be explained by the fact that the cheap generation offered by the nuclear unit was not available in this scenario.

Table 7.12 Scenario III GEP Results

	Generator Added	Bus	Hour
1	CCGT	58	42
2	CCGT	19	81
3	CT	34	17
4	CT	19	17
	Total Investment Cost:	**$428,288,668.32**	

Table 7.13 Scenario III TEP Results

Line Added	121	122	123	124	125
Hour	81	81	63	88	56
	Total Investment Cost:		**$2,937,267.96**		

Table 7.14 Scenario III Operational Results

	Operational Years	8760 Hr x 2 SCED Cost ($)
1	1 & 10	1,454,933,000.00

The water consumption data for the additional generation in the system can be seen in Table 7.15. The water consumption is seen to be much less than in the reference scenario and Scenario I because the unit which were added were much more thermally efficient and thus require less water consumption for the unit's cooling cycle.

Table 7.15 Scenario III Environmental Results

Generator Added	On time (Hrs)	Energy (MWH)	Water Consumption (AF)
CCGT	2280	220.0×10^3	210.69
CCGT	1183	146.8×10^3	140.56
CT	2093	81.75×10^3	57.95
CT	2457	95.56×10^3	67.75
	Total 476.95 AF = 1.554×10^8 gal		

Finally, a visual comparison of the results for each of the scenarios can be seen in Figure 7.2 through Figure 7.4 with the investment costs, operational costs, and total water consumption shown. Note that the reference case is "Scenario 1" on the x-axis in the plots.

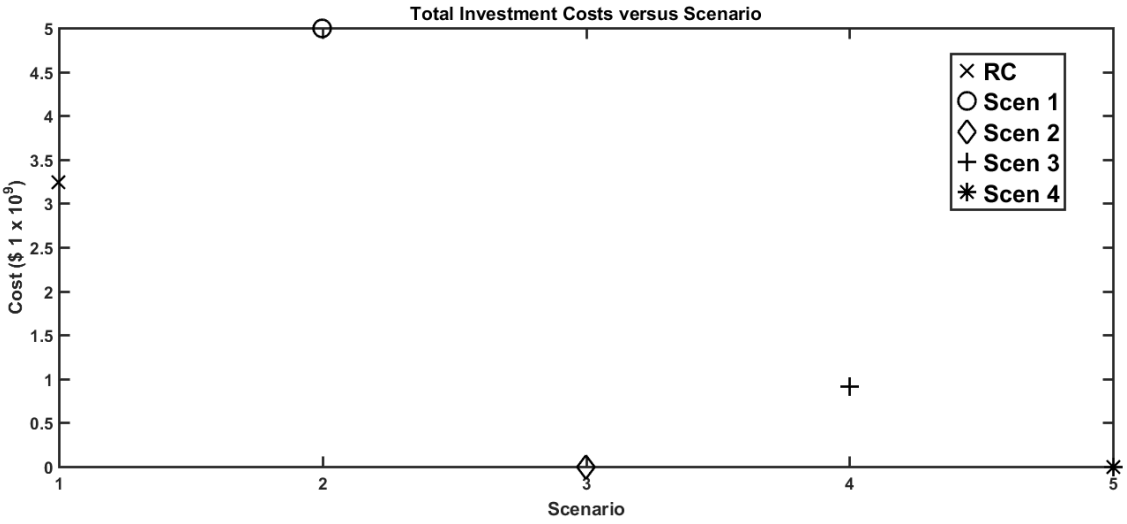

Figure 7.2 Total Investment Cost Comparison for GEP/TEP Scenarios

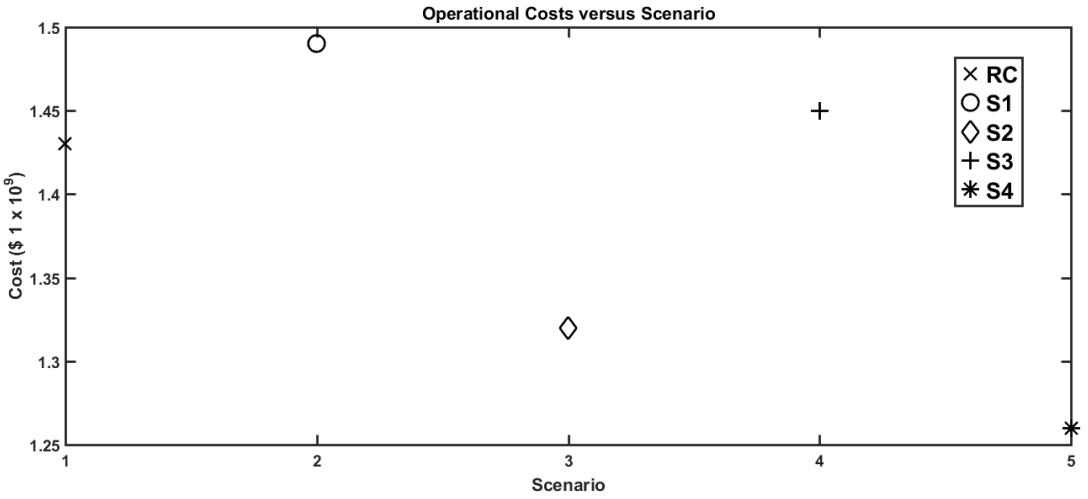

Figure 7.3 Total Year 1 & Year 10 Operational Cost Comparison for GEP/TEP Scenarios

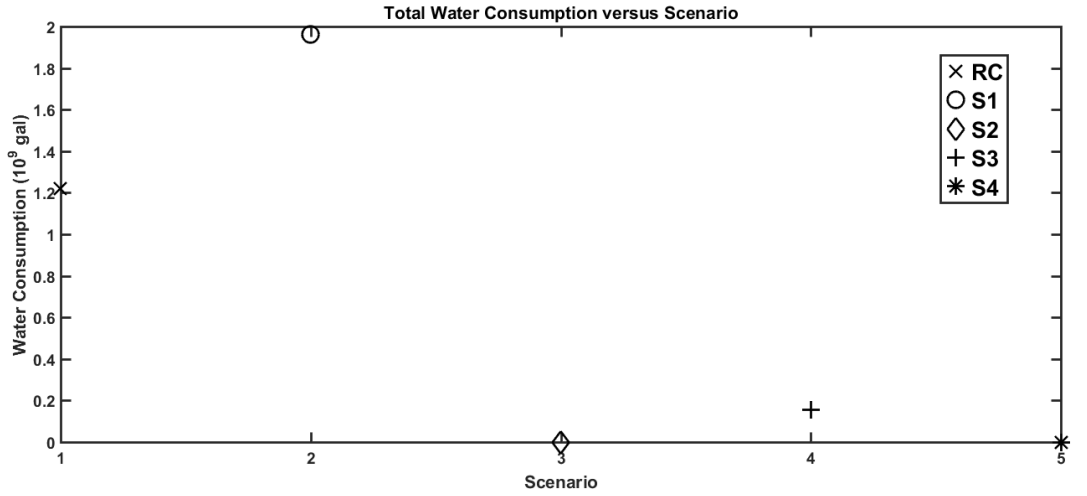

Figure 7.4 New Generation Total Water Consumption for GEP/TEP Scenarios

7.4 Summary

This chapter has presented the results for the implemented optimal investment-SCUC model to solve the GTEP problem. The novel idea presented is the calculation of the water consumption for new (and/or existing) generation with consideration of scenarios

where the anticipated water availability at a generation location or the amount of water rights obtained can be added to the planning model.

CHAPTER 8

POWER SYSTEM RESILIENCE: QUANTIFICATION THROUGH OPERATIONAL AND INFRASTRUCTURAL METRICS

Historically, it has been observed that the electric power system and the water distribution system are very reliable in their operation and resilient to normal disturbances that affect the systems. This is the result of extensive and thorough design and planning procedures for the two systems. The results of the previous studies, especially in the realm of an operational time-scale, have confirmed this fact even for the simplified test systems used. These results show that the satisfactory operation of the two systems is possible even under the extreme contingencies simulated.

Reliability [67] is composed of two parts with one part pertaining to static, steady-state performance and the other pertaining to transient stability. Resilience is another measure of satisfactory performance that has garnered more attention recently as it desired to have a more comprehensive understanding and more insight into how the systems will behave when subjected to increasingly extreme system or external conditions. The disturbances that are to be studied here are similar to what was considered earlier, namely extreme incidents that fall into the category of so-called high impact, low probability events.

This chapter builds up the resilience computation methodology step-by-step, starting with the concept of index functions, the formulation for operational resilience and

the infrastructural robustness metrics, and finally the infrastructural-operational resilience formulation. The work presented in this chapter is based upon the work in [108], [109].

8.1 Concept of "Index" Functions

The index functions defined in later sections are the starting point for all of the resilience calculations. These functions are meant to be indices that allow for the current system operating conditions to be gauged with respect to the values of the selected quantities (e.g. bus voltages).

8.2 Operational Resilience Calculation Methodology

The operational resilience (OR) calculation method that is presented here is done in three steps. First, an *index function* is used to compare a specific operational parameter or variable in the power system with its ideal value. Second, that index is used to calculate what was called in Chapter 2 a *resilience measure of performance* (RMP). Because the power system is a complex system and it is not reasonable to assume that resilience can be quantified by just one system characteristic, several RMPs are presented in this chapter. The goal of these measures of performance is to relate the index function values to the current and past overall performance of the system. Following the calculation of the desired or specified RMPs, a weighted sum of these RMPs is calculated and normalized appropriately and this value can be viewed as the actual measure of resilience. Figure 8.1 shows the flow chart for the implementation of this calculation procedure. Here, it is noted that this analysis was implemented by using simulation results from Chapter 6. The calculations were performed after the simulations were completed, although this procedure

could be implemented to perform the resilience calculations within the simulation framework presented.

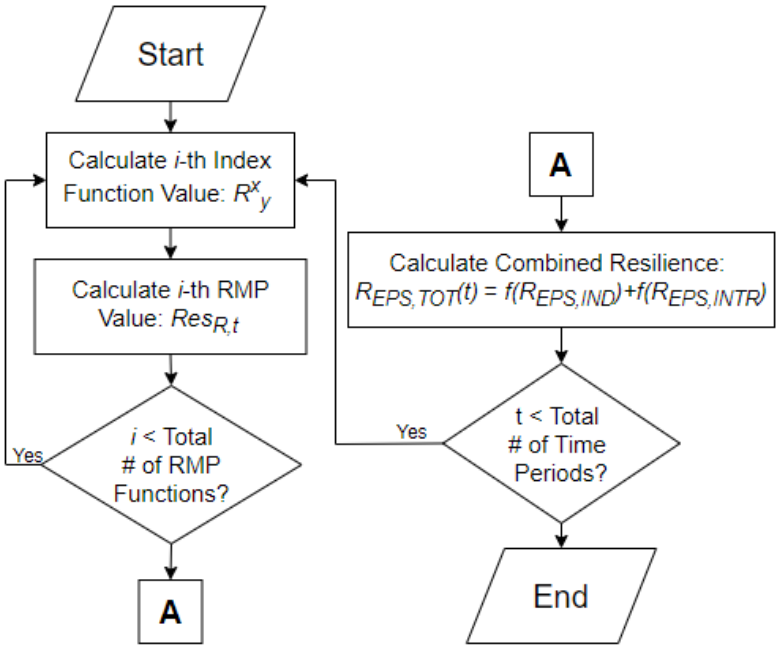

Figure 8.1. Resilience calculation flow chart

8.3 Mathematical Formulation for OR Index Functions and OR RMPs

The metrics that are used as a weighted sum to quantify resilience are directly related to the present and historical operating condition of the power system. These metrics, from which the overall system resilience value is determined, are defined in terms of quantities related to both the independent operation of the power system as well as to the interdependent operation of the electricity and water systems. The weighting of each of the terms comprising the overall resilience can be determined by a decision maker or by other means such as assigning weights according to a component's calculated structural vulnerability, as will be discussed in a later section.

With the power system quantities that were examined in Chapter 6 in mind, the following quantities are used for calculating the OR index function values:

1. Bus voltage magnitude

2. Line thermal limits

3. *Thermoelectric cooling water demand satisfaction*

4. Load (overall) supply satisfaction

5. *Load (WDS pump) supply satisfaction*

The terms in italics above denote quantities that aim to capture resilience in terms of explicit interdependencies between the EPS and WDS. Each of these five quantities is defined for every iteration (time-period) within the simulation, so it is noted here that the functions defined below are functions of time.

The OR calculation is based on defining resilience to characterize how well the system performs satisfactorily following unsatisfactory operation. For a given performance index function, *R*, the OR value [110] in time-period *t* is given as:

$$Res_{R,t} = \frac{\#\ of\ satisfactory\ operations\ following\ unsatisfactory}{\#\ of\ unsatisfactory\ operations} \tag{8.1}$$

Unsatisfactory operation is defined as the resilience index function being less than that function's value in the previous simulation hour (and satisfactory operation denoted by an increase in the index function's value). For the interdependent infrastructure metrics, a

more restrictive definition of unsatisfactory operation in a given time-period is defined. For those cases, if the index function is less than its maximum value of 1, this is considered unsatisfactory. The RMPs are defined as values between 0 and 1. The relationship between the various index functions and the RMP is clearly seen in the flowchart of the presented methodology shown in Figure 8.1.

8.3.1.Bus Voltage Index Function and OR RMP

The voltage magnitudes in the EPS are kept within a small range of values during normal system operation. The reason for this is that electrical equipment is designed for operation at certain rated voltages and operation under conditions which differ too greatly from the rated specifications can have adverse effects. These effects can include insulation breakdown for equipment that is operated at voltage levels that are too high. The index function relating the operational performance of the power system to bus voltages is therefore defined to have a value of 1 for voltages within a small, nominal operating range. Outside of this range, the resilience is assumed to decrease as the deviation away from the nominal operating conditions is increased and reach a value of zero at some point. Following the description above and using the quantities given in Table 8.1 below, the resilience index function for bus voltage magnitude is defined mathematically as:

$$R_V^n = \begin{cases} 0 & V_n < V_{min} \\ 13.\overline{3} \cdot V_n - 12 & V_{min} \le V_n \le V_{thr,min} \\ 1 & V_{thr,min} \le V_n \le V_{thr,max} \\ -13.\overline{3} \cdot V_n + 14.\overline{6} & V_{thr,max} \le V_n \le V_{max} \\ 0 & V_{max} < V_n \end{cases} \tag{8.2}$$

Table 8.1 Parameters for Bus Voltage Resilience Index Function

Symbol	Quantity	Value (pu)
V_{min}	Lower-Cut Out for Index Function	0.900
$V_{thr,min}$	Minimum Bus Voltage Value for Maximum Index Function	0.975
$V_{thr,max}$	Maximum Bus Voltage Value for Maximum Index Function	1.025
V_{max}	Upper-Cut Out for Index Function	1.100

where V_n is the bus voltage magnitude in pu and the parameters $V_{thr,min/max}$ and $V_{min/max}$ are the values where R_V^n starts decreasing and the values where it reaches zero, respectively, as described above. The values of $13.\overline{3}$, 12, and $14.\overline{6}$ are due to the numerical values chosen for $V_{thr,min/max}$ and $V_{min/max}$ and where, for completeness, $13.333\ldots = 13.\overline{3}$ and $14.666\ldots = 14.\overline{6}$. The behavior of this resilience function for different voltage magnitude values and over the course of a simulation will now be demonstrated. First, the resilience index function given in (8.2) is shown in Figure 8.2 below.

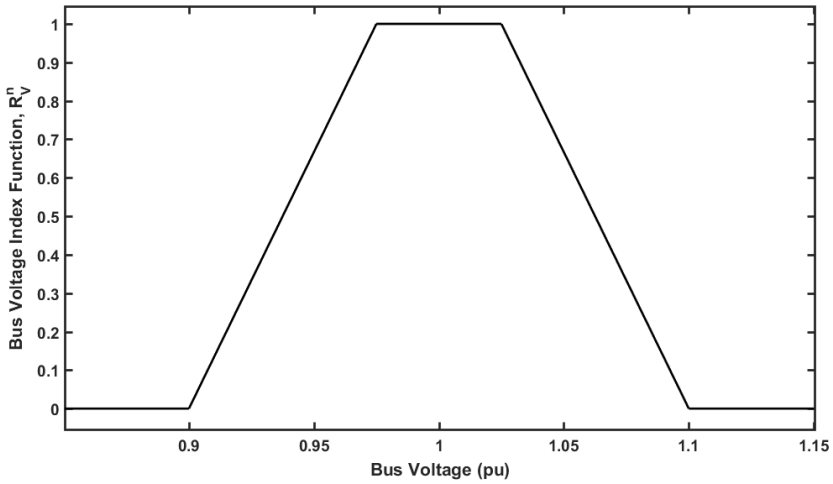

Figure 8.2 Bus Voltage Resilience Index Function versus Bus Voltage

The next two figures show the plots of bus voltages for the IEEE 14-bus test system followed by the plots of the index function values.

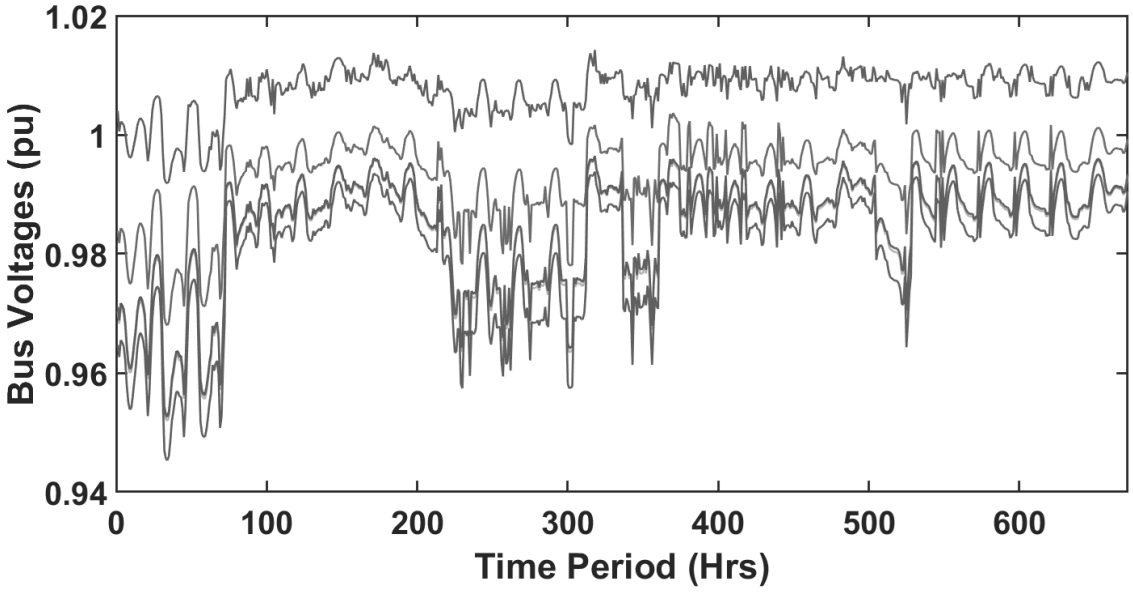

Figure 8.3 Bus Voltages (pu) versus Time (Hrs)

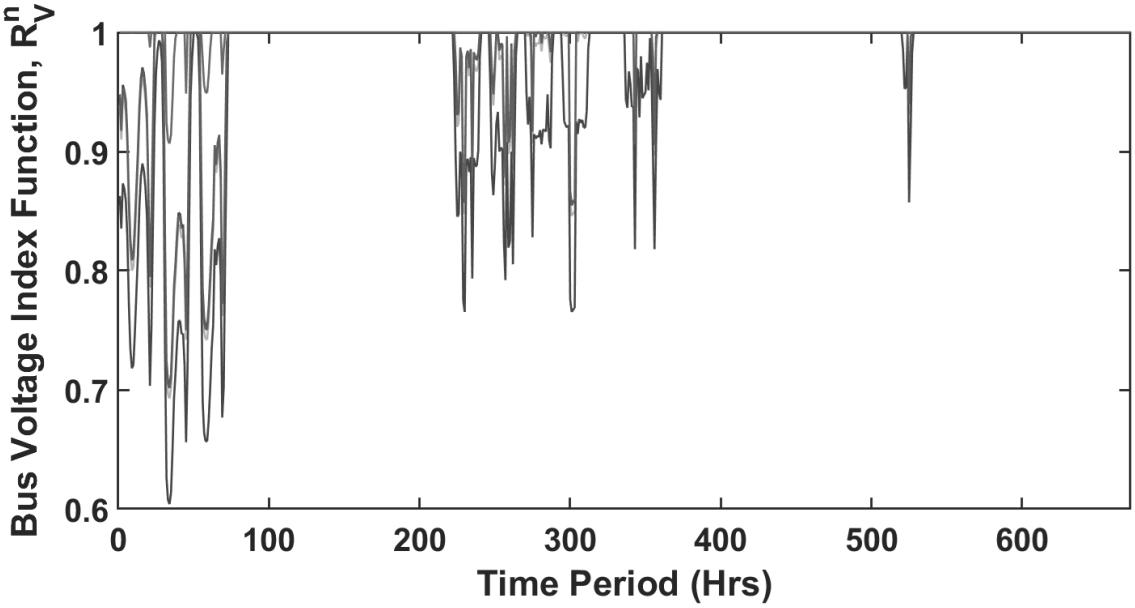

Figure 8.4 Bus Voltage Index Function versus Time (Hrs)

The voltage profile indicates periods of high system loading (low voltage) and periods with smaller total load (high voltage). The resilience index function follows the

behavior illustrated in Figure 8.2. For example, the system voltages increase, decrease and reach a minimum, the begin to increase again. The resilience index values correspondingly decrease while the voltage magnitudes are below $V_{thr,min}$, peak, then return to one for magnitudes which return to a value between $V_{thr,min}$and $V_{thr,max}$.

The RMP for bus voltages in time *t* of the simulation is formulated using (8.1) and the voltage index function (R_V^n) given in (8.2) for each time *t* of the simulation and calculated as:

$$Res_{R_V^n,t} = \frac{\sum_{n=1}^{NB} max(0, R_V^n(t) - R_V^n(t-1))}{\sum_{n=1}^{NB} ceil(R_V^n(t-1) - R_V^n(t))} \tag{8.3}$$

Note that this is just an expansion of (8.1) in terms of the index function R_V^n.

8.3.2.Transmission Line Index Function and OR RMP

Similar to the voltage magnitudes in the power system, the transmission lines are designed to be operated under specific rated current magnitude levels. The reason for this is that the transmission level equipment consisting of conductors, terminating equipment such as transformers, and protection equipment, all have thermal ratings and operation of this equipment above these temperatures can cause permanent damage to what are often some of the most expensive components in the power system. In addition, transmission lines will sag under increasing current (and therefore temperatures) which can cause regulatory issues regarding minimum clearance criteria as well as pose a potential hazard for objects beneath the transmission lines.

Because power is proportional to current, lines are normally given several different maximum apparent power operating limits. These include the familiar normal, continuous Rate A MVA equipment rating as well as the emergency, Rate C MVA limit. Because there are multiple limits, there is some flexibility on the magnitude of power flow on a line. Therefore, instead of being based on the instantaneous line flow magnitude, a moving average of the line flow is calculated and used for the transmission line thermal limit index function. The planner or operator performing this study then has the flexibility to adjust the summing length parameter, *sl*, to make the index function value more or less sensitive to temporary line flows exceeding the Rate A value. The index function is given as:

$$R_{TL}^{l} = min\left(1, \frac{P_{l,max} \cdot sl}{\sum_{r=t-sl}^{t-1} P_{l,r}}\right) \tag{8.4}$$

where $P_{l,max}$ is the Rate A MVA line limit and $P_{l,r}$ is the line flow in time-period *r*.

An example of what this quantity looks like is shown below. First, Figure 8.5 shows the actual line flow, in MW, over a 10-day (240 hour) window. Figure 8.6 shows the value of the running sum of the line flow for different *sl* values along with a presumed maximum flow of 39.5 MW. Lastly, Figure 8.7 shows the value of the index function R_{TL}^{l} over the 240-hour window with the previously stated assumptions. The lowest value of the index function value of approximately 0.92 is seen for an averaged line flow value of 42.8 MW corresponding to the *sl* value of 4 hours. Note that for *sl* values greater than 12 hours, the resilience index function is not seen to drop below 1.

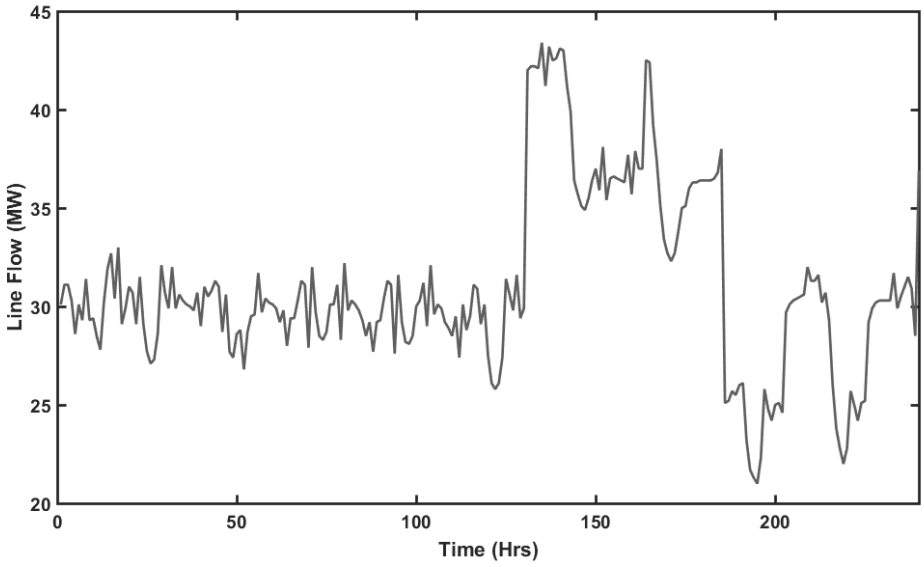

Figure 8.5 Line Active Power Flow

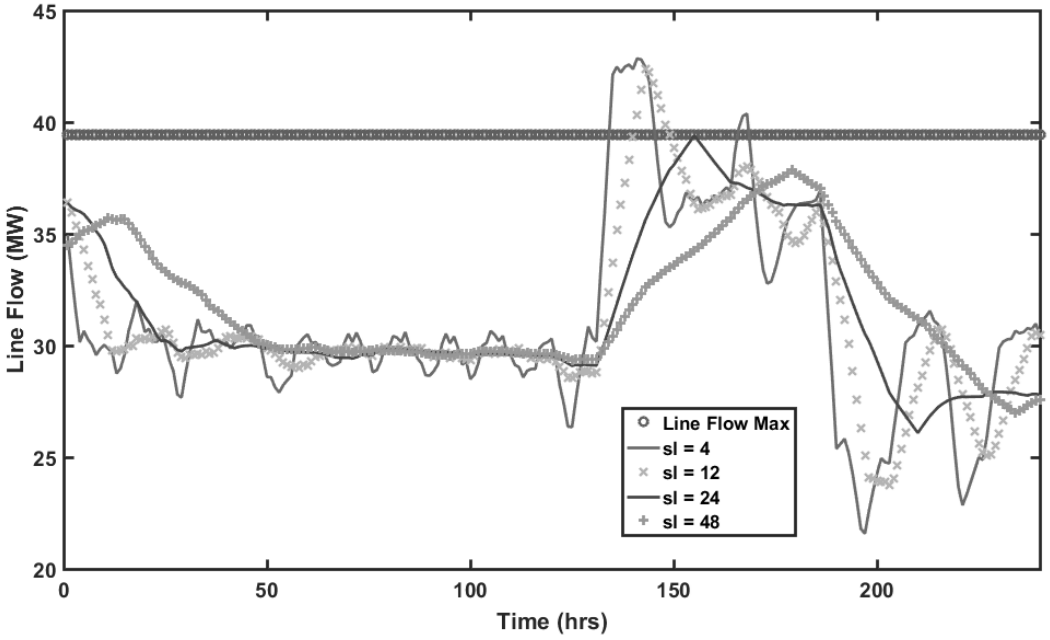

Figure 8.6 Transmission Line Active Power Flow Maximum and Running Sum

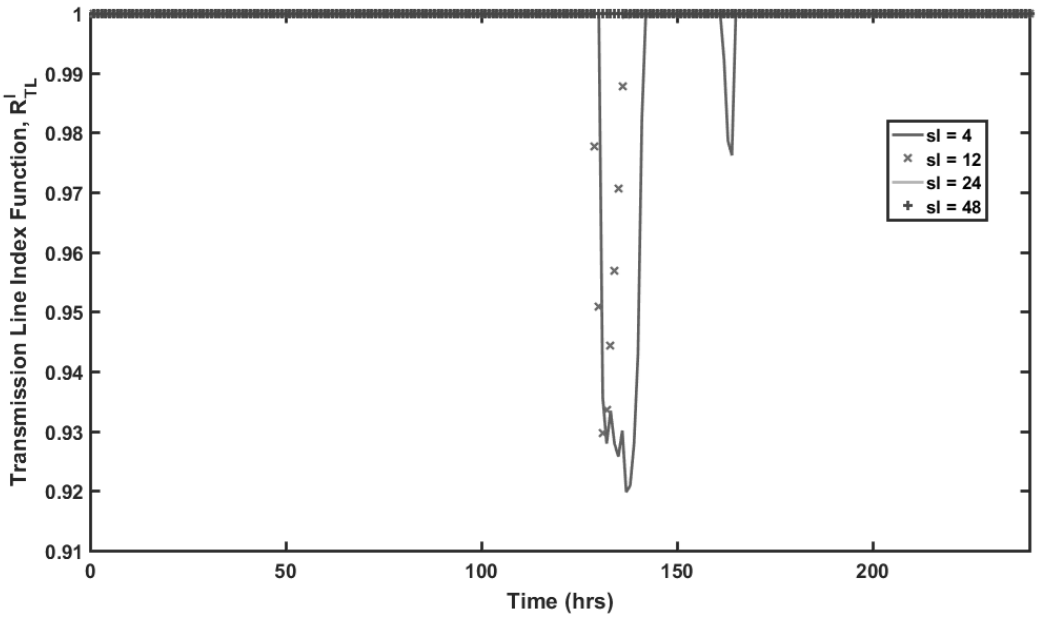

Figure 8.7 Transmission Line Resilience Index Function

The RMP for transmission line thermal limits is formulated using (8.1) and the thermal limit index function (R^l_{TL}) given in (8.4) for each time *t* of the simulation and is calculated as:

$$Res_{R^l_{TL},t} = \frac{\sum_{l=1}^{NL} max(0, R^l_{TL}(t) - R^l_{TL}(t\text{-}1))}{\sum_{l=1}^{NL} ceil(R^l_{TL}(t\text{-}1) - R^l_{TL}(t))} \quad (8.5)$$

8.3.3.Cooling Water Demand Satisfaction Index Function and OR RMP

Thermoelectric generation requires water for the cooling cycle in the process of converting the heated working fluid from steam back to water via heat transfer. As discussed in Chapter 2, the cooling cycle can be an open or closed cycle, with the latter exemplified by power plants using cooling towers. The use of cooling towers introduces losses through drift, blowdown and evaporation and the water needed to replenish the

amount lost represents a key dependency of the power system on the water system. Since the amount of onsite storage for cooling water is normally substantial, it is reasonable to assume that the onsite tank levels will not change vary rapidly either under normal conditions or even when operating under sub-optimal conditions related to the re-supply of consumed cooling water. Given the substantial storage and the slow rate of change in that storage, the system will be able to function at a satisfactory level even with changes in the level of onsite water storage. The index function relating system performance to the amount of cooling water that is supplied is presented here as a conservative estimate of the storage tank level and given a piece-wise linear form as follows:

$$R_{CW}^{g} = \frac{ceil\left(\frac{TL_{g,t}}{TL_{g,initial}} \cdot 10\right)}{10} \tag{8.6}$$

The formulation of the index function in this way means that the index function tracks the tank level but with a slight lag in the functions value as changes in the level in the water storage tank occur. This can be seen by examining how the value of R_{CW}^{g} changes as the tank level decreases. For example, it is not until the tank level is under 90% of its initial value that the index function decreases and becomes 0.9. This gives the desired behavior of tracking the tank level while also not responding to small, rapid fluctuations in the storage tank levels.

In summary, this formulation quantifies resilience with respect to cooling water as a piece-wise linear function based on the ratio between the current on-site cooling water to

the initial tank level. The plot of (8.6) versus normalized tank level and a plot as tank level changes in simulation are shown in Figure 8.8 and Figure 8.9 below.

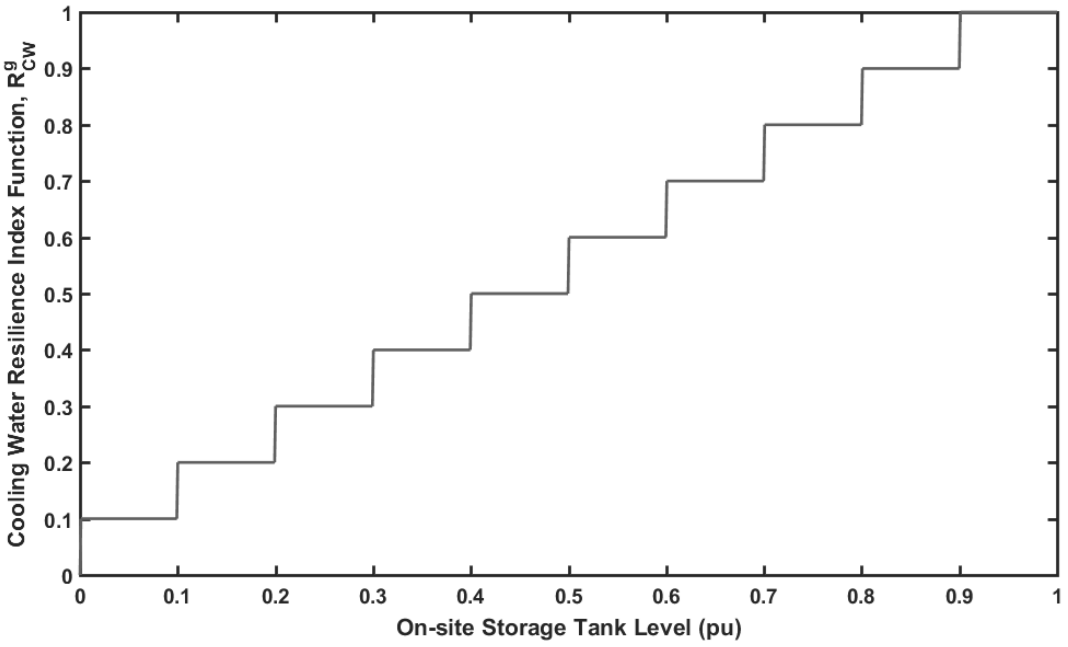

Figure 8.8 Cooling Water Index Function versus Time (Hrs)

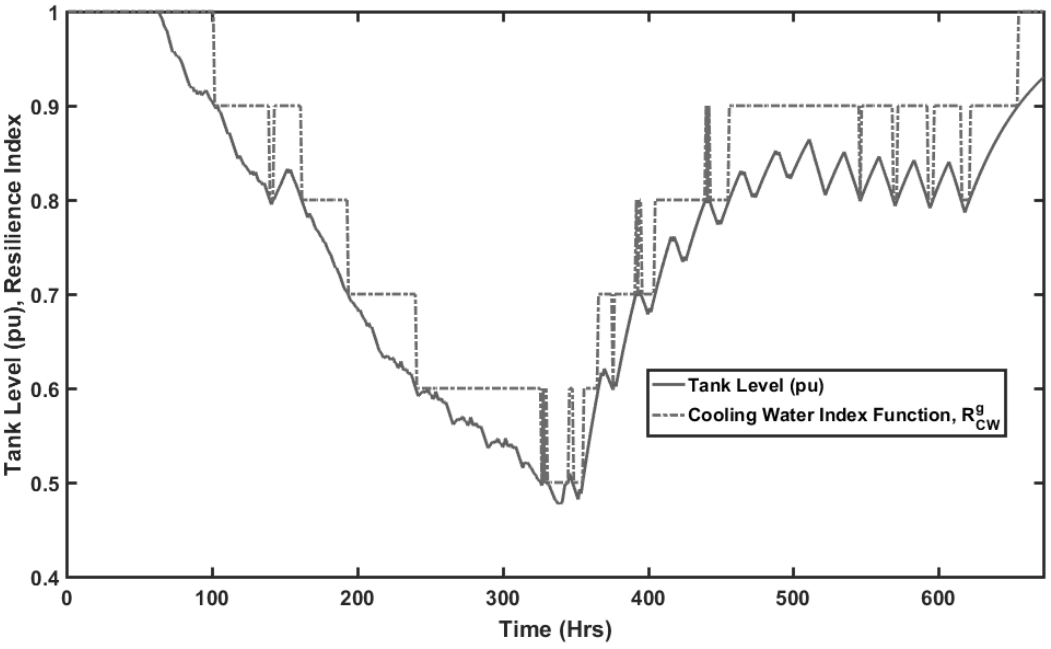

Figure 8.9 On-site Storage Tank Level and Resilience Function versus Time

The RMP for the thermoelectric generation's cooling water supply is then formulated using (8.1) and the cooling water index function (R^{g}_{CW}) value given in (8.6) for each time *t* in the simulation as:

$$Res_{R^{g}_{CW},t} = \frac{\sum_{l=1}^{NL} max(0, R^{g}_{CW}(t) - R^{g}_{CW}(t-1))}{\sum_{g=1}^{NG} ceil(1 - R^{g}_{CW}(t))} \tag{8.7}$$

Here, the difference between (8.7) as compared with (8.3) and (8.5) is seen in the denominator where the number of unsatisfactory performances in (8.7) is given a more strict definition.

8.3.4.Load Supplied (Overall) Index Function and OR RMP

The goal of operation in the power system is to satisfactorily supply the requested electrical power demands of consumers while satisfying constraints related to the quality of the power delivered. A resilience measure along these lines is formulated in order to quantify how well the system demands were met under extreme system operating conditions where the probability of load being shed or at least the necessity of additional power needing to be imported into the area under study was non-negligible. From the simulations results for the case studies under consideration, it was seen that with the implemented control strategy of de-rating units suffering cooling water shortages, there would be times during which the total electrical demand would not be satisfied. In addition, it is know from consumer surveys [111] that they (consumers) are willing to adjust their demands based on what the perceived weather conditions are. These consumers have also been shown to have slightly different amounts of willingness to change their consumption

based on their knowledge of how the water and power system interact as well as whether the curtailment of the usage of water and energy is mandatory or not. For representation of this fact within this resilience calculation, the bus loads are decomposed into representative percentages for industrial, commercial and residential components. Within the residential load component, it is further sub-divided into single family (*sf*) and multi-family (*mf*) elements based on recent census data for Arizona [112].

An example of how incorporation of this consumer data will affect the load curve over time is demonstrated below. First, Scenario 1-R from the consumer data, corresponding to a chronic water shortage is selected. The consumer survey data regarding how usage of water and electricity would change in such a scenario was collected for sub-categories of each domain as shown below in Table 8.2.and Table 8.3.

Table 8.2 Sub-Categories Surveyed for Usage in the Energy Domain

Domain	**Sub-Category**
Energy	Cooling
-	Dryer
-	Washing Machine
-	Oven
-	Dishwasher
-	Water Heater
-	Refrigeration
-	Lighting
-	Outdoor
-	Cooking
-	Other

These sub-categories represent the major end-uses of electricity and water for the residential sector in the United States. A scenario corresponding to a chronic water shortage was then selected from the consumer survey results and the proportion of electricity usage

that consumers would be willing to curtail was used to calculate the amount that would still be used. This was then weighted against a given sub-category's proportion of the total

Table 8.3 Sub-Categories Surveyed for Usage in the Water Domain

Domain	Sub-Category
Water	Toilet
-	Shower
-	Washing Machine
-	Bath
-	Dishwasher
-	Outdoor
-	Leaks
-	Faucet
-	Other

energy use in the US and aggregated in order to give the demand adjustment factors for the peak hours surveyed, as shown in Table 8.4. The interpretation is then that consumers would be willing to reduce their overall consumption by a factor equal to these values in the corresponding hour.

Table 8.4 Peak Hour Demand Coefficients for Single and Multi-Family Homes

Time	Demand Coefficient - *sf*	Demand Coefficient - m*f*
6am - 6:59am	0.75444906	0.7093457
7am -7:59am	0.79997816	0.7314116
8am - 9am	0.78636656	0.7292784
5pm - 5:59pm	0.8309073	0.7605177
6pm - 6:59pm	0.82466484	0.7514394
7pm - 7:59pm	0.8223109	0.7490517
8pm - 9pm	0.82880098	0.7518957

These values were then used to alter the nominal value of *LMF* at any given time-period for load buses. The new *LMF*s for both the single-family and the multi-family components of the load is given by the product of the nominal LMF curve and the demand

coefficient (*sf* or *mf*) at that hour. For the hours which are not peak hours and hence no demand coefficient is given, an assumption that the demand adjustment is equal to the average of that during the peak hours was used. The plot in the top of Figure 8.10 show the nominal *LMF* and the adjusted *LMF*, assuming percentages of single-family and multi-family houses as stated above and assuming that residential loads are 1/3rd of the total load. The plot in the bottom of Figure 8.10 shows the *LMF* factor corresponding to multi-family and single-family homes.

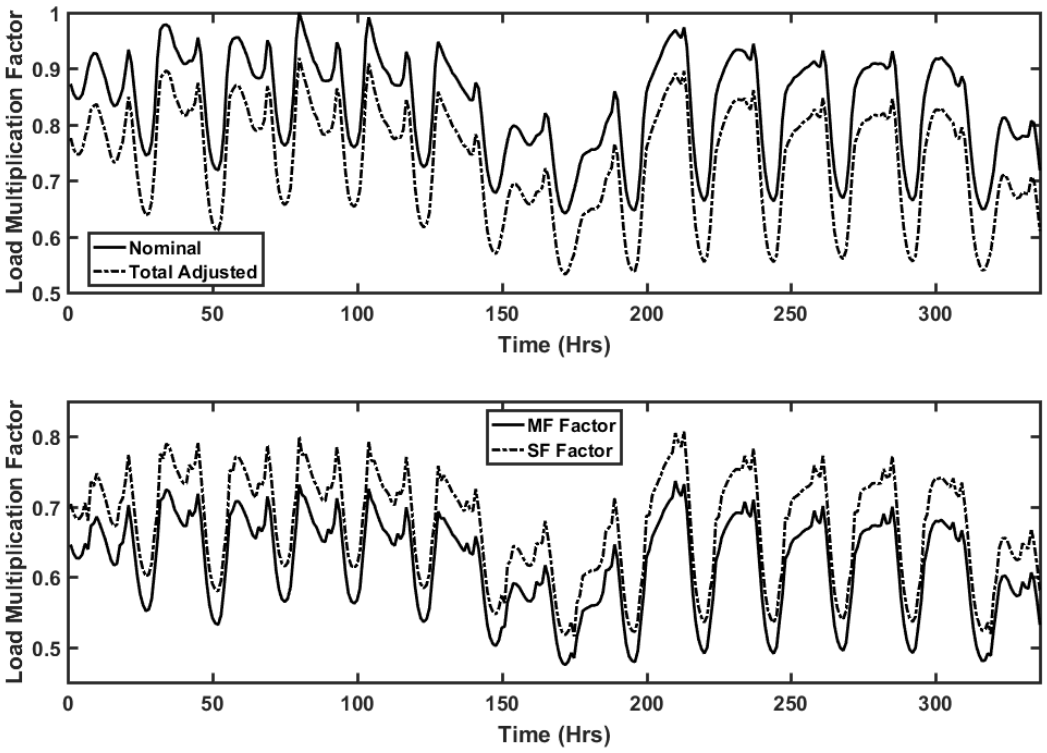

Figure 8.10 *LMF* Curves

With the previous values defined and examined, the resilience index function for overall load satisfaction can now be defined. The expression is as shown below:

$$R_{DS}^{n} = ceil\left(\left(P_{load,nt}\text{-}LOL_{n,t}\right)\text{-}\left(P_{load,nt}\text{-}sf_{n}\cdot dAdj_{sf,t}\text{-}mf_{n}\cdot dAdj_{mf,t}\right)\right)$$
$$= ceil\left(sf_{n}\cdot dAdj_{sf,t}+mf_{n}\cdot dAdj_{mf,t}\text{-}LOL_{n,t}\right) \quad (8.8)$$

This function can be understood by examining one term at a time. From the top equation in (8.8), the first term can be seen to be the present bus load less any load that is lost and the second term is a best case load assuming the present demand is adjusted by a reduction equal to what consumers have said they would be willing to decrease their amount of consumption by. From this, the function is assigned a value of 1 if the actual load (less any lost) is greater than the best case, consumer adjusted load and zero if the opposite is true.

The resilience measure of performance related to the supplied demand at time *t* is then formulated using (8.1) and the overall load supplied index function (R_{DS}^{n}) given in (8.8) and can be calculated as:

$$Res_{R_{DS}^{n},t} = \frac{\sum_{n=1}^{NBL} max(0, R_{DS}^{n}(t)\text{-}R_{DS}^{n}(t\text{-}1))}{\sum_{n=1}^{NBL} ceil(R_{DS}^{n}(t\text{-}1)\text{-}R_{DS}^{n}(t))} \quad (8.9)$$

8.3.5.Load supplied (WDS pumps) Index Function and OR RMP

To further capture the interdependencies of the water and electric systems during operation, an additional index function is defined which is related to the satisfaction of the pump load directly serving the water distribution system. In contrast to the previous load metric, this one does not consider any consumer survey data but instead directly generates

a zero or one based on whether the pump demand is satisfied or not. The index function is given mathematically as:

$$R_{PL}^{n} = \begin{cases} 1, & PL_{demand} = PL_{supply} \\ 0, & PL_{demand} > PL_{supply} \end{cases} \tag{8.10}$$

where PL_{demand} is the active power demand which would have been requested and PL_{supply} is the value determined by the scenario definition (e.g. $PL_{demand} = PL_{supply}$ with no contingency).

The resilience measure of performance related to the supplied demand of pump loads in the WDS at time *t* is then formulated using (8.1) and the WDS pump load supplied index function (R_{PL}^{n}) given in (8.10) and can be calculated as:

$$Res_{R_{PL}^{n},t} = \frac{\sum_{n=1}^{NPL} max(0, R_{PL}^{n}(t) - R_{PL}^{n}(t-1))}{\sum_{n=1}^{NPL} ceil(1 - R_{PL}^{n}(t))} \tag{8.11}$$

8.3.6.Total System OR

The overall system resilience is then calculated as a weighted sum of the voltage, thermal limit, cooling water, demand supplied (overall) and demand supplied (WDS pumps) resilience measure of performance values. The terms compose what are recognized as quantities pertaining solely to the operation of the power system, $f(Res_{PS,IND})$, as well as quantities concerned explicitly with the interdependent operation of the two systems, $f(Res_{PS,INTR})$. The weights used in (8.13) for the calculation of $Res_{PS,TOT}(t)$ can be determined through sensitivity analysis for the power system in order to judge each

parameters effect in correctly assessing the overall performance of the system. The total OR can be calculated at each time-period as:

$$Res_{EPS,TOT}(t) = f(Res_{EPS,IND}) + f(Res_{EPS,INTR}) \tag{8.12}$$

$$Res_{EPS,TOT}(t) = \frac{w_{ov}Res_{R_V^n,t} + w_{otl}Res_{R_{TL}^l,t} + w_{ocw}Res_{R_{CW}^g,t} + w_{ods}Res_{R_{DS}^n,t} + w_{opl}Res_{R_{PL}^n,t}}{w_{ov}+w_{otl}+w_{ocw}+w_{ods}+w_{opl}} \tag{8.13}$$

8.4 Example of Proposed OR RMPs and Case Study Results

The following results are based on the results for Case I and Case III in Chapter 6 and were done after the assigning of line limits based on the observed line flows over the course of many simulations. Figure 8.11-Figure 8.13 contain the plots of the individual RMPs that were calculated using the results from Case III. The system is heavily loaded towards the beginning of the simulation and this is reflected in Figure 8.11 where the bus voltage and transmissions line resilience values that are less than 1 at the beginning of the simulation.

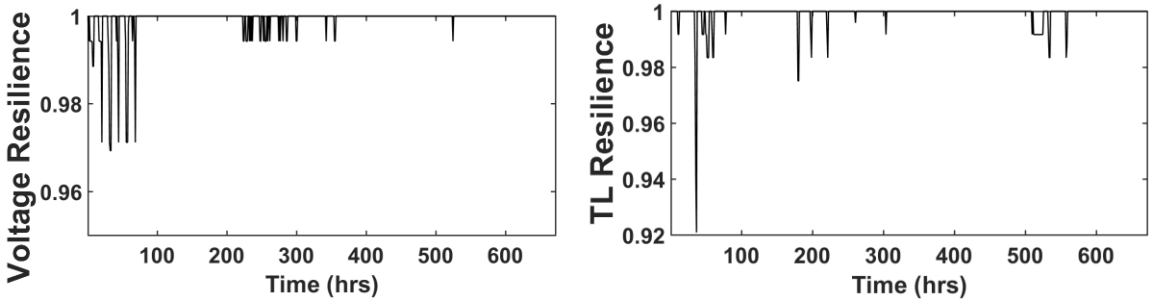

Figure 8.11 Bus Voltage (L) and Transmission Line (R) Resilience Value

The restriction of water, representing drought conditions, is seen to quickly degrade the cooling water RMP in Figure 8.12 as the cooling water demand requirements of the thermoelectric generation is not met and the on-site storage tank levels begin to decrease. The demand satisfied (overall) RMP is seen to decrease later in the simulation as the implemented control scheme reduces the maximum power outputs of the units as the level of water in the on-site storage decreases. As mentioned in Chapter 6, this loss of load is an artifact of the small test system being used and can instead be interpreted as the amount of power needing to be imported for a large, interconnected system.

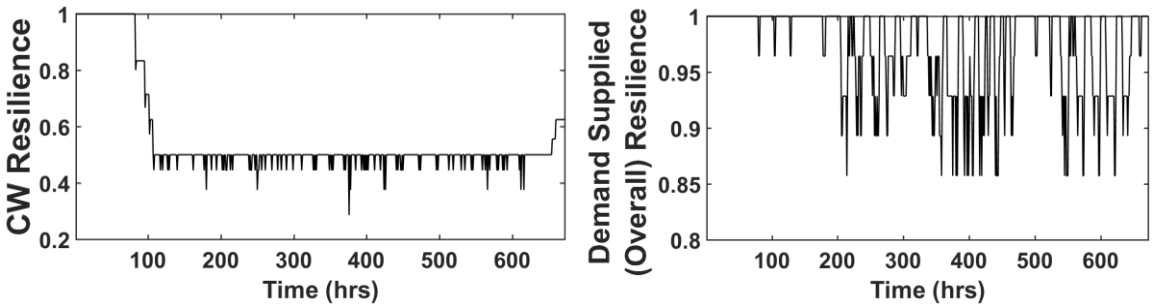

Figure 8.12 Cooling Water (L) and Demand Supplied (Overall) (R) Resilience Values

The plot on left in Figure 8.13 shows resilience value for the demand satisfied for the WDS pumps. This plot is seen to follow the trend in Figure 6.12 in that these pumps are specified to be outaged in the scenario definition.

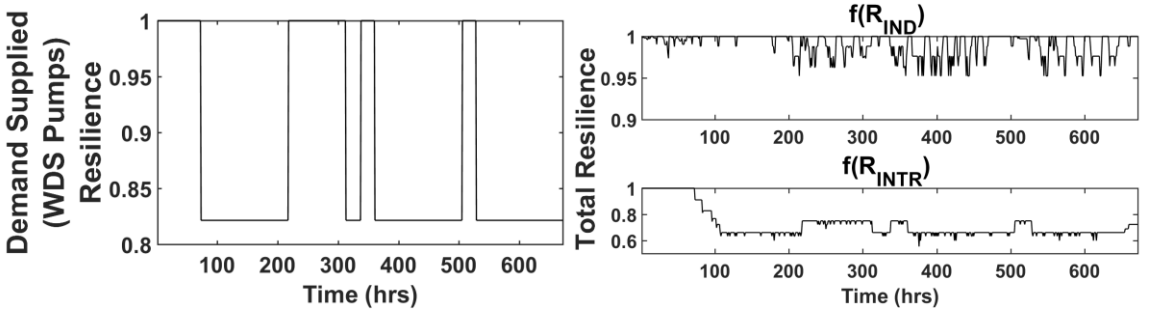

Figure 8.13 Demand Supplied (WDS Pumps) (L) and Total Resilience Components (L)

The plots on the right in Figure 8.13 above show the components of the total resilience calculation in terms of the independent and interdependent measures of performance.

Figure 8.14 plots the combined resilience metric for increasing weights of the terms capturing interdependent operation. Because these resilience values are the dominant component of the overall resilience value, it is seen that increasing values of these weights results in smaller decreases of the overall function value. Lastly, it can be noted that selection of the specified indices results in capturing the desired system behavior, in that the measures of performance reflect the degradation in system conditions that were observed. The combined resilience value also reflects the fact that this test system is resilient in that the resilience value begins to increase at the end of the simulation. This is seen to be directly as a result of a larger volume of water available to the WDS to meet the thermoelectric generation demand in addition to its commercial and residential demands.

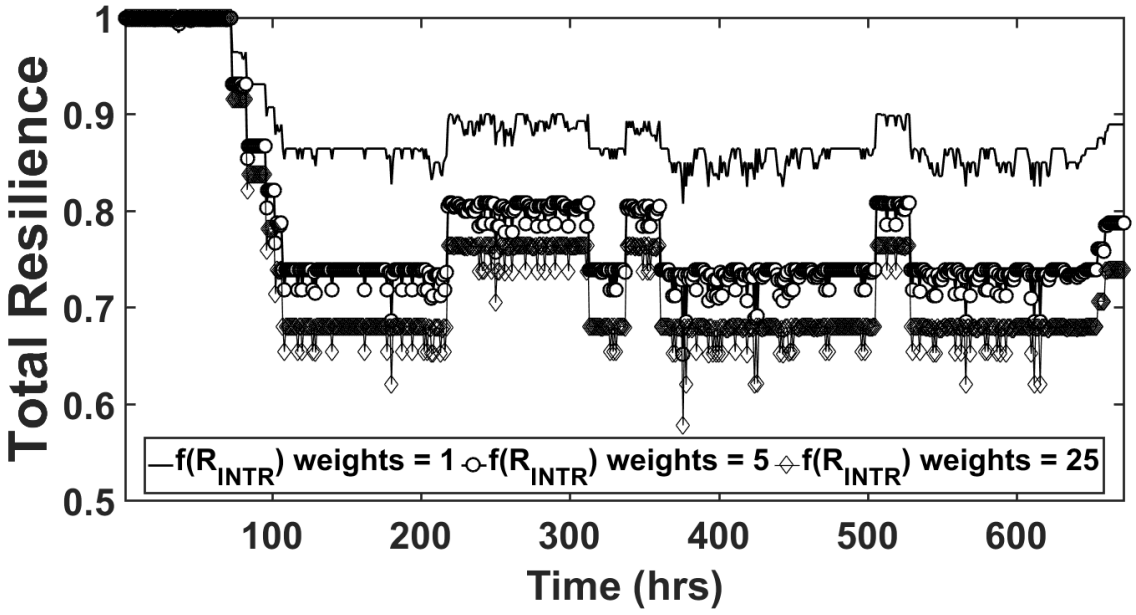

Figure 8.14 Sensitivity Analysis for Total Resilience, Case III

Figure 8.15 shows a comparison of the resilience values from Case I and Case III, because the contingencies contained within the simulated scenario were much more severe in Case III, the total resilience value is seen to be much lower. The momentary increases in resilience value for Case III are the result of the demand satisfied (WDS Pumps) resilience value increasing during time when there are no pump outages. Because the total resilience function value is seen to be dominated by the $f(Res_{PS,INTR})$ terms, the difference in resilience values can be seen to be the result of primarily the cooling water resilience function value, calculated in (8.6) and (8.7).

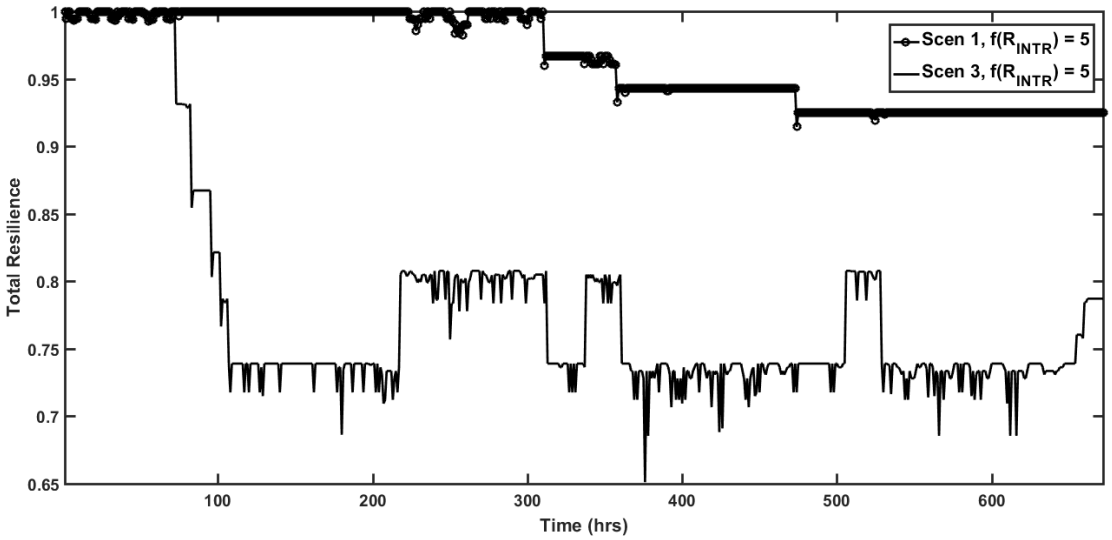

Figure 8.15 Resilience Comparison for Case I and Case III

8.5 Mathematical Formulation for Infrastructural Robustness Metrics (IRM)

Robustness is the inherent ability of a system to resist failures and this ability is intrinsic to a particular system based on its structure and configuration. This section details several *infrastructural robustness metrics* (IRM) which are used in order to determine a

weight for each RMP in preparation for its inclusion in the final *infrastructural-operational resilience* (IOR) value.

The reasoning for including the IRMs is as follows, taking the voltage RMP as an example. The voltage RMP in a given time-period will be calculated as the sum of all of the bus voltage RMP's. However, it is likely that not all the buses are equally important to a system's operation or integrity and therefore the contribution of some bus voltage values to the overall resilience value should be less as compared with other buses.

The IRM's therefore allow for a systematic way of weighting the RMP's to give a more complete view of system resilience since both the system operating conditions as well as the system network topology are taken into consideration for the total IOR value. Although the above example considered the EPS voltage RMP, the same logic can be easily extended to the other OR quantities. The first three robustness metrics for the EPS that are defined in the following sections are based upon those in [113]–[115] and are uniquely applied here as weights to the RMP's.

8.5.1.Connectivity Metric

The principal purpose of this metric is to determine a node's (bus) importance. The development of this metric follows the progression for determining the importance of a vertex by degree (for an unweighted network), strength (for a weighted network), or "entropic degree", which is the metric presented. The benefit of using this metric is that it provides the ability to capture [114], in graph theory terms, 1) vertex connection strength to an edge 2) distribution of weights between the edges connected to a vertex and 3) the

total number of edges connected to a vertex. For each bus, this connectivity metric is determined by the impedance of the lines connected to it. The metric is defined as:

$$M_{ED,n} = \left(1 - \sum_m p_{nm} \cdot log\left(p_{nm}\right)\right) \sum_m w_{nm} \tag{8.14}$$

where the weight of the edge, w_{nm}, is the weight of a transmission line (edge) and is assigned a value equal to the primitive impedance of the transmission element and p_{nm} is defined as the weight w_{nm} divided by the sum of all weights. Figure 8.16 and Figure 8.17 show the connectivity metric for each bus in the IEEE 14-bus test system and the components that make up that metric, respectively. The IRM metric values for each bus in the RTS96 system are shown Figure 8.18.

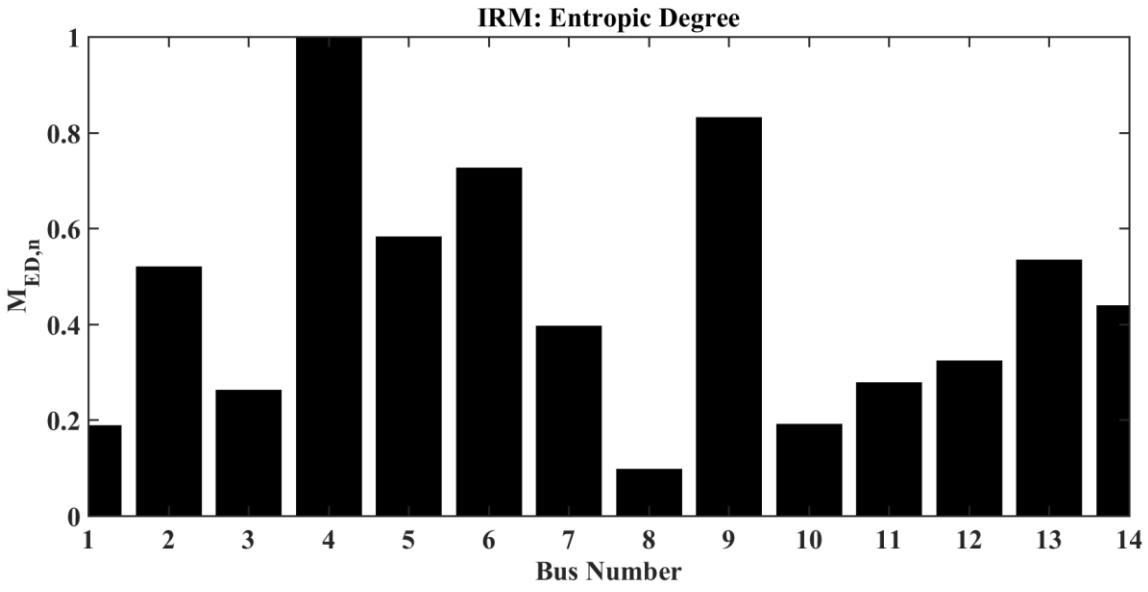

Figure 8.16 IRM: Bus Connectivity, IEEE 14-Bus System

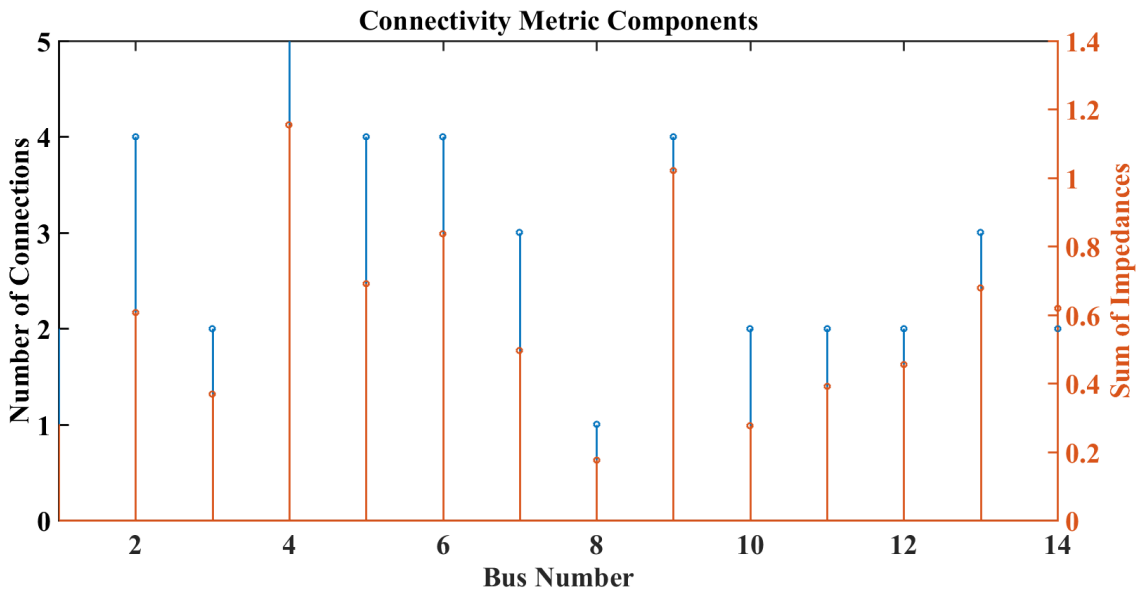

Figure 8.17 IRM: Bus Connectivity Components, IEEE 14-Bus System

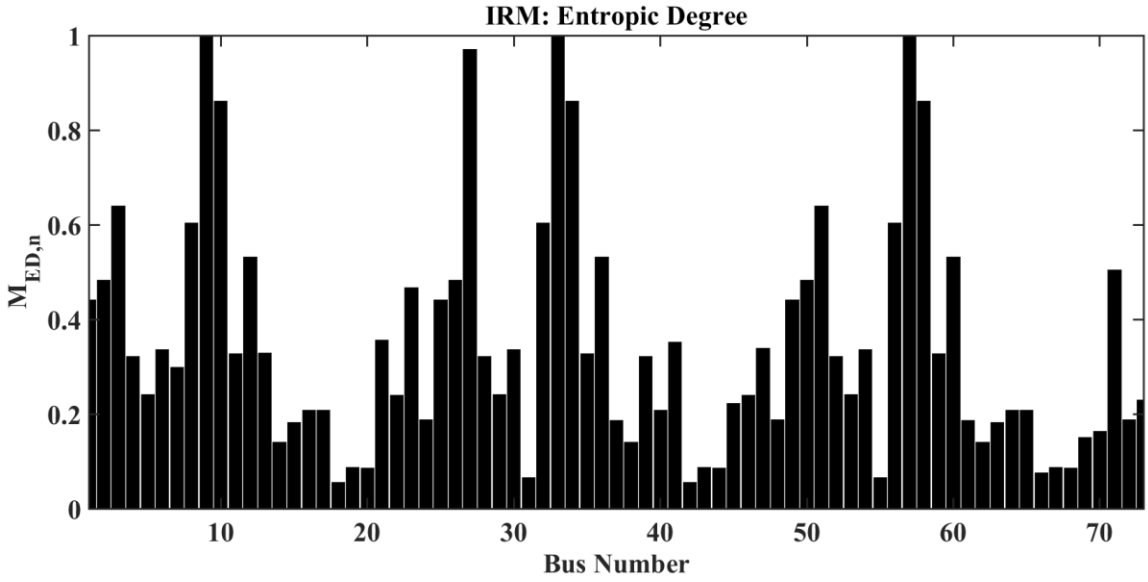

Figure 8.18 IRM: Bus Connectivity Metric, RTS96 System

8.5.2.Betweenness Metric

Similar to the connectivity measure above but for a transmission line (edge) rather than a bus (node), the betweenness metric captures the importance of a given transmission line in the resilience calculation for line thermal limits. The calculation for the extended betweenness for a transmission element *l* is given by:

$$M_{EB,l} = \left| \sum_g \sum_d C_{g,d} PTDF_{l,g,d} \right| \tag{8.15}$$

where $C_{g,d}$ is the minimum ratio for all lines of the quantity $P_{max,l}$, the maximum active power across transmission element *l,* and the power transfer distribution factor from generator *g* to load *d* across line *l.* Figure 8.19 and Figure 8.20 provide examples of the magnitude of these values for the branches in the short-term and long-term test systems used in this work.

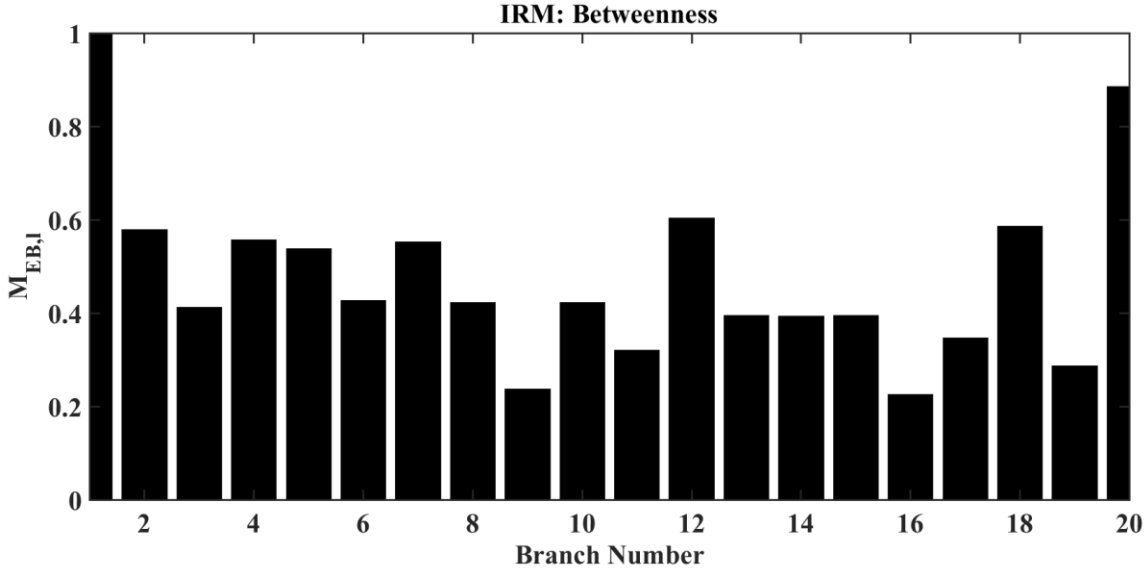

Figure 8.19 IRM: Branch Betweenness, IEEE 14-Bus Test System

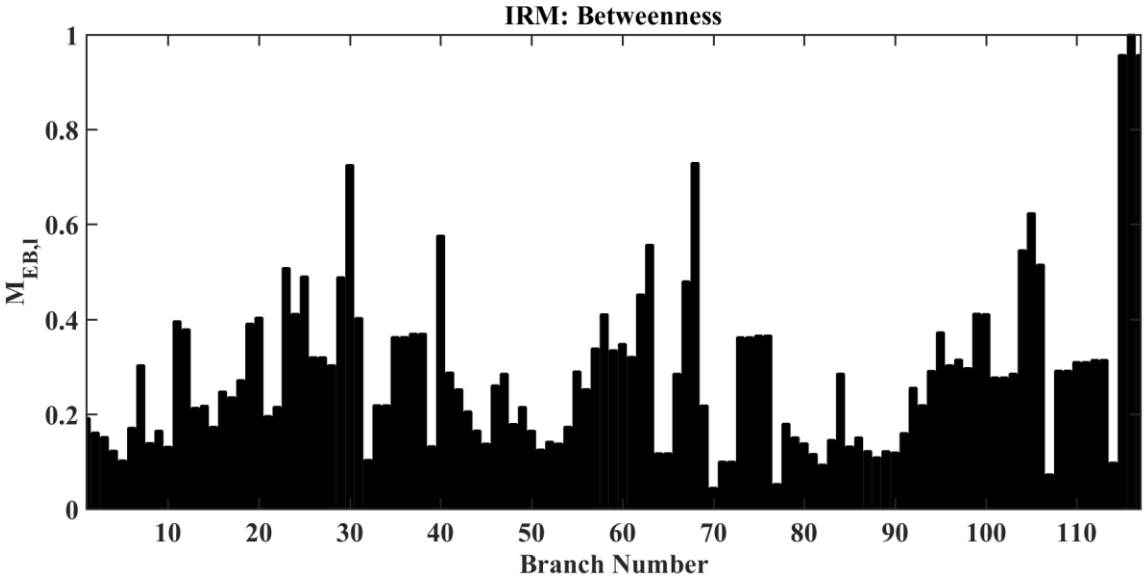

Figure 8.20 IRM: Branch Betweenness, RTS96 Test System

8.5.3.Efficiency Metric

The efficiency metric uses the electrical distance between generators and a load to determine the importance of a given load in the calculation of its resilience value. Defining the equivalent impedance between generator *g* and load *n* as:

$$Z_g^n = z_{gg} - 2z_{gn} + z_{nn} \tag{8.16}$$

where the z_{ij} values are the *ij*-th entry in the bus impedance matrix. The efficiency metric for the load at bus *n* can be calculated as:

$$M_{EFF,n} = \frac{1}{N_g} \sum_g \frac{1}{Z_g^n} \tag{8.17}$$

This IRM can be used as a weight for loads either inversely proportional or directly proportional to the impedance between the load and generation. For a highly networked

system, the impedance of loads will be less than that of loads connected radially to the system. Thus, the inversely proportional relationship is chosen here as this will give higher importance to loads that are electrically close to generation and may highlight issues within the system if they are not being served as opposed to radially connected loads. Figure 8.21 and Figure 8.22 show the load IRMs for the two test systems.

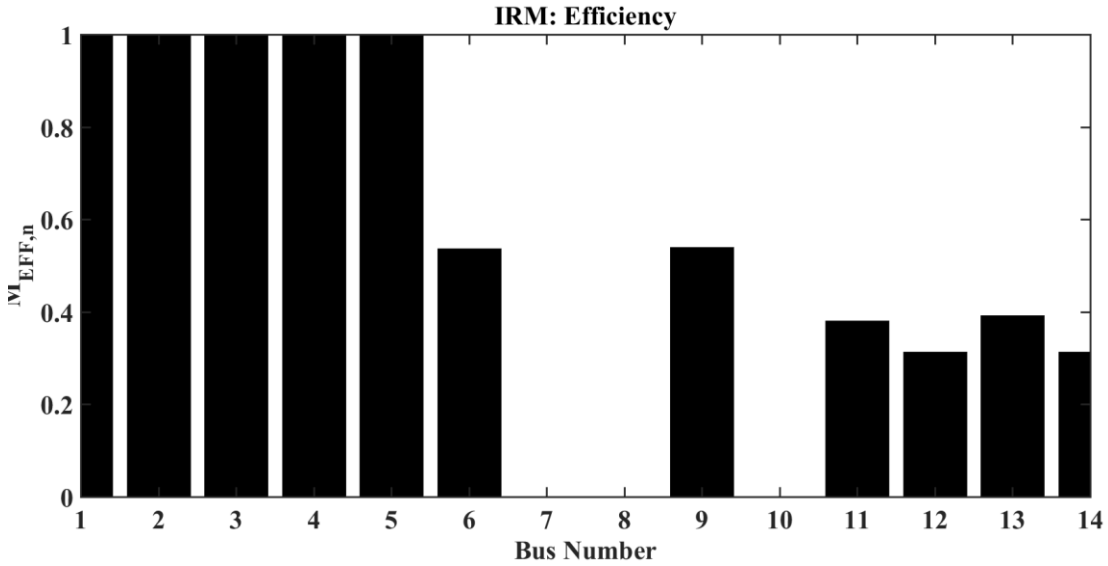

Figure 8.21 IRM: Load Efficiency, IEEE 14-Bus Test System

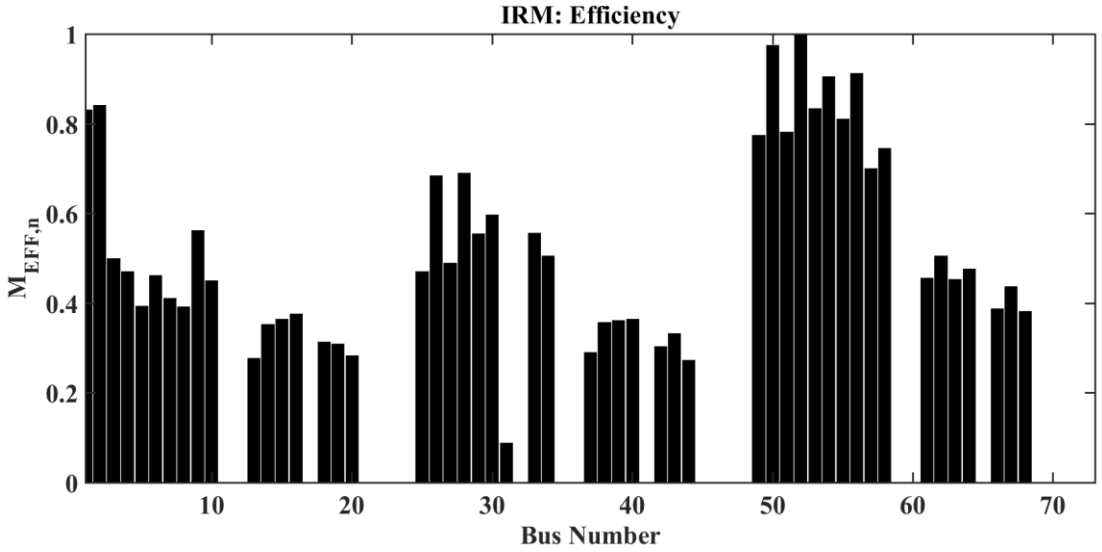

Figure 8.22 IRM: Load Efficiency, RTS96 Test System

8.5.4.Generator Metric

This metric combines the generator's type (base-load (*bl*), load-following (*lf*), peaking (*pk*)), contribution to system generation capacity, and the unit's historical capacity factor [116]. The importance factor characterizing the significance of cooling water supplied to generator *g* is expressed as the sum of these values:

$$M_{SCW,g} = G_{TP,g} + \frac{P_{g,max}}{\sum_j P_{j,max}} + HCF_g \tag{8.18}$$

The values for $G_{TP,g}$ and HCF_g for each unit in the calculation of this IRM were assigned for the unit's fuel type from the values shown in Table 8.5. The generators in the two test systems used in this work were assigned values as shown in Table 8.6 and in Table 8.7. Figure 8.23 and Figure 8.24 show the CW importance IRM for the five generators in the IEEE 14-bus system and for the 99 units in the RTS96 system.

Table 8.5 IRM: Generator CW Importance Parameter Values

	Generator Fuel Type	$G_{TP,g}$	HCF_g
1	IGCC	1	0.54
2	Npp	1	0.926
4	CT	0.5	0.116
5	CCGT	0.75	0.576

Table 8.6 IRM: Generator CW Importance Parameter Values, IEEE 14-Bus Test System

	Generator Fuel Type	Generator Bus	Generator Type (Value)
1	CF	1	*bl* (1)
2	Npp	2	*bl* (1)
3	CT	3	pk (0.5)
4	CT	6	*pk* (0.5)
5	CCGT	8	*lf* (0.75)

Table 8.7 IRM: Generator CW Importance Parameter Values, RTS96 Test System

Generator P_{max} (MW)	Generator Fuel Type	Generator Type (Value)
100, 155, 197, 350	CF	*l f* (0.75), *bl* (1), *bl*, *bl*, *bl*
400	Npp	*bl*
12, 20	CT	*pk*
50	Hydro	-
76	CCGT	*lf* (0.75)

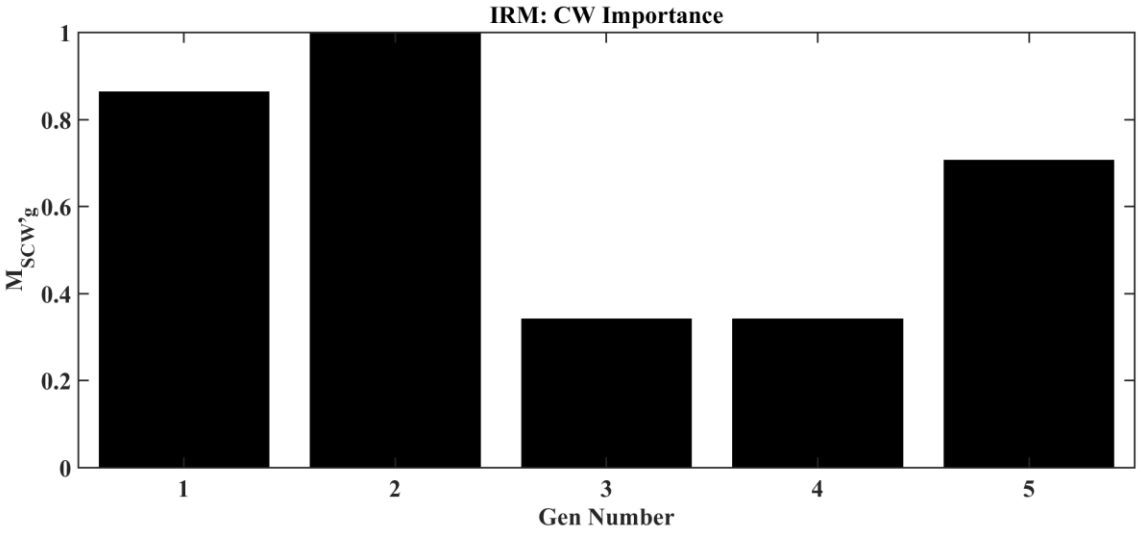

Figure 8.23 IRM: Generator CW Importance, IEEE 14-Bus Test System

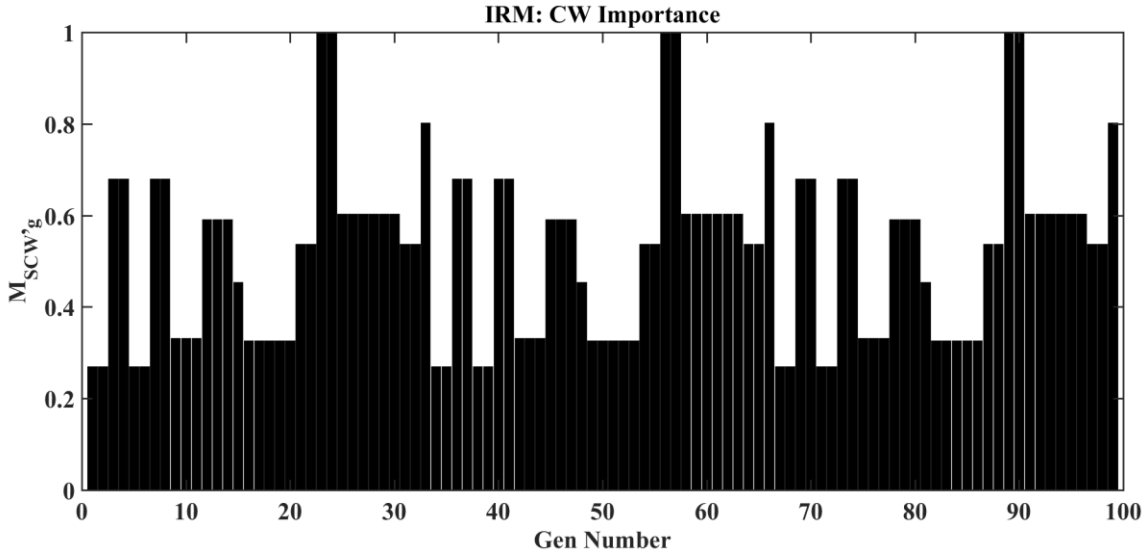

Figure 8.24 IRM: Generator CW Importance, RTS96 Test System

8.6 Infrastructural-Operational Reslience Formulation

A computational overlay methodology utilizing the presented RMPs and IRMs was used for the computation of infrastructural-operational resilience (IOR). The final IOR values are calculated by weighting the OR RMPs with the appropriate IRM. A depiction of the methodology for the resilience calculations is shown in Figure 8.25 and considers the impacts of both reduced water availability and electric power supply. The final IOR formulations are shown in the following sections.

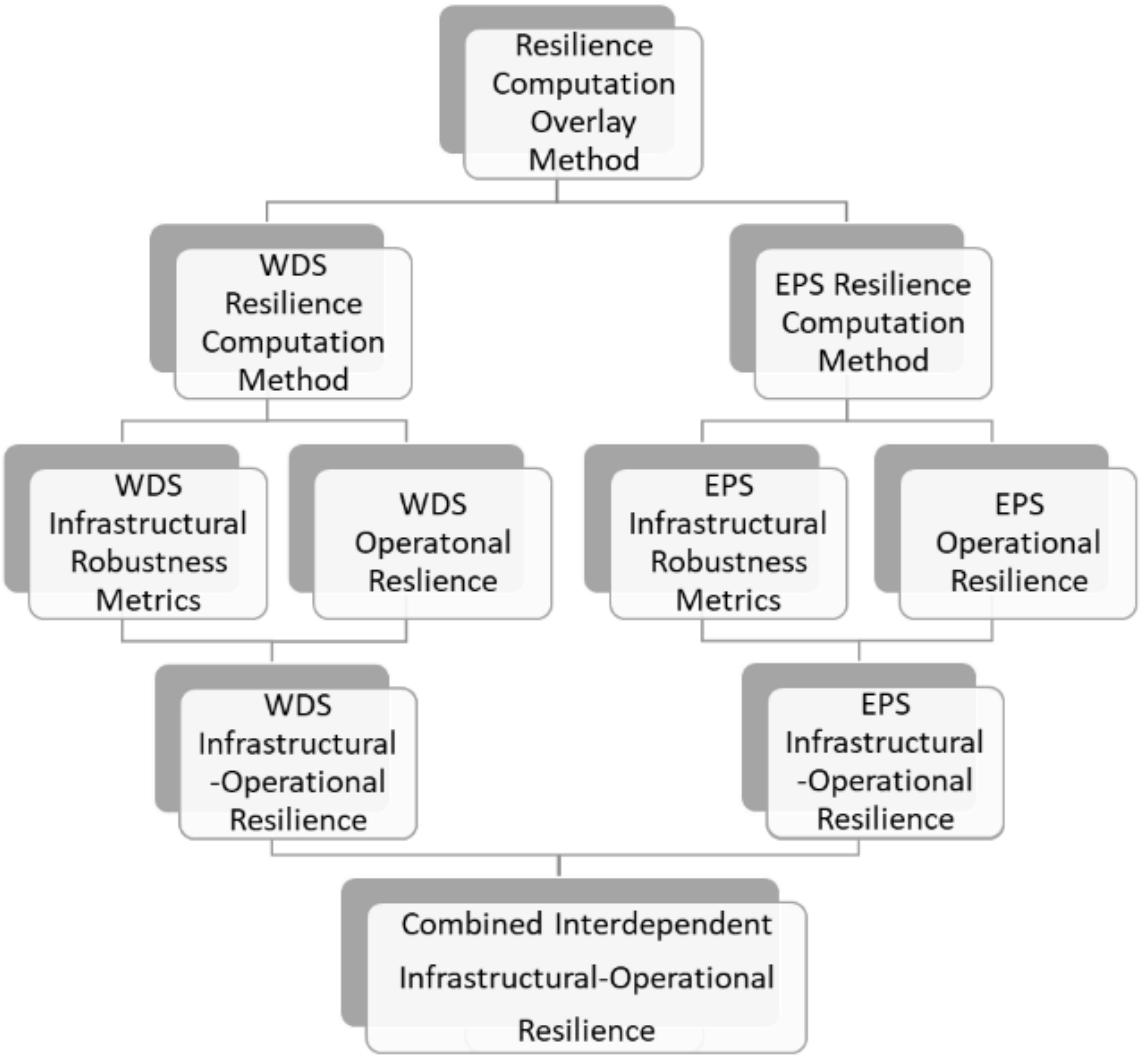

Figure 8.25 Resilience Computation Methodology

8.6.1.Bus Voltage IOR

Resilience for bus voltages in the IOR context is calculated by weighting the OR bus voltage RMP in (8.3) with the IRM in (8.14) and is expressed as:

$$R_{R_{V,t}^n} = \frac{\sum_{n=1}^{NB} \left(\left(1 - \sum_m p_{nm} \cdot log\left(p_{nm}\right)\right) \sum_m w_{nm}\right) \cdot max(0, R_V^n(t) - R_V^n(t\text{-}1))}{\sum_{n=1}^{NB} ceil(R_V^n(t\text{-}1) - R_V^n(t))} \tag{8.19}$$

8.6.2.Transmission Line Thermal Limit IOR

The IOR value for transmission line thermal limit resilience is calculated by weighting the operational thermal limit RMP (8.5) with the extended betweenness metric (8.15):

$$R_{R_{TL,t}^l} = \frac{\sum_{l=1}^{NL} \left(\left|\sum_g \sum_d C_{g,d} PTDF_{l,g,d}\right|\right) max(0, R_{TL}^l(t) - R_{TL}^l(t\text{-}1))}{\sum_{l=1}^{NL} ceil(R_{TL}^l(t\text{-}1) - R_{TL}^l(t))} \tag{8.20}$$

8.6.3.Load Supplied IOR

Both the load supplied operational resilience values (overall and WDS pumps) given in (8.9) and (8.11) are weighted at each node according to the proposed electrical efficiency metric (8.17):

$$R_{R_{DS,t}^n} = \frac{\sum_{n=1}^{NBL} \left(\frac{1}{N_g} \sum_g \frac{1}{Z_g^n}\right) max(0, R_{DS}^n(t) - R_{DS}^n(t\text{-}1))}{\sum_{n=1}^{NBL} ceil(R_{DS}^n(t\text{-}1) - R_{DS}^n(t))} \tag{8.21}$$

for the load supplied (overall) IOR and

$$R_{R^n_{PL},t} = \frac{\sum_{n=1}^{NPL} \left(\frac{1}{N_g}\sum_g \frac{1}{Z_g^n}\right) max(0, R^n_{PL}(t) - R^n_{PL}(t-1))}{\sum_{n=1}^{NPL} ceil(1 - R^n_{PL}(t))} \quad (8.22)$$

for the load (WDS pumps) IOR.

8.6.4.Thermoelectric Generation IOR

The IOR values for thermoelectric generation are calculated by weighting the RMP for thermoelectric generation cooling water (8.7) by the thermoelectric generator cooling water significance metric (8.18):

$$R_{R^g_{CW},t} = \frac{\sum_{g=1}^{NG} \left(G_{TP,g} + \frac{P_{g,max}}{\sum_j P_{j,max}} + HCF_g\right) \cdot max(0, R^g_{CW}(t) - R^g_{CW}(t-1))}{\sum_{g=1}^{NG} ceil(1 - R^g_{CW}(t))} \quad (8.23)$$

8.6.5.EPS Total System IOR

The overall EPS IOR, $R_{EPS,TOT}(t)$, is then calculated at each time-period t as a normalized weighted sum of the voltage, thermal limit, cooling water, demand supplied (overall) and demand supplied (WDS pumps) IOR values.

$$R_{EPS,TOT}(t) = \frac{w_v R_{R^n_V,t} + w_{tl} R_{R^l_{TL},t} + w_{cw} R_{R^g_{CW},t} + w_{ds} R_{R^n_{DS},t} + w_{pl} R_{R^n_{PL},t}}{w_v + w_{tl} + w_{cw} + w_{ds} + w_{pl}} \quad (8.24)$$

The calculation methodology shown in Figure 8.1 can then be updated for the inclusion of the IRMs in the process of calculating the total IOR as shown below in Figure 8.26.

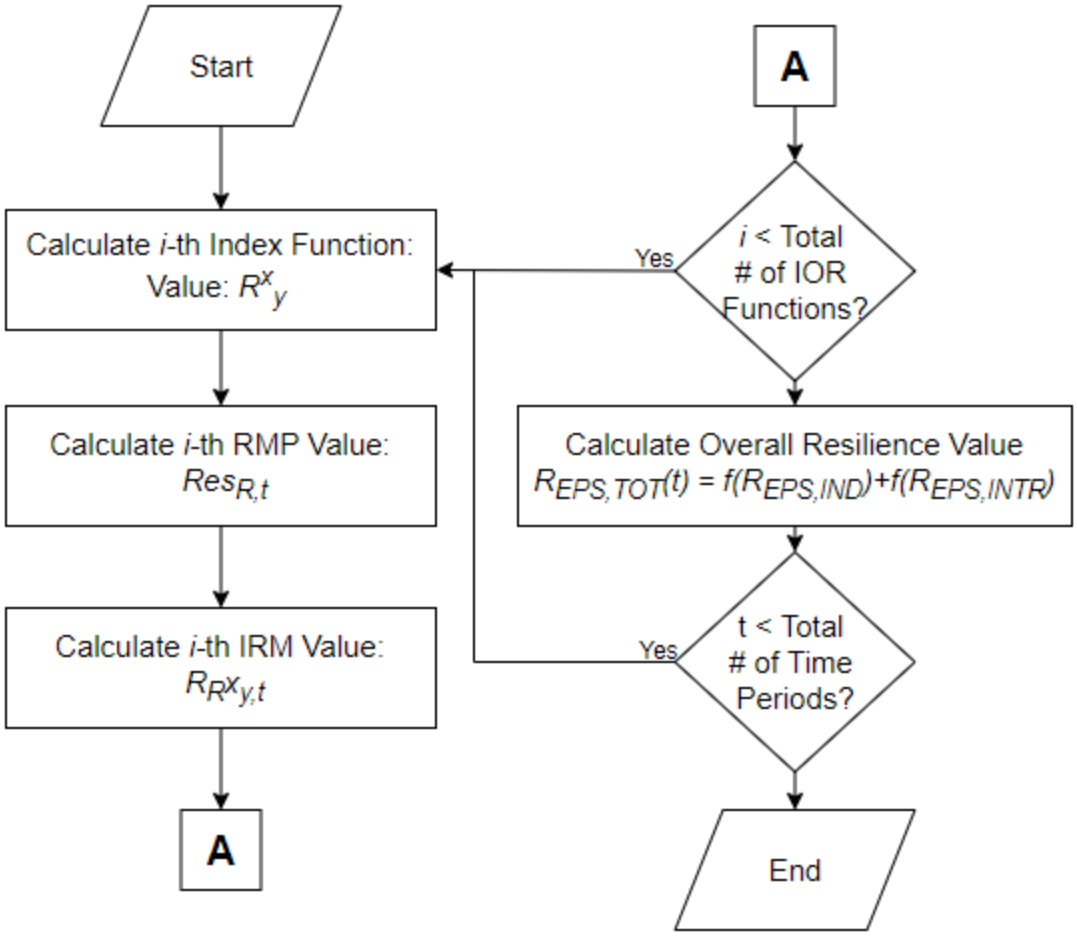

Figure 8.26 IOR Calculation Flow Chart

8.6.6.EPS and WDS Combined calculations

For the purpose of completeness concerning some of the results shown in a later section, the IOR formulation developed for inclusion in an interdependent infrastructure resilience calculation will now be summarized and a complete discussion found in [109].

Following the same progression for the development of EPS OR and IOR, the WDS index functions are based on:

1) Node Pressures index function based on whether pressures lie within the acceptable upper and lower pressure bounds

2) Power availability based on whether pumps that are experiencing a power outage are scheduled after pump schedule optimization

3) Demand satisfaction based on the ration of demand satisfied to demand required

IRMs for the WDS are then formulated from standard graph theory metrics and are:

1) Connectivity metric based on the number of links (pipes/pumps) connected to a given node

2) Betweenness metric based on the type (pipe, pump or valve) and size (diameter for pipe/valves or flow for pumps) of the connecting links at a given node

3) Demand priority metric based on the importance of the demands in a given WDS service area based on the type of demands (residential, commercial, industrial or cooling water for power plants) in the service area

The WDS total system IOR is then formulated and repeated here for completeness:

$$R_{WDS,TOT}(t) = \frac{w_p R_{R_P^{n,tim},t} + w_{pow} R_{R_{Pow}^{pump,tim},t} + w_{dem} R_{R_{Dem}^{z,tim},t}}{w_p + w_{pow} + w_{dem}} \qquad (8.25)$$

It is again noted here that the calculation of IOR for the two interdependent infrastructure systems contains terms that are recognized as quantities pertaining solely to the operation of that particular system (EPS or WDS), $f(R_{IND})$, as well as quantities concerned explicitly with the interdependent operation of the two systems, $f(R_{INTR})$. Table 8.8 summarizes the independent and interdependent quantities.

Table 8.8 EPS and WDS IOR Quantity Summary

System	Independent Quantity	Interdependent Quantity
EPS	Bus Voltage Magnitude Line Thermal Limits Load (overall) supply satisfied	Thermoelectric cooling water demand satisfied Load (WDS pump) supply satisfied
WDS	Nodal Pressure	Pump Power Availability Zonal Demand Satisfaction

The total resilience for the two systems at each time-period can be calculated as:

$$R_{TOT}(t) = f(R_{EPS,IND}) + f(R_{EPS,INTR}) + f(R_{WDS,IND}) + f(R_{WDS,INTR})$$

$$= f(R_{IND}) + f(R_{INTR})$$

$$= \frac{w_1\left(R_{R_V^n,t} + R_{R_{TL}^l,t} + R_{R_{DS}^n,t} + R_{R_P^{n,tim},t}\right) + w_2\left(R_{R_{CW}^g,t} + R_{R_{PL}^n,t} + R_{R_{Pow}^{pump,tim},t} + R_{R_{Dem}^{z,tim},t}\right)}{w_3} \quad (8.26)$$

where the weights for the interdependent (w_2) and independent (w_1) terms can be determined through sensitivity analysis or by a decision maker and $w_3$is the normalizing weight used to keep the final value between 0 and 1.

8.7 Disturbance Severity Quantification Framework for IOR

The overall IOR value is expected (in addition to the individual values) to have a certain behavior as a function of time before, during, and after system disturbances. Figure

8.27 shows this expected behavior for a generic system disturbance and denotes the key points that will be used in the quantifying metrics below. The severity of a disturbance is measured by the degree to which the measure of performance drops, how fast it both drops and recovers, and to what value the measure settles at. This severity can be quantified using four metrics (e.g. [72], [75]) including system robustness, resourcefulness of the operational control, recovery rapidity and recovery ability, adaptability. An additional quantity also used to capture these behaviors is the time averaged performance loss.

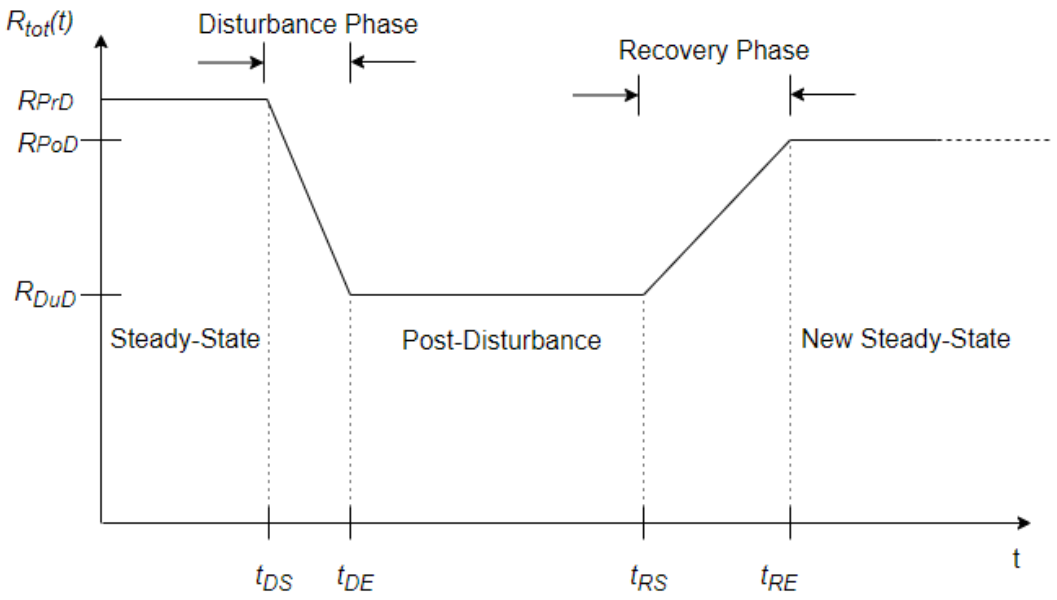

Figure 8.27 IOR versus Time (modified from [75])

This type of behavior has already been demonstrated and is observed in the case study results of Section 8.4. Metrics that are adequate to study these high impact, low probability extreme events will now be presented in order to more closely examine the IOR case study results.

Robustness of a system is the measure of capability of its absorptive capability. Robustness in terms of IOR is given by the minimum value of IOR between the time at which the disturbance phase starts, t_{DS}, and when the recovery ends, t_{RE}, as follows:

$$M_{ROB}=min(R_{TOT}(t),\ t_{DS}<t<t_{RE}) \tag{8.27}$$

Rapidity and performance loss are metrics used to quantify the disruption caused to the system performance during a certain disruptive phase. The rapidity quantification metrics are computed using the average slope of the IOR in both the disturbance phase and the recovery phase and are defined as:

$$M_{RAPI,DP}=\frac{R_{PrD}-R_{DuD}}{t_{DE}-t_{DS}} \tag{8.28}$$

$$M_{RAPI,RP}=\frac{R_{PoD}-R_{DuD}}{t_{RS}-t_{RE}} \tag{8.29}$$

The recovery ability of the system is quantified by using the ratio of the post-disturbance IOR value to the pre-disturbance value.

$$M_{RA}=\left|\frac{R_{PoD}-M_{ROB}}{R_{PrD}-M_{ROB}}\right| \tag{8.30}$$

The area between the pre-disturbance IOR value and the IOR value during the disturbance is used in order to specify the performance loss during a disruption phase.

$$M_{TAPL} = \frac{\int \left(R_{PrD} - R_{TOT}(t) \right) dt}{t_{RE} - t_{DS}} \tag{8.31}$$

Finally, the total resilience metric integrates the above five metrics in (8.27) - (8.31):

$$M_{TOT} = M_{ROB} \cdot \frac{M_{RAPI,RP}}{M_{RAPI,DP}} \cdot \frac{M_{RA}}{M_{TAPL}} \tag{8.32}$$

A quick examination shows that the M_{TOT} value will be larger for larger values of robustness, rapidity of IOR increase in the recovery phase and recovery ability. Conversely, this value will be smaller for fast (or large) decreases in IOR value during the disruption phase and for large deviations of IOR from its pre-disturbance value.

8.8 IOR Case Study Results

The following sub-sections contain results for various scenarios that demonstrate the application of the IOR methodology as well as the interdependent infrastructure calculation methodology and the disturbance severity metrics.

8.8.1. Inclusion of IRM in Chapter 6, Case III scenario

This case demonstrates the effects of including the IRMs and can be contrasted with the results shown in Figure 8.14. The results in that figure consider resilience as calculated using the OR RMPs only. Figure 8.28 shows a comparison of the final IOR values in the modified 14-bus system with different values for the weight on interdependent quantities (w_2 in (14), with w_1 being equal to unity). The main takeaways are as follows. First, the final IOR formulation still captures the scenario definition in that the resilience value

begins decreasing as the electric power outages are placed on the system and the effects of the water-shortage begin to propagate from the WDS to the EPS. Following this, there are periods of increased resilience as these disturbances are cycled throughout the simulation.

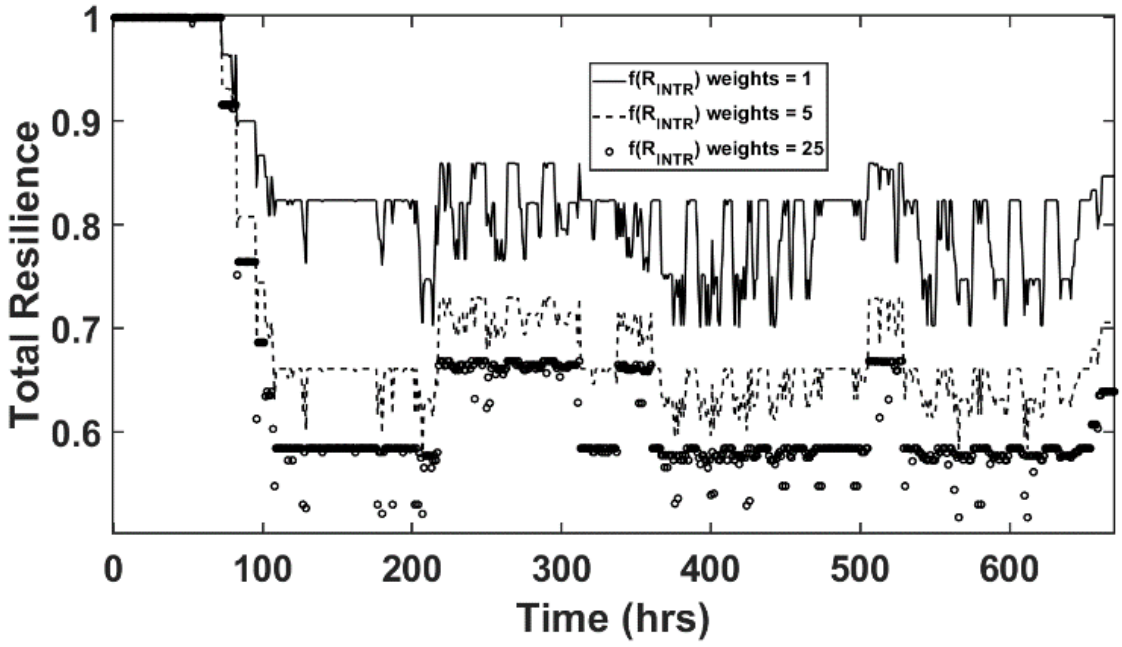

Figure 8.28 . IOR – Interdependent Quantity Weight Comparison

The resilience then begins to recover at the end of the simulation as expected and as was seen before. Second, with the $f(R_{EPS,INTR})$ weights being 1 and in comparison with the results in Section 8.4, the larger fluctuations in the magnitude of overall IOR can be attributed to more important $f(R_{EPS,IND})$ quantities having a larger impact do to the increased importance given to them by their IRM's. Lastly, the decrease in the magnitude of those fluctuations and the smaller decrease in the overall resilience values as w_2 goes from five to twenty-five as compared with the change from one to five again shows that the resilience value becomes dominated by the interdependent system quantities.

8.8.2.Application of the IOR Methodology to a Larger Test System

The results in this section utilize simulation results from Section 6.4 by using the same methodology described in Section 6.7. It was assumed that one scaled version of the WDS test system developed for use with the 14-bus system could supply one (of the three) areas within the larger system. The ratio of cooling water supplied to cooling water consumed from the simulation in Section 6.4 was again used to determine how much make-up water was supplied to each of the generator types. Figure 8.29 shows the results for the drought/outage scenario applied to one area in the 73-bus system. This figure shows how the resilience value changes with the inclusion of the IRMs. The effect of including the IRMs on the final resilience value is noted as more clearly emphasizing both the slow fluctuations in resilience value due to interdependent system quantities as well as an increased magnitude in the higher-frequency fluctuations in the resilience value. These higher-frequency changes are the result of changing bus voltages and line flows.

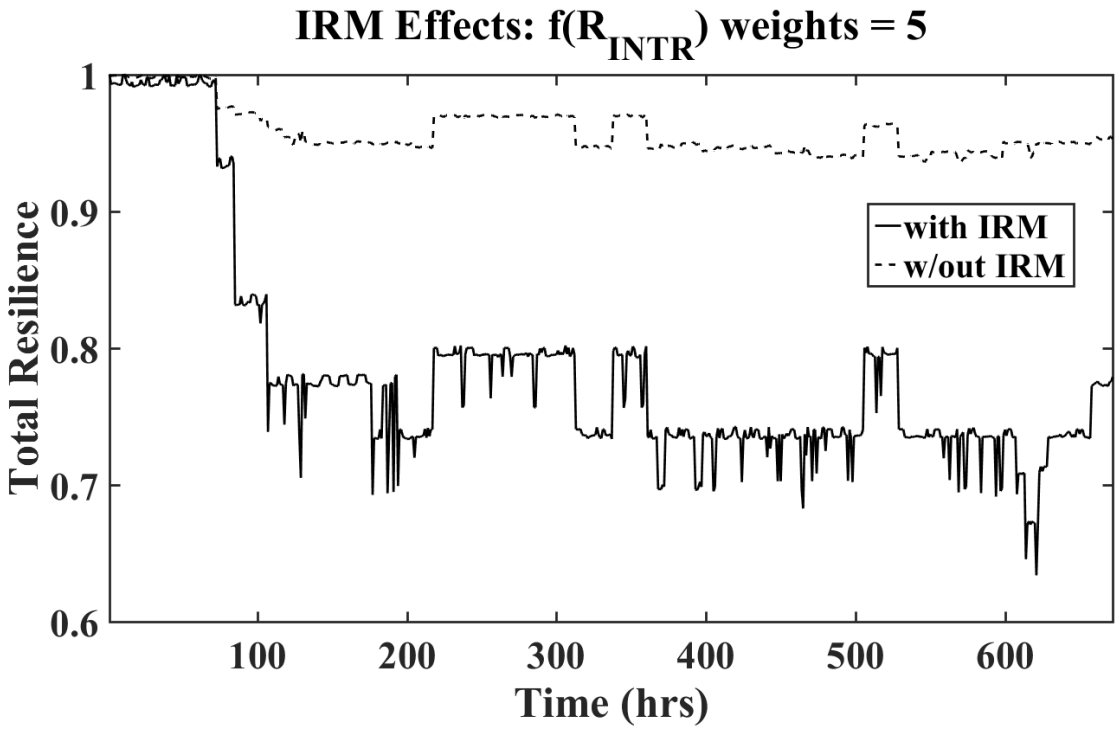

Figure 8.29 Impact of IRM Inclusion – 73-Bus

Figure 8.30 provides some insight into how this decrease in the magnitude of the resilience value occurs with the inclusion of the IRMs into the resilience calculation. This figure contains plots for 10 of the generators that are within the drought area and it is noted that Unit 89 experiences a significant drop in its tank level. Given that this is a baseload unit, this means that the unit's $M_{SCW,g}$ value will be much greater than a peaking unit since it has both a larger $G_{TP,g}$ value as well as HCF_g value (Figure 8.23, Figure 8.24).

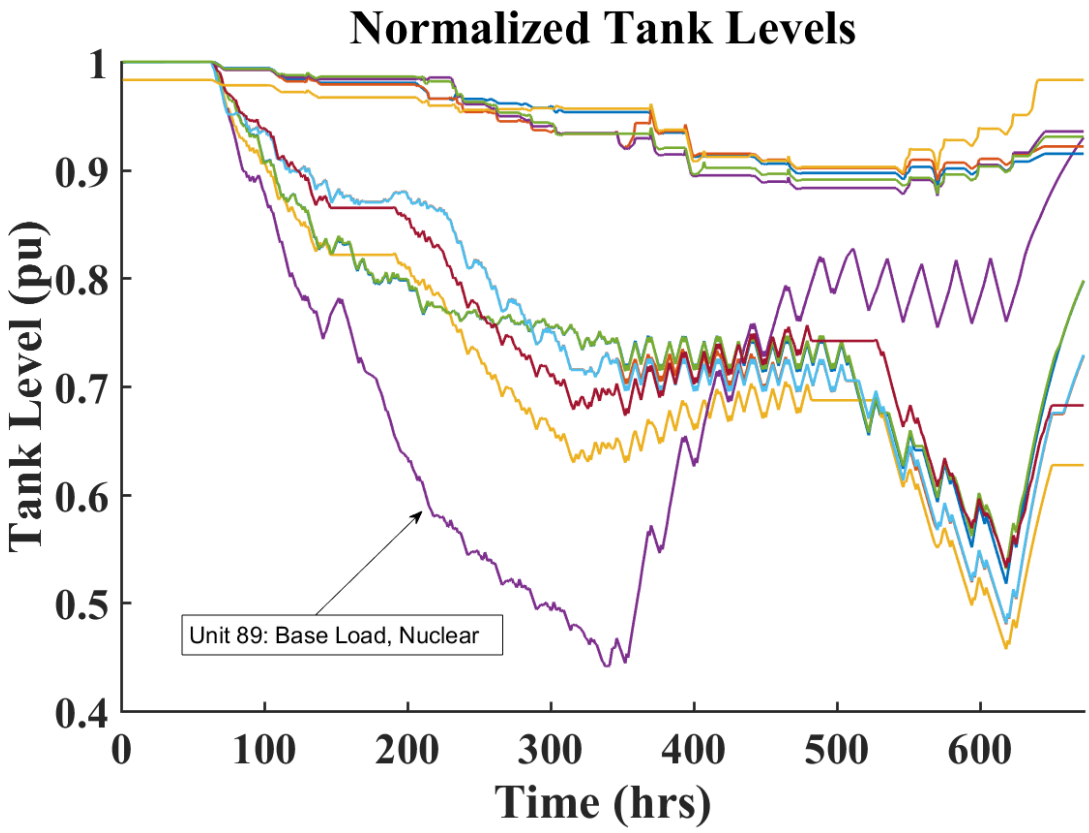

Figure 8.30 Normalized Onsite Water Storage for Generators Supplied by WDS under Drought Conditions – 73-Bus System

Thus, the drop in this tank level will contribute relatively more to the overall decrease in magnitude of the cooling water IOR and therefore will contribute more to the decrease in the final IOR value as well.

It is desired to extend the operation of critical or necessary generation for system security in these periods of extreme weather conditions. Following the analysis conducted throughout Chapter 6, the sensitivity of system resilience to the dispatch of generation was examined. As was done in that chapter, this is accomplished by changing the value of the

$\delta_{fuelCost}$ weight for use in the combined economic and environmental dispatch formulation. The effect of the change in this value is to move the dispatch from one having balanced considerations for fuel and water costs to a pure environmental dispatch. Figure 8.31 shows the system resilience value for the two cases and it is seen that an environmental dispatch does result in a higher system resilience value in most time-periods throughout the simulations.

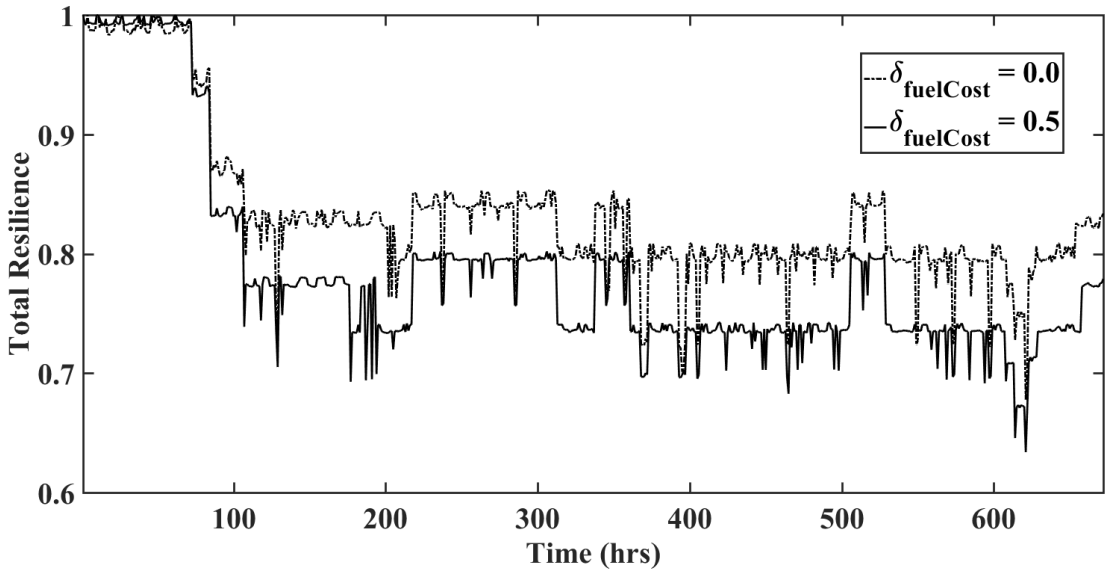

Figure 8.31 System Resilience Comparison for Different Generation Dispatch Priorities – 73-Bus System

Figure 8.32 shows a plot of the smoothed arithmetic difference in resilience values between simulations having an environmental dispatch and a simulation having a balanced dispatch (equal weight on fuel and operational water costs). As can be clearly seen, the improvement in the resilience value for the pure economic dispatch is evident with the positive value of the plot in this figure. At the beginning of the simulation, there are small fluctuations in this difference due to different operating conditions, but this difference

grows larger in magnitude as the disturbances in the WDS and EPS system begin to occur. At the end of the simulation, this difference remains relatively constant, meaning the resilience values are increasing at approximately the same rate.

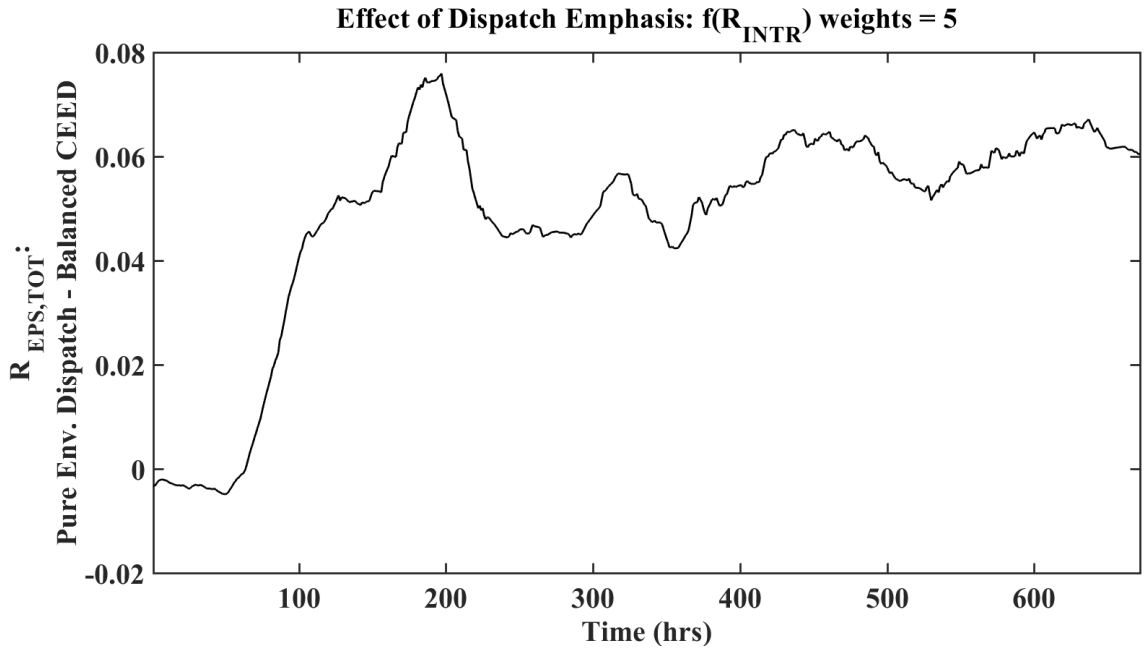

Figure 8.32 System Resilience Comparison for Different Generation Dispatch Priorities – 73-Bus System

The averaged improvement in system resilience over the course of the 28-day simulation is seen to be approximately 4.87 percent, proving that this is one possible way to both extend the operation of plants experiencing such conditions and, in the process, improve the overall system resilience.

The last scenario that was considered for this test system is one where the same drought conditions are experienced in both Area 2 and in Area 3 within this 73-bus system, as denoted in Figure 6.55. Figure 8.33 shows the plots that contrast the IOR value for the

scenario of drought in only one area with this one. Here, the resilience value is lower overall during the disturbance, as expected, and in addition to the decrease in system resilience during the drought periods attributed to the $R^{g}_{R^{g}_{CW},t}$ IOR term, the large decreases and increases in the total IOR that are due to the pump outages is more clearly seen.

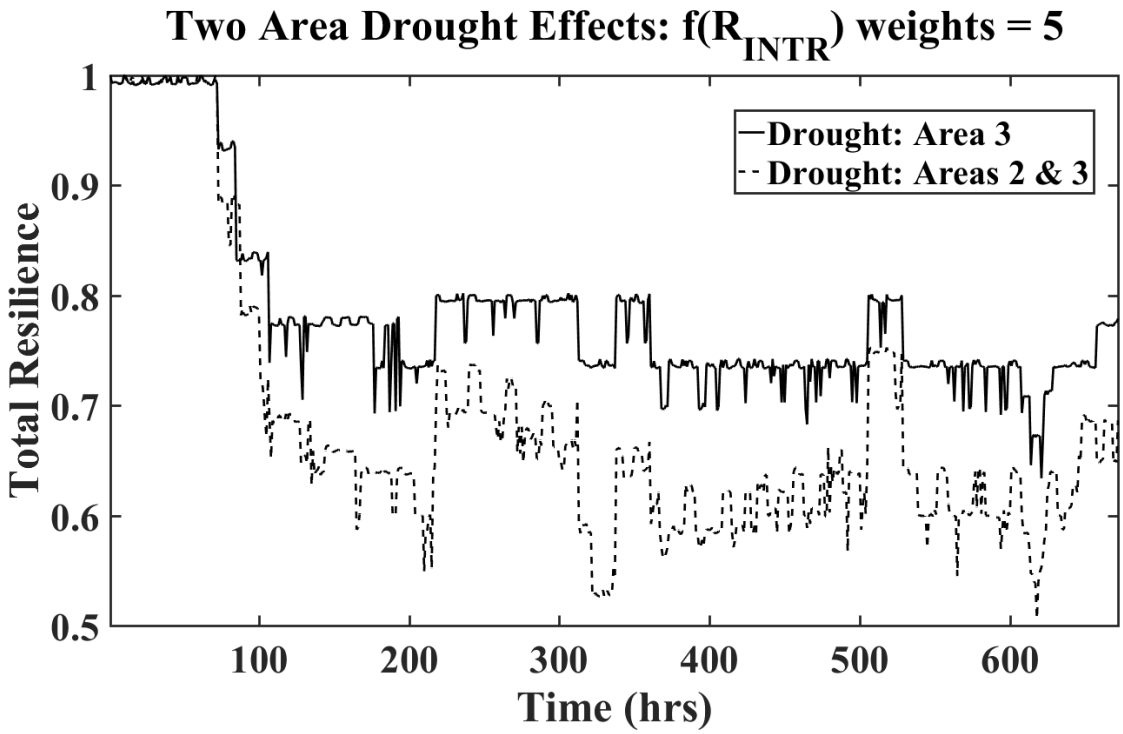

Figure 8.33 Effect Comparison of One-Area vs. Two-Area Drought on System Resilience – 73-Bus System

8.8.3.Examination of Combined EPS and WDS IOR and IOR Quantification During Disturbances

The scenario considered here was detailed in Section 6.3 and summarized here as having extended period power outage contingencies for the WDS pumping stations and large water shortages within the WDS emulating severe drought conditions. Figure 8.34 shows the trends of EPS IOR that was calculated using (8.24), WDS IOR that was

calculated using (8.25), and the combined, total IOR value that was calculated using (8.26). The top two subplots show the IOR value for both the independent systems while the total IOR is shown in the bottom subplot. The shaded areas in the WDS IOR graph show the contingency periods due to limited water availability as shown in Figure 6.1, while the shaded areas in the EPS IOR graph show the contingency periods due to power outages of the pumps shown in Table 6.1 and for hours shown in Figure 6.12.

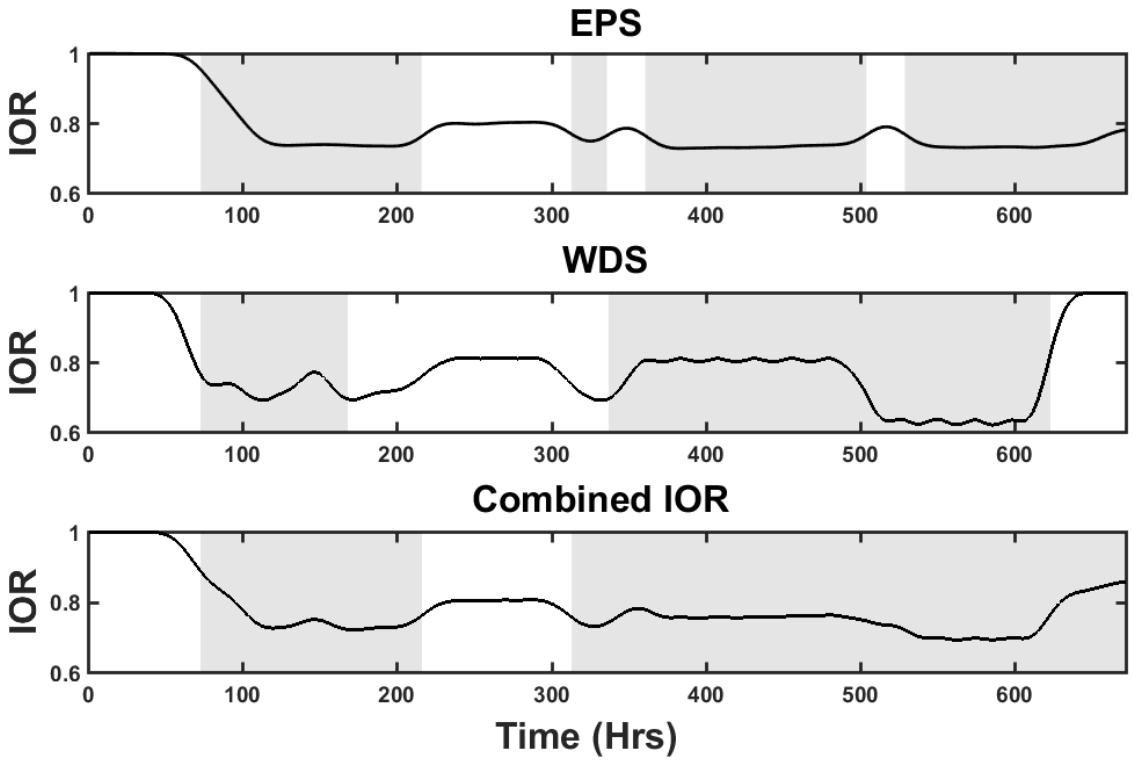

Figure 8.34 IOR for EPS and WDS, Combined with Contingency Overlay

The shaded areas in the bottom subplot of the combined IOR plot depict contingency periods due to limited water and/or power outage during the total simulation period. The values of weights used for the independent (w_1) and interdependent terms (w_2) within the total IOR calculation were 1 and 5, respectively. The trends of EPS and WDS IOR are observed to decline from simulation times slightly before the contingency starts at the

beginning of day three due to the use of a moving average of the IOR values that was used to post-process the result calculations. The lag observed in the decline of EPS IOR compared with WDS IOR is due to the EPS being more resilient to limited water availability because of the on-site cooling water storage that the power plants have. The EPS and WDS IOR values are seen to follow similar trends during the later parts of the simulation. The WDS is observed to recover from the reduced IOR values at the end of the simulation period even though pump power outages still persist. This means that the WDS optimization procedure was successfully scheduling pumps that were not outaged and because there is not a shortage of available water during the last 48 hours of the simulation. Thus, the effect that is noted here is that the pump power outages are successfully mitigated in the WDS as the simulation progresses.

Figure 8.35 shows the independent, $f(Res_{IND})$, and interdependent, $f(Res_{INTR})$, IOR values for the simulation where the terms were calculated with normalizing weights on all of the terms equal to one. Again, the shaded areas in the figure depict the periods during which there is limited water availability and/or power outage contingencies. A quick comparison of the two plots shows that the interdependent IOR values were observed to decrease during the periods which had contingencies, while throughout the simulation the

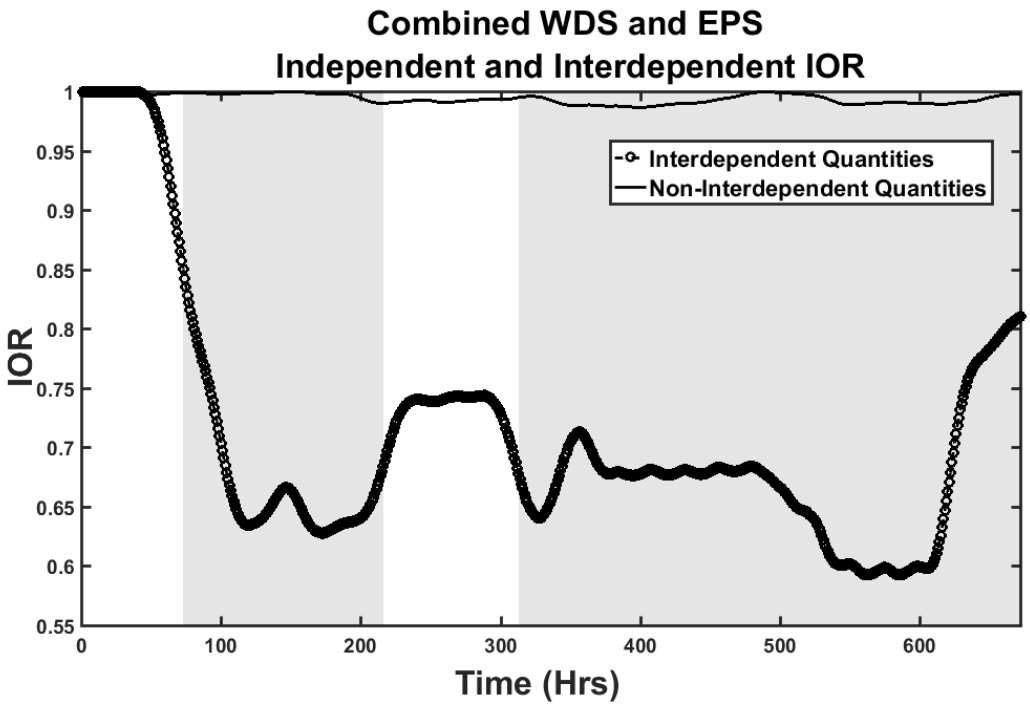

Figure 8.35 Independent and Interdependent IOR Quantities versus Time

decrease in the independent IOR value during these periods is seen to be much smaller in comparison. It is also seen that the effect on the IOR values from the second round of severe contingencies beginning at the start of the third week is not as severe as the effect of the first contingency that begins in day 3 of week one.

This demonstrates that the implemented control strategies are effective at attenuating the impact of the second contingency and successfully manoeuvre the interdependent systems to a more hardened system operating conditions prior to hour 337. This simulation also shows the benefits that occur with the consideration of separate computations for the independent and interdependent IOR quantities. This is shown by the fact that the decline in IOR value captured by the interdependent IOR quantities is not observed in the independent IOR quantities.

A sensitivity analysis was performed for the weights of independent and interdependent IOR quantities as it is these values that allow for the consideration of the effect that each quantity has on the overall IOR value. In the course of conducting this sensitivity analysis, it was observed that increasing the interdependent IOR weight (w_2) beyond 10 has a diminishing effect on the overall resilience value (with the independent IOR weight w_1 kept constant) because the final IOR value is dominated by the interdependent terms, $f(Res_{INTR})$. Similar effects were observed in the OR resilience calculations in Section 8.4 and in the sensitivity analysis shown in Figure 8.14.

An effort will now be made to examine the resilience of the system for this scenario using the disturbance severity metrics that were presented in Section 8.7. The expected behavior of IOR versus time was shown in Figure 8.27. Along these lines, Figure 8.36 shows the final IOR value, (8.26), which was calculated using a weight for the independent quantities of one and a weight for the interdependent quantities equal to five. Also shown in this figure is a linear approximation of that curve. In contrast to Figure 8.27, Figure 8.35 has what appears to be more than one disturbance and therefore the IOR, an accompanying linear approximation to that curve and accompanying visuals are shown in Figure 8.36 in order to aid in understanding the application of the metrics presented in Section 8.7 . As a direct result of the contingency scenarios used in both networks, there are three distinct disturbance periods that are identified. The numbers in the plot that are encircled draw attention to the beginning of each disturbance period, with the disturbance and recovery phase for the first disturbance period shown explicitly.

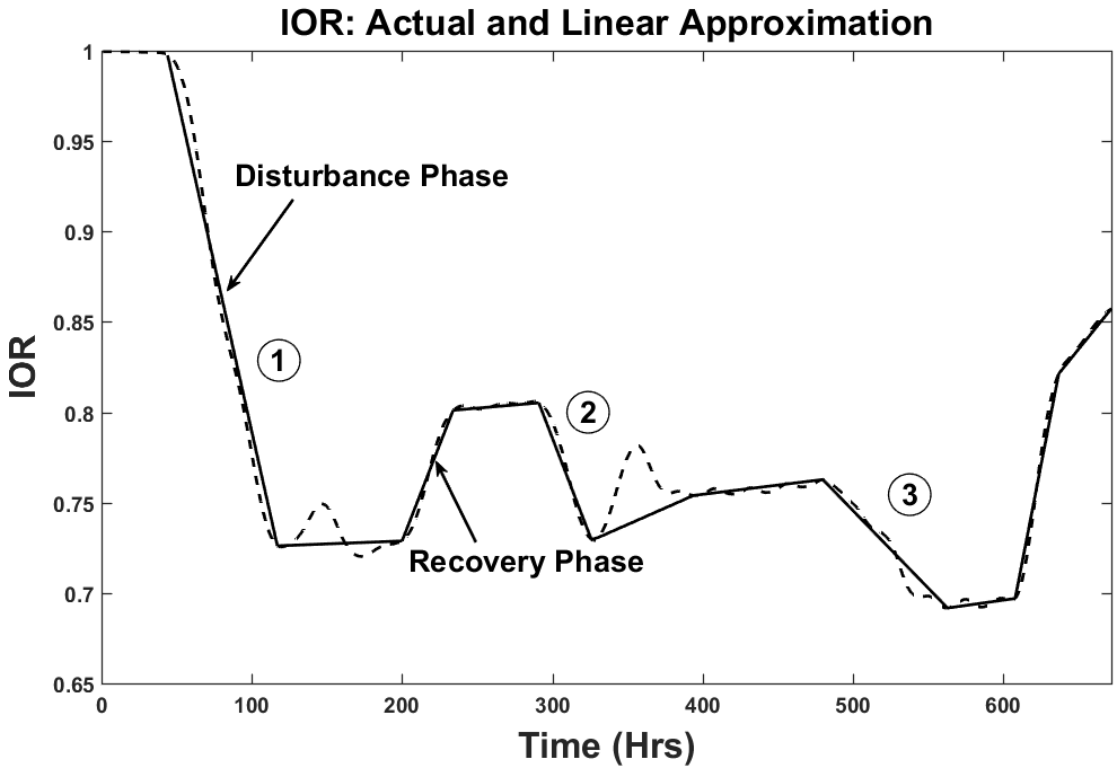

Figure 8.36 IOR with Linear Approximation for Metric Application

The severity quantification metrics which were defined in (8.27) - (8.32) were then calculated for each of the three disturbance periods and Table 8.6 contains the numerical values for each of these quantities. Interestingly, the robustness of the system, as quantified by M_{ROB}, is seen to be very close for all three periods. The monotonically decreasing value of $M_{RAPI,DP}$ for cases 1, 2, and 3, respectively, is confirmed visually by the decreasing slope and increased time to reach a minimum IOR value.

The fact that the magnitude of the slope of the recovery phase, captured by $M_{RAPI,RP}$, in disturbance period 2 is smaller as compared with disturbance period 1 aids in the resulting lower value of M_{TOT} for disturbance period 2. Because there is a relatively larger decrease in the post-disturbance steady state value of IOR (M_{RA}) for disturbance

period 2 as compared with period 1 explains the increase in this value for disturbance 2. A lower value of the time averaged performance loss, M_{TAPL}, for period 2 as compared with 1 is due to the reasons just mentioned and because of the larger value of M_{TAPL} for period 3. This value, in comparison with periods 1 and 2, results from the post-disturbance IOR value being greater than the pre-disturbance IOR value. Lastly, even though period 3 has the lowest minimum IOR value, $M_{ROB,}$ the fact that this period has a faster recovery in IOR value, $M_{RAPI,RP}$, combined with the much larger M_{RA} and significantly lower M_{TAPL} values results in the fairly large difference in the final M_{TOT} value.

Table 8.9 Numerical Results for IOR Quantification Metrics

Disturbance #	M_{ROB}	$M_{RAPI,DP}$	$M_{RAPI,RP}$	M_{RA}	M_{TAPL}	M_{TOT}
1	0.7261	0.0037	0.0021	0.2789	10.0893	0.0114
2	0.7296	0.0022	0.0004	0.3386	9.6786	0.0046
3	0.6917	0.0009	0.0043	2.3291	3.4585	2.2256

8.8.4.Feasibility for the Implementation of the IOR Calculation Methodology

The scalability of this calculation methodology can be accomplished by examining the computation times required to complete the post-simulation resilience calculations. The calculations were performed using MATLAB on a machine with a 3.6 GHz i7 processor and the results are shown in Table 8.10. Because the resilience calculations for the test systems shown are not computationally expensive (total calculation time of 1.90 sec was

recorded for the WDS), it seems that the IOR computation methodology is suitable for both real-time and post-simulation analysis for EPS – WDS performance assessment.

Table 8.10 Post-Simulation Resilience Computation Times

	Test System	IRM Calculation	Time (sec)
1	Modified 14-Bus	No	1.6431
2	73-Bus	No	2.5374
3	Modified 14-Bus	Yes	1.7412
4	73-Bus	Yes	3.2692

8.9 Summary

A formulation for the calculation of power system resilience and a methodology for this calculation using operational measures of performance related to several quantities of interest in the power system was presented. The methodology was then extended with the use of infrastructural metrics that were used as weights for the operational resilience quantities. This calculation methodology was coined infrastructural-operational resilience. The resilience calculations have consideration of measures of performance that are explicit functions of power system operation only, including bus voltages and transmission line thermal limits, as well as measures of performance reflecting the interdependent water-energy system operation, including on-site water storage tank levels. Application of the presented OR and IOR calculation methodologies was then performed using several case studies using the results of long term, time-domain simulations. These case studies included sensitivity analysis for IOR weights and examination of a possible method to improve system resilience.

CHAPTER 9

CONCLUSION AND FUTURE WORK

9.1 Conclusions and Key Contributions

The background on the water-energy nexus and relative modeling information has been given. The analytical framework for the control schemes that were presented have been detailed and implemented within a complex simulation procedure for operational time-scale simulations. Simulations of the coordinated operation of the water distribution system and the electric power system have been conducted and results from several different case studies have been presented. Lastly, metrics for quantifying the resilience of the interdependent systems have been formulated within a novel calculation methodology. These metrics were used within several case studies to examine the resilience of the test systems using results from the case studies conducted in the operational scale time-frame.

Some key contributions of this work are as follows: Long-term simulations were performed which capture the inherent slow dynamics that exist between the EPS and WDS. Explicit representation of the main dependencies of each system on the other are included in the modeling and repeated here: cooling water for thermoelectric generation and power for WDS pumps. The developed simulation engine allows the planner to conduct analysis of the type normally done by a water utility (pump scheduling) and an electric utility or ISO/RTO (Unit Commitment and Unit Dispatch) while allowing for the additional benefits that come from having knowledge of the infrastructure system that each is dependent on. The ability to tailor the defined scenarios allows for the inclusion of a wide variety of network and external contingencies in either system. The CEED formulation explicitly

considers system conditions with respect to the WDS via the operational water cost. This operational cost can be adjusted by the application of one of the presented control policies. Another of the policies presents formulations that provide an explicit and systematic approach to de-rate thermoelectric plants during droughts based on the current levels in the on-site water storage tanks at the plant location. As information sharing between entities in the EPS with those in the WDS is virtually non-existent, the approach to modeling, simulation and control presented in this work offers a reasonable attempt at optimizing operations of the two systems with limited data exchange.

9.2 Future Work

9.2.1. Operational Length Model:

Inclusion of middleware architecture: Easy data exchange between the EPS and the WDS was assumed in this work. The two systems, however, have supervisory control and data acquisition systems (SCADA) which are completely separate in operation. A middleware architecture representative of what would be needed to actually interface the SCADA systems of the two networks has been developed [117]. The inclusion of this into the simulation platform presented in this work will also allow for multiple WDSs to be incorporated and coupled with larger EPS test systems and will allow for the simulation computational burden to be distributed to multiple computers.

Sensitivity analysis on the relation of fuel cost to operational water cost: While conducting the various case studies presented in this work, it was seen that the dispatch of generation was extremely sensitive to the weights given to the CEED objective function terms. Therefore, it is proposed that sensitivity analysis be performed with the goal of

providing guidelines on how to properly determine and/or set the operational cost of water. This can be accomplished by examining simulation results and comparisons of the ratio of fuel cost to operational water cost versus time. Tuning of model in this way will allow for some insight into appropriate initial values for the operational water cost.

Inclusion of environmental considerations into the SCUC model: From the case study with the larger test system, it was noted that the inclusion of the reduced maximum active power outputs from the de-rating method caused units to be dispatched differently than if they were not. was not possible as this made the SCUC model infeasible (generation-load imbalance). Therefore, it is proposed that environmental considerations be included in the unit commitment problem. This would be especially applicable for cases where part of a system is experiencing extreme conditions, but the control policies are not implemented system wide (e.g. UC in AZ, which is interconnected with WECC).

9.2.2.Planning Length Model:

Incorporation of water availability scenarios: The compilation of data related to regional water availability is desired. This data can then be used along with water usage policies in order to see how water restrictions or limits on water availability effect expansion planning. GTEP is a large and complex problem so a decomposition routine implementing Benders decomposition using the master/slave problems listed in Figure 5.5 has been formulated and analysis of the results is ongoing.

9.2.3.Resilience:

Addition of resilience feedback into CEED formulation: It was noted that the IOR value could be increased if the dispatched was changed by altering the objective function term weights in the CEED. Therefore, it is proposed to investigate including feedback of some type that can adjust this weight within the simulation. This would accomplish:

1) Modification of the control methodology mid-simulation in order to actively increase resilience

2) Include a feedback loop which would enable the "adaptability within the system and its operating procedures and policies in order to improve the robustness, resourcefulness, and recovery characteristics for future events," as was described in the definition of desirable characteristics for a resilient system in Chapter 2.

REFERENCES

[1] California Energy Commission, “Integrated energy policy report,” Sacremento, CA, USA, 2005.

[2] S. C. Jones and R. B. Sowby, “Quantifying energy use in the U.S. public water industry — a summary,” *ASCE EWRI Currents*, vol. 16, no. 4, pp. 6–9, 2014.

[3] M. A. Maupin *et al.*, “Estimated use of water in the United States in 2010,” US DOI, USGS, Reston, Virginia, USA, USGS Circular 1405, 2014.

[4] *Net Generation by State by Type of Producer by Energy Source*, US EIA. [Online]. Available: https://www.eia.gov/electricity/data/state/

[5] R. Danielson, “Treatment plant power outage means all of tampa must boil water,” *Tampa Bay Times*, 2013. [Online]. Available: https://www.tampabay.com/news/localgovernment/boil-water-notice-issued-for-all-tampa-water-customers/1276215.

[6] K. Gerdes and C. Nichols, “Water requirements for existing and emerging thermoelectric plant technologies,” National Energy Technology Laboratory, Golden, CO, USA, Tech. Rep. DOE/NETL-402/080108, 2009.

[7] Admin, “Lessons from 1993 guide flood fight now,” *Radio Iowa*, 2008. [Online]. Available: https://www.radioiowa.com/2008/06/10/lessons-from-1993-guide-flood-fight-now/.

[8] A. Metcalf, “Millions of gallons of raw sewage overflows into little patuxent,” *Patch*, 2012. [Online]. Available: https://patch.com/maryland/columbia/report-millions-of-gallons-of-raw-sewage-overflows-in8e907dc022.

[9] A. Yeage, “On eve of Sandy anniversary, Ulman breaks ground on sewage plant backup generators,” *The Baltimore Sun*, 2013. [Online]. Available: https://www.baltimoresun.com/news/maryland/howard/lisbon-fulton/ph-sewage-power-fail-safe-story.html.

[10] U.S. EPA, “Power reslience: Guide for water and wastewater utilities,” U.S. EPA Office of Water, Washington, D.C., USA, June 2019.

[11] B. I. Cook, T. R. Ault, and J. E. Smerdon, “Unprecedented 21st century drought risk in the American southwest and central plains,” *Sci. Adv.*, vol. 1, no. 1, pp. 1–8, 2015.

[12] “High-impact, low-frequency event risk to the north American bulk power system,” North American Electric Reliability Corporation, U.S. Department of Energy, Washington, D.C., USA, 2010.

[13] President’s Commission on Critical Infrastructure Protection, “Critical foundations: Protecting america’s infrastructures,” Washington, D.C., USA, Oct. 1997.

[14] FEMA, “Power outage incident annex to the response and recovery federal interagency operational plans,” U.S. Department of Homeland Security, Washington, D.C., USA, June 2017.

[15] S. M. Rinaldi, J. P. Peerenboom, and T. K. Kelly, “Identifying, understanding, and analyzing critical infrastructure interdependencies,” *IEEE Control Systems Magazine*, pp. 11–25, Dec. 2001.

[16] F. Petit *et al.*, “Analysis of Critical Infrastructure Dependencies and Interdependencies,” Argonne National Laboratory, Argonne, IL, USA, June 2015.

[17] J. Gao, S. V. Buldyrev, H. E. Stanley, and S. Havlin, “Networks formed from interdependent networks,” *Nat. Phys.*, vol. 8, no. 1, pp. 40–48, 2012.

[18] M. Ouyang, “Review on modeling and simulation of interdependent critical infrastructure systems,” *Reliab. Eng. Syst. Saf.*, vol. 121, pp. 43–60, Jan. 2014.

[19] L. Duenas-Osorio, J. I. Craig, and B. J. Goodno, “Seismic response of critical interdependent networks,” *Earthq. Eng. Struct. Dyn.*, vol. 36, no. 2, pp. 285–306, Sep. 2006.

[20] G. J. Baxter, S. N. Dorogovtsev, A. V. Goltsev, and J. F. F. Mendes, “Avalanche collapse of interdependent networks,” *Phys. Rev. Lett.*, vol. 109, no. 24, pp. 1–5, Dec. 2012.

[21] U. Lee, J. Han, and A. Elgowainy, “Water consumption factors for electricity generation in the United States,” Argonne National Laboratory, Energy Systems Division, Argonne, IL, USA, Oct. 2016.

[22] S. Miller, “Personal Communication,” APS, Tempe, AZ, USA2017.

[23] P. Torcellini, N. Long, and R. Judkoff, “Consumptive water use for U. S. power production - technical report,” National Renewable Energy Laboratory, Golden, CO, USA, Tech. Rep. NREL/TP-550-33905, Dec. 2003.

[24] T. J. Feeley, L. Green, J. T. Murphy, J. Hoffmann, and B. A. Carney, “Department of energy/office of fossil energy’s power plant water management r&d program,” U.S. Department of Energy, National Energy Technology Laboratory, Washington, D.C., USA, Tech. Rep., 2005.

[25] T. Feeley *et al.*, “Addressing the critical link between fossil energy and water,” U.S. Department of Energy, National Energy Technology Laboratory,

Washington, D.C., USA, Jul. 2005.

[26] J. Maulbetsch and B. Barker, “Water use for electric power generation,” Electric Power Research Institute, Palo Alto, CA, USA, Tech. Rep. 1014026, Feb. 2008.

[27] S. Roy and L. Chen, “Water use for electricity generation and other sectors: recent changes (1985-2005) and future projections (2005-2030),” Electric Power Research Institute, Palo Alto, CA, USA, Tech. Rep. 1023676, Nov. 2011.

[28] J. Macknick, R. Newmark, G. Heath, and K. Hallett, “A Review of operational water consumption and withdrawal factors for electricity generating technologies,” National Renewable Energy Laboratory, Golden, CO, USA, Tech. Rep. NREL/TP-6A20-50900, Mar. 2011.

[29] L. Badr, G. Boardman, and J. Bigger, “Review of water use in U.S. thermoelectric power plants,” *J. Energy Eng.*, vol. 138, no. 4, pp. 246–257, Mar. 2012.

[30] G. Blair *et al.*, “Guidelines for managing water in cooling systems: For owners, operators, and environmental managers,” San Jose/Santa Clara Water Pollution Control Plant, City of San José Environmental Service Department, San Jose, CA, USA, Tech. Rep. 0707/Q1.5:4980, Jul. 2002.

[31] D. R. Baker and H. A. Shryock, “A comprehensive approach to the analysis of cooling tower performance,” *J. Heat Transfer*, vol. 83, no. 3, pp. 339–349, 1961.

[32] J. C. Hensley and SPX Cooling Technologies Staff, “Cooling tower fundamentals,” SPX Cooling Technologies, Inc., Overland Park, KS, USA, 2009.

[33] “Program on technology innovation: An energy/water sustainability research program for the electric power industry,” Electric Power Research Institute, Palo Alto, CA, USA, Tech. Rep. 1015371, Jul. 2007.

[34] J. L. Tsou, J. Maulbetsch, and J. Shi, “Power plant cooling system overview for researchers and technology developers,” Electric Power Research Institute, Palo Alto, CA, USA, Tech. Rep. 3002001915, May 2013.

[35] R. W. Healy *et al.*,“The water-energy nexus — an earth science perspective: U.S. geological survey circular 1407,” U.S. Department of the Interior, U.S. Geological Survey, Reston, VA, USA, U.S. Geological Survey Circular 1407, 2015.

[36] T. H. Diehl, M. A. Harris, J. C. Murphy, S. S. Hutson, and D. E. Ladd, “Methods for estimating water consumption for thermoelectric power plants in the United States,” U.S. Department of the Interior, U.S. Geological Survey, Reston, VA, USA, Scien. Invest. Rep. 2013–5188, 2013.

[37] International Energy Agency, “Water for energy,” in *World Energy Outlook*, 2012, ch. 17, pp. 1–33.

[38] J. Macknick, S. Sattler, K. Averyt, S. Clemmer, and J. Rogers, “The water implications of generating electricity: Water use across the United States based on different electricity pathways through 2050,” *Environ. Res. Lett.*, vol. 7, no. 4, Dec. 2012.

[39] L. Poch, G. Conzelmann, and T. Veselka, “An analysis of the effects of drought conditions on electric power generation in the Western United States,” U.S. Department of Energy, National Energy Technology Laboratory, Tech. Rep. DOE/NETL-2009/1365, 2009.

[40] C. B. Harto *et al.*, “Analysis of drought impacts on electricity production in the western and texas interconnections of the United States,” Argonne National Laboratory, U.S. Department of Energy, Office of Electricity Delivery and Energy Reliability, Tech. Rep. ANL/EVS/R-11/14, Dec. 2011.

[41] C. W. King, I. Duncan, and M. E. Webber, “Water demand projections for power

generation in texas," Texas Water Development Board, The University of Texas at Austin, Austin, TX, USA, Tech. Rep., Aug. 2008.

[42] W. Mills, A. Gabriel, and D. Gabriel, "Variability and impacts of implementing various power plant cooling technologies in texas," Electric Power Research Institute, Texas A&M, College Station, TX, USA, Aug. 2012.

[43] B. R. Scanlon, I. Duncan, and R. C. Reedy, "Drought and the water-energy nexus in texas," *Environ. Res. Lett.*, vol. 8, no. 4, pp. 1–14, Dec. 2013.

[44] A. M. Hamiche, A. B. Stambouli, and S. Flazi, "A review of the water-energy nexus," *Renew. Sustain. Energy Rev.*, vol. 65, pp. 319–331, Nov. 2016.

[45] M. Bazilian *et al.*, "Considering the energy, water and food nexus: Towards an integrated modelling approach," *Energy Policy*, vol. 39, no. 12, pp. 7896–7906, Oct. 2011.

[46] A. Endo, I. Tsurita, K. Burnett, and P. M. Orencio, "A review of the current state of research on the water, energy, and food nexus," *J. Hydrol. Reg. Stud.*, vol. 11, pp. 20–30, 2017.

[47] M. A. D. Larsen and M. Drews, "Water use in electricity generation for water-energy nexus analyses: The european case," *Sci. Total Environ.*, vol. 651, pp. 2044–2058, Feb. 2019.

[48] L. Lin and Y. D. Chen, "Evaluation of future water use for electricity generation under different energy development scenarios in china," *Sustain.*, vol. 10, no. 30, pp. 1–16, Dec. 2017.

[49] F. Kahrl and D. Roland-holst, "China's water-energy nexus," Center for Energy, Resources, and Economic Sustainability, UC Berkely, Berkeley, CA, USA,

Research Paper No. 0709071, Sep. 2007.

[50] C. Li, A. Svoboda, C. Tseng, and B. Johnson, “Hydro unit commitment in hydro-thermal optimization,” *IEEE Trans. Power Syst.*, vol. 12, no. 2, pp. 764–769, May 1997.

[51] W. Snyder, H. Powell, and J. Rayburn, “Dynamic programming approach to unit commitment,” *IEEE Trans. Power Syst.*, vol. 2, no. 2, pp. 339–348, May 1987.

[52] G. Morales-España, J. M. Latorre, and A. Ramos, “Tight and compact milp formulation of start-up and shut-down ramping in unit commitment,” *IEEE Trans. Power Syst.*, vol. 28, no. 4, pp. 1288–1296, Nov. 2013.

[53] H. Pandzic, T. Qiu, and D. S. Kirschen, “Comparison of state-of-the-art transmission constrained unit commitment formulations,” in *IEEE Power and Energy Society General Meeting*, 2013.

[54] B. Stott, J. Jardim, and O. Alsac, “DC power flow revisited,” *IEEE Trans. Power Syst. power Syst.*, vol. 24, no. 3, pp. 1290–1300, May 2009.

[55] H. Dommel and W. F. Tinney, “Optimal power flow solutions,” *IEEE Trans. Power Appar. Syst.*, vol. PAS-87, no. 10, pp. 1866–1876, Nov. 1968.

[56] H. Huneault and F. D. Galiana, “A survey of the optimal power flow literature,” *IEEE Trans. Power Syst.*, vol. 6, no. 2, pp. 762–770, May 1991.

[57] O. Alsac, J. Bright, M. Prais, and B. Stott, “Further developments in lp-based optimal power flow,” *IEEE Trans. Power Syst.*, vol. 5, no. 3, pp. 697–711, Aug. 1990.

[58] B. Stott and J. L. Marinho, “Linear programming for power-system network security applications,” *IEEE Trans. Power Appar. Syst.*, vol. PAS-98, no. 3, pp. 837–848, May 1979.

[59] J. H. Talaq, F. El-Hawary, and M. E. El-Hawary, “A summary of environmental/economic dispatch algorithms,” *IEEE Trans. Power Syst.*, vol. 9, no. 3, pp. 1508–1516, Aug. 1994.

[60] R. Yokoyama, S. H. Bae, T. Morita, and H. Sasaki, “Multiobjective optimal generation dispatch based on probability security criteria,” *IEEE Trans. Power Syst.*, vol. 3, no. 1, pp. 317–324, Feb. 1988.

[61] D. Fooladivanda and J. A. Taylor, “Dispatching thermal power plants under water constraints,” in *53rd Annual Allerton Conference*, Sep./Oct., 2015, pp. 396–401.

[62] V. C. Tidwell, M. Bailey, K. M. Zemlick, and B. D. Moreland, “Water supply as a constraint on transmission expansion planning in the western interconnection,” *Environ. Res. Lett.*, vol. 11, no. 12, pp. 1–15, Nov. 2016.

[63] G. A. Bakirtzis, P. N. Biskas, and V. Chatziathanasiou, “Generation expansion planning by milp considering mid-term scheduling decisions,” *Electr. Power Syst. Res.*, vol. 86, pp. 98-112, Dec. 2011.

[64] V. Hui Zhang, G. T. Vittal, J. Heydt, and J. Quintero, “A mixed-integer linear programming approach for multi-stage security-constrained transmission expansion planning,” *IEEE Trans. Power Syst.*, vol. 27, no. 2, pp. 1125–1133, May 2012.

[65] S. M. Shan Jin and S. M. Ryan, “A tri-level model of centralized transmission and decentralized generation expansion planning for an electricity market - part I,” *IEEE Trans. Power Syst.*, vol. 29, no. 1, pp. 132–141, 2014.

[66] S. Kamalinia, M. Shahidehpour, and A. Khodaei, “Security-constrained expansion planning of fast-response units for wind integration,” *Electr. Power Syst. Res.*, vol. 81, no. 1, pp. 107–116, Jan. 2011.

[67] A. R. Berkeley III and M. Wallace, “A framework for establishing critical infrastructure resilience goals: final report and recommendations,” National Infrastructure Advisory Council, DHS, Washington, D.C., USA, Oct. 2010.

[68] “Keeping the country running: natural hazards and infrastructure,” Cabinet Office, London, UK, Guide, Oct. 2011.

[69] S. Hosseini, K. Barker, and J. E. Ramirez-Marquez, “A review of definitions and measures of system resilience,” *Reliab. Eng. Syst. Saf.*, vol. 145, pp. 47–61, Jan. 2016.

[70] Executive Office of the President, “Economic benefits of increasing electric grid resilience to weather outages,” President’s Council of Economic Advisers,U.S. Department of Energy Office of Electricity Delivery and Energy Reliability, White House Office of Science and Technology, Washington, D.C., USA, Aug. 2013.

[71] M. Panteli and P. Mancarella, “The Grid: Stronger, Bigger, Smarter?: Presenting a Conceptual Framework of Power System Resilience,” *IEEE Power Energy Mag.*, vol. 13, no. 3, pp. 58–66, May/Jun. 2015.

[72] M. Panteli, P. Mancarella, D. Trakas, E. Kyriakides, and N. Hatziagyriou, “Metrics and quantification of operational and infrastructure resilience in power systems,” *IEEE Trans. Power Syst.*, vol. 32, no. 6, pp. 4732–4742, Nov. 2017.

[73] M. Panteli, C. Pickering, S. Wilkinson, R. Dawson, and P. Mancarella, “Power System Resilience to Extreme Weather: Fragility Modeling, Probabilistic Impact Assessment, and Adaptation Measures,” *IEEE Trans. Power Syst.*, vol. 32, no. 5, pp. 3747–3757, Sep. 2017.

[74] Y. Zhou, P. Mancarella, B. Wang, and M. Panteli, “Quantifying the system-level resilience ofelectric power generation to extreme temperature and water scarcity events,” *IEEE Syst. J.*, accepted for publication, pp. 1–11, 2019.

[75] C. Nan and G. Sansavini, “A quantitative method for assessing resilience of interdependent infrastructures,” *Reliab. Eng. Syst. Saf.*, vol. 157, pp. 35–53, Jan. 2017.

[76] K. Oikonomou and M. Parvania, “Optimal coordination of water distribution energy flexibility with power systems operation,” *IEEE Trans. Smart Grid*, vol. 10, no. 1, pp. 1101–1110, Jan. 2019.

[77] A. S. Zamzam, E. Dall’Anese, C. Zhao, J. A. Taylor, and N. D. Sidiropoulos, “Optimal Water-Power Flow-Problem: Formulation and Distributed Optimal Solution,” *IEEE Trans. Control Netw. Syst.*, vol. 6, no. 1, pp. 37–47, Mar. 2019.

[78] Q. Li, S. Yu, A. Al-Sumaiti, and K. Turitsyn, “Micro Water-Energy Nexus: Optimal Demand-Side Management and Quasi-Convex Hull Relaxation,” *IEEE Trans. Control Netw. Syst.*, vol. 6, no. 4, p. 1313-1322, Nov. 2018.

[79] Q. Li, S. Yu, A. Al-Sumaiti, and K. Turitsyn, “Modeling and co-optimization of a micro water-energy nexus for smart communities,” in *Innovative Smart Grid Technologies Conference Europe (ISGT-Europe), 2018 IEEE PES*, 2018, pp. 1–5.

[80] P. M. Anderson and A. A. Fouad, *Power system control and stability*, 2nd ed.. Piscataway, N.J.: IEEE Press ; Wiley-Interscience, 2003.

[81] V. Vittal, J. McCalley, P. M. Anderson, and A. A. Fouad, *Power system control and stability*, 3rd ed. Hoboken, NJ: IEEE Press ; Wiley-Interscience, 2020.

[82] P. Kundur, *Power system stability and control*. New York, NY: McGraw-Hill,

1994.

[83] W. D. Stevenson, *Elements of power system analysis*, 4th ed. New York, NY: McGraw-Hill, 1982.

[84] J. D. Glover, M. Sarma, and T. J. Overbye, *Power system analysis and design*, 5th ed. Stamford, CT: Cengage Learning, 2012.

[85] A. J. Wood, B. F. Wollenberg, and G. B. Sheblé, *Power generation, operation and control*, 3rd ed. New York, NY: John Wiley and Sons, 2013.

[86] C. L. Fortescue, "Method of Symmetrical Co-Ordinates Applied to the Solution of Polyphase Networks," *Trans. Am. Inst. Electr. Eng.*, vol. XXXVII, no. 2, pp. 1027–1140, Jul. 1918.

[87] PowerWorld, "Solving the powerflow." [Online]. Available: https://www.powerworld.com/WebHelp/Content/MainDocumentation_HTML/Solving_the_Power_Flow.htm.

[88] L. A. Rossman, "EPANET 2 users manual," National Risk Management Research Laboratory, US EPA, Cincinnati, OH, USA, 2000.

[89] M. B. Cain, R. P. O'Neill, and A. Castillo, "History of optimal power flow and formulation," Federal Energy Regulatory Commision, Washington, D.C, USA, Tech. Rep, Dec. 2012.

[90] R. J. Campbell, "Weather-related power outages and electric system resiliency," Washington, D.C., USA, CRS Rep. for Congress, Aug. 2012.

[91] J. McCall, J. Macknick, and D. Hillman, "Water-related power plant curtailments: An overview of incidents and contributing factors," National Energy Technology

Laboratory, Albany, OR, USA, Tech. Rep. NREL/TP-6A20-67084, Dec. 2016.

[92] P. Khatavkar and L. Mays, "Model for the real-time operation of water distribution systems under limited power availability," in *Proc. World Environmental and Water Resources Congress 2017*, 2017, pp. 171–183.

[93] P. Khatavkar and L. W. Mays, "Testing an optimization/simulation model for the real-time operations of water distribution systems under limited power availability," in *Congress on Technical Advancement 2017: Infrastructure Resilience and Energy - Papers from Sessions of the 1st Congress on Technical Advancement*, 2017, 2017, pp. 1–9.

[94] S. Zuloaga, P. Khatavkar, V. Vittal, and L. W. Mays , "Interdependent electric and water infrastructure modeling, optimization and control," IET Energy Syst. Integr. J., vol. 2, no. 1, pp. 9–21, March, 2020.

[95] R. Fourer, D. M. Gay, and B. W. Kernighan, "A modeling language for mathematical programming," *Manage. Sci.*, vol. 36, no. 5, pp. 519–554, May 1990.

[96] Z. Gu, E. Rothberg, and R. Bixby, "Gurobi Optimizer Reference Manual, Version 5.1," 2013.

[97] S. Barnes, R. D'Aquila, and B. Thomas, "PSLF user manual." General Electric (GE), Schenectady, NY, USA, 2011.

[98] D. G. Elíades, M. Kyriakou, S. Vrachimis, and M. M. Polycarpou, "EPANET-MATLAB toolkit: an open-source software for interfacing EPANET with MATLAB," in *Proc. 14th International Conference on Computing and Control for the Water Industry (CCWI)*, 2016, pp. 1–8.

[99] "Reliability requirements." California ISO. [Online]. Available: http://www.caiso.com/planning/Pages/ReliabilityRequirements/Default.aspx#Historical.

[100] WECC Scenario Planning Steering Group, "WECC Long-term planning scenario report: In support of the regional transmission expansion planning project," Western Electricity Coordinating Council, Salt Lake City, UT, USA, Tech. Rep., Mar. 2013.

[101] C. Grigg *et al.*, "The IEEE Reliability Test System-1996. A report prepared by the Reliability Test System Task Force of the Application of Probability Methods Subcommittee," *IEEE Trans. Power Syst.*, vol. 14, no. 3, pp. 1010–1020, Aug. 1999.

[102] WECC Staff, "2013 interconnection-wide plan tools and models," Western Electricity Coordinating Council, Salt Lake City, UT, USA, Tech. Rep., Sep. 2013.

[103] WECC, "LTPT final recommended scenario modeling parameters," Western Electricity Coordinating Council, Salt Lake City, UT, USA, Tech. Rep., 2014.

[104] Illinois Center for a Smarter Electric Grid, "IEEE 14-bus system," 2018. [Online]. Available: http://icseg.iti.illinois.edu/ieee-14-bus-system.

[105] Schneider Electric, "Recommended electrical network design for efficient plant and energy operations," Schneider Electric, Rueil-Malmaison, France, Tech. Rep., 2012.

[106] K. P. Schneider *et al.*, "Analytic considerations and design basis for the IEEE distribution test feeders," *IEEE Trans. Power Syst.*, vol. 33, no. 3, pp. 3181–3188, May 2018.

[107] "Net generation by energy source: total (all sectors), 2007 - 2017," Energy Information Administration, 2017. [Online]. Available: https://www.eia.gov/electricity/annual/html/epa_03_01_a.html.

[108] S. Zuloaga and V. Vittal, "Metrics for Use in Quantifying Power System Resilience with Water-Energy Nexus Considerations: Mathematical Formulation and Case Study," in *IEEE Power and Energy Society General Meeting*, 2019.

[109] S. Zuloaga, P. Khatavkar, L. W. Mays, and V. Vittal, "Resilience of Cyber-Enabled Electrical Energy and Water Distribution Systems Considering Infrastructural Robustness Under Conditions of Limited Water and/or Energy Availability," *IEEE Trans. Eng. Manag.*, Early Access, pp. 1–17, Sep. 2019.

[110] N. Y. Aydin, L. Mays, and T. Schmitt, "Sustainability assessment of urban water distribution systems," *Water Resour. Manag.*, vol. 28, no. 12, pp. 4373–4384, Jul. 2014.

[111] V. S. Y. Kwan, E. S. Naidu, and M. T. Bixter, "Controlling environmental crisis appraisal through knowledge, vividness, and timing," *J. Environ. Psychol.*, vol. 61, pp. 93–100, Feb. 2019.

[112] U.S. Census Bureau, "Census of housing," *U.S. Department of Commerce*. [Online]. Available: https://www.census.gov/hhes/www/housing/census/histcensusofhsg.html.

[113] E. Bompard, E. Pons, and D. Wu, "Analysis of the structural vulnerability of the interconnected power grid of continental europe with the integrated power system and unified power system based on extended topological approach," *Int. Trans. Electr. Energy Syst.*, vol. 23, no. 5, pp. 620–637, Jul. 2013.

[114] E. Bompard, R. Napoli, and F. Xue, "Analysis of structural vulnerabilities in power transmission grids," *Int. J. Crit. Infrastruct. Prot.*, vol. 2, no. 1, pp. 5–12,

May 2009.

[115] E. Bompard, R. Napoli, and F. Xue, “Extended topological approach for the assessment of structural vulnerability in transmission networks,” *IET Gener. Transm. Distrib.*, vol. 4, no. 6, pp. 716–724, May 2010.

[116] “Electric Power Monthly: with Data for July 2019,” U.S. Energy Information Agency and U. S. Department of Energy, Washington, D.C., USA, 2019.

[117] B. Liu, “A software-defined networking (sdn) assisted middleware interconnecting supervisory control and data acquisition (scada) systems,” M.S. thesis, ECEE, Arizona State University, Tempe, AZ, 2018.

APPENDIX A

MODIFIED IEEE 14-BUS TEST CASE .RAW FILE

0 , 100.000, 33, 0,1, 60.00

1,'Bus 1 ',138.0000,3, 1, 1, 1,1.060000,
0.000000,1.100000,0.900000,1.100000,0.900000

2,'Bus 2 ',138.0000,2, 1, 1, 1,1.045000,-
4.982411,1.100000,0.900000,1.100000,0.900000

3,'Bus 3 ',138.0000,2, 1, 1, 1,1.010000,-
12.724711,1.100000,0.900000,1.100000,0.900000

4,'Bus 4 ',138.0000,1, 1, 1, 1,1.017716,-
10.313436,1.100000,0.900000,1.100000,0.900000

5,'Bus 5 ',138.0000,1, 1, 1, 1,1.019541,-
8.773617,1.100000,0.900000,1.100000,0.900000

6,'Bus 6 ',138.0000,2, 1, 1, 1,1.069993,-
14.217169,1.100000,0.900000,1.100000,0.900000

7,'Bus 7 ',138.0000,1, 1, 1, 1,1.061678,-
13.360950,1.100000,0.900000,1.100000,0.900000

8,'Bus 8 ',138.0000,2, 1, 1, 1,1.090003,-
13.360951,1.100000,0.900000,1.100000,0.900000

9,'Bus 9 ',138.0000,1, 1, 1, 1,1.056239,-
14.939865,1.100000,0.900000,1.100000,0.900000

10,'Bus 10 ',138.0000,1, 1, 1, 1,1.051233,-
15.097814,1.100000,0.900000,1.100000,0.900000

11,'Bus 11 ',138.0000,1, 1, 1, 1,1.057016,-
14.789227,1.100000,0.900000,1.100000,0.900000

12,'Bus 12 ',138.0000,1, 1, 1, 1,1.055431,-
15.075738,1.100000,0.900000,1.100000,0.900000

13,'Bus 13 ',138.0000,1, 1, 1, 1,1.050862,-
15.166369,1.100000,0.900000,1.100000,0.900000

14,'Bus 14 ',138.0000,1, 1, 1, 1,1.036477,-
16.051870,1.100000,0.900000,1.100000,0.900000

15,'Bus 15 ', 69.0000,1, 1, 1, 1,1.051156,-
15.168376,1.100000,0.900000,1.100000,0.900000

16,'Bus 16 ', 69.0000,1, 1, 1, 1,1.051249,-15.175210,1.100000,0.900000,1.100000,0.900000

17,'Bus 17 ', 69.0000,1, 1, 1, 1,1.051249,-15.175210,1.100000,0.900000,1.100000,0.900000

18,'Bus 18 ', 12.7000,1, 1, 1, 1,1.051249,-15.175210,1.100000,0.900000,1.100000,0.900000

19,'Bus 19 ', 12.7000,1, 1, 1, 1,1.051249,-15.175210,1.100000,0.900000,1.100000,0.900000

20,'Bus 20 ', 12.7000,1, 1, 1, 1,1.051249,-15.175210,1.100000,0.900000,1.100000,0.900000

21,'Bus 21 ', 12.7000,1, 1, 1, 1,1.051249,-15.175210,1.100000,0.900000,1.100000,0.900000

22,'Bus 22 ', 12.7000,1, 1, 1, 1,1.051249,-15.175210,1.100000,0.900000,1.100000,0.900000

23,'Bus 23 ', 12.7000,1, 1, 1, 1,1.051249,-15.175210,1.100000,0.900000,1.100000,0.900000

24,'Bus 24 ', 12.7000,1, 1, 1, 1,1.051249,-15.175210,1.100000,0.900000,1.100000,0.900000

25,'Bus 25 ', 12.7000,1, 1, 1, 1,1.051249,-15.175210,1.100000,0.900000,1.100000,0.900000

26,'Bus 26 ', 12.7000,1, 1, 1, 1,1.051249,-15.175210,1.100000,0.900000,1.100000,0.900000

27,'Bus 27 ', 12.7000,1, 1, 1, 1,1.051249,-15.175210,1.100000,0.900000,1.100000,0.900000

28,'Bus 28 ', 12.7000,1, 1, 1, 1,1.051249,-15.175210,1.100000,0.900000,1.100000,0.900000

29,'Bus 29 ', 12.7000,1, 1, 1, 1,1.051249,-15.175210,1.100000,0.900000,1.100000,0.900000

30,'Bus 30 ', 12.7000,1, 1, 1, 1,1.051249,-15.175210,1.100000,0.900000,1.100000,0.900000

31,'Bus 31 ', 69.0000,1, 1, 1, 1,1.036767,-16.053877,1.100000,0.900000,1.100000,0.900000

32,'Bus 32 ', 69.0000,1, 1, 1, 1,1.036859,-16.060709,1.100000,0.900000,1.100000,0.900000

33,'Bus 33 ', 69.0000,1, 1, 1, 1,1.036859,-16.060709,1.100000,0.900000,1.100000,0.900000

34,'Bus 34 ', 12.7000,1, 1, 1, 1,1.036859,-16.060709,1.100000,0.900000,1.100000,0.900000

35,'Bus 35 ', 12.7000,1, 1, 1, 1,1.036859,-16.060709,1.100000,0.900000,1.100000,0.900000

36,'Bus 36 ', 12.7000,1, 1, 1, 1,1.036859,-16.060709,1.100000,0.900000,1.100000,0.900000

37,'Bus 37 ', 12.7000,1, 1, 1, 1,1.036859,-16.060709,1.100000,0.900000,1.100000,0.900000

38,'Bus 38 ', 12.7000,1, 1, 1, 1,1.036859,-16.060709,1.100000,0.900000,1.100000,0.900000

39,'Bus 39 ', 12.7000,1, 1, 1, 1,1.036859,-16.060709,1.100000,0.900000,1.100000,0.900000

40,'Bus 40 ', 12.7000,1, 1, 1, 1,1.036859,-16.060709,1.100000,0.900000,1.100000,0.900000

41,'Bus 41 ', 12.7000,1, 1, 1, 1,1.036859,-16.060709,1.100000,0.900000,1.100000,0.900000

42,'Bus 42 ', 12.7000,1, 1, 1, 1,1.036859,-16.060709,1.100000,0.900000,1.100000,0.900000

43,'Bus 43 ', 12.7000,1, 1, 1, 1,1.036859,-16.060709,1.100000,0.900000,1.100000,0.900000

44,'Bus 44 ', 12.7000,1, 1, 1, 1,1.036859,-16.060709,1.100000,0.900000,1.100000,0.900000

45,'Bus 45 ', 12.7000,1, 1, 1, 1,1.036859,-16.060709,1.100000,0.900000,1.100000,0.900000

46,'Bus 46 ', 12.7000,1, 1, 1, 1,1.036859,-16.060709,1.100000,0.900000,1.100000,0.900000

47,'Bus 47 ', 12.7000,1, 1, 1, 1,1.036859,-16.060709,1.100000,0.900000,1.100000,0.900000

48,'Bus 48 ', 12.7000,1, 1, 1, 1,1.036859,-16.060709,1.100000,0.900000,1.100000,0.900000

49,'Bus 49 ', 12.7000,1, 1, 1, 1,1.036859,-16.060709,1.100000,0.900000,1.100000,0.900000

50,'Bus 50 ', 12.7000,1, 1, 1, 1,1.036859,-16.060709,1.100000,0.900000,1.100000,0.900000

51,'Bus 51 ', 12.7000,1, 1, 1, 1,1.036859,-16.060709,1.100000,0.900000,1.100000,0.900000

52,'Bus 52 ', 12.7000,1, 1, 1, 1,1.036859,-16.060709,1.100000,0.900000,1.100000,0.900000

0 / END OF BUS DATA, BEGIN LOAD DATA

2,'1 ',1, 1, 1, 21.700, 12.700, 0.000, 0.000, 0.000, -0.000, 1,1,0

3,'1 ',1, 1, 1, 94.200, 19.000, 0.000, 0.000, 0.000, -0.000, 1,1,0

4,'1 ',1, 1, 1, 47.800, -3.900, 0.000, 0.000, 0.000, -0.000, 1,1,0

5,'1 ',1, 1, 1, 7.600, 1.600, 0.000, 0.000, 0.000, -0.000, 1,1,0

6,'1 ',1, 1, 1, 11.200, 7.500, 0.000, 0.000, 0.000, -0.000, 1,1,0

9,'1 ',1, 1, 1, 29.500, 16.600, 0.000, 0.000, 0.000, -0.000, 1,1,0

10,'1 ',1, 1, 1, 9.000, 5.800, 0.000, 0.000, 0.000, -0.000, 1,1,0

11,'1 ',1, 1, 1, 3.500, 1.800, 0.000, 0.000, 0.000, -0.000, 1,1,0

12,'1 ',1, 1, 1, 6.100, 1.600, 0.000, 0.000, 0.000, -0.000, 1,1,0

13,'1 ',1, 1, 1, 13.500, 5.800, 0.000, 0.000, 0.000, -0.000, 1,1,0

14,'1 ',1, 1, 1, 14.900, 5.000, 0.000, 0.000, 0.000, -0.000, 1,1,0

20,'1 ',1, 1, 1, 0.000, 0.000, 0.000, 0.000, 0.000, 0.000, 1,1,0

21,'1 ',1, 1, 1, 0.000, 0.000, 0.000, 0.000, 0.000, 0.000, 1,1,0

22,'1 ',1, 1, 1, 0.000, 0.000, 0.000, 0.000, 0.000, 0.000, 1,1,0

23,'1 ',1, 1, 1, 0.000, 0.000, 0.000, 0.000, 0.000, 0.000, 1,1,0

24,'1 ',1, 1, 1, 0.000, 0.000, 0.000, 0.000, 0.000, 0.000, 1,1,0

25,'1 ',1, 1, 1, 0.000, 0.000, 0.000, 0.000, 0.000, 0.000, 1,1,0

26,'1 ',1, 1, 1, 0.000, 0.000, 0.000, 0.000, 0.000, 0.000, 1,1,0

27,'1 ',1, 1, 1, 0.000, 0.000, 0.000, 0.000, 0.000, 0.000, 1,1,0

28,'1 ',1, 1, 1, 0.000, 0.000, 0.000, 0.000, 0.000, 0.000, 1,1,0

29,'1 ',1, 1, 1, 0.000, 0.000, 0.000, 0.000, 0.000, 0.000, 1,1,0

30,'1 ',1, 1, 1, 0.000, 0.000, 0.000, 0.000, 0.000, 0.000, 1,1,0

36,'1 ',1, 1, 1, 0.000, 0.000, 0.000, 0.000, 0.000, 0.000, 1,1,0

37,'1 ',1, 1, 1, 0.000, 0.000, 0.000, 0.000, 0.000, 0.000, 1,1,0

38,'1 ',1, 1, 1, 0.000, 0.000, 0.000, 0.000, 0.000, 0.000, 1,1,0

39,'1 ',1, 1, 1, 0.000, 0.000, 0.000, 0.000, 0.000, 0.000, 1,1,0

40,'1 ',1, 1, 1, 0.000, 0.000, 0.000, 0.000, 0.000, 0.000, 1,1,0

41,'1 ',1, 1, 1, 0.000, 0.000, 0.000, 0.000, 0.000, 0.000, 1,1,0

42,'1 ',1, 1, 1, 0.000, 0.000, 0.000, 0.000, 0.000, 0.000, 1,1,0

43,'1 ',1, 1, 1, 0.000, 0.000, 0.000, 0.000, 0.000, 0.000, 1,1,0

44,'1 ',1, 1, 1, 0.000, 0.000, 0.000, 0.000, 0.000, 0.000, 1,1,0

45,'1 ',1, 1, 1, 0.000, 0.000, 0.000, 0.000, 0.000, 0.000, 1,1,0

46,'1 ',1, 1, 1, 0.000, 0.000, 0.000, 0.000, 0.000, 0.000, 1,1,0

47,'1 ',1, 1, 1, 0.000, 0.000, 0.000, 0.000, 0.000, 0.000, 1,1,0

48,'1 ',1, 1, 1, 0.000, 0.000, 0.000, 0.000, 0.000, 0.000, 1,1,0

49,'1 ',1, 1, 1, 0.000, 0.000, 0.000, 0.000, 0.000, 0.000, 1,1,0

50,'1 ',1, 1, 1, 0.000, 0.000, 0.000, 0.000, 0.000, 0.000, 1,1,0

51,'1 ',1, 1, 1, 0.000, 0.000, 0.000, 0.000, 0.000, 0.000, 1,1,0

52,'1 ',1, 1, 1, 0.000, 0.000, 0.000, 0.000, 0.000, 0.000, 1,1,0

0 / END OF LOAD DATA, BEGIN FIXED SHUNT DATA

9,' 1',1, 0.000000, 19.000000

0 / END OF FIXED SHUNT DATA, BEGIN GENERATOR DATA

1,'1 ', 232.385, -16.560, 0.000, 0.000,1.060000, 0, 615.000, 0.00000, 1.00000, 0.00000, 0.00000, 1.00000,1, 100.0, 10000.000,-10000.000, 1,1.0000,0,1,0,1,0,1,0,1

2,'1 ', 40.000, 43.514, 50.000, -40.000,1.045000, 0, 60.000, 0.00000, 1.00000, 0.00000, 0.00000, 1.00000,1, 100.0, 10000.000,-10000.000, 1,1.0000,0,1,0,1,0,1,0,1

3,'1 ', 0.000, 25.048, 40.000, 0.000,1.010000, 0, 60.000, 0.00000, 1.00000, 0.00000, 0.00000, 1.00000,1, 100.0, 10000.000,-10000.000, 1,1.0000,0,1,0,1,0,1,0,1

6,'1 ', 0.000, 12.102, 24.000, -6.000,1.070000, 0, 25.000, 0.00000, 1.00000, 0.00000, 0.00000, 1.00000,1, 100.0, 10000.000,-10000.000, 1,1.0000,0,1,0,1,0,1,0,1

8,'1 ', 0.000, 17.535, 24.000, -6.000,1.090000, 0, 25.000, 0.00000, 1.00000, 0.00000, 0.00000, 1.00000,1, 100.0, 10000.000,-10000.000, 1,1.0000,0,1,0,1,0,1,0,1

0 / END OF GENERATOR DATA, BEGIN BRANCH DATA

1, 2,'1 ', 0.01938, 0.05917, 0.05280, 0.00, 0.00, 0.00, 0.00000, 0.00000, 0.00000, 0.00000,1,1, 0.00, 1,1.0000

1, 5,'1 ', 0.05403, 0.22304, 0.04920, 0.00, 0.00, 0.00, 0.00000, 0.00000, 0.00000, 0.00000,1,1, 0.00, 1,1.0000

2, 3,'1 ', 0.04699, 0.19797, 0.04380, 0.00, 0.00, 0.00, 0.00000, 0.00000, 0.00000, 0.00000,1,1, 0.00, 1,1.0000

2, 4,'1 ', 0.05811, 0.17632, 0.03400, 0.00, 0.00, 0.00, 0.00000, 0.00000, 0.00000, 0.00000,1,1, 0.00, 1,1.0000

2, 5,'1 ', 0.05695, 0.17388, 0.03460, 0.00, 0.00, 0.00, 0.00000, 0.00000, 0.00000, 0.00000,1,1, 0.00, 1,1.0000

3, 4,'1 ', 0.06701, 0.17103, 0.01280, 0.00, 0.00, 0.00, 0.00000, 0.00000, 0.00000, 0.00000,1,1, 0.00, 1,1.0000

4, 5,'1 ', 0.01335, 0.04211, 0.00000, 0.00, 0.00, 0.00, 0.00000, 0.00000, 0.00000, 0.00000,1,1, 0.00, 1,1.0000

6, 11,'1 ', 0.09498, 0.19890, 0.00000, 0.00, 0.00, 0.00, 0.00000, 0.00000, 0.00000, 0.00000,1,1, 0.00, 1,1.0000

6, 12,'1 ', 0.12291, 0.25581, 0.00000, 0.00, 0.00, 0.00, 0.00000, 0.00000, 0.00000, 0.00000,1,1, 0.00, 1,1.0000

6, 13,'1 ', 0.06615, 0.13027, 0.00000, 0.00, 0.00, 0.00, 0.00000, 0.00000, 0.00000, 0.00000,1,1, 0.00, 1,1.0000

7, 8,'1 ', 0.00000, 0.17615, 0.00000, 0.00, 0.00, 0.00, 0.00000, 0.00000, 0.00000, 0.00000,1,1, 0.00, 1,1.0000

7, 9,'1 ', 0.00000, 0.11001, 0.00000, 0.00, 0.00, 0.00, 0.00000, 0.00000, 0.00000, 0.00000,1,1, 0.00, 1,1.0000

9, 10,'1 ', 0.03181, 0.08450, 0.00000, 0.00, 0.00, 0.00, 0.00000, 0.00000, 0.00000, 0.00000,1,1, 0.00, 1,1.0000

9, 14,'1 ', 0.12711, 0.27038, 0.00000, 0.00, 0.00, 0.00, 0.00000, 0.00000, 0.00000, 0.00000,1,1, 0.00, 1,1.0000

10, 11,'1 ', 0.08205, 0.19207, 0.00000, 0.00, 0.00, 0.00, 0.00000, 0.00000, 0.00000, 0.00000,1,1, 0.00, 1,1.0000

12, 13,'1 ', 0.22092, 0.19988, 0.00000, 0.00, 0.00, 0.00, 0.00000, 0.00000, 0.00000, 0.00000,1,1, 0.00, 1,1.0000

13, 14,'1 ', 0.17093, 0.34802, 0.00000, 0.00, 0.00, 0.00, 0.00000, 0.00000, 0.00000, 0.00000,1,1, 0.00, 1,1.0000

15, 16,'1 ', 0.13250, 0.09850, 0.00170, 0.00, 0.00, 0.00, 0.00000, 0.00000, 0.00000, 0.00000,1,1, 0.00, 1,1.0000

15, 17,'1 ', 0.13250, 0.09850, 0.00170, 0.00, 0.00, 0.00, 0.00000, 0.00000, 0.00000, 0.00000,1,1, 0.00, 1,1.0000

16, 17,'1 ', 0.00770, 0.00570, 0.00010, 0.00, 0.00, 0.00, 0.00000, 0.00000, 0.00000, 0.00000,1,1, 0.00, 1,1.0000

18, 20,'1 ', 0.00000, 0.00001, 0.00000, 0.00, 0.00, 0.00, 0.00000, 0.00000, 0.00000, 0.00000,1,1, 0.00, 1,1.0000

18, 21,'1 ', 0.00000, 0.00001, 0.00000, 0.00, 0.00, 0.00, 0.00000, 0.00000, 0.00000, 0.00000,1,1, 0.00, 1,1.0000

18, 22,'1 ', 0.00000, 0.00001, 0.00000, 0.00, 0.00, 0.00, 0.00000, 0.00000, 0.00000, 0.00000,1,1, 0.00, 1,1.0000

18, 23,'1 ', 0.00000, 0.00001, 0.00000, 0.00, 0.00, 0.00, 0.00000, 0.00000, 0.00000, 0.00000,1,1, 0.00, 1,1.0000

18, 24,'1 ', 0.00000, 0.00001, 0.00000, 0.00, 0.00, 0.00, 0.00000, 0.00000, 0.00000, 0.00000,1,1, 0.00, 1,1.0000

19, 25,'1 ', 0.00000, 0.00001, 0.00000, 0.00, 0.00, 0.00, 0.00000, 0.00000, 0.00000, 0.00000,1,1, 0.00, 1,1.0000

19, 26,'1 ', 0.00000, 0.00001, 0.00000, 0.00, 0.00, 0.00, 0.00000, 0.00000, 0.00000, 0.00000,1,1, 0.00, 1,1.0000

19, 27,'1 ', 0.00000, 0.00001, 0.00000, 0.00, 0.00, 0.00, 0.00000, 0.00000, 0.00000, 0.00000,1,1, 0.00, 1,1.0000

19, 28,'1 ', 0.00000, 0.00001, 0.00000, 0.00, 0.00, 0.00, 0.00000, 0.00000, 0.00000, 0.00000,1,1, 0.00, 1,1.0000

19, 29,'1 ', 0.00000, 0.00001, 0.00000, 0.00, 0.00, 0.00, 0.00000, 0.00000, 0.00000, 0.00000,1,1, 0.00, 1,1.0000

19, 30,'1 ', 0.00000, 0.00001, 0.00000, 0.00, 0.00, 0.00, 0.00000, 0.00000, 0.00000, 0.00000,1,1, 0.00, 1,1.0000

31, 32,'1 ', 0.13250, 0.09850, 0.00170, 0.00, 0.00, 0.00, 0.00000, 0.00000, 0.00000, 0.00000,1,1, 0.00, 1,1.0000

31, 33,'1 ', 0.13250, 0.09850, 0.00170, 0.00, 0.00, 0.00, 0.00000, 0.00000, 0.00000, 0.00000,1,1, 0.00, 1,1.0000

32, 33,'1 ', 0.00770, 0.00570, 0.00010, 0.00, 0.00, 0.00, 0.00000, 0.00000, 0.00000, 0.00000,1,1, 0.00, 1,1.0000

34, 36,'1 ', 0.00000, 0.00001, 0.00000, 0.00, 0.00, 0.00, 0.00000, 0.00000, 0.00000, 0.00000,1,1, 0.00, 1,1.0000

34, 37,'1 ', 0.00000, 0.00001, 0.00000, 0.00, 0.00, 0.00, 0.00000, 0.00000, 0.00000, 0.00000,1,1, 0.00, 1,1.0000

34, 38,'1 ', 0.00000, 0.00001, 0.00000, 0.00, 0.00, 0.00, 0.00000, 0.00000, 0.00000, 0.00000,1,1, 0.00, 1,1.0000

34, 39,'1 ', 0.00000, 0.00001, 0.00000, 0.00, 0.00, 0.00, 0.00000, 0.00000, 0.00000, 0.00000,1,1, 0.00, 1,1.0000

34, 40,'1 ', 0.00000, 0.00001, 0.00000, 0.00, 0.00, 0.00, 0.00000, 0.00000, 0.00000, 0.00000,1,1, 0.00, 1,1.0000

34, 41,'1 ', 0.00000, 0.00001, 0.00000, 0.00, 0.00, 0.00, 0.00000, 0.00000, 0.00000, 0.00000,1,1, 0.00, 1,1.0000

34, 42,'1 ', 0.00000, 0.00001, 0.00000, 0.00, 0.00, 0.00, 0.00000, 0.00000, 0.00000, 0.00000,1,1, 0.00, 1,1.0000

34, 43,'1 ', 0.00000, 0.00001, 0.00000, 0.00, 0.00, 0.00, 0.00000, 0.00000, 0.00000, 0.00000,1,1, 0.00, 1,1.0000

35, 44,'1 ', 0.00000, 0.00001, 0.00000, 0.00, 0.00, 0.00, 0.00000, 0.00000, 0.00000, 0.00000,1,1, 0.00, 1,1.0000

35, 45,'1 ', 0.00000, 0.00001, 0.00000, 0.00, 0.00, 0.00, 0.00000, 0.00000, 0.00000, 0.00000,1,1, 0.00, 1,1.0000

35, 46,'1 ', 0.00000, 0.00001, 0.00000, 0.00, 0.00, 0.00, 0.00000, 0.00000, 0.00000, 0.00000,1,1, 0.00, 1,1.0000

35, 47,'1 ', 0.00000, 0.00001, 0.00000, 0.00, 0.00, 0.00, 0.00000, 0.00000, 0.00000, 0.00000,1,1, 0.00, 1,1.0000

35, 48,'1 ', 0.00000, 0.00001, 0.00000, 0.00, 0.00, 0.00, 0.00000, 0.00000, 0.00000, 0.00000,1,1, 0.00, 1,1.0000

35, 49,'1 ', 0.00000, 0.00001, 0.00000, 0.00, 0.00, 0.00, 0.00000, 0.00000, 0.00000, 0.00000,1,1, 0.00, 1,1.0000

35, 50,'1 ', 0.00000, 0.00001, 0.00000, 0.00, 0.00, 0.00, 0.00000, 0.00000, 0.00000, 0.00000,1,1, 0.00, 1,1.0000

35, 51,'1 ', 0.00000, 0.00001, 0.00000, 0.00, 0.00, 0.00, 0.00000, 0.00000, 0.00000, 0.00000,1,1, 0.00, 1,1.0000

35, 52,'1 ', 0.00000, 0.00001, 0.00000, 0.00, 0.00, 0.00, 0.00000, 0.00000, 0.00000, 0.00000,1,1, 0.00, 1,1.0000

0 / END OF BRANCH DATA, BEGIN TRANSFORMER DATA

4, 7, 0,'1 ',2,2,1, 0.00000, 0.00000,2,' ',1, 1,1.0000

0.00000, 0.20912, 100.00

134.964005,138.000000,0.000000, 0.00, 0.00, 0.00, 0, -0,207.000000,70.379997,1.500000,0.510000, 159, 0, 0.00, 0.00, 0.00

138.000000,138.000000

4, 9, 0,'1 ',2,2,1, 0.00000, 0.00000,2,' ',1, 1,1.0000

0.00000, 0.55618, 100.00

133.722000,138.000000,0.000000, 0.00, 0.00, 0.00, 0, -
0,207.000000,70.379997,1.500000,0.510000, 159, 0, 0.00, 0.00, 0.00

138.000000,138.000000

5, 6, 0,'1 ',2,2,1, 0.00000, 0.00000,2,' ',1, 1,1.0000

0.00000, 0.25202, 100.00

128.615997,138.000000,0.000000, 0.00, 0.00, 0.00, 0, -
0,207.000000,70.379997,1.500000,0.510000, 159, 0, 0.00, 0.00, 0.00

138.000000,138.000000

13, 15, 0,'1 ',2,2,1, 0.00000, 0.00000,2,' ',1, 1,1.0000

0.01000, 0.08000, 100.00

138.000000,138.000000,0.000000, 0.00, 0.00, 0.00, 0, -
0,207.000000,70.379997,1.500000,0.510000, 159, 0, 0.00, 0.00, 0.00

69.000000,69.000000

14, 31, 0,'1 ',2,2,1, 0.00000, 0.00000,2,' ',1, 1,1.0000

0.01000, 0.08000, 100.00

138.000000,138.000000,0.000000, 0.00, 0.00, 0.00, 0, -
0,207.000000,70.379997,1.500000,0.510000, 159, 0, 0.00, 0.00, 0.00

69.000000,69.000000

16, 18, 0,'1 ',2,2,1, 0.00000, 0.00000,2,' ',1, 1,1.0000

0.01900, 0.04800, 100.00

69.000000,69.000000,0.000000, 0.00, 0.00, 0.00, 0, -
0,103.500000,35.189999,1.500000,0.510000, 159, 0, 0.00, 0.00, 0.00

12.700000,12.700000

17, 19, 0,'1 ',2,2,1, 0.00000, 0.00000,2,' ',1, 1,1.0000

0.01900, 0.04800, 100.00

69.000000,69.000000,0.000000, 0.00, 0.00, 0.00, 0, -
0,103.500000,35.189999,1.500000,0.510000, 159, 0, 0.00, 0.00, 0.00

12.700000,12.700000

32, 34, 0,'1 ',2,2,1, 0.00000, 0.00000,2,' ',1, 1,1.0000

0.01900, 0.04800, 100.00

69.000000,69.000000,0.000000, 0.00, 0.00, 0.00, 0, -
0,103.500000,35.189999,1.500000,0.510000, 159, 0, 0.00, 0.00, 0.00

12.700000,12.700000

33, 35, 0,'1 ',2,2,1, 0.00000, 0.00000,2,' ',1, 1,1.0000

0.01900, 0.04800, 100.00

69.000000,69.000000,0.000000, 0.00, 0.00, 0.00, 0, -
0,103.500000,35.189999,1.500000,0.510000, 159, 0, 0.00, 0.00, 0.00

12.700000,12.700000

0 / END OF TRANSFORMER DATA, BEGIN AREA DATA

1, 2, 0.0,999.990,'IEEE14 '

0 / END OF AREA DATA, BEGIN TWO-TERMINAL DC DATA

0 / END OF TWO-TERMINAL DC DATA, BEGIN VOLTAGE SOURCE DC DATA

0 / END OF VOLTAGE SOURCE DC DATA, BEGIN IMPEDANCE CORRECTIOIN DATA

0 / END OF IMPEDANCE CORRECTION DATA, BEGIN MULTI-TERMINAL DC DATA

0 / END OF MULTI-TERMINAL DC DATA, BEGIN MULTI-SECTION LINE DATA

0 / END OF MULTI-SECTION LINE DATA, BEGIN ZONE DATA

1,'IEEE 14 '

0 / END OF ZONE DATA, BEGIN INTER-AREA TRANSFER DATA

0 / END OF INTER-AREA TRANSFER DATA, BEGIN OWNER DATA

1,'1 '

0 / END OF OWNER DATA, BEGIN FACTS DEVICE DATA

0 / END OF FACTS DEVICE DATA BEGIN SWITCHED SHUNT DATA

0 / END OF SWITCHED SHUNT DATA, BEGIN GNE DATA

0 / END OF GNE DATA, BEGIN INDUCTION MACHINE DATA

0 / END OF INDUCTION MACHINE DATA

APPENDIX B

PYTHON CODE: DRIVER CODE AND EXAMPLE CLASS

SOFTWARE PACKAGE DRIVER:

```
import AMPL.runAmpl
import MATLAB.runMatlab
import PSLF.runPslf
import EPANET.modifyInpFile_v13
import EPANET.runEpanet
import os
import time
t0 = time.clock()
numIters = 2*14*24
timeStep = '1' #HAS TO BE IN HOURS

#Pickle File Names
baseAmplPickle = 'amplPickle'
baseMatlabPickle = 'matlabPickle'
basePslfPickle = 'plsfPickle'
baseModEpaPickle = 'modEpaPickle'
baseRunEpaPickle = 'runEpaPickle'
basePickleHour = 6
pickleRestartHour = 72
pickleRestartFlag = 1
##################   Save Files
import combinedSaveSimFilesToFolder
saveFiles = combinedSaveSimFilesToFolder.SaveSimFilesToFolder()
```

```
saveFolderName =  'z_testResults_' + str(numIters) +'Hrs'
saveAmpl = '1'
saveEpanet = '1'
saveMatlab = '1'
savePslf = '1'

#AMPL fileNames
baseBranchContingencyFile = '1_branchData_Contingency'
baseRunFile = '1_lp_Base_run'
baseModFile = '1_lp_Base'
baseUCRunFile = '2_UC1_run'
delta = '0.5'

#MATLAB fileNames
basePgenPdfFile = 'Pgen'
baseGenWaterConsFile = 'Unit'

#Pslf.writeLoadPgenEpcl(epclFileName, savFileName, pGens, loads, timePeriod)
baseEpclInputChange = 'changeLoadPgen'
basePumpLoadChange = 'changePumpLoads'
baseSavFile = '14busDistr1'
basePgenFile = 'UpdatedPgen'
baseLoadFile = 'UpdatedLoads'
```

```
#Pslf.writePgenWaterConsEpcl(epclFileName, savFileName, genData, resultsPW,
resultsV, timePeriod)

baseEpclOutputPrint = 'printPgenWaterCons'

basePWResults = 'results_Pw'

baseNetworkResults = 'results_V'

baseGenData = 'genData'


#EPANET fileNames

mFileRunScript = 'runTestSystem'

baseInpFile = 'TestSystem1'

totalDemandFile = 'totalDemand'

pumpSchedFile = 'pumpSchedule'

baseRptFile = 'waterReport'

baseRptEnergyFile = 'waterReport_Energy'

basePumpLoadFile = 'pumpLoads'

baseGenNodeFlowFile = 'genNodeFlow'

baseGenTankLevelFile = 'tankLevels'

baseMultiplierFile = 'newNodeDemandMultipliers'

basePumpScheduleFile = 'pumpSchedule'

basePumpLoadFileML = 'pumpPowers'

baseHeadFile = 'heads'

simDuration = '25'

hydTS = '1:00'

patternTS = '1:00'

patternStart = '0:00'
```

```
reportTS = '1:00'


#instantiate classes
if pickleRestartFlag == 0:
    ml = MATLAB.runMatlab.Matlab(baseSavFile)
    ampl = AMPL.runAmpl.Ampl()
    pslf = PSLF.runPslf.Pslf()
    modEpa = EPANET.modifyInpFile_v13.ModifyInpFile()
    runEpa = EPANET.runEpanet.RunEpanet()


    ml.createFiles()
    ampl.getMatlabUpdates()
    pslf.getMatlabUpdates()
    ml.startEpanetEngine()
    i = 0
else:
    ml = MATLAB.runMatlab.Matlab(baseSavFile)
    ml.startEpanetEngine()
    lastPickleHour = pickleRestartHour - pickleRestartHour%basePickleHour
    i = lastPickleHour



timeSynchFlag = 1
```

```
while i < numIters:


   timePeriod = str(i+1)


   if pickleRestartFlag == 1:

      pickleRestartFlag = 0

      lastPickleHour = str(lastPickleHour)

      ampl, pslf, modEpa, runEpa = saveFiles.unPickleObjects(baseAmplPickle,
basePslfPickle, baseModEpaPickle, baseRunEpaPickle, lastPickleHour)


   ##UC: if not wanted, create desired GenStatus files using "createGenStatusFiles.py"

   if 1 == int(timePeriod) % 24:

      ampl.writeLoadPercentagesUC(timePeriod)

      ampl.solveUC(baseUCRunFile)


   if timePeriod == '1' and 1 == timeSynchFlag:

       ampl.writeLoadPercentage(timePeriod)

       ampl.checkNetworkStatus(baseBranchContingencyFile, timePeriod)

       if 1 == ampl.contingencyFlag:

          ampl.reWriteRunFileCont(baseRunFile, baseModFile, delta, timePeriod)

          ampl.reWriteModFileCont(baseModFile, baseBranchContingencyFile,
timePeriod)

          ampl.solveOPFCont(baseRunFile, timePeriod)

       else:

          ampl.reWriteModFile(baseModFile, timePeriod)
```

```
            ampl.solveOPF(baseRunFile)

        pslf.getAmplUpdates(baseLoadFile,pumpSchedFile, basePumpLoadFile,
timeSynchFlag, timePeriod)

        if 0 == ampl.contingencyFlag:

            pslf.writeLoadPgenEpcl(baseEpclInputChange, baseSavFile, basePgenFile,
baseLoadFile, timePeriod)

        else:

            pslf.writeLoadPgenEpclCont(baseEpclInputChange, baseSavFile, basePgenFile,
baseLoadFile, baseBranchContingencyFile, timePeriod)

            ampl.contingencyFlag == 0



        pslf.writeChangePumpLoadEPCL(basePumpLoadChange, baseSavFile, timePeriod)

        pslf.writePgenWaterConsEpcl(baseEpclOutputPrint, baseSavFile, baseGenData,
basePWResults, baseNetworkResults, timePeriod)

        pslf.writeCallEpclBat(baseEpclInputChange, baseEpclOutputPrint,
basePumpLoadChange, timePeriod)

        pslf.runPslf()



        modEpa.getGenNodeDemands(basePWResults, timePeriod)

        modEpa.read(baseInpFile, timePeriod, timeSynchFlag)

        modEpa.getPumpSchedule(pumpSchedFile, timePeriod)

        modEpa.reWriteForGA(baseInpFile, baseMultiplierFile, timePeriod, simDuration,
hydTS, patternTS, patternStart, reportTS,timeSynchFlag)

        runEpa.runEpanet(baseInpFile, baseRptFile, timePeriod)



        modEpa.getW4Pdata(baseRptFile, basePumpLoadFile, baseGenNodeFlowFile,
simDuration, timePeriod)
```

```
        ampl.getEpanetUpdates(basePumpLoadFile, baseGenNodeFlowFile, timePeriod)


        timeSynchFlag = 0
    else:
        ampl.writeLoadPercentage(timePeriod)
        ampl.checkNetworkStatus(baseBranchContingencyFile, timePeriod)
        if 1 == ampl.contingencyFlag:
            ampl.reWriteRunFileCont(baseRunFile, baseModFile, delta, timePeriod)
            ampl.reWriteModFileCont(baseModFile, baseBranchContingencyFile,
timePeriod)
            ampl.solveOPFCont(baseRunFile, timePeriod)
        else:
            ampl.reWriteModFile(baseModFile, timePeriod)
            ampl.solveOPF(baseRunFile)


        pslf.getAmplUpdates(baseLoadFile,pumpSchedFile, basePumpLoadFile,
timeSynchFlag, timePeriod)


        if 0 == ampl.contingencyFlag:
            pslf.writeLoadPgenEpcl(baseEpclInputChange, baseSavFile, basePgenFile,
baseLoadFile, timePeriod)
        else:
            pslf.writeLoadPgenEpclCont(baseEpclInputChange, baseSavFile, basePgenFile,
baseLoadFile, baseBranchContingencyFile, timePeriod)
            ampl.contingencyFlag == 0
```

```
pslf.writeChangePumpLoadEPCL(basePumpLoadChange, baseSavFile, timePeriod)

pslf.writePgenWaterConsEpcl(baseEpclOutputPrint, baseSavFile, baseGenData,
basePWResults, baseNetworkResults, timePeriod)

pslf.writeCallEpclBat(baseEpclInputChange, baseEpclOutputPrint,
basePumpLoadChange, timePeriod)

pslf.runPslf()

pslf.printNewPumpPowers(baseNetworkResults, basePumpLoadFileML,
simDuration, timePeriod)

modEpa.getGenNodeDemands(basePWResults, timePeriod)

modEpa.read(baseInpFile, timePeriod, timeSynchFlag)

if int(timePeriod) > 1:

   modEpa.getInitTankLevels(baseInpFile, baseHeadFile, simDuration, timePeriod)



modEpa.getPumpSchedule(pumpSchedFile, timePeriod)

modEpa.reWriteForGA(baseInpFile, baseMultiplierFile, timePeriod, simDuration,
hydTS, patternTS, patternStart, reportTS,timeSynchFlag)

runEpa.reWriteRunScript(mFileRunScript, baseInpFile, baseRptFile,
baseMultiplierFile, basePumpScheduleFile, basePumpLoadFile, simDuration,
timePeriod)

runEpa.runMfileFromShell(mFileRunScript)

modEpa.deleteTempFile(baseInpFile, timePeriod)



modEpa.getW4Pdata(baseRptFile, basePumpLoadFile, baseGenNodeFlowFile,
simDuration, timePeriod)



modEpa.updateGenTankLevels(baseGenNodeFlowFile, baseGenTankLevelFile,
timeStep, timePeriod)

modEpa.storeGenParams()
```

```
        ampl.getEpanetUpdates(basePumpLoadFile, baseGenNodeFlowFile, timePeriod)

        modEpa.printGenParams()


        #print i, '\n'

        i += 1


    if 0 == (i % basePickleHour):

        saveFiles.pickleObjects(ampl, baseAmplPickle, pslf, basePslfPickle, modEpa,
baseModEpaPickle, runEpa, baseRunEpaPickle, timePeriod)

ml.printResults(timePeriod, basePWResults, basePgenPdfFile, baseGenNodeFlowFile,
baseGenWaterConsFile)

modEpa.printGenParams()

ml.closeMatlab()

ml.closeEpanetMatlab()


t1 = time.clock()

print t1-t0


saveFiles.moveFiles(saveFolderName, saveAmpl, saveEpanet, saveMatlab, savePslf)
```

MATLAB CLASS DEFINITION:

```
class Matlab(object):
    def __init__(self, rawFile):
        ####################################################
        # starts matlab engine in the MATLAB dir
        ####################################################
        import os
        import matlab.engine

        self.rawFileName = rawFile + '.raw'
        self.startDir = os.getcwd()
        os.chdir('..')
        os.chdir('MATLAB')
        self.directory = os.getcwd()

        self.ml = matlab.engine.start_matlab()

        os.chdir(str(self.startDir))

    def createFiles(self):
        ####################################################
        # create data files from raw file for ampl
        ####################################################
        self.ml.createDataFiles(self.directory, self.rawFileName, nargout=0)
```

```
    def closeMatlab(self):
        ##################################################
        # stops matlab engine
        ##################################################
        self.ml.close()


    def printResults(self, timePeriod, basePWResults, basePgenPdfFile,
baseGenNodeFlowFile, baseGenWaterConsFile):
        ##################################################
        # calls m file to gather pslf simulation results
        ##################################################
        self.ml.resultsCollection(timePeriod, basePWResults, basePgenPdfFile,
baseGenNodeFlowFile, baseGenWaterConsFile, nargout=0)


    def printResultsWS(self, timePeriod):


        self.ml.resultsExtract(timePeriod, nargout=0)


    def startEpanetEngine(self):
        import os
        import matlab.engine


        self.startDir = os.getcwd()
        os.chdir('..\MATLABWS')
```

```
    self.mlEpanet = matlab.engine.start_matlab()

    os.chdir(str(self.startDir))

def closeEpanetMatlab(self):
    ##################################################
    # stops matlab engine
    ##################################################
    self.mlEpanet.close()

def fileCleanup(self):
    ##################################################
    # deletes simulation results from MATLAB dirs
    ##################################################
    resp = raw_input('Do you want to cleanup MATLAB folder data files (y/n)? '
    if 'y' == str(resp):
        import subprocess
        import os
        self.startDir = os.getcwd()
        os.chdir('..\MATLAB')
        subprocess.call(['del', '1_*.dat'], shell = True)
        os.chdir(str(self.startDir))
    else:
        pass
```